Noise and Vibration of Electrical Machines

Edited by

P. L. TÍMÁR

NOISE AND VIBRATION OF ELECTRICAL MACHINES

Noise and Vibration of Electrical Machines

P. L. TÍMÁR
A. FAZEKAS
J. KISS
A. MIKLÓS
S. J. YANG

Edited by
P. L. Tímár

LIST OF CONTRIBUTORS

P. L. Tímár

Department of Electrical Machines Technical, University of Budapest

Introduction, 2, 3.1–3.3, 3.5, 4, 4.1, 4.3, 5, 6, 7, 8.3, 8.4, 9, 10, 11.1 –11.4, 11.6, 12, 13, 14.1–14.3, 17, 18, Appendix 1

A. Fazekas

Central Office of the Hungarian Academy of Sciences, Budapest

1, 3.4, 3.6, 4.2, 8.1, 8.2

J. Kiss

Instruments and Measuring Technique Service of the Hungarian Academy of Sciences, Budapest
11.5, 11.7, 14.4, 15.1, 15.2, 16.1, 16.2, 17.2, Appendices 2 to 6.

A. Miklós

Institute of Isotopes of the Hungarian Academy of Sciences, Budapest
14.5, 15.3, 15.4, 16.3, Appendices 7

S. J. Yang

Department of Electrical Engineering, Heriot-Watt University, Edinburgh
3.1.5, 3.3, 13.4

CONTENTS

Contents

FOREWORD

Noise pollution is one of the most unpleasant environmental hazards of this age. The factories, workshops and the living quarters in the cities are noisy and sometimes even the peaceful countryside as well. According to physicians and pathologists, noise can even cause permanent damage to the organs of hearing and it can also bring on disorders of the vegetative nervous system. Richard Katz, the well known writer, wrote in the thirties his witty book entitled: "Three Features of Lucifer: Noise, Machine and Business". In his book we can read the accurate statement: "If engineers devoted only a small fraction of the time spent on constructing new machines to acoustics then most noises of machines and equipment could be eliminated."

In most cases electrical machines are used to drive engines. These generate noise in the factories. Trams, trolley-buses and even transformers increase this noise level and this has a negative effect on the people living in a city. This is why the question of a silent electrical machine and transformer plays a significant role in reducing the noise level. This book deals with the above-mentioned subjects: It discusses the acoustics and noise-measuring systems of electrical machines in detail; presents both the theoretical and practical question of the field and gives a detailed description of the mechanical and magnetic noise of electrical machines. It also shows the possibilities of decreasing the noise level. Thus it not only gives an analysis of the various causes of noise production in electrical machines but also presents guidelines for the reduction of noise level of electrical machines. The authors succeeded in summarizing the latest results from the field and they also published the results of their own observations regarding techniques of reducing the noise level of electrical machines and transformers. The present book can be a useful aid for engineers engaged in the design of electrical machines. It expands their knowledge and assists them in choosing new machines.

Special attention should be devoted to those chapters which deal with the specific causes of noises generated by up-to-date, electronically controlled machines. The book can be used as a text-book by universities and postgraduate students. For specialists engaged in reducing the noise level of electrical machines and generally of machines, the book can even be recommended as a handbook.

<div align="right">Pál K. Kovács</div>

LIST OF SYMBOLS

a	path, distance, length, m	i	integer, mode number
	acceleration, m s^{-2}		current, A
	linear current density, A m^{-1}	I	current, A
A	damping, system parameter,		sound intensity, W m^{-2}
	absorption factor, area, m^2		moment of inertia, kg m^2
	linear current density, A m^{-1}	ΔI	rotor imbalance, mm g
b	relative bandwidth	j	integer mode number, $\sqrt{-1}$
	flux density, T	J	moment of inertia, kg m^2
	distance, width, m	k	integer, wave number, correction
B	stiffness factor		factor
	magnetic flux density, T	k_c	Carter factor
	diameter of phase bundle, cm	k	correction factor, constant, winding
	bandwidth, Hz		factor,
c	distance, m		force, N
	speed of sound, m s^{-1}	l	distance, length, path, m
C	capacity, Fa	L	level, dB
	spring constant, m N^{-1}		inductance, H
d	distance, m	m	integer, number of phases
	thickness, diameter of strands, cm		mass, kg
D	directivity factor, damping factor,	M	mass, kg
	determinant, diameter, distance, m	n	integer, number of elements
e	distance, m, eccentricity, cm		speed of rotation (rpm) s^{-1}
E	Young's modulus of elasticity, Pa	N	number of turns
f	frequency, Hz	o	variable
F	force, N	p	number of pole-pairs
F_m	magnetomotive force (mmf), A		pressure, sound pressure, tensile stress,
g	integer		Pa
g	field strength, kV cm^{-1}	P	power, sound power, W
G	weight, N		amplitude of tensile stress, Pa
G_m	specific magnetic conductivity,	q	coordinate, number of slots per pole
	Hm^{-2}		phase
h	height, length m	Q	factor
	thickness, mm		charge, Cb
H	system function	r	mode number
	magnetic field strength, A m^{-1}		distance, radius, m

r_{sf}	specific flow resistance, $N\,s\,m^{-3}$	η	quotient
R	mode number, range	ϑ	angle, rad
	room constant, m^2, radius, m	Θ	second degree polar moment,
	transmission loss, dB		$kg\,m^2\,rad^{-1}$
	resistance, Ω	$\varkappa$	adiabat power
$\mathfrak{s}$	slip	λ	order (rotor), wave length, m
S	number of slots, slew rate	μ	magnetic permeability, $H\,cm^{-1}$, order
	area, surface, m^2		(stator)
t	tooth pitch	ν	integer, order (in time)
	time, s	ϱ	factor, angle, rad
T	time period, time constant,		density, $kg\,m^{-3}$
	reverberation time, s	σ	standard deviation, radiation
	temperatur, °C		factor angle, rad
	torque, N m	τ	variable, mode number, acoustic
u, U	voltage, V		transmission factor time, delay time, s
v	velocity, vibration velocity, $m\,s^{-1}$	φ	angle, rad
V	volume, m^3	Φ	torsional vibration, $rad\,s^{-1}$
$\dot{V}$	volumetric flow, $m^3\,s^{-1}$		magnetic flux, Wb
w	energy density, $J\,m^{-3}$	ψ	angle, rad
W	energy, J	ω	angular frequency, $rad\,s^{-1}$
x	variable	Ω	mechanical angular velocity,
	space coordinate along the bore		$rad\,s^{-1}$
	periphery, rad	Δ	factor
X	variable		
	specific deformation, dispacement, m		
	reactance, Ω		*List of subscripts and superscripts*
y	variable		
	displacement, m	A	A-weighted
Y	displacement, m	b	blade, ball
z	residuum, number of conductors in	cs	commutator segments
	one slot	e	eccentricity
Z	number of commutator segments,	eq	equivalent
	number of balls, impedance, $V\,A^{-1}$;	fr	frequency
		g	geometrical
		h	homopolar
		i	integer, ideal
Greek letters		I	sound intensity
		j	integer
α	absorption coefficient, confidence level	crit	critical
	angle, space coordinate along the	l	on-load, lower
	bore periphery, rad	m	magnetic, maximum, measuring,
β	constant, factor, power		mechanical
	angle, rad	max	maximum
γ	angle, rad	p	fundamental wave, sound pressure
δ	distance, length, m, radial air-gap, mm	r	rotor, rth mode number, ring
δ_s	virtual air-gap increase, mm	rad	radiating
ε	megnetostriction factor, specific ec-	ref	reference, reflected
	centricity	res	resonance
	rotational acceleration, $rad\,s^{-2}$		

s	tooth width, stator, static	ump	unbalanced magnetic pull
sat	saturation	w	winding, wall
sc	short, circuit	W	sound power
sl	slot	0 (zero)	no-load, syschronous, reference
spec	specific	λ	order (rotor)
s, l	sound longitudinal	μ	order (stator)
s, tr	sound transversal	ν	order (in time)
tg	tangential	1	main, stator, integer
u	upper	2	rotor, integer

INTRODUCTION

Noise is an audible sound or mixture of sounds which have an unpleasant effect on human beings, disturbs the concentration and does not convey any useful information. The above definition clearly implies that noise is a subjective concept, associated with humans.

In general, the unpleasantness and disturbing effect of sound lie in its uncertainty, even if we consider a Beethoven symphony! We call it beautiful art in the concert hall and enjoy it. But when our neighbour wakes us with it from peaceful slumber, it is noise; or perhaps we are better tuned into a light Schubert song; or else we just do not like Beethoven; or we want to whisper something important into the ear of our companion just as the crescendo of the brass strikes through the air. An electrical machine may be called silent if the noise of the milling machine, lathe or the ventilator driven by it is at least 10 dB louder than the noise from the machine itself. On the other hand, almost any electric motor would seem noisy in a watchmaker's shop. We do not even notice the sound of the elevator during the day when we are wide awake and surrounding noise level is high, but it disturbs our rest during the night. Further, we must not forget that the hearing of people varies and changes with age.

Standards try to provide a certain degree of objectivity with which to assess the subjective and relative concepts of noisiness by incorporating such components in the noise measuring system which simulate average human hearing, and by setting noise limits for the various kinds of electrical machines. These limits, however, are not derived from physical laws but rather reflect the typical technical level of a given period. This clearly implies that the mere fact that an electrical machine complies with standards as far as its noise characteristics are concerned does not necessarily mean that it is considered silent under all circumstances at any time. As the acoustic phenomenon produced by the electrical machine is an undesirable byproduct of the energy transforming function of the machine, we consider it to be noise, regardless of its magnitude, nature or spectrum.

It was about seven decades ago that engineers first started to pay attention to

noise produced by electrical machines. As machines were oversized at that time, the aerodynamic noise was negligible, while the bearing noise was a well-known phenomenon from the operation of other machine types, and so research turned to noise of electromagnetic origin. The number of asynchronous motors increased rapidly, so that they became the subject of the first experiments. In the first fifteen years, engineers used rotors of different slot number in the same stator and deduced that there are favourable and unfavourable slot number combinations. A large number of publications recommended "optimum" slot numbers which scattered over a wide range. In the thirties, it came as an unpleasant shock to realize that a slot number combination that had proved acceptable or unacceptable before, could behave quite differently in machines of different power rating. Therefore, attention turned to the mechanical structure of motors, their vibration properties, and their effect on noise generation.

Since the forties, numerous analytical studies have been published world-wide. In Central Europe, Professor H. Jordan and his colleagues, in the U.S.A., Prof. E. Erdélyi and P. L. Alger, in England, A. J. Ellison, and in the Soviet Union, Professor N. V. Astachov established successfully operating research centres. In their publications, they evaluated a steady-state of the electromagnetic field and managed to solve numerous noise-related problems. Meanwhile, technical development gradually resulted in better specific machine parameters (e.g., kW/kg) and improved exploitation of active and passive machine components. As the weight and dimensions of machine parts decreased, the noise of electrical machines increased. According to British sources, for example, the noise of 30 kW asynchronous squirrel-cage motors increased by more than 10 dB in the period between 1957 and 1967. The situation was further complicated by the fact that the scope of application of electrical machines extended beyond the boundaries of factories, entering homes and apartment buildings which are extremely sensitive to noises. In this area, the spreading of lightweight construction panels in the building construction industry is the breeding ground of noise pollution. Noise, as one of the environmental harms, has a doubly adverse effect on men. On one hand, it damages the organs of hearing and, on the other hand, it brings on disorders of the vegetative nervous system. As it diminishes human performance, it gives rise indirectly to economic losses.

By the end of the sixties, engineers had achieved substantial results in decreasing steady-state noise levels of electromagnetic origin. Then, attention turned to noises of aerodynamic origin, i.e., ventilation noise. The more extensive exploitation of the active material resulted in an increase of losses and, consequently, in the requirement of stronger and more effective ventilation. The solid-state drive systems appeared in the seventies and have ever since been spreading raised new questions, as the time harmonics present at the motor terminals very often

considerably enhanced the noise level. In recent times engineers have encountered the new challenge of measuring short-time noise phenomena in the transient operation of the electrical machine.

The mechanical vibration of electrical machines, which can by no means be separated from the noise of the machine, manifests itself in many ways. Vibration means a permanent deformation of the machine, hence it reduces lifetime. Part of the vibration is transferred to objects in close mechanical contact with the machine, e.g., to the machine tool, adversely affecting the working accuracy and, in turn, degrading machine tool quality. In most cases there are people working close to the vibrating machine, whose health and performance may also be affected.

The requirements as regards the noise and vibration levels of electrical machines are increasingly stringent and wider in scope, since reduction of noise and vibration is equally important to health, economics and productivity.
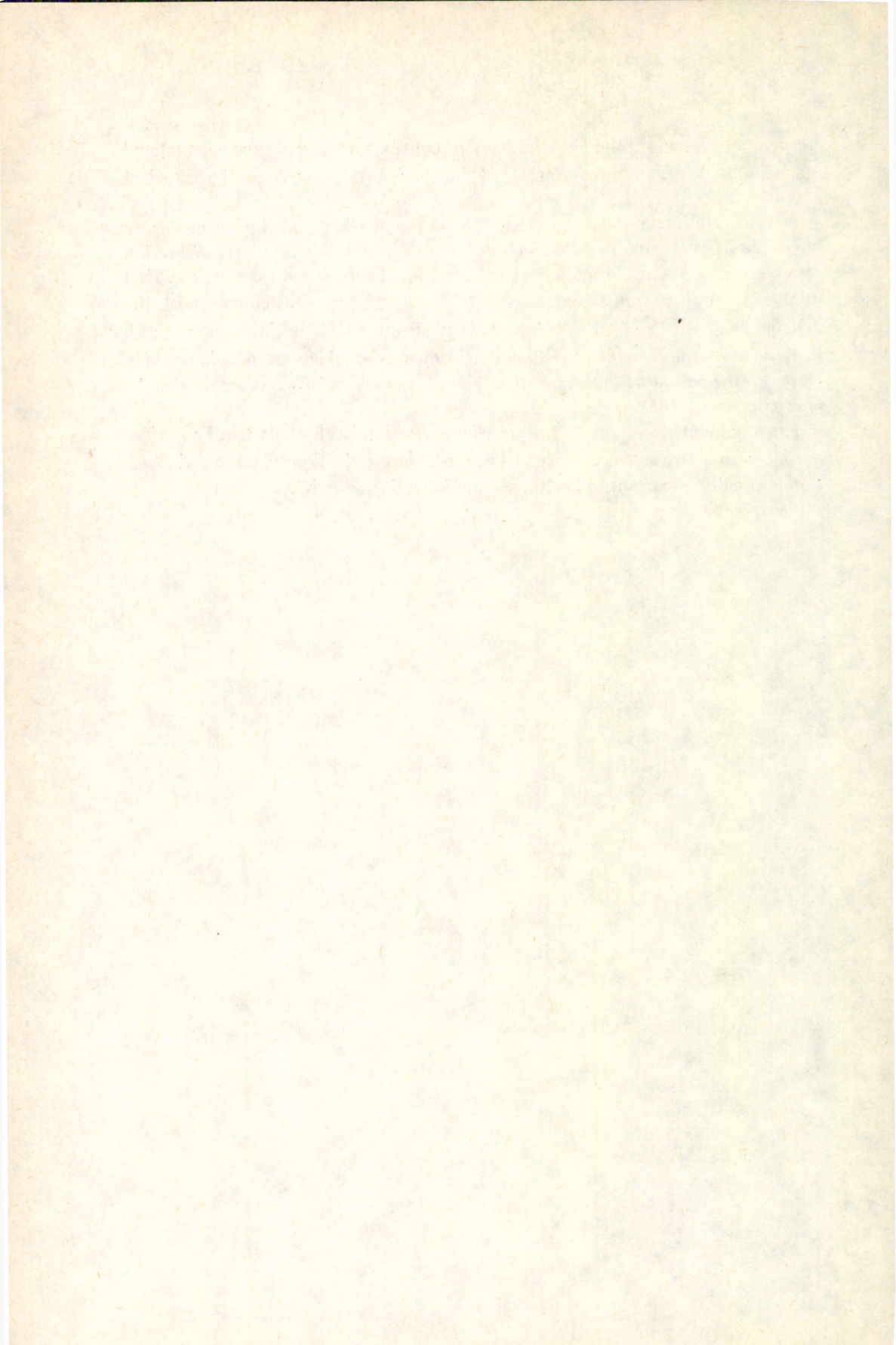
A. GENERATION AND ELIMINATION
OF NOISE AND VIBRATION

1. BASIC ACOUSTIC TERMS

1.1 Sound generation and sound radiation

In our everyday life, sound is a spatial phenomenon sensed in the air or under, water by our ears which transform it into information about our surroundings. This information may contribute to our knowledge or serve as an element of our culture, but can still be the cause of discomfort.

According to our senses, sound is a vibration with characteristic amplitude and frequency. The general definition of vibration is as follows. The time function $q(t)$ of a mechanical model's coordinate given by q can be regarded as a vibratory motion if the function $q(t)$ satisfies the following criteria:

(1) $q(t)$ is bounded (i.e. the absolute value of $q(t)$ for any t is less than a given finite number),

(2) the velocity of motion, expressed as dq/dt, changes sign at least twice in the time interval examined.

In further discussions, to avoid misunderstanding, sound is defined as the mechanical vibration of an elastic material medium. This vibration is the result of a single or periodic force that displaces the smallest material particles of the medium from its position of balance, causing them to oscillate about their rest position through their inertia and elastic forces, normally following a harmonic pattern, transferring their motion to adjacent particles.

According to our definition, the medium transmitting sound is elastic, capable of mechanical oscillation. This elastic medium can be gaseous, liquid or solid material.

The sound (or oscillation), in a general sense, can be classified by two characteristics, its frequency and amplitude, as shown in Fig. 1.1. Of course, the ranges identified in the figure indicate only the order of magnitude relations in the direction of both axes. Oscillations of very low (<5 Hz) frequency are called LF vibrations, and then up to 20 Hz, infrasound. Audible sounds occupy the range from 20 Hz to 16 kHz (though the limit real value can depend on the individual and could be something else). The next range is that of ultrasound with an upper frequency limit of 1 GHz, which represents the maximum frequency obtainable by tech-

nical means of today. The two important limits that depend on the amplitude of
oscillation are the threshold of hearing and the threshold of feeling.
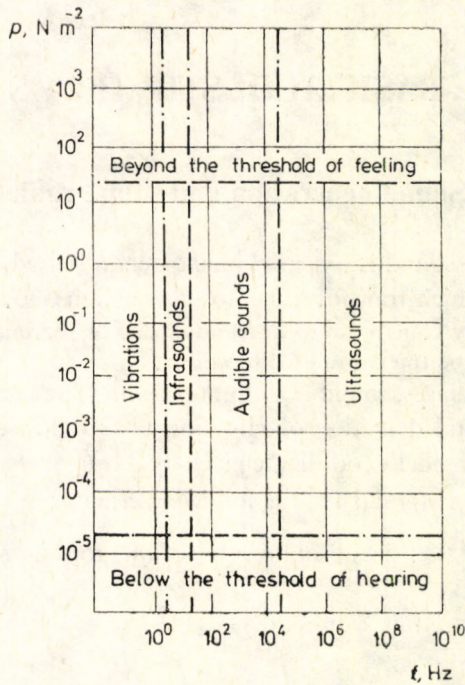
Fig. 1.1. The sound pressure–frequency plane

In everyday use, the term sound is understood to be the part of the sound which
falls into the audible frequency range, and we will also use the term in that sense.
Sounds propagating in a gaseous medium or air are called airborne sounds, while
in the case of a liquid or solid medium, liquidborne or structure-borne, respec-
tively. For convenience, airborne sounds will simply be called sounds in this book,
but we should not forget to add the "air" prefix, at least mentally.

Vibration is a more general term, but in engineering practice, oscillations of a
solid media with relatively low frequencies (below 1 kHz) are called vibration.

The vibration emitted by the source passes through different media or even
a mixture of them in the form of airborne or structure-borne sound depending on
the media, until it dies away completely. The damping of the travelling wave
depends on the material characteristics and geometry of the medium. The interface
between two different media reflects the sound; the propagation speed is charac-
teristic of the medium, while the waveform is a function not only of the medium
but also of the geometry. In gases and liquids, sound propagates in the form of

longitudinal waves, where the particles oscillate in the same direction as that of propagation. In solid bodies, however, transverse waves are also present owing to the fact that elastic strain is accompanied by transversal constuction. Depending on the wavelength, the geometry of the body and their ratio, bending, dilatational and torsional waves may also be generated. The natural frequencies of mechanical components have significant effects on wave propagation.

Sound waves, just as other types of oscillations, may be characterized by their peak, effective and mean value, their frequency and, in the case of complex sound, their spectra. The classification of sounds will be detailed later.

The complex system of sound generation, propagation and sensation incorporates the exciting forces, the sound source, the medium and its properties, and the whole space occupied by the sound, the so-called sound space. The exciting forces act on a mechanical system or medium capable of vibrating, and generate vibrations determined by the vibrating and radiating properties of the source. The involved active (time-dependent) and passive elements can be analysed by means of adequate models.

The input parameters of the system would be the exciting forces arising by chance or for a known reason.

The detailed discussion and calculation of these forces form a very important part of this book. At this point we will classify the forces by their functions of time, not forgetting, however, that in concrete practical analyses the function describing spatial behaviour also plays a very important role.

Classification of exciting forces:

Shock-type exciting forces described by functions (a) and (b):

(a)

$$x(t) = \hat{X} \cos (\omega t - \varphi) \tag{1.1}$$

and

$$x(t) = X_0 + \sum_{n=1}^{\infty} \hat{X}_n \cos (n\omega t - \varphi_n), \tag{1.2}$$

(b)

$$x(t) = 1(t) \tag{1.3}$$

and

$$x(t) = \delta(t), \tag{1.4}$$

(c) Transient-type exciting forces,
(d) Non-periodic, irregular, stochastic exciting forces.

In the generation of noise and vibration in electrical machines, it is mostly type (a) exciting forces that take part. The energy transferred by the exciting forces will set the mechanical system vibrating, as determined by the system's response,

weight, geometry, material, etc. The induced vibration can be of two kinds: free and forced.

We refer to free vibration if vibration continues, even when the force that acted on the mechanical system to induce vibration is no longer present to transfer energy to the system. In this case, the vibration of the system is damped, and the amplitude of vibration will gradually decay, depending on the degree of damping within the system, until it returns to rest position.

Forced vibration is produced when a steady $F(t)$ exciting force acts on the system. If the frequency of the periodic force is identical with the natural frequency of the system ($\omega=\omega_0$), then the system will exhibit resonance with a maximum amplitude of oscillation.

We can detect the vibration of the medium in sound space, that is the space where sound waves are present, by means of our ears, hands or a proper instrument set up there.

The sound produced can be one of the following types:
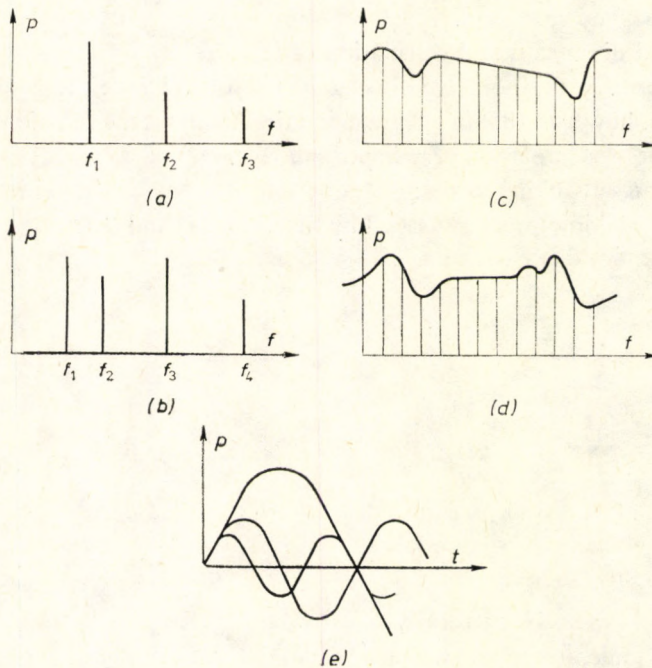
Fig. 1.2. Sound types: (a) f_2 and f_3 are the whole number multiples of f_1, the vibrations are harmonic, (b) f_1, f_2, f_3 and f_4 are independent, the vibrations are not harmonic, (c) continuous frequency distribution, no useful information, (d) continuous frequency distribution with several components standing out, (e) multiple-wave harmonics [see (a)]

— Pure tone, when the vibration of the medium is sinusoidal (harmonic) with a single characteristic frequency.

— Complex sound, when the vibration of the medium is made up from a finite or infinite number of pure tones. Periodic complex sounds may be broken down into harmonic components. Under special conditions and restrictions, the components of non-periodic vibrations may be analysed as well.

— Noisy sound, generally with a continuous spectrum that may include several dominant frequencies. The amplitude and frequency of components fluctuates randomly.

The sound, or vibration of a medium, may be represented graphically as a function of time or frequency. The time response is used mostly for the analysis or demonstration of pure tones or a selected component or a series of selected components of a complex sound. The frequency spectrum of complex sounds is useful in illustrating the general character of the sound and identifying the sensible direction for further analysis. Figure 1.2(e) shows an example for time response. Some frequency spectra for typical complex sounds are shown in Fig. 1.2.

1.2 Characteristics of sound field

To describe sound field, the time and space distribution of sound pressure and particle velocity is the common means. Driven by the force of vibration, the density and pressure of the medium and the velocity of its particles oscillate about a constant mean value characteristic of the medium in the state of "rest" before vibrating. The motion of particles results in compression in one place and rarefaction is another, increasing and decreasing the density of the medium, respectively. Normally there is no time for heat exchange between the medium and the ambient owing to the relatively rapid change of state within each period, so the sound pressure can be expressed in the following form:

$$p = \frac{p_{const}^{\varkappa}}{\varrho_{const}} \varrho, \tag{1.5}$$

where p_{const} — normal pressure at normal temperature,

ϱ_{const} — density of the medium at normal condition,

$\varkappa$ — heat capacity ratio of the gas (constant).

(a) The sound pressure is characterized by the root mean square (r.m.s.) value of the pressure change induced by the vibration:

$$p = \sqrt{\frac{1}{T} \int_0^T [p(t)]^2 \, dt}. \tag{1.6}$$

When there are more components of different frequency, as is the case in most technical applications, the sound pressure is described by the resultant r.m.s. value calculated from the component r.m.s. values according to the following formula:

$$p = \sqrt{p_1^2 + p_2^2 + p_3^2 + \dots .} \tag{1.7}$$

(b) The particle velocity is the fluctuating speed of particles within the medium. Its value is expressed, just as for the sound pressure, by the r.m.s. velocity:

$$v = \sqrt{\frac{1}{T} \int_0^T [v(t)]^2 \, dt.} \tag{1.8}$$

(c) The speed of sound is the wave velocity of sound in a given medium. It is a function of temperature, i.e., it varies with the square root of the absolute temperature. Its value
  for gases:

$$c = \sqrt{\frac{\varkappa p_{const}}{\varrho_{const}}}, \tag{1.9}$$

  for air:

$$c = 344 \text{ m s}^{-1}$$

for

$$\varkappa = 1.4 \quad \text{and} \quad T = 20°C,$$

  for solid materials:

— for three-dimensional wave propagation, assuming that the dimensions of the body are much larger than the wavelength in each direction:

$$c_{sl} = \sqrt{\frac{E(1-\mu)}{\varrho_{const}(1+\mu)(1-2\mu)}}, \tag{1.10}$$

where E — modulus of elasticity,
        μ — Poisson's number (e.g., for steel $\mu = 0.3$) (the above formula applies
               only within the scope of Hooke's law),
— for two-dimensional wave propagation (e.g., plate):

$$c_{str} = \sqrt{\frac{E}{2\varrho_{const}(1+\mu)}}. \tag{1.11}$$

(d) The specific acoustic impedance is the ratio sound pressure to particle velocity:

$$Z_{spec} = \frac{p}{v}. \tag{1.12}$$

(e) The sound intensity is the rate of flow of energy through unit area perpendicular to the direction of travel of the sound:

$$I=\frac{1}{T}\int\limits_{0}^{T} pv\, dt,\qquad (1.13)$$

where v is the component of speed perpendicular to the surface.

(f) The acoustic power is the sound intensity over an optional surface S perpendicular to the direction of travel of sound:

$$P=\int\limits_{0}^{S} I\, dS.\qquad (1.14)$$

(g) The directivity factor describes the propagation of waves generated by a radiator in various directions:

$$D=\frac{p^2(r,\varphi,v)}{p^2(r,\varphi_0,v_0)},\qquad (1.15)$$

where $p(r,\varphi_0,v_0)$ — the sound pressure at the reference point defined by asimuthal angle φ_0 and polar angle v_0 at a distance of r from the radiator,

$p(r,\varphi,v)$ — the sound pressure at a point defined by asimuthal angle φ and polar angle v at a distance of r from the radiator.
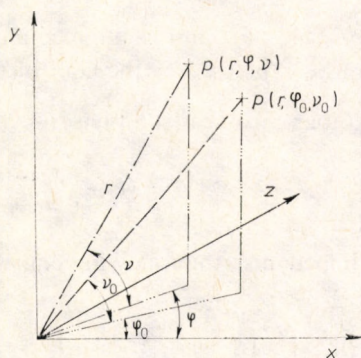
Fig. 1.3. The sound source in the spatial coordinate system

Figure 1.3 illustrates the concept of directivity in space. The complete set of directivity factors makes up the directivity pattern.

1.3 Modelling sound radiators

As the feature of the propagation of sound waves emitted by radiators—because of their complex physical inherence—is difficult to calculate, we use model radiators of known parameters to facilitate the analysis.

In technical practice, and elsewhere, point sources, spherical and plane radiators of various orders, etc. are used as the commonest model types. With careful model selection, we can approximate the real physical conditions quite well. For the analysis of electrical machines, spherical or cylindrical radiation models are usually used.

Let us start off from the formula of spherical waves. First we consider a pulsating spherical radiator, when mode numbers $R=0$. The amplitude of the pressure wave is inversely proportional to the distance from the centre:

$$p=\frac{p_{a1}}{r}\,e^{j(\omega t-kr)}, \qquad (1.16)$$

where p_{a1} — pressure amplitude at a distance of $r_1=1$ m from the centre of radiator,

r — distance from the centre,

ω — angular velocity of vibration,

t — time,

$k=\dfrac{2\pi}{\lambda}$ — wave number,

$\lambda=\dfrac{c}{f}$ — wavelength of vibration,

c — travelling speed of sound in the medium.

The particle velocity can be expressed as the sum of two components, one in phase with pressure, the other $\dfrac{\pi}{2}$ ahead of phase:

$$v=\frac{1}{\varrho c}\frac{p_{a1}}{r}\,e^{j(\omega t-kr)}+\frac{1}{\varrho c}\frac{1}{kr}\frac{p_{a1}}{r}\,e^{j\left(\omega t-kr+\frac{\pi}{2}\right)}. \qquad (1.17)$$

For the specific radiation impedance, the following equation is found:

$$Z=\frac{p}{v}=\varrho c\,\frac{k^2r^2}{1+k^2r^2}+j\varrho c\,\frac{kr}{1+k^2r^2}. \qquad (1.18)$$

The radiated power can be calculated by applying the real part of the radiation impedance, just as in the case of electrical power:

$$P=v^2\varrho c\,\frac{k^2r^2}{1+k^2r^2}\,S. \qquad (1.19)$$

This formula gives us the acoustic power emitted by the radiating surface to air, when v is the mechanical vibration velocity of the radiating spherical surface, r is the radius of the radiating sphere, S is the surface area of the sphere and ϱ is the density of air. The general formula that gives the value of radiated acoustic power for a mechanical system of surface S in terms of the radiation wave imped-ance for any mode number R is:

$$P = v^2 \, \mathrm{Re} \, \{Z\}S. \tag{1.20}$$

The characteristics of various radiators are covered by factor $\mathrm{Re} \, \{Z\}$:

$$\mathrm{Re} \, \{Z\} = Z_0 \sigma, \tag{1.21}$$

where σ — the radiation factor,
$\quad Z_0 = \varrho c$.

The σ is a function of the mode number, and thus of the spatial distribution of exciting forces as well. Taken this into consideration, according to [40] we obtain:

$$P_R = v^2 Z_0 S \, \sigma \tag{1.22}$$

If the sound radiator emits a complex acoustic power and thus various mode numbers are in effect, then:

$$P = \sum_R P_R. \tag{1.23}$$

Formulae of radiation factor for typical acoustic radiators are reviewed below.

For a spherical radiator:

$$\sigma = \mathrm{Re} \left\{ jkr \, \frac{\displaystyle\sum_{v=0}^{R} \frac{(R+v)!}{(R-v)!} \frac{R!}{v!} (2jkr)^{R-v}}{\displaystyle\sum_{v=0}^{R} \frac{(R+v)!}{(R-v)!} \frac{R!}{v!} (2jkr)^{R-v}(1+jkr+v)} \right\}, \tag{1.24}$$

where R — mode number,
$\quad v$ — integer.

For some significant mode numbers and limiting conditions, the acoustic power is if $R = 0$, (pulsating sphere):

$$\sigma = \frac{k^2 r^2}{1 + k^2 r^2} \cdot \quad \text{(see eqn. (1.21))} \tag{1.25}$$

(a) If the frequency and r is very small, i.e., $kr \ll 1$, then the acoustic radiator approximates a point source. Then:

$$\sigma \cong k^2 r^2. \tag{1.26}$$

(b) If the frequency or the sphere radius is large, i.e., $kr \gg 1$, then the radiator approximates a plane source and

$$\sigma \cong 1. \tag{1.27}$$

So, in order to select an adequate model in terms of acoustical requirements, it is essential to consider not only the geometry and dimensions of the radiator but also the relation of frequency, wavelength and radiator dimensions.

Depending on the frequency, the same radiator may produce different types of sound wave.

For practical purposes, eqn. (1.24) is difficult to handle, and therefore the curves shown in Fig. 1.4, which were calculated applying eqn. (1.24) may be used with
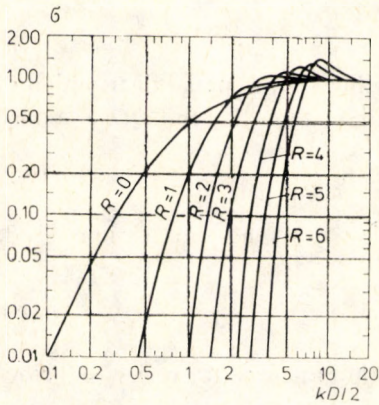
Fig. 1.4. The radiation factor curves of a spherical radiator
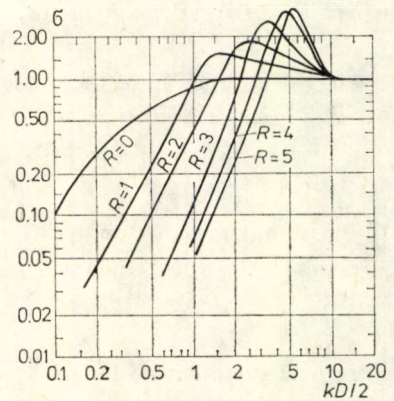
Fig. 1.5. The radiation factor curves of a cylindrical radiator

acceptable accuracy. For computer analysis, the following approximating formulae may be used if $K = kr$, $(K = k\frac{D}{2})$:

for $R = 0$,

$$\sigma_0 = \frac{K^2}{1 + K^2}, \tag{1.28}$$

for $R = 1$,

$$\sigma_1 = \frac{K^4}{4 + K^4}, \tag{1.29}$$

for $R = 2$,

$$\sigma_2 = \frac{K^6}{10^2 + K^6}[0.4 \times 10^{-3}(K - 20)^2 + 1], \tag{1.30}$$

for $R = 3$,

$$\sigma_3 = \frac{K^8}{5 \times 10^3 + K^8}[1.11 \times 10^{-3}(K - 20)^2 + 1], \tag{1.31}$$

for $R=4$,

$$\sigma_4 = \frac{K^{10}}{5 \times 10^5 + K^{10}} [1.51 \times 10^{-3}(K-20)^2 + 1], \tag{1.32}$$

for $R=5$,

$$\sigma_5 = \frac{K^{12}}{10^8 + K^{12}} [2.11 \times 10^{-3}(K-20)^2 + 1]. \tag{1.33}$$

The specific radiated power of a cylindrical radiator is expressed as:

$$\sigma = (kr)^2 \frac{N_R I_{R+1} - I_R N_{R+1}}{[RI_R - (kr)I_{R+1}]^2 + [RN_R - (kr)N_{R+1}]^2} \tag{1.34}$$

where N_R and N_{R+1} are Neumann functions,

I_R and I_{R+1} are Bessel functions.

For manual calculations, as for the spherical radiators above, the plotted representation of the equation is given in Fig. 1.5.

1.4 Levels and their mathematical expression

The acoustic power of sound sources varies over a wide range spreading from the rustle of leaves ($\sim 10^{-9}$ W) to the noise level of jets or rockets taking off ($\sim 10^{5 \text{ to } 7}$ W). The range of the human ear allows the sensation of sounds with pressure of 2×10^{-5} N m^{-2} (threshold of feeling) to about 20 N m^{-2} (threshold of pain), which is quite a wide dynamic span. To better fit the sensation of human hearing and to facilitate classification and measurement, relative quantities have been introduced. These units relate the quantity to a reference value and express the value as the logarithm of the ratio of the actual quantity to the reference value.

The introduction of levels is also justified by the fact that their perception changes in a non-linear way with sound pressure.

The human ear is practically unable to sense changes in sound pressure level below 1 dB.

Level quantities:

— sound power level

$$L_W = 10 \log \frac{P}{P_0} \quad \text{dB}, \tag{1.35}*$$

where

$$P_0 = 10^{-12} \quad \text{W},$$

— sound intensity level

$$L_I = 10 \log \frac{I}{I_0} \quad \text{dB}, \tag{1.36}$$

* In the following $\log_{10} = \log$.

where

$$I_0 = 10^{-12} \quad \text{W m}^{-2},$$

— sound pressure level

$$L_p = 20 \log \frac{p}{p_0} \quad \text{dB}, \tag{1.37}$$

where p — the r.m.s. sound pressure,

$p_0 = 2 \times 10^{-5}$ Pa (this value corresponds to the threshold of sensitivity of human hearing at 1000 Hz).

(From now on, following standard practice, symbol L will stand for sound pressure level, and subscript p will be omitted.)

Now we have introduced the levels, the basic elements in our acoustical calculations. Owing to their logarithmic character and taken into consideration their physical content as well, the addition and subtraction of levels cannot be achieved through basic arithmetic operations.

The essence of the calculation is better characterized by the determination of the resultant component, and therefore this will be used in further discussions. The complex algorithm can be simplified. For example, let us consider equipment with sound power levels of L_{W1} and L_{W2}, where $L_{W1} \neq L_{W2}$. The resultant level, L_{Wr} is given by

$$L_{Wr} = L_{W1} + \Delta L, \tag{1.38}$$

where

$$\Delta L = 10 \log \left(1 + \frac{1}{10^{0.1(L_{W1} - L_{W2})}} \right).$$

To ease the process of calculation, Fig. 1.6 is provided. The lower, linear scale shows the values of $(L_{W1} - L_{W2})$, while the upper, logarithmic scale shows the corresponding ΔL values.

The formula given to determine the resultant level is equally applicable to sound power, sound pressure and intensity levels.
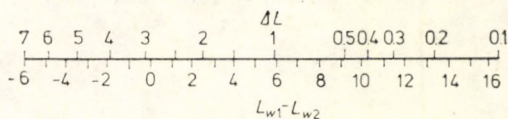
Fig. 1.6. Nomogram to help level addition

The only limitation of the method of addition given above is that it applies only to the determination of the resultant of two levels and to its inverse operation. For this reason, we have to determine the value of a series of partial resultants of components in order to get the resultant for all the components making up a spectrum. We should point out that the sequence of calculations determining the resultant level does not influence the final result.

Let us consider n measurements that give us n different sound pressure level values. The resultant sound pressure level is obtained by:

$$L_r = 10 \log \sum_{i=1}^{n} 10^{0.1L_i}.\tag{1.39}$$

The mean sound pressure level is:

$$\bar{L} = 10 \log \left(\frac{\overline{p^2}}{p_0^2}\right) = 10 \log \left[\frac{1}{n} \sum_{i=1}^{n} 10^{0.1L_i}\right].\tag{1.40}$$

1.5 Build-up of sound field in open and closed space

The structure of sound pressure level that builds up in acoustical space depends on the specifications of the space surrounding the sound source, i.e., on the acoustical properties of the medium, the dimensions and shape of boundary surfaces and their material characteristics, etc. Sound spaces are classified as follows:

— Free space: homogeneous, isotropic space that does not modify the spreading of sound. In free space, sound spreads out in the form of travelling plane waves or spherical waves.

— Closed space: the space surrounding the sound source is limited in all directions. Reflecting and absorbing surfaces, materials are essential parts of closed space. Reflected sound waves substantially affect the build up of spatial sound field.

— Limited space: the propagation of sound waves exhibits a direction-specific pattern and the boundary surfaces may modify the sound field.

Let us consider the relationship between the sound pressure level L at distance r from the inducing ideal point source and the emitted sound power level L_W in free space under ideal acoustical conditions, that is, only waves directly generated by the source are present.

Combining eqns (1.13) and (1.14):

$$p^2 = \frac{P\varrho c}{S},$$

and for the reference level:

$$p_0^2 = \frac{P_0\varrho_0 c_0}{S_0},$$

where $S_0 = 1\ m^2$.

The sound pressure level is obtained by taking the logarithm of the ratio of the two above equations, multiplied by ten:

$$L = L_W + 10 \log \frac{S_0}{S} = L_W - 10 \log \frac{S}{S_0}, \tag{1.41}$$

as in most cases ϱc and $\varrho_0 c_0$ are assumed to be equal.

Since S is proportional to the square of r, the distance between the evaluation point in question and the point source, it can be shown from eqn. (1.41) that the sound pressure level in an ideal sound space decreases with the square of the distance. In the case of directional sound source with directivity factor D, the sound pressure level is expressed as:

$$L = L_W + D - 10 \log \frac{S}{S_0}. \tag{1.42}$$

In common language, open or free space implies an unenclosed, roofless air space. In an ideal, homogeneous, non-absorbing air space, the sound pressure is inversely proportional to the square of the distance. The value of sound pressure level for ideal circumstances is given by eqn. (1.41). If the source is above an ideally hard floor, then the sound field is hemispherical.

In a real air space, the absorption in air, the meteorological conditions and obstacles scattered in space, all give excess damping. Now the sound pressure level is given by:

$$L = L_W + D - 10 \log \frac{S}{S_0} - A_t, \tag{1.43}$$

where

$$A_t = A_a + A_p + A_{lm} + A_{am},$$

where A_a — damping due to absorption in air,
$\quad\quad A_p$ — damping due to precipitation, i.e., mist, snow, rain,
$\quad\quad A_{lm}$ — damping due to the presence of landmarks (e.g., trees, buildings and other obstacles),
$\quad A_{am}$ — damping due to air motion.

As electrical machines are mostly working in closed areas, we will concentrate our efforts on the discussion of closed spaces. A detailed description of the various damping effects that prevail in open air spaces is outside the scope of this work.

Figure 1.7 illustrates the changing sound pressure level in closed space as a function of the distance from the sound source. We note that the position of the interfaces between the various fields may vary with frequency.

Zone *I* depends on the phase difference between particle velocity and sound pressure, the characteristic dimensions of the sound source and the phase of the parts of the radiating surface. It is very hard to describe the overall effect of these factors in an explicit numerical value and the boundaries of the near field can often be determined only by measurement.
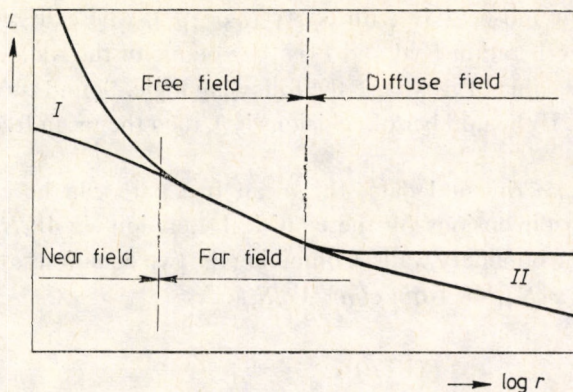
Fig. 1.7. The characteristic domains of the sound field in a closed space

Zone *II* develops as a result of interference between the direct and reflected wave-trains in the reverberation field. This interference can result in the widest range of superposition patterns that could lead to a uniform sound pressure zone of considerable extent. Another factor is the frequency-dependence of the absorption coefficient, which may affect the reflected sound power.

Now let us discuss the basic characteristics of the various fields shown in the figure.

Near field: its most important characteristic is that the sound pressure leads on the particle velocity, that is, they are not in phase. This phenomenon is predominant within a range of about 2λ around the source.

We will consider its effect on the accuracy of sound pressure level measurement later.

Far field: here the phase difference between particle velocity and pressure wave is negligible. If there is no other effect, e.g., reflection, the sound pressure level decreases by 6 dB when the distance is doubled.

Free field: this is that part of the far field, where the reflected sound waves do not modify or interfere with the sound field generated by the source. The sound pressure depends only on the output of the sound source, the acoustical properties of the medium and the distance from the source.

Diffuse field: the sound pressure within this zone is determined by the direct sound pressure produced by the source, and the reflected pressure. It is into the reverberation field that power not absorbed by the walls or the air medium is transmitted. If absorption in air is neglected and absorption by walls is represented by an average absorption coefficient, $\bar{a}$, then the reflected power can be expressed as $P(1-\bar{a})$. If there are n reflections per minute, then the energy

possessed by the sound field is reduced by $(n\bar{a}w_{\mathrm{ref}}V)$, where w_{ref} is the energy density of the reverberation field and V is the volume of the room.

To estimate the value of n, we use the following logic. Sound travels a distance of ct in a period t. If the number of collisions is n, then the mean free path is given by $d=ct/n$.

According to experimental data, the mean free path can be expressed as a function of room dimensions by the empirical equation $d\cong 4V/S_{\mathrm{ref}}$, where S_{ref} is the surface of the boundary walls. Combining the two equations and substituting $t=1$ s, we have $n=cS_{\mathrm{ref}}/4V$ from $ct/n=4V/S_{\mathrm{ref}}$. As

$$P(1-\bar{a})=\frac{cS_{\mathrm{ref}}}{4V}w_{\mathrm{ref}}\bar{a}V, \tag{1.44}$$

we get

$$P=\frac{S_{\mathrm{ref}}\bar{a}}{1-\bar{a}}\frac{c}{4}w_{\mathrm{ref}}. \tag{1.45}$$

Factor $\dfrac{S_{\mathrm{ref}}\bar{a}}{1-\bar{a}}$ is called room constant and is denoted by the symbol R. This depends only on the internal surfaces of the room and the average absorption coefficient.

Let us substitute the energy density $w_{\mathrm{ref}}=\dfrac{p_{\mathrm{ref}}^{2}}{\varrho c^{2}}$ into the equation:

$$P=R\frac{c}{4}\frac{p_{\mathrm{ref}}^{2}}{\varrho c^{2}}=\frac{R}{4}\frac{p_{\mathrm{ref}}^{2}}{\varrho c}.$$

Now the reflected sound pressure is:

$$p_{\mathrm{ref}}^{2}=P\varrho c\frac{4}{R}. \tag{1.46}$$

For small rooms the neglection of absorption in air is justified. For larger air spaces, it can be incorporated in $\bar{a}$ as an additional term. For laboratories, workshops and assembly halls which are not too large, $\bar{a}$ is in the range 0.05 to 1.1. For higher frequencies, the damping effect of air increases significantly. The mean free path provides a proper means of qualifying the size of a closed space. Such a closed space is considered large, when the ratio d/λ is large.

Above we have determined the direct (p_d) and reflected (p_{ref}) sound pressure, and so it is possible to formulate the sound pressure level in a steady-state closed sound field. From the above equations:

$$p_{\mathrm{res}}^{2}=p_{d}^{2}+p_{\mathrm{ref}}^{2}=P\varrho c\left(\frac{1}{4r^{2}\pi}+\frac{4}{R}\right). \tag{1.47}$$

The sound pressure level is:

$$L = 10 \log \frac{p_{\text{res}}^2}{p_0^2} = 10 \log \frac{P \varrho c}{p_0^2} \left(\frac{1}{4r^2\pi} + \frac{4}{R} \right). \qquad (1.48)$$

Assuming again that $\varrho c = \varrho_0 c_0$, the resultant sound pressure level is:

$$L = L_W + 10 \log \left(\frac{1}{4r^2\pi} + \frac{4}{R} \right). \qquad (1.49)$$

In open space, also taking the directivity, which depends on the sound source and its relative position into consideration, the sound pressure level is found to be:

$$L = L_W + 10 \log \left(\frac{D}{4r^2\pi} + \frac{4}{R} \right). \qquad (1.50)$$

2. GENERATION PROCESS OF NOISE
AND VIBRATION IN ELECTRICAL MACHINES

2.1 The process of noise generation

The objects, elements and human beings involved in the noise generation process, constitute a well-defined, clear-cut system. This system comprises three basic constituents. On one hand there is the noise source as the fundamental cause that generates the noise phenomenon. On the other hand lies the sensing or perceiving element which can be a human being or an instrument.

In between source and sensor, there is the so-called ambient, the medium that connects them. From the point of view of our discussion, the characteristics of this system can be divided into two groups. Parameters that are independent of time are called passive parameters. The passive parameters of the system determine the ability of the system to respond to outside interference. These parameters are determined by the geometry, materials and conditions of the system or its components. The active parameters include physical phenomena that vary with time and influence the passive parameters. In Fig. 2.1, a block is designated to each system parameters.

Arrows interconnecting the blocks indicate the casual relations and the process flow. At the starting point of the system, there are the causes which give rise through complex interactions to exciting forces. Owing to the harmonic or at least periodic nature of the generated exciting forces, applying Fourier series, they can be handled as the sum of numerous sinusoidal waves. Any exciting force can be characterized by its amplitude, mode number (vibration mode), frequency and angular position. These exciting forces act on the machine which is seen as a mechanical passive system capable of vibrating, and gives rise to the vibratory motion.

The vibrating capability of the electronic machine can be thought of as a transfer parameter of the system, since the exciting force applied at the input produces vibration at the output of the mechanical system. The vibrating capability of the machine is a function of two parameters, namely the mode number and the frequency. At least one natural frequency of the machine corresponds to each vibration mode. Of course, a dangerous situation arises where the frequency of the

Passive system parameters

Active system parameters (physical phenomena)
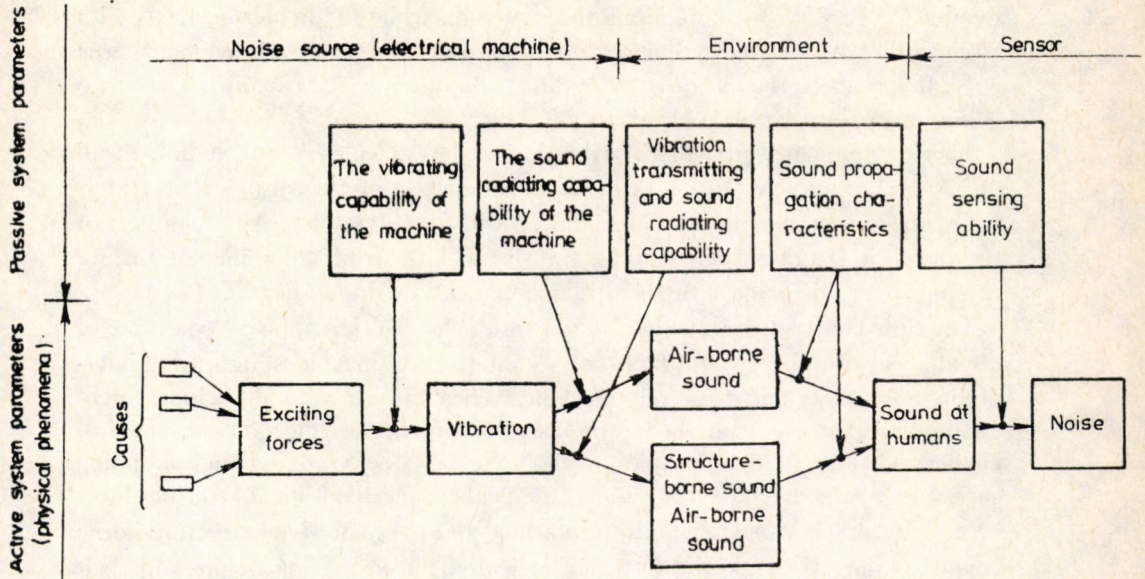
Fig. 2.1. Noise generation by the electrical machine

periodic exciting force is identical with or close to one of the natural frequencies of the machine.

Part of the vibrational energy within the audible range transforms into sound energy. The "efficiency" of this transformation depends on the radiating ability of the machine, which is, in turn, dependent on the mode number and the frequency. The radiation factor appears as a term in the equation describing the sound radiating capability of the machine. The sound power arises over the machine surface only after the above transformation.

The acoustic properties of the surroundings determine the amount of this power transmitted to the observer and the means. The end point of the process is human hearing which comprises two parts. One is the ear with its frequency transfer characteristic dependent on frequency, loudness and exposure time, and the second one is the state of the mind.

Now, on the subject of the human mind, we can introduce the concept of noise, or rather the concept of so-called airborne noise. Until now, we have implicitly assumed that the machine is not coupled mechanically with its ambient. In reality, however, there is mechanical connection or coupling, between the machine and the surroundings through the base plate, support or shaft, or through the vibration damper itself. The major part of the vibrational energy of the audible range is transmitted to the surroundings in the form of structure-borne sound. The trans-

mission process is spreading along the structure, while the lighter elements with large surface area act as secondary radiators, so the end-product is again airborne noise that adds to the airborne noise directly emitted by the machine. These two components together make up the noise itself.

The low-frequency part of the vibrational energy, which is not audible at all ($f < 30$ Hz) or audible but with considerable damping by the ear ($f < 1000$ Hz), is called the vibration of the machine and we will treat it as such. Although part of the energy in the range below 30 Hz transforms into air pressure fluctuations, we can pass over this point in further discussion, since we do not hear it.

The flow chart shown in Fig. 2.1 illustrates the multidisciplinary character of the analysis of noise generating processes in electrical machines, indicating interdisciplinary areas and their relationships. When the causes and exciting forces are investigated, we need the knowledge of experts in electrotechnics, mechanical engineering and fluid mechanics, while to assess the vibrating and radiating capability of the machine as a system, the fields of mechanics and acoustics must be employed. The transmission of vibrations and the analysis of structure-borne sounds require the expertise of a mechanical engineer and an architect in their study. The acoustical field is analysed by an acoustical engineer while the investigation of human response and behaviour is a medical task.

Thus it is obvious that noise analysis is a very complex activity, and effective cooperation of numerous disciplines is needed to solve problem of noise reduction.

The mental process illustrated in Fig. 2.1 provides useful assistance in identifying the casual and quantitative relations for noise analysis, highlighting the physical phenomena involved to aid comprehension. A flow chart or process block diagram has many didactical advantages for both educational and industrial purposes. It is useful for the engineer as it develops views about the system structure concerned. The dominant exciting forces, vibration and noise components are obvious at first sight, and not only are the steady-state conditions seen but also the transient characteristics.

The third, and perhaps most important, advantage of the flow chart shown in Fig. 2.1 is the easy identification of the tasks regarding noise reduction. It is evident, as it is from an engineer's common-sense, that the first thing to do when dealing with vibration and noise reduction is to identify and then eliminate the causes, or at least to reduce them below acceptable limits. If the causes cannot be eliminated as required for whatever reasons, then the passive parameters of the machine (e.g., vibrating and radiating capacity) must be mismatched. If this is not the best solution for technical, economical or other reasons, then we have to turn to the last, costly solution, one of designing a vibration damping and noise insulating enclosure as an after-measure to control noise. If none of the above solutions is

feasible, or they cannot provide the required reduction in noise, then finally, the personnel must be protected directly and individually. The technical measures that can be taken to reduce noise level will be discussed in detail later.

2.2 Classification of causes of vibration and noise

The various causes of vibration and noise in electrical machines arise unequally in vibration and noise generation. The basic function of an electrical machine is to transform energy. Certain factors connected with the generation of the electromagnetic field cause noise production (e.g. winding configuration and arrangement, saturation effects, the fluctuation in permeance due to air gap, slotting and eccentricity). These factors give rise to measurable mechanical deformations and vibrations, and only a fraction of the vibrational energy is transformed into sound energy. This process can be followed in Fig. 2.2 where causes of electromagnetic origin, denoted by *Em*, are shown.

All the other components of the electrical machine can be thought of as parts assisting in the energy transformation process with indirect function. In this group we can class bearings of rotating machines (marked *M*1 in Fig. 2.2), which allow changes in the relative position of stator and rotor windings; the sliding contacts
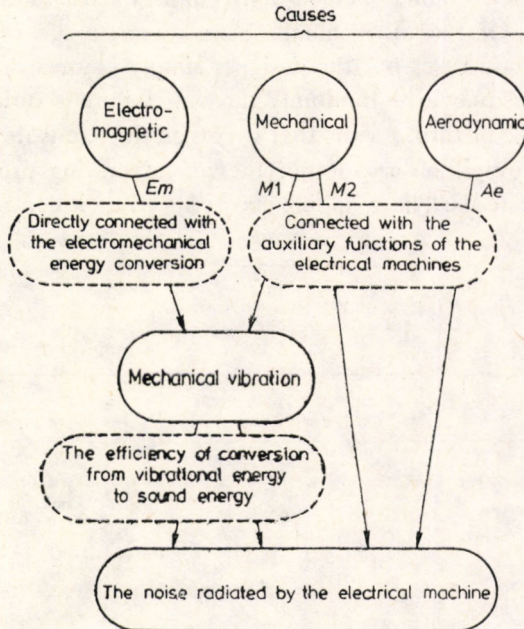
Fig. 2.2. The relationship between noise and vibration of electrical machines

(*M2*) that provide the electrical link between the moving coil and the stationary circuit through the commutator or slip rings; the fan and the ventilation duct system (*Ae*) which is designed to vent the excessive heat developed owing to losses in the electrical machine. Some of these auxiliary elements, like the bearings, give rise to substantial mechanical vibrations of the machine because of their inherent geometrical defects of random nature.

Type *M2* mechanical causes of noise are characterized by the low weight of the oscillating brushes which, owing to their flexible mounting, hardly produce any noticeable vibration of the machine body or housing. These sliding contacts contribute directly to the sound generation without involvement of the machine mass, just as in the case of noises of aerodynamic origin, which are not detectable in the vibration of the electrical machine.

The ease of control of the many sources of noise varies substantially for each cause. Let us examine this by considering an asynchronous machine. The frequency and amplitude of slot and winding harmonics arisen from slotting are controlled by the designer. The correct slot number combination and the frequency and amplitude of winding and slot harmonics for a given standard machine size can be predicted at a given load and material quality. An upper limit can be specified for the dynamic unbalance of the rotor in the manufacturing procedure and compliance can be checked by Quality Control. Of course, the technological procedure specifies only a tolerance limit, but below this limit, the true unbalance of the rotor can lie anywhere. On the other hand, there are certain causes whose effect is predictable in certain cases but the designer simply ignores them in the calculations. These causes may arise randomly through failure to observe technological requirements. This, in turn, means that they can be controlled within realistic tolerance limits by rigid observation of the manufacturing procedure and using precision machine tools. The grouping according to their controllability is shown in Fig. 2.3.
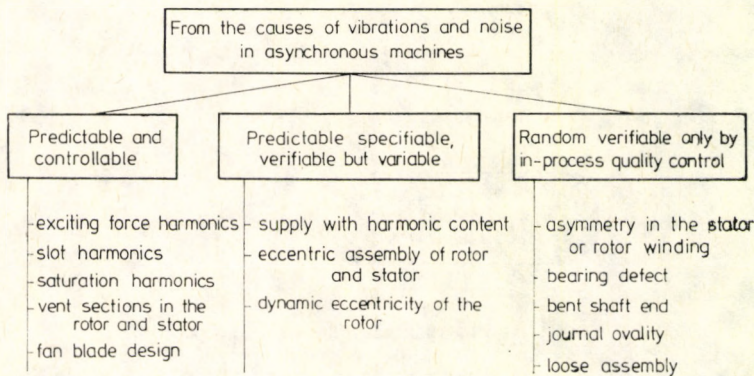
Fig. 2.3. Classification of the causes of noise in asynchronous machines on the basis of their controllability

3. CAUSES OF ELECTROMAGNETIC NOISE
AND VIBRATION

3.1 Asynchronous motor

3.1.1 Theory of the development of flux in the air gap

The main task in creating electromechanical energy conversion by asynchronous machine is to get a rotating sinusoidal magnetic field with pole number 2p. In machines of standard construction, the magnetic flux in the air gap is induced by the current flowing through the conductors in the slots.

Slotting has two consequences. First, the magnetomotive force (mmf) is staggered round the circumference, and consequently the mmf wave has a strong harmonic content superposed on the fundamental. Secondly, the slots, in particular the open slots, break up the uniformity of the air gap round the circumference, and the gap, which represents almost the total reluctance of the magnetic circuit, will change periodically as the relative position of the stator and the rotor changes. The local maximum and minimum values of permeance correspond to tooth-faces-tooth and slot-faces-slot situations, respectively. The total magnetizing current of an asynchronous machine is supplied from the mains, and therefore the air gap is designed to be as small as possible. In this case, however, even the smallest deviation of the air gap from the shape of a cylindrical sleeve of uniform thickness will result in considerable relative distortion of air gap permeance. The eccentricity of the rotor and iron saturation will also give rise to permeance harmonics. The air gap flux density harmonics induce periodic exciting forces which act on the mechanical system of the machine. Figure 3.1 illustrates the generating process of exciting forces of electromagnetic origin. The rotor and stator are both slotted and operate in complex magnetic interaction, therefore we will determine the order, frequency and amplitude of composing harmonics first. In order to comprehend the problem itself and then its solution, it is worthwhile following the process of how the flux density distribution is established in the air gap, as shown in Fig. 3.2, where the block diagram only outlines the infinite cycle without being readily suitable for the development of an algorithm for computation.

In the stator of a symmetrical unsaturated three-phase machine (i.e., with identical phase windings of symmetrical arrangement, fed from a symmetrical mains supply of voltage U_{sup} and free of harmonics, uniform and constant air gap), there is a symmetric current system of angular frequency ω_1, assuming, for the

Causes	Phenomena	Modelling the electromagnetic phenomenon

Mechanical	Electromagnetic

Laminated core slotting

Eccentric stator-bore with respect to the rotor

Elliptic stator-bore

Elliptical rotor surface

Unbalanced rotor

Heterogeneous material

Static eccentricity

Dynamic eccentricity

Stepped m.m.f. curve → m.m.f. harmonics

Non-uniform cross-section of the pole flux path, local saturation → Saturation harmonics

The magnetic permeance of the air gap varies periodically round the periphery because $\delta \neq$ constant → Slot harmonics

Eccentricity harmonics

Exciting forces

Fig. 3.1. The influence diagram of exciting force generation of electromagnetic origin

time being, that only fundamental currents are present. This current lags on the voltage by a given phase angle. All three phase currents set up an m.m.f. varying with time, staggered round the circumference, so in addition to the funda-mentals of pole pair number p, space harmonics of pole pair number μp will be produced as well. The alternating m.m.f. established by the three phase wind-ings make up a rotating m.m.f., but the permeance of the air gap is not uniform. It is altered by slotting, saturation and rotor position. The former is called the m.m.f. wave, the latter, the permeance wave. All the m.m.f. waves interact with the constant term of the permeance, and excite the stator fundamental wave and the winding flux density harmonics. The pole pair number of these equals the pole pair number of the m.m.f. waves. In addition, all the m.m.f. waves interact with each permeance wave, inducing further flux density waves of pole number and frequency equal to the sum or difference of the corresponding orders of the stator m.m.f. and permeance waves. This infinite series of flux density waves (Σb_μ), passing through the air gap, acts on the rotor winding (squirrel-cage), inducing in it voltages having identical order of harmonics. The induced voltages drive currents in the closed rotor circuit, depending on the impedance of rotor winding. This impedance is a function of, among others, the frequency, the number of turns (or, for squirrel-cage motors, the number of slots), the permeability of iron, the shape of the slots, etc. Owing to the rotor slotting, each of the above cur-
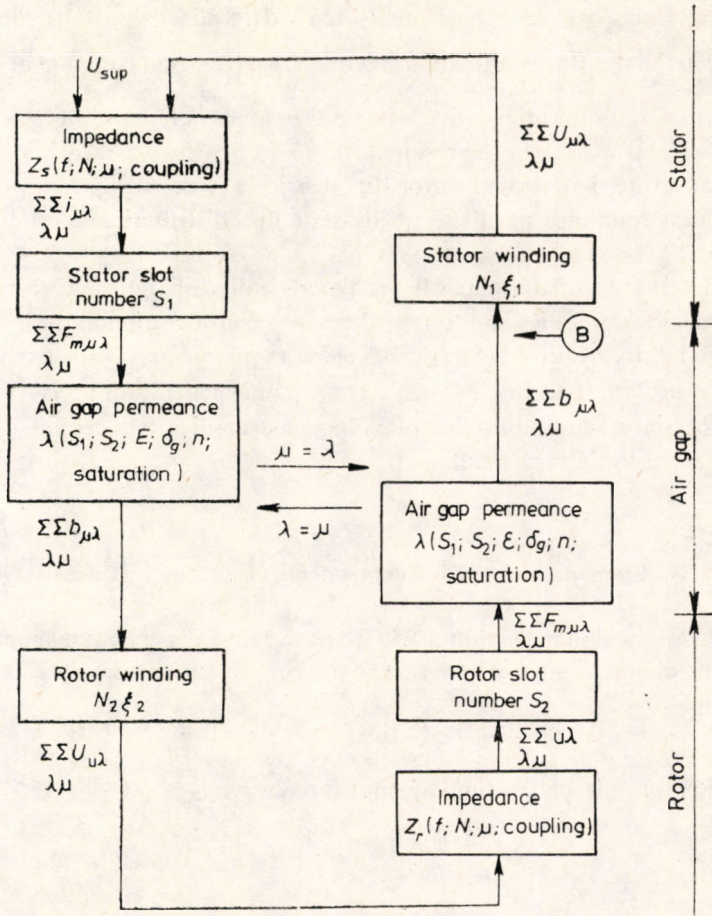
Fig. 3.2. The building-up of the air gap field in asynchronous machines

rents gives rise to m.m.f. waves having mode number $\lambda \left(\sum_{\lambda} \sum_{\mu} F_{m\mu\lambda} \right)$ that contains a theoretically infinite excitation number harmonics. As a result of interaction between the m. m. f. waves and the permeance waves of the air gap, a new set of flux density waves is generated $\left(\sum_{\lambda} \sum_{\mu} b_{\mu\lambda} \right)$. Out of these flux density waves, those with order equal to that of the stator flux density waves ($\lambda = \mu$) react on the corresponding stator flux density harmonics (armature reaction). The remaining waves are called residual rotor flux density waves. These residual rotor fields induce voltage again in the stator windings, with frequency different from that of the network frequency. For these voltages, the stator circuit is virtually short-circuited

via the supply network, and therefore currents determined by stator impedance Z_s will flow in the winding conductors. Of course, each current component $\sum_\lambda \sum_\mu i_{\mu\lambda}$

flowing in the stator windings gives rise to new m.m.f. harmonics a part of which (when $\lambda = \mu$) reacts on the residual rotor flux density waves, while the other part will constitute the residual stator flux density waves.

This process continues until the steady-state flux distribution is established in the air gap.

It is unnecessary to determine all the theoretically infinite number of steady-state flux density harmonics and to take them into consideration in the calculation of the radial force. Even the most stringent requirements are satisfied by an analysis that according to Fig. 3.2 neglects harmonic generation processes following letter B, since the amplitudes of voltage harmonics induced in the stator windings are generally very small.

3.1.2 Computing the radial components of air gap flux density

Based on the discussion in Section 3.1.1, space and time dependent magnetomotive forces arising along the air gap of asynchronous motors can be classified as follows:

$$\bar{F}_m(x, t) = \bar{F}_{m1p}(x, t) + \bar{F}_{m1}(x, t) + \bar{F}_{m2}(x, t) + \bar{F}_{m2', 1}(x, t). \tag{3.1}$$

The complex formula of the fundamental force wave is:

$$\bar{F}_{m1_p}(x, t) = \frac{S_1 z_s \sqrt{2} I_m \xi_p}{2p\pi} e^{j(px - \omega_1 t - \varphi_m)} = F_{m1_p} e^{j(px - \omega_1 t - \varphi_m)}, \tag{3.2}$$

where S_1 — stator slot number,
$\quad z_s$ — number of conductors in one slot,
$\quad I_m$ — no-load stator current,
$\quad p$ — number of pole pairs,
$\quad \varphi_m$ — phase angle of no-load current,
$\quad \xi_p$ — winding factor for the first harmonic wave,
$\quad x$ — space coordinate in radians round the circumference of bore.

The complex Fourier series of stator m. m. f. space harmonics is:

$$F_{m1}(x, t) = \sum_\mu F_{m1p} \frac{I_1}{I_m} \frac{\xi_\mu}{\xi_p} \frac{1}{\mu} \cdot \frac{\Sigma F_m}{F_{m\,\text{airgap}}} e^{j(\mu px - \omega\, t - \psi_\mu)} =$$

$$= \sum_\mu F_{m\mu} e^{j(\mu px - \omega_\mu t - \psi_\mu)}, \tag{3.3}$$

where $\mu = 2mg + 1$ — the order of the space harmonics,

$\omega = \omega_1$,

$\psi = \varphi_1$,

m — number of phases,

$g = 0, \pm 1, \pm 2, \ldots$

For a squirrel-cage rotor, the complex Fourier series of rotor m. m. f. space harmonics (induced by current I_2 with frequency sf_1) is written as:

$$\bar{F}_{m_2}(x, t) = \sum_\lambda -(-1)^g \frac{\sqrt{2}mI_1 \cos \varphi_1 N_1 \xi_p \xi_\lambda}{p\lambda\pi} e^{j(\lambda px - \omega_\lambda t - \psi_\lambda)} =$$

$$= \sum_\lambda F_{m_2} e^{j(\lambda px - \omega_\lambda t - \psi_\lambda)}, \tag{3.4}$$

where $\lambda = \frac{gS_2}{p} + 1$ — the order of the rotor space harmonics,

$\quad I_1$ — stator current,

$\quad \varphi_1$ — phase angle of stator current,

$\quad N_1$ — number of turns per stator phase,

$\quad \xi_\lambda$ — winding factor for the λth harmonic,

$$\omega_\lambda = \omega_1 \left(\frac{gS_2}{p} (1-s) + 1 \right), \quad \psi_\lambda = \varphi_1 + \tan^{-1} \frac{\frac{I_m}{I_{sc}} s_{max}}{s},$$

where s_{max} — slip belonging to maximum torque,

$\quad s$ — slip,

$\quad I_{sc}$ — short-circuit current,

$\quad S_2$ — rotor slot number.

For a wound slip ring rotor, the m. m. f. harmonics can be calculated in a similar way to the stator. The complex Fourier series of m. m. f. space harmonics produced by current time harmonics flowing in the rotor wires is found to be:

$$\bar{F}_{m2, 1}(x, t) = \sum_{\lambda\mu} F_{m\lambda\mu} e^{j(\lambda_\mu px - \omega_{\lambda\mu} t - \psi_{\lambda\mu})}, \tag{3.5}$$

where $\lambda_\mu = \frac{gS_2}{p} + \mu$,

$$\omega_{\lambda\mu} = \omega_1 \left[\frac{gS_2}{p} (1-s) + 1 \right],$$

$$\psi_{\lambda\mu} = \varphi_1 + \tan^{-1} \frac{\frac{I_m}{I_{sc}} s_{max}}{s}.$$

For the permeance, slotting, eccentricity and saturation harmonics are taken into account:

$$\bar{G}_m(x, t) = \bar{G}_{mo} + \bar{G}_{m_1}(x) + \bar{G}_{m_2}(x, t) + \bar{G}_{m_{12}}(x, t) + \bar{G}_{m_e}(x, t) + \bar{G}_{m_{sat}}(x, t) \quad (3.6)$$

The mean permeance of the air gap is calculated by using a larger air gap in the formula, obtained as a product of the real air gap and the two Carter factors k_c for stator and rotor, respectively:

$$G_{mo} = \frac{\mu_0}{\delta_g k_{c1} k_{c2}}. \quad (3.7)$$

For a smooth rotor, the complex Fourier series of permeance harmonics due to stator slotting is:

$$\bar{G}_{m_1}(x) = G_{mo} k_{c1} \sum_{g=1}^{\infty} -(-1)^g \frac{\sin g\pi}{g\pi} \frac{2(k_{c1}-1)}{k_{c1}} e^{jgS_{1x}}. \quad (3.8)$$

For a smooth stator, the complex Fourier series of permeance space harmonics due to rotor slotting is expressed as:

$$\bar{G}_{m_2}(x, t) = G_{mo} k_{c2} \sum_{g=1}^{\infty} -(-1)^g \frac{\sin g\pi}{g\pi} 2 \frac{k_{c2}-1}{k_{c2}} e^{jgS_2(x-\omega t)}. \quad (3.9)$$

The permeance wave $\bar{G}_{m_{12}}$ due to double slotting is negligible compared with the other waves, so we will no longer take it into account. The first harmonic term of the complex Fourier expansion of the permeance wave due to eccentricity is found to be:

$$\bar{G}_{m_e}(x, t) = \frac{\mu_0 e}{\delta_g^2 k_{c1}^2 k_{c2}^2} e^{j(x-\omega_e t - \psi_e)}, \quad (3.10)$$

where

$$\omega_e = \begin{cases} e \text{ — eccentricity,} \\ 0 \text{ — for static eccentricity,} \\ \dfrac{\omega_1}{p}(1-s) \text{ — for dynamic eccentricity.} \end{cases}$$

The first harmonic term of the Fourier series of the permeance wave due to saturation is:

$$\bar{G}_{m_{sat}}(x, t) = -\frac{G_{mo}\delta_s}{\delta_g k_{c1} k_{c2}} \left(\frac{F_{mairgap}}{\Sigma F_m}\right)^2 e^{j(2px-2\omega_1 t - 2\varphi_m)}, \quad (3.11)$$

where δ_s is the virtual air gap increase that affects the air gap flux density to the same extent as saturation.

The air gap flux density is given by the following product:

$$\bar{B}(x, t) = \bar{F}_m(x, t) \bar{G}_m(x, t).$$

From eqns (3.1) and (3.6), the product consists of $4 \times 6 = 24$ terms, but for practical purposes it is enough to consider the following.

The product of the fundamental m. m. f. and the constant term of the permeance gives the fundamental air gap flux density. Combining eqns (3.2) and (3.7), we obtain the following complex formula:

$$\bar{B}_{1p}(x, t) = G_{mo}\bar{F}_{m1_p}(x, t) = B_{1p}e^{j(px - \omega_1 t - \varphi_m)}.$$

The instantaneous value of the fundamental flux density wave is given by the real part of the complex wave expression, that is:

$$b_{1p}(x, t) = B_{1p}\cos(px - \omega_1 t - \varphi_m), \tag{3.12}$$

where the amplitude is $b_{1p} = G_{mo}F_{m1_p}$.

The term $G_{mo}[\bar{F}_{m_1}(x, t) + \bar{F}_{m_2}(x, t) + \bar{F}_{m_{21}}(x, t)]$ defines the so-called excitation harmonics of the air gap flux density.

The Fourier series of the stator winding harmonics is:

$$\bar{B}_1(x, t) = G_{mo}\bar{F}_{m_1}(x, t).$$

Using a w subscript to mark the parameters (w stands for winding), the instantaneous value of the μ_wth harmonic is found to be:

$$\bar{B}_{\mu w}(x, t) = B_{\mu w}e^{j(\mu_w px - \omega_{\mu w} t - \psi_{\mu w})}.$$

In view of the fact that the Fourier series has been established in such a way that the real part of its terms gives the corresponding harmonic Fourier terms, the formula that provides the instantaneous value of any of the stator winding harmonics is:

$$b_{\mu w}(x, t) = B_{\mu w}\cos(\mu_w px - \omega_{\mu w} t - \psi_{\mu w}). \tag{3.13}$$

In a similar way, any term of the complex Fourier series of any other harmonic may be rewritten in the form of a harmonic Fourier series. The order, frequency and phase angle are covered by eqn. (3.3).

The amplitude is expressed as:

$$B_{\mu w} = G_{mo}\bar{F}_{m_n}.$$

The Fourier series of rotor winding harmonics can be written as:

$$\bar{B}_2(x, t) = G_{mom}\bar{F}_2(x, t).$$

For a squirrel-cage rotor, the instantaneous value of harmonic with order λ_t is obtained by combining eqns (3.4) and (3.7):

$$\bar{B}_{\lambda w}(x, t) = B_{\lambda w}e^{j(\lambda_w px - \omega_{\lambda w} t - \psi_{\lambda w})}, \tag{3.14}$$

where

$$B_{\lambda w} = G_{mo}F_{m_\lambda}.$$

The order, frequency and phase angle are covered by eqn. (3.4).

The Fourier series of the residual field of rotor current harmonics is:

$$\bar{B}_{21}(x, t) = G_{mo}\bar{F}_{m21}(x, t).$$

The instantaneous value of the λ_μth flux density harmonic from eqn. (3.5) is:

$$\bar{B}_{\lambda\mu}(x, t) = B_{\lambda\mu}e^{j(\lambda_\mu px - \omega_{\lambda\mu}t - \omega_{\lambda\mu})},$$

$$b_{\lambda_{\shortparallel}}(x, t) = B_{\lambda\mu}\cos(\lambda_\mu px - \omega_{\lambda\mu}t - \psi_{\lambda\mu}). \tag{3.15}$$

The amplitude is:

$$B_{\lambda_{..}} = -(-1)^g\sqrt{2}I_{..}\frac{\mu}{\lambda_\mu}\xi_{\lambda_\mu}G_{m\mu}.$$

The formula for the calculation of harmonic ring currents $I_{r\mu}$ is given in ref. [58], where Jordan *et al.* use the stator winding and slotting flux density harmonics to determine the rotor current harmonics, also taking into account the angle of skew of slots and magnetic leakage. The following formula describes the permeance waves of air gap flux density:

$$\bar{F}_{m1p}(x, t)[\bar{G}_{m_1}(x) + \bar{G}_{m_2}(x, t) + \bar{G}_{m_e}(x, t) + \bar{G}_{m_{sat}}(x, t)].$$

The Fourier series of stator slot harmonics is expressed as:

$$\bar{B}_{\mu s}(x, t) = \bar{F}_{m1_p}(x, t)\bar{G}_{m_1}(x).$$

If the multiplication is done with complex variables, the complex series of $B_{\mu s}(x, t)$ is obtained:

$$\bar{B}_{\mu s}(x, t) = \frac{1}{2}[\bar{F}_{m1_p}(x, t)\bar{G}_{m_1}(x) + \bar{F}_{m1_p}(x, t)\bar{G}^*_{m_1}(x)],$$

so

$$\bar{B}_{\mu s}(x, t) = \sum_{\mu s}B_{\mu s}e^{j(\mu_s px - \omega_1 t - \varphi_m)},$$

where $$b_{\mu s}(x, t) = B_{\mu s}\cos(\mu_s px - \omega_1 t - \varphi_m), \tag{3.16}$$

$$\mu_s = 6g_1q_1 + 1, \quad q_1 = \frac{S_1}{2pm}.$$

The amplitude of stator slot harmonics is expressed as:

$$B_{\mu s} = -(-1)^{g_1}B_{1p}(k_{c1} - 1)\xi_{\mu s},$$

where

$$\xi_{\mu s} = \frac{\sin g_1\dfrac{k_{c1}-1}{k_{c1}}\pi}{g_1\dfrac{k_{c1}-1}{k_{c1}}\pi}.$$

The Fourier series of rotor slot harmonics is:

$$\bar{B}_{\lambda s}(x, t) = \bar{F}_{m_{1p}}(x, t)\bar{G}_{m_2}(x, t).$$

Using the complex formula:

$$\bar{B}_{\lambda s}(x, t) = \frac{1}{2}[\bar{F}_{m_{1p}}(x, t)\bar{G}_{m_2}(x, t) + \bar{F}_{m_{1p}}(x, t)\bar{G}_{m_2}^*(x, t)],$$

$$\bar{B}_{\lambda s}(x, t) = \sum_{\lambda s} B_{\lambda s} e^{j(\lambda_s px - \omega_{\lambda s} t - \psi_{\lambda s})},$$

$$(3.17)$$

$$b_{\lambda s}(x, t) = B_{\lambda s} \cos(\lambda_s px - \omega_{\lambda s} t - \psi_{\lambda s}).$$

λ_s and $\omega_{\lambda s}$ are consequently equal to λ and ω_λ in eqn. (3.4), respectively.
    The phase angle: $\psi_{\lambda s} = \varphi_m$.

    The amplitude: $B_{\lambda s} = -(-1)^{g_2} B_{1p}(k_{c2} - 1)\xi_{\lambda s}$,
where

$$\xi_{\lambda s} = \frac{\sin g_2 \dfrac{k_{c2} - 1}{k_{c2}} \pi}{g_2 \dfrac{k_{c2} - 1}{k_{c2}} \pi}.$$

The angular frequencies of winding and slotting harmonics are identical, while the set of winding harmonic orders also contains the orders of the slotting harmonics. Slotting and winding harmonics appear simultaneously when the ratio g/q is an integer. The two field components have different phase angles, and so the rules of vector addition must be applied for the stator and rotor separately. The angular frequency of the resultant harmonic will be the same.
    The eccentricity flux density harmonic is found to be:

$$\bar{B}_{\mu e}(x, t) = \bar{F}_{m_{1p}}(x, t)\bar{G}_{m_e}(x, t).$$

Using the complex version of eqns (3.2) and (3.10) and assuming a parallel displacement of the rotor axis, we find [52]:

$$\bar{B}_{\mu e}(x, t) = \frac{1}{2}[\bar{F}_{m_{1p}}(x, t)\bar{G}_{m_e}(x, t) + \bar{F}_{m_{1p}}(x, t)\bar{G}_{m_e}^*(x, t)] =$$

$$= B_{\mu e} e^{j(\mu_e px - \omega_{\mu e} t - \varphi_{\mu e})},$$

$$b_{\mu e}(x, t) = B_{\mu e} \cos(\mu_e px - \omega_{\mu e} t - \varphi_{\mu e}), \qquad (3.18)$$

where

$$B_{\mu e} = B_{1p} \frac{e}{2\delta_0},$$

$$\mu_e = 1 \pm \frac{1}{p},$$

$$\omega_{\mu e} = \omega_1 \pm \omega_e,$$

$$\varphi_{\mu e} = \varphi_m \pm \varphi_e.$$

The flux density harmonic originating from saturation is given by

$$\bar{B}_{\mu \text{sat}}(x, t) = \bar{F}_{m1_p}(x, t) \bar{G}_{m\text{sat}}(x, t).$$

Using the complex form of the factors, the following formula is obtained:

$$\bar{B}_{\mu \text{sat}}(x, t) = \frac{1}{2}[\bar{F}_{m1_p}(x, t)\bar{G}_{m\text{sat}}(x, t) + \bar{F}_{m1_p}(x, t)\bar{G}^*_{m\text{sat}}(x, t)] =$$

$$= -\frac{1}{2}\frac{\mu_0}{\delta_0} F_{m1_p} \frac{\delta_s}{\delta_0} e^{j[(1\pm 2)px - (1\pm 2)\omega_1 t - (1\pm 2)\varphi_m]}.$$

Note that apart from the flux density harmonic of order $3p$, a fundamental of order $-p$ is also produced. The flux density harmonic of order $3p$ due to saturation is found to be:

$$\bar{B}_{\mu \text{sat}}(x, t) = -B_{\mu \text{sat}} e^{j(3px - 3\omega_1 t - 3\varphi_m)},$$

$$b_{\mu \text{sat}}(x, t) = B_{\mu \text{sat}} \cos (3px - 3\omega_1 t - 3\varphi_m), \qquad (3.19)$$

$$B_{\mu \text{sat}} = \frac{F_{m_t}}{3(F_{m1_p} + F_{m_y})} B_{1p}.$$

where F_{m_t} — the m. m. f. on the tooth,

F_{m_y} — the m. m. f. on the yoke.

To analyse the residual rotor field due to saturation and eccentricity, we have to return to the rotor and the residual flux density waves. We saw that the flux density harmonics of any origin in the air gap induce harmonic currents in the rotor, which in turn react on the field that has induced them and give rise to the undamped residual field of the rotor.

An air gap flux density harmonic:

$$\bar{B}_\mu(x, t) = B_\mu e^{j(\mu px - \omega_\mu t - \psi_\mu)}$$

of any origin will produce a rotor m. m. f. according to eqn. (3.5).

On this m. m. f.

$$\bar{B}_{\lambda \mu}(x, t) = B_{\lambda \mu} e^{j(\lambda_\mu px - \omega_{\lambda \mu} t - \psi_{\lambda \mu})}$$

flux density harmonics are produced.

As above, we again consider the flux density harmonics due to eccentricity (3.18) and saturation (3.19).

The residual field due to eccentricity is:

$$\bar{B}_{\lambda e}(x, t) = \sum_{\lambda e} B_{\lambda e} e^{j(\lambda_e px - \omega_{\lambda e} t - \psi_{\lambda e})},$$

$$b_{\lambda e}(x, t) = B_{\lambda e} \cos (\lambda_e p x - \omega_{\lambda e} t - \psi_{\lambda e}). \tag{3.20}$$

Based on eqns (3.5) and (3.18), the order is:

$$\lambda_e = \frac{g_2 S_2}{p} + \mu_e = \frac{g_2 S_2}{p} + \left(1 \pm \frac{1}{p}\right),$$

the angular frequency:

$$\omega_{\lambda e} = \omega_{\mu e} + \frac{g_2 S_2}{p} (1-s)\omega_1,$$

the phase angle:

$$\psi_{\lambda e} = \varphi_{\mu e} + \tan^{-1} \frac{\dfrac{I_m}{I_{sc}} S_{max}}{s}.$$

The residual flux density field due to saturation is:

$$\bar{B}_{\lambda sat}(x, t) = \sum_{\lambda s} B_{\lambda sat} e^{j(\lambda_{sat} p x - \omega_{\lambda sat} t - \psi_{\lambda sat})},$$

$$b_{\lambda sat}(x, t) = B_{\lambda sat} \cos (\lambda_{sat} p x - \omega_{\lambda sat} t - \psi_{\lambda sat}), \tag{3.21}$$

where

$$\omega_{\lambda sat} = \omega_1 \left[3 + \frac{g S_2}{p} (1-s)\right], \quad \lambda_{sat} = \frac{g_2 S_2}{p} + 3,$$

$$\psi_{\lambda sat} = 3\varphi_m + \tan^{-1} \frac{\dfrac{I_m}{I_{sc}} S_{max}}{s}.$$

For squirrel-cage and slip ring machines, the calculation of $B_{\lambda e}$ and $B_{\lambda sat}$ is covered in ref. [29].

In Fig. 3.2, it can be seen that the rotor reacts back on the fundamental wave and on the harmonic field of the stator. The reaction on the fundamental wave has been taken into consideration by using the magnetizing current in eqn. (3.2) to calculate the fundamental m. m. f. The damping effect of the rotor on the resultant of winding and slotting harmonics of the stator can be covered by multiplying the flux density amplitude by a damping factor [53].

The resultant of the air gap flux density is made up from the fundamental and the stator and rotor harmonics:

$$b(x, t) = b_{1p}(x, t) + \sum_{\mu} b_{\mu}(x, t) + \sum_{\lambda} b_{\lambda}(x, t). \tag{3.22}$$

In many cases it is practical to break down $\sum b_{\lambda}$ to the sum of the groups of winding, slotting and eccentricity harmonics. From the flux density harmonics derived above in this chapter the harmonics originating from double slotting, saturation and rotor harmonic currents can be neglected according to the literature [54], [120] and the results of practical noise research.

3.1.3 Deformational force waves of electromagnetic origin and modifying effects

According to Maxwell's equation, the tensile stress on the stator bore and rotor cylinder surface, i.e., the magnitude of the radial force, is proportional to the square of the normal component of the air gap flux density:

$$p(x, t) = \frac{b^2(x, t)}{2\mu_0} = \frac{1}{2\mu_0} \left[b_{1p}^2 + 2 \left(\sum_\mu b_{1p} b_\mu + \sum_\lambda b_{1p} b_\lambda \right) + \sum_\mu b_\mu^2 + \sum_\lambda b_\lambda^2 + \right.$$

$$\left. + 2 \left(\sum_{\mu 1 < \mu 2} b_{\mu 1} b_{\mu 2} + \sum_{\lambda 1 < \lambda 2} b_{\lambda 1} b_{\lambda 2} + \sum_{\mu \lambda} b_\mu b_\lambda \right) \right]. \tag{3.23}$$

The Maxwell tensile stresses comprise three groups of the infinite number of radial force waves. The squares of stator flux density waves produce force waves in the 0 to 100 Hz frequency range, which are uninteresting from the acoustical point of view. However, the 100 Hz force wave must be considered in the vibration calculations. The product of stator fundamental b_{1p} and the first harmonic of eccentricity origin, $b_{\mu e}$, generates the unbalanced magnetic tensile force with angular frequency ω_e, which received detailed coverage elsewhere in the literature (Hasse, Kovács, and Jordan [39], Schuisky [98]). We will also return to this subject at a later stage. The rotor and stator waves multiplied by themselves are also of no interest in terms of acoustics and vibrations because the mode number of the force waves is high and the amplitude is negligibly small. It is the interaction of rotor and stator waves which is really important to us. Any component of the force wave induced by this interaction, acting over unit area, may be written in the following form:

$$p_r(x, t) = P_r \cos (rx - \omega_r t - \psi_r), \tag{3.24}$$

where the mode number of the force wave is expressed as $r = (\mu_i \pm \lambda_j)p$. The negative sign means that the fundamental and harmonic force waves rotate in opposite directions.

The angular frequency: $\omega_r = \omega_{\mu i} \pm \omega_{\lambda j}$,

The phase angle: $\psi_r = \psi_{\mu i} \pm \psi_{\lambda j}$,

The amplitude: $P_r = \frac{B_{\mu i} B_{\lambda j}}{2\mu_0}$.

As mentioned before, the extent of deformation and noise becomes excessive when the frequency of the exciting force f_r is close or equals to one of the natural frequencies of the machine. This coincidence which results in the phenomenon of resonance can occur under steady-state running condition at working speed but

also in transient operation. If we look at the formula of angular frequency in the force wave equation (3.24), we find the following frequencies:

— If the mixed product of stator and rotor winding space harmonics is concerned then:

$$f_r = f_1 \left[\frac{gS_2}{p} (1-s) + \genfrac{<}{.}{0pt}{}{2}{0} \right]. \tag{3.25}$$

— If the mixed product of stator winding and rotor eccentricity space harmonics is concerned then:

$$f_r = f_1 \left[\frac{gS_2}{p} (1-s) + \genfrac{<}{.}{0pt}{}{2}{0} \pm \genfrac{<}{.}{0pt}{}{0}{(1-s)/p} \right]. \tag{3.25a}$$

— If the mixed product of stator winding and rotor saturation harmonics is concerned then:

$$f_r = f_1 \left[\frac{gS_2}{p} (1-s) + \genfrac{<}{.}{0pt}{}{4}{2} \right]. \tag{3.25b}$$

The two choices within the square brackets (2 or 0 and 4 or 2) indicate whether the arguments were added or subtracted for the harmonics determined by multiplying the flux density harmonic components. The 0 or $(1-s)/p$ choice in eqn. (3.25a) covers the cases of static or dynamic eccentricity.

Both (3.25) and (3.25a and b) indicate that the frequency of the exciting force is directly proportional to the speed of the machine. When the machine does not rotate ($s=1$), the frequency is 0, $2f_1$ or $4f_1$, then increases linearly during acceleration. Therefore resonance may occur in the acceleration period in cases when the mechanical natural frequency of the machine in continuous operation is much lower than the frequency of the exciting force. In other words, the smoothly running machine might "roar up" during the acceleration period. This transient resonance may show up under other types of transient operating condition, like reversing, or in the generator braking mode of multiple-speed motors. Based on theoretical considerations and practical experience, the force waves classified as dangerous in terms of vibration or noise can be selected on the basis of their mode number and frequency. The low and medium power asynchronous machines have proved to be extremely rigid against force waves with mode numbers over 6, and therefore we can neglect the analysis of force waves with mode numbers above six. From experience, the following frequency ranges must be considered for asynchronous machines:

$$\text{for noise} - 200 \text{ Hz} \leq f_r \leq 4000 \text{ Hz}, \tag{3.26}$$
$$\text{for vibration} - 10 \text{ Hz} \leq f_r \leq 1000 \text{ Hz}.$$

For manual calculations it is advisable to use the mode number table compiled by Jordan [53], where the dangerous mode numbers and corresponding frequencies can be marked.

More recent investigations suggest that the above assumption regarding the mode numbers is not evident in all cases. It can be proved by calculation, and is also observable in practice, that even air gap force waves with mode number equal to or higher than the order of magnitude of tooth numbers may result in force and deflection waves in the yoke with lower frequency, owing to the anisotropy caused by the presence of teeth. The radial forces are transmitted to the yoke through the teeth from the air gap. The radial force wave acts directly on the tooth tips. The stator bore surface is not smooth but is covered by alternating slots and teeth. The waves are also present in the slotted zones. The total force exerted on the teeth is given by the integral sum of the force over the area within the tooth pitch. This force is then transmitted to the yoke through the tooth root. Depending on the root cross-sectional area, the mechanical stress varies round the circumference. If the frequency of the force wave is low compared with the number of teeth, then the amplitude change of the force wave is negligible within a given tooth range and the radial force wave is transmitted to the yoke. If, however, the mode number of the air gap force wave is close to the number of teeth, then, in addition to the resultant radial force, a sensible amount of bending moment is also transferred to the yoke, owing to substantial changes in stress distribution within the tooth tip area. Weh proved by calculation [140] that for force waves with mode number $r > S_1/2$, the assumption that the air gap force wave is transmitted to the yoke without suffering any modification is not justified and—a very important point—the fundamental mode number of the yoke wave is reduced. This phenomenon is called subwave generation.

The time function of the radial tensile stress wave acting on the stator yoke is given by:

$$p_n(x, t) = P_n \cos (nx - \omega_r t - \psi_r).$$ (3.27)

The mode number: $n = gS_1 - r$.

The amplitude: $P_n = \xi_i \xi_j P_r$,

where

$$\xi_i = \frac{\sin (r\pi/S_1)}{r\pi/S_1}, \quad \xi_j = \frac{\sin \left(n \dfrac{b_s}{D}\right)}{n \dfrac{b_s}{D}},$$

b_s — tooth width (as seen in Fig. 3.3).

If $g=0$, then $n=|r|$. Let the value of r/S_1 converge on 0, that is, if the frequency of force wave is low as compared with the number of teeth, then the value of ξ_i and ξ_j converges on 1, and the general calculating procedure stands. The magnitude of error depends on the value of ξ_i and ξ_j, and, indirectly, on the ratio r/S_1.
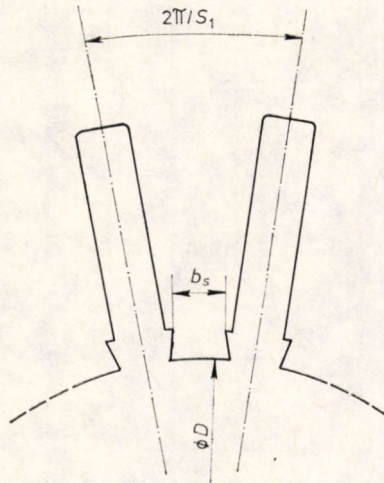
Fig. 3.3. A slot and a tooth of a high-powered asynchronous motor

3.1.4 Numerical example

Noise of electromagnetic origin is an important factor in low-speed, high pole number asynchronous motors, because noises of other (aerodynamic and mechanical) origins are relatively small.

For noise calculation, first the potentially dangerous mode numbers and frequencies of exciting forces must be identified. To facilitate the work, we may prepare so-called mode number tables for each of the products $b_\mu b_{\lambda w}$, $b_\mu b_{\lambda e}$ and $b_\mu b_{\lambda \mathrm{sat}}$ (Tables 3.1, 3.2 and 3.3, respectively). The stator orders are the headers for the columns of the tables (every pth order is also a slot harmonic), while the rows are headed by the λ_w, λ_e and λ_{sat} values, respectively. The elements of the tables are the force mode numbers $r=(\mu\pm\lambda)p$ of eqn. (3.24). If we see that the mode number is high and not dangerous from vibroacoustical point of view, we do not even enter it in the table. Under the mode number, the exciting force frequency, determined by eqns (3.25) or (3.25a, b) assuming an average slip value, is entered. The analysis is illustrated by a six-pole squirrel-cage asynchronous motor with slot numbers $S_1=36$ and $S_2=30$.

Table 3.1. The mode number table of exciting forces $b_\mu b_{\lambda w}$
($S_1/S_2 = 36/30$ and $p = 3$)

λ_w	μ											
	−15	+21	−33	+39	−51	+57	−69	+75	−87	+93	−105	+111
−27		−6 / 390	−6 / 490									
+33			0 / 590	+6 / 490								
−57					+6 / 980	0 / 880						
+63						−6 / 980	−6 / 1080					
−87									0 / 1470	+6 / 1370		
+93									+6 / 1570	0 / 1470		
−117												−6 / 1860

In the Fourier series of flux density harmonics, the amplitudes of harmonics decrease sharply with increasing order. The heavy framed boxes indicate the stator winding harmonics (e.g., −33, +39) that are also slot harmonics (e.g., b_{-33}, b_{+39}), because their amplitude is very large, and which are therefore of special interest in terms of noise generation. Reviewing Tables 3.1 to 3.3, we can verify that for the given slot numbers, forces with mode number $r = 1$ are produced under the first slot harmonic in Table 3.2 at frequencies of about 600 Hz, and mode numbers $r = 0, 5, 6$ and 7, i.e., relatively low mode numbers, at frequencies around 1100 to 1200 Hz in all three tables, but especially in Table 3.3.

Figure 3.4 shows the third octave band frequency spectrum of the sound pressure level produced by an asynchronous motor. The square of the fundamental flux density wave shows up around 100 Hz.

In the one-third octave band with a centre frequency of 630 Hz (within the range of 560 Hz to 710 Hz) the dominant noise component appears, which determines the noise of the machine. There is considerable noise in the third octave

Table 3.2. The mode number table of exciting forces $b_\mu b_{\lambda e}$
($S_1/S_2 = 36/30$ and $p=3$)

λ_e						μ						
	−15	+21	−33	+39	−51	+57	−69	+75	−87	+93	−105	+111
−26		−5 374	−7 474									
−28		−7 417	−5 517									
+32			−1 574	+7 474								
+34			+1 606	+5 506								
−56					+5 964	+1 864						
−58					+7 996	−1 896						
+62						−5 964	−7 1064					
+64						−7 996	−5 1096					
−86							−1 1454	+7 1354				
−88							+1 1486	+5 1386				
+92									+5 1553	+1 1453		
+94									+7 1586	−1 1486		
−116												−5 1483
−118												−7 1876

band of 1250 Hz as well, as expected on the basis of preliminary calculations. From the appearance of forces of $b_\mu b_{\lambda e}$ origin with mode number $r=1$, we can conclude that the 36/30 slot number combination in six-pole machines is very sensitive to eccentricity which, owing to fabrication tolerances, cannot be completely eliminated.

Table 3.3. The mode number table of exciting forces $b_\mu b_{\lambda sat}$
($S_1/S_2 = 36/30$ and $p = 3$)

λ_s	-15	$+21$	-33	$+39$	-51	$+57$	-69	$+75$	-87	$+93$	-105	$+111$
-21	+6 390	0 290										
$+39$			+6 690	0 590								
-51					0 780	+6 880						
$+69$							0 1180	+6 1080				
-81								-6 1270	-6 1370			
$+99$									-6 1570	-6 1670		
-111											+6 1860	0 1760

Potentiometer range: __50__ dB Rectifier: __r.m.s.__ Lower lim. freq: __50__ Hz Writing speed: _____ mm s⁻¹

Multiply frequency scale by: __1__   Zero level: __30 dB__
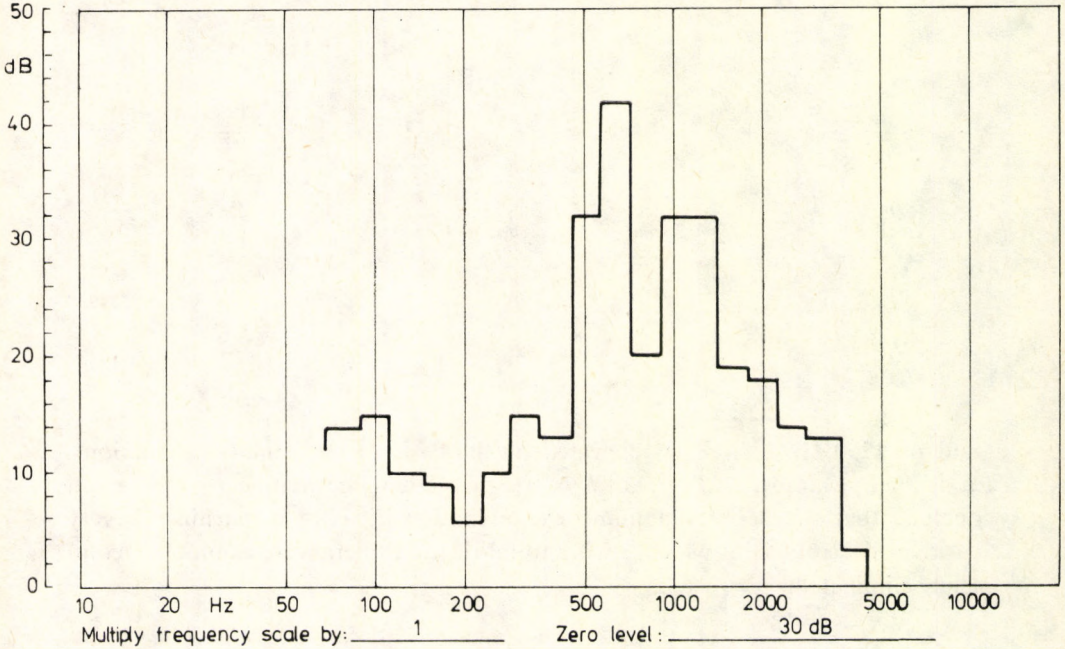
Fig. 3.4. The frequency spectrum of the sound pressure level of an asynchronous motor
($S_1/S_2 = 36/30$ and $p = 3$)

3.1.5 Homopolar flux and unbalanced magnetic pull in two-pole asynchronous motors

Owing to manufacturing asymmetries and material inhomogenities, homopole fluxes may be produced in two-pole asynchronous motors. This homopolar flux is unidirectional in the air gap, i.e., it passes through the air gap from, say, the rotor to the stator, then follows the magnetic circuit through the yoke, housing, shield, bearing and shaft. The most usual cause of homopolar flux build-up is the eccentricity of the rotor, and therefore this phenomenon can be introduced with the aid of the following example.

The m. m. f. of a three-phase, two-pole asynchronous motor is expressed as:

$$F_{m_{1p}}(x, t) = F_{m_{1p}} \cos (x - \omega_1 t - \varphi_m) + \Sigma F_{m_{misc}}.(x, t), \tag{3.28}$$

where the value of $F_{m_{1p}}$ is determined with the aid of eqn. (3.2) and the term $\Sigma F_{m_{misc}}(x, t)$ represents the m. m. f. harmonics.

When both static and dynamic eccentricity are present in the machine, but their level is below 0.2 to 0.3, the air gap permeance is found as:

$$G_m(x, t) = G_{mo} + G_{me;s} \cos (x - \varphi_{e,s}) + G_{me;d} \cos [x - (1 - s)\omega_1 t - \varphi_{e,d}] +$$

$$+ \Sigma G_{m_{misc}}.(x, t), \tag{3.29}$$

where

$$G_{mo} = \frac{\mu_0}{\delta_g k_{c1} k_{c2}}; \quad G_{me,s} = G_{mo}\varepsilon_s; \quad G_{me,d} = G_{mo}\varepsilon_d;$$

$$\varepsilon_s = \frac{e_s}{\delta_g}; \quad \varepsilon_d = \frac{e_d}{\delta_g}.$$

$\Sigma G_{m_{misc}}$ stands for the slotting, saturation and permeance waves. We confine further discussion to the fundamental and the first order permeance waves of static and dynamic origin, since the effects of others have been covered before. The product of eqns (3.28) and (3.29) gives the flux density in the air gap. It comprises the following five terms:

$$b(x, t) = B_{1p} \cos (x - \omega_1 t - \varphi_m) + B_{e,s,h} \cos [\omega_1 t - (\varphi_m - \varphi_{e,s})] +$$
$$+ B_{e,s} \cos [2x - \omega_1 t - (\varphi_m - \varphi_{e,s})] + B_{e,d,h} \cos [s\omega_1 t - (\varphi_m - \varphi_{e,d})] +$$
$$+ B_{e,d} \cos [2x - (2 - s)\omega_1 t - (\varphi_m - \varphi_{e,d})]. \tag{3.30}$$

The subscript h indicates the homopolar components. Note that the second and fourth terms are of uniform distribution round the circumference. At any instant the direction of the flux points from the rotor to the stator or vice versa all through the air gap, i.e. these terms represent homopolar fluxes. The frequencies of the homopolar flux due to static and dynamic eccentricity equal the supply and

slip frequencies, respectively. The value of B_{1p} is given by the product $G_{mo}F_{m1p}$, while $B_{e,s}=0.5B_{1p}\varepsilon_s$ and $B_{e,d}=0.5B_{1p}\varepsilon_d$. In the calculation of homopolar flux density amplitudes, it must be borne in mind that the reluctance of machine parts in the path of the flux is not negligible compared with the air gap reluctance. Therefore, based on the literature [68], we introduce factor Q' as follows:

$$Q'=\left[1+\frac{lD\pi}{2\delta_g}\sum_n\frac{l_n}{\mu_nA_n}\right]^{-1}, \tag{3.31}$$

where δ_g — geometrical air gap length,

$\quad l$ — effective magnetic length of rotor,

$\quad D$ — rotor diameter,

$\quad l_n$ — length of the nth section of the homopolar flux path,

$\quad A_n$ — cross-sectional area of the nth section of the homopolar flux path,

$\quad \mu_n$ — relative permeability of the nth section of the homopolar flux path.

Now

$$B_{e,s,h}=0.5B_{1p}\varepsilon_sQ',$$

and

$$B_{e,d,h}=0.5B_{1p}\varepsilon_dQ'.$$

From our interest in the amplitude and frequency of the produced force waves, omitting the phase angles of the individual flux density waves (which corresponds to the arbitrary decision of taking the zero of the circumferential coordinate x to the air gap minimum due to eccentricity), we find that the radial tensile stress is expressed by the following formula:

$$p(x,t)=\frac{b^2(x,t)}{2\mu_0}=\frac{B_{1p}^2}{4\mu_0}[1+\cos(2x-2\omega_1t)]+\frac{B_{1p}^2\varepsilon_s^2Q'^2}{16\mu_0}[1+\cos 2\omega_1t]+$$

$$+\frac{B_{1p}^2\varepsilon_s^2}{16\mu_0}[1+\cos(4x-2\omega_1t)]+\frac{B_{1p}^2\varepsilon_d^2Q'^2}{16\mu_0}[1+\cos 2s\omega_1t]+$$

$$+\frac{B_{1p}^2\varepsilon_d^2}{16\mu_0}\{1+\cos[4x-2(2-s)\omega_1t]\}+\frac{B_{1p}^2\varepsilon_sQ'}{4\mu_0}[\cos x+\cos(x-2\omega_1t)]+$$

$$+\frac{B_{1p}^2\varepsilon_s}{4\mu_0}[\cos x+\cos(3x-2\omega_1t)]+\frac{B_{1p}^2\varepsilon_dQ'}{4\mu_0}\{\cos[x-(1-s)\omega_1t]+$$

$$+\cos[x-(1+s)\omega_1t]\}+\frac{B_{1p}^2\varepsilon_d}{4\mu_0}\{\cos[x-(1-s)\omega_1t]+\cos[3x-(3-s)\omega_1t]\}+$$

$$+\frac{B_{1p}^2\varepsilon_s^2Q'}{8\mu_0}[\cos 2x+\cos(2x-2\omega_1t)]+\frac{B_{1p}^2\varepsilon_s\varepsilon_dQ'^2}{8\mu_0}[\cos(1-s)\omega_1t+\cos(1+s)\omega_1t]+$$

$$+\frac{B_{1p}^2\varepsilon_s\varepsilon_dQ'}{8\mu_0}\{\cos[2x-(1-s)\omega_1t]+\cos[2x-(3-s)\omega_1t]\}+$$

$$+\frac{B^2_{1p}\varepsilon_s\varepsilon_d Q'}{8\mu_0}\ \{\cos\ [2x-(1-s)\omega_1 t]+\cos\ [2x-(1+s)\omega_1 t]\}+$$

$$+\frac{B^2_{1p}\varepsilon_s\varepsilon_d}{8\mu_0}\ \{\cos\ (1-s)\omega_1 t+\cos\ [4x-(3-s)\omega_1 t]\}+$$

$$+\frac{B^2_{1p}\varepsilon_d^2 Q'}{8\mu_0}\ \{\cos\ [2x-2(1-s)\omega_1 t]+\cos\ (2x-2\omega_1 t)\}. \tag{3.32}$$

Analysing eqn. (3.32), we can see that the square terms of flux density waves produce force waves of angular frequencies of $2\omega_1$, $2s\omega_1$ and $2(2-s)\omega_1$, while the mixed products describe waves with angular frequencies of 0, $2\omega_1$, $(3-s)\omega_1$, $(1+s)\omega_1$ and $2(1-s)\omega_1$, and, of course, the corresponding vibration and noise. The amplitude of these rotating force waves is generally constant but, as we shall see, the amplitude of certain components varies with time, and therefore the amplitude of the deforming force wave pulsates.

Special attention must be paid to terms 6, 7, 8 and 9 of eqn. (3.32), because they contain tensile stresses of mode number $r=1$. These stresses when multiplied by the surface area, could be potentially dangerous, especially in high power ma-chines where the distance between the supporting bearings is large. The net radial force over the whole rotor surface is called unbalanced magnetic pull in the literature (see Fig. 3.5), because round the circumference, it has one maximum and one minimum point. Nevertheless, we should bear in mind that force wave
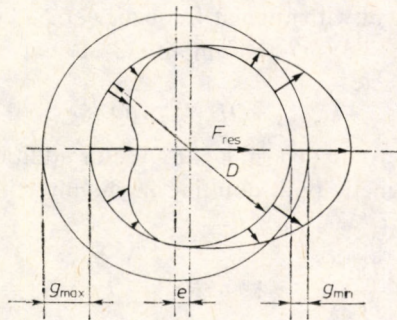
Fig. 3.5. Peripheral distribution of the unbalanced magnetic pull

with mode number $r=1$ may appear in machines with higher pole numbers as well, and it might originate from slotting, saturation, asymmetry in the three-phase supply system or asymmetry in the flux density distribution round the circumference arising from a broken rotor bar. These phenomena can be analysed by means of the flux density space harmonics model discussed in Section 3.1.2, while the exciting force waves are calculated as covered in Section 3.1.3. In all

cases, when the mode number of the exciting force is $r=p(\mu_i\pm\lambda_j)=1$, we can talk about unbalanced magnetic pull.

Let us now return to the two-pole asynchronous motor. First we take the force waves of mode number $r=1$, produced by the mixed product of the space funda-mental and the homopolar $B_{e,s,h}$ and heteropolar $B_{e,s}$ flux density waves due to static eccentricity (see the 6th term and the first part of the 7th term in eqn. (3.32)).

The unbalanced magnetic pull pointing in the direction of static eccentricity (minimum air gap) distributed sinusoidally round the circumference, is found as:

$$f_{\text{ump},s}(x,t)\Big|=\frac{D\pi l}{8\mu_0}B_{1p}^2\varepsilon_s[(1+Q')\cos x+Q'\cos(x-2\omega_1 t)]_{x=0}. \qquad (3.33)$$

Freise and Jordan [28] noticed in 1962 that the value of unbalanced magnetic pull calculated by the above procedure is higher than the value actually measured on the machines. They also found that the difference between the calculated and measured value becomes smaller with increase in pole number. Wright *et al.* [141] suggested in 1982 that the unbalanced magnetic pull be multiplied by a pole-number-dependent factor Q. The value of Q is 0.25 for two-pole machines, 0.712 for four-pole machines, 0.86 for six-pole machines and 0.896 for eight-pole ma-chines. The force pointing in the direction of minimum air gap has a constant component,

$$F'_{\text{ump},s}=QD\pi lB_{1p}^2\varepsilon_s(1+Q')/8\mu_0,$$

and a rotating component with angular frequency of $2\omega_1$. (i.e., the real component of the rotating complex vector) and amplitude of

$$F''_{\text{ump},s}=QD\pi lB_{1p}^2\varepsilon_s Q'/8\mu_0.$$

The resultant force has to be determined by vector addition (i.e., cosine formula), so the unbalanced magnetic pull, pointing in the direction of minimum air gap, varies in time as:

$$F_{\text{ump},s}(t)\Big|_{x=0}=Q\frac{D\pi l}{8\mu_0}B_{1p}^2\varepsilon_s\sqrt{1+2Q'+2Q'^2+2(1+Q)Q'\cos 2\omega_1 t}, \qquad (3.34)$$

i.e., pulsates at an angular frequency of $2\omega_1$ The circumferential distribution follows the cos x curve. The ratio of the maximum value to the minimum value is $f_{\text{ump},s,\text{ max}}/f_{\text{ump},s,\text{ min}}=1+2Q'$.

If the reluctance of the homopolar flux path outside the air gap is negligible, then $Q'=1$, so the ratio of largest to smallest unbalanced magnetic pull is 3. The other extreme case is $Q'=0$ which can be achieved by increasing the magnetic reluctance, e.g., by using a non-magnetic shield or applying between the bearing and shield a non-magnetic ring, thus eliminating most of the homopolar flux.

In this latter case, the unbalanced magnetic pull hardly pulsates, and the ratio $f_{ump, s, max}/f_{ump, s, min}$ is approximately 1.

In the formula for the unbalanced magnetic pull, (3.33), it can be seen that the rotating term has a component perpendicular to the minimum air gap direction, which can be written as:

$$\left. f_{ump, s}(x, t) \right|_{x=\frac{\pi}{2}} = F''_{ump, s} \sin 2\omega_1 t. \tag{3.35}$$

(The distribution round the circumference, of course, follows the $\cos x$ curve again.)

As for dynamic eccentricity, the force wave of mode number $r=1$ is produced by the mixed product of the space fundamental B_{1p} and the homopolar $B_{e, d, h}$ and heteropolar $B_{e, d}$ flux density waves (see the 8th term and the first part of the 9th term in eqn. (3.32)). As we see, the dynamic eccentricity gives rise to rotating unbalanced magnetic pull waves of different angular frequency, $(1-s)\omega_1$ and $(1+s)\omega_1$. The two rotating force vectors can be added, so the following equation is obtained for the unbalanced magnetic pull due to dynamic eccentricity:

$$f_{ump, d}(x, t) = \left\{ Q \frac{D\pi l}{8\mu_0} B_{1p}^2 \varepsilon_d \sqrt{1+2Q'+2Q'^2+2(1+Q')Q'\cos 2s\omega_1 t} \right\} \times$$
$$\times \cos\left[x-(1-s)\omega_1 t\right]. \tag{3.36}$$

It can be seen that the unbalanced magnetic pull amplitude fluctuates at twice the slip frequency, while rotates at an angular frequency of $(1-s)\omega_1$. The ratio of the largest value to the smallest is again $1+2Q'$. If $Q'=1$, that is, the homopolar flux is at its maximum, the ratio is 3, while if the homopolar flux is eliminated (i.e., $Q'=0$), then the amplitude of the unbalanced magnetic pull will not pulsate.

When the static and dynamic eccentricities appear simultaneously in the asynchronous motor, then all the components of the unbalanced magnetic pull will be present according to eqns (3.34), (3.35) and (3.36). As a matter of interest, we note that not only the amplitude of the unbalanced magnetic pull fluctuates from the force waves described by eqn. (3.32), but also the mixed products $B_{e,s, h}B_{e,d}$ and $B_{e,s}B_{e, d,h}$ give rise to a force wave which rotates at an angular frequency of $(1-s)\omega_1$ with its amplitude pulsating at twice the slip frequency, but only when both dinamic and static eccentricity are present simultaneously in the machine. The expression of this force wave (from the 12th and 13th terms of eqn (3.32)) is found to be:

$$f_{e, s, d}(x, t) = Q \frac{D\pi l}{8\mu_0} B_{1p}^2 \varepsilon_s \varepsilon_d Q' \sqrt{5+4\cos 2s\omega_1 t} \, e^{j[2x-(1-s)\omega_1 t]}. \tag{3.37}$$

If the homopolar flux is eliminated, this component of the exciting force is also eliminated completely. Calculating the unbalanced magnetic pull we should note, however, that the above equations do not provide the exact value of the unbalanced magnetic pull. There are other factors that should be considered. On the one hand, the above procedure overestimates the magnitude of the unbalanced magnetic pull in that it omits the effect of saturation that tends to decrease the flux and the effect of slotting on the flux distribution below the tooth curve. On the other hand, the pull is underestimated in that higher order slotting and force harmonics may also generate unbalanced magnetic pull components. The accuracy of the above calculation is further reduced by the difficulty of determining the correct value of Q', the empirical character of Q, and most of all, by the fact that the degree of static and dynamic eccentricity can be only predicted but cannot be known with certainty. Only the static eccentricity can be measured at the price of dismantling the motor, but the dynamic eccentricity can only be estimated indirectly in most cases. If the degree of relative eccentricity exceeds $0.2 \sim 0.3$, then it is not enough to consider only the first term of the eccentricity permeance wave: we saw an approximation in eqns (3.10) and (3.29) but the higher order harmonics must also be taken into account [28]. The adverse effects of the homopolar flux and the unbalanced magnetic pull discussed in this chapter can be summarized as follows:

— in two-pole machines, the eccentricity of the rotor results in the establishment of a homopolar flux that may give rise to shaft flux and shaft stresses,

— the amplitude of certain force waves will pulsate at a frequency of $2sf_1$ because of the homopolar flux, which results in a low-frequency fluctuation of the motor noise near the nominal speed,

— eccentricity fields induce voltage in the parallel paths of stator windings, which give rise to equilizing currents, and therefore the connecting scheme of the parallel paths is crucially important [62],

— the unbalanced magnetic pull produced by eccentricity tends to bend the shaft, thus further increases the eccentricity and the magnetic pull. This self-exciting effect, especially in the case of a flexible shaft, may result in the rotor touching the surface of the stator bore (i.e., mechanical friction),

— as increasing eccentricity corresponds to increasing pull force on the shaft, the phenomenon can be represented by a spring with negative characteristic, which reduces the mechanical spring constant of the shaft and consequently the critical angular frequency of the shaft.

The first critical angular frequency of the shaft is expressed, for the basic situation, as follows:

$$\omega_{crit} = \sqrt{\frac{C_{mech}}{m_2}}, \tag{3.38}$$

where m_2 is the mass of rotor and C_{mech} is the mechanical spring constant of the shaft. C_{mech} can be determined as the ratio of the rotor weight to the deflection under this weight. By analogy, the magnetic spring constant C_{magn} can be written as the ratio of the unbalanced magnetic pull f_{ump} to the eccentricity. Since a constant pull acts on the shaft through static eccentricity in the direction of minimum air gap, and therefore:

$$C_{magn} = -Q\frac{D\pi l}{4\mu_0\delta_g}.$$

(3.39)

The effect of unbalanced magnetic pull modifies the critical angular frequency:

$$\omega'_{crit} = \sqrt{\frac{C_{mech}+C_{magn}}{m_2}}.$$

(3.40)

The decrement in critical angular frequency is given by the formula $(1-\sqrt{1+C_{magn}/C_{mech}})$.

3.1.6 Tangential vibration

The interaction of flux density waves in the air gap and the circumferential currents of the rotor gives rise to tangential forces according to the Biot–Savart law. The tangential force wave acting on unit area of the bore surface is found to be:

$$P_{tan}(x, t) = \sum_\mu \sum_\lambda b_\mu(x, t)a_\lambda(x, t),$$

(3.41)

where $b_\mu(x, t)$ — an optional radial component of the stator flux density space

harmonic $b_\mu = B_\mu \cos(\mu px - \omega_\mu t - \psi_\mu)$,

$a_\lambda(x, t)$ — an optional component of the circumferential current of the rotor.

The relationship between the circumferential current of the rotor and its flux density space harmonics is:

$$a_\lambda(x, t) = \frac{\delta_g}{\mu_0 R}\frac{\partial b_\lambda(x, t)}{\partial x},$$

(3.42)

where $b_\lambda(x, t)$ — any radial component of the flux density space harmonic of the rotor $b_\lambda = B_\lambda \cos(\lambda px - \omega_\lambda t - \psi_\lambda)$,

R — the radius of the rotor,

δ_g — the geometrical radial air gap length.

Substituting the expressions for b_μ and b_λ, eqn. (3.41) becomes:

$$p_{tan}(x, t) = -\sum_\mu \sum_\lambda \frac{p\lambda\delta_g B_\mu B_\lambda}{\mu_0 R}\sin(\lambda px - \omega_\lambda t - \psi_\lambda)\cos(\mu px - \omega_\mu t - \psi_\mu).$$

Applying the well known trigonometrical formula for the multiplication of harmonic functions:

$$p_{\tan}(x, t) = -\sum_{\mu} \sum_{\lambda} \frac{p\lambda\delta_g B_\mu B_\lambda}{2\mu_0 R} \sin (r_{\tan}x - \omega_{p,\tan}t - \psi_{r,\tan}), \qquad (3.43)$$

where　　$r_{\tan} = p(\lambda_j \pm \mu_i)$,

$\omega_{r,\tan} = \omega_{\lambda j} \pm \omega_{\mu i}$,

$\psi_{r,\tan} = \psi_{\lambda j} \pm \psi_{\mu i}$.

Comparing eqns (3.24) and (3.43) we see that the mode number, angular frequency and phase angle of the radial and tangential force waves are identical, that is, the spectrum of the tangential vibration is identical to that of the radial vibration. If the magnitudes of the two force waves are compared, we find that the amplitude of the tangential force wave is $p\lambda\delta_g/R$ times that of the radial force wave. Normally the value of this ratio is considerably less than 1, and consequently the tangential vibrations are generally much smaller than the radial ones.

3.1.7 Parasite torque

By multiplying the expression of tangential force wave acting upon a unit area of the bore surface (3.41) with the differential surface element $lRdx$, the differential force, and by multiplying this with the radius, the differential torque is obtained:

$$dT = \left[-\sum_{\mu} \sum_{\lambda} b_\mu(x, t)a_\lambda(x, t) \, dx \right] lR^2. \qquad (3.44)$$

Substituting the expressions for b_μ and a_λ and integrating eqn. (3.44) round the total circumference, the torque T is given as:

$$T = -\sum_{\mu} \sum_{\lambda} \frac{lRp\lambda\delta_g B_\mu B_\lambda}{2\mu_0} \int_0^{2\pi} \sin (r_{\tan}x - \omega_{r,\tan}t - \psi_{r,\tan}) \, dx, \qquad (3.45)$$

where 1 is the length of the rotor.

If $r_{\tan} \neq 0$ in the argument of the harmonic function the value of the integration will be zero. If the mode number $r_{\tan}$ is equal to zero in expression (3.45) of the torque, which means that the order (number of pole pairs) of the stator and rotor harmonics are equal ($|\lambda| = |\mu|$) then parasitic torque is created. There are two types of the parasitic torque.

The stator flux density space harmonic rotates in the stationary coordinate system with a constant space angular velocity, which depends on the supply frequency, the number of pole-pairs and the order of the harmonic $\Omega_\mu = \omega_1/(\mu p)$.

The rotor current space harmonic rotates in the stationary coordinate system with a space angular velocity which also depends on the mechanical speed of the rotor $\Omega_\lambda = \omega_1[(\lambda-1)(1-s)+1]/(\lambda p)$.

If the two space angular velocities equals only at a given rotor speed, synchronous like torque, the so-called synchronous parasitic torque will develop at this common speed which has the magnitude of

$$T_{sy} = pD\pi l\lambda\delta_g \frac{B_\mu B_\lambda}{2\mu_0}.$$

At speeds outlying this given speed pulsating torque acts in the asynchronous motor which pulsates with the frequency $(\omega_\lambda + \omega_\mu])/2\pi$. The amplitude of the torque pulsation is the same as the synchronous parasitic torque.

Example

At $p=2$, $S_1=24$ there appears a stator flux density space harmonic with the order of $\mu=13$. If the slot number in the rotor is $S_2=28$ there is a $\lambda=-13$ harmonic development on the rotor as well, that is, one condition of creating torque, the equality of the number of pole-pairs is true. By solving the equation describing the equality of the space angular velocities of the harmonics

$$\frac{\omega_1}{\mu p} = \frac{\omega_1}{\lambda p}[(\lambda-1)(1-s)+1]$$

it can be seen that at $n=n_0/7$ speed (at one seventh of the synchronous speed belonging to the fundamental harmonic), the synchronous parasitic torque will develop. This torque can prevent in unfavourable cases, the rotor from surpassing this speed when accelerating.

If a stator and a rotor flux density harmonic, besides having the same order $(\mu=\lambda)$, will rotate with the same space angular velocity $(\Omega_\mu = \Omega_\lambda)$ independent of the rotor speed, then asynchronous type parasitic torque, the asynchronous crowling is created, with a magnitude of

$$T_{as} = pD\pi l\lambda\delta_g \frac{B_\mu B_\lambda}{2\mu_0} \cos(\varphi_\lambda \pm \varphi_\mu).$$

The physical explanation for this is the following: The μth stator space harmonic of the flux density acts as if there were a winding of μp number of pole-pairs on the stator, which is supplied with a frequency of f_1. The magnetic field rotates with the space angular velocity of Ω_μ. The caged rotor has no definite number of poles and tries to reach Ω_μ space angular velocity. The order of the current system induced in the rotor by μth stator harmonic flux density is $\lambda = \mu + gS_2/p$. If $g=0$ (that is, the spatial fundamental harmonic of this current system), the order of the rotor harmonic is $\lambda = \mu$, so according to the previous equations the angular frequency of the rotor harmonic is:

$$\omega_\lambda = \omega_1 \left[\frac{gS_2}{p}(1-s)+1 \right] = \omega_1.$$

The space angular velocity of the rotor harmonic is $\Omega_\lambda = \omega_1/(\lambda p)$ that is condition $\Omega_\mu = \Omega_\lambda$ is fulfilled. The shape of the asynchronous parasitic torque curve is similar to that of the fundamental harmonic wave only the synchronous speed is different. Of course, the magnitude of the torque decreases by $1/\mu^2$.

There are "saddles" on the resultant speed-torque curves which are able to prevent the motor from reaching the desirable speeds in certain cases. The asynchronous crawling caused by the 7th harmonic is for instance capable of preventing the motor from accelerating at one seventh of the fundamental harmonic synchronous speed, when the slip is:

$$s_\mu = \frac{n_0 \pm n_0/\mu}{n_0} = 1 \pm 1/\mu = 1 - 1/7 = 0.86.$$

The asynchronous crawling is the most dangerous in the case of not-skewed squirrel-caged motors. It is well known that by using step-shortening in the stator winding, or by proper skewing of the rotor slots, the biggest stator space harmonic will decrease to near zero. The asynchronous crowling do not disturb the running up of the asynchronous motors with slip-ring rotor, since the adequate accelerating torque is usually ensured with an external starting resistor.

3.2 Asynchronous motor drives with controllable solid-state power-supply system

Through the rapid development in power electronics, more and more controlled solid-state power-supply systems are being used in various drive applications. For electric drives, the use of asynchronous motors is preferred owing to their reliability, simplicity and subsequently low cost, although it is a major drawback that their speed variation is complicated. The problem of speed variation can be solved by controlled solid-state devices. In terms of connection, the solid-state applications can be divided into four basic groups. In the case of squirrel-cage asynchronous machines, we can only interfere on the primary side of the circuit by connecting, say, an inverter to the terminals of the motor, providing a variable-frequency supply for the machine. In crane drives, for example, we use antiparallel connected symmetrical or asymmetrical thyristor–thyristor (TT) or thyristor–diode (TD) semiconductor element pairs, usually at slip-ring type rotors. In the rotor circuit, two types of connection are used. The rotor current is first rectified, then connected to a resistor through a controlled solid-state device, so a chopper is built in the rotor circuit. The effective resistance of this d.c. circuit is set by the variable

duty cycle of a thyristor incorporated in the circuit. The wattage in this case is dissipated as heat in the rotor circuit. The fourth solution requires higher invest-ment cost, but the loss, on the other hand, is much less. Here the rectified rotor current of frequency sf_1 is fed back to the supply network by an inverter. Apart from elegantly solving the problem of speed variation in asynchronous motors, the use of solid-state devices has numerous secondary effects like torque oscilla-tions, increased losses, noise and vibration.

In this chapter, we are discussing the possibility of noise and vibration generation induced by changes in exciting forces through two different primary-side inter-ferences. According to theoretical considerations and practical experiments, the secondary-side interferences do not contribute to noise or vibration generation at all. Other noises and vibrations of mechanical or aerodynamical origin, mentioned in Chapter 2, depend on the speed of the machine. They are independent of the supply configuration. The passive characteristics, the vibrating and sound radiating capabilities of the machine are also independent of the power-supply. Therefore it is thus adequate to focus our investigation on electromagnetic forces. Considering the order of magnitude of flux density space harmonics of different origin, we still maintain our simplifying assumptions outlined under 3.1.1.

We assumed before that the supply voltage is purely sinusoidal. The model outlined in Fig. 3.2, however, is suitable for the analysis of the vth time harmonic supply, produced by the solid-state device.

The spatial distribution of these time harmonics corresponds to the pole pair number p, and their angular frequency is $v\omega_1$. Each time harmonic induces space harmonics for the reasons outlined above, as illustrated in Fig. 3.2, just as the time fundamental does with frequency f_1. The amplitude of time harmonics is generally smaller than that of time fundamentals.

As the amplitude of the force wave varies with the square of the voltage, the space harmonics of time harmonics must only be taken into account when the amplitude of the time harmonics is greater than 70 percent of that of the time fundamental. If the amplitude of the time harmonics is greater than 30 percent but less than 70 percent of the amplitude of the time fundamental, then the space harmonics of the time harmonics as small in second order, can be neglected. If, however, the amplitude of the time harmonics is smaller than 30 percent of the time fundamental, then even the space fundamental of time harmonics can be neg-lected.

The voltage across the stator winding can be expanded into a Fourier series, with an instantaneous value of

$$u(t) = \sum_v U_v \cos(v\omega_1 t). \tag{3.46}$$

Symmetry considerations generally state that

$$v = 1 + 6k$$

where $k = 0, \pm 1, \pm 2, \ldots,$

and for asymetrical TD (antiductor) operation:

$$v = 1 + 3k.$$

For $k = 0$, $v = 1$, that is, we get the time fundamental voltage.

Under steady-state conditions, the amplitude of the vth current harmonic is:

$$I_v = \frac{U_v}{Z(v, \omega)} . \tag{3.47}$$

As the individual voltage harmonics constitute a symmetrical three-phase system, the impedance $Z(v, \omega)$ of the motor can be calculated from the equivalent circuit shown in Fig. 3.6 which is similar to the standard equivalent circuit.
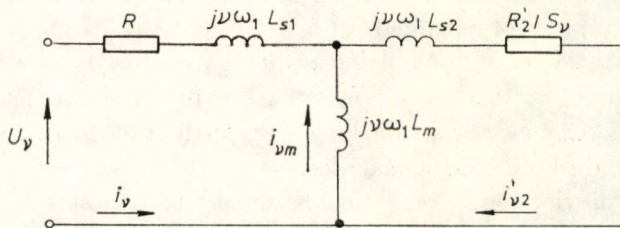
Fig. 3.6. Equivalent circuit of the asynchronous motor in the case of harmonic supply that differs from the supply frequency

In the figure, s_v is the slip of the vth harmonic which can be expressed in terms of the fundamental slip, s_1, as:

$$s_v = \frac{v\omega_1 - \omega}{v\omega_1} = \frac{v - 1 + s_1}{v} . \tag{3.48}$$

The flux density space fundamental waves, established by the time fundamental and time harmonics of the supply are found to be:

$$b_{f_v}(x, t) = \sum_v B_{f_v} \cos(px - v\omega_1 t - \psi_v), \tag{3.49}$$

where B_{f_v} can be determined from eqns. (3.2),(3.12) and (3.47), while ψ_v is approximately $\pi/2$.

The Fourier series of the flux density space harmonics, induced by the time fundamental and harmonics of the supply, is expressed as:

$$b_\mu(x, t) = \sum_\mu B_\mu \cos(\mu px - v\omega_1 t - \psi_\mu), \tag{3.50}$$

where $\mu = 1 + 6g.$

Since the space fundamental of the time fundamental has been covered in eqn. (3.49), thus in this equation $\mu \neq 1$, $\nu \neq 1$. The amplitude of the flux density space harmonic is the resultant of the winding and slotting harmonics and can be calculated from eqns (3.13) and (3.16).

The voltages induced in the rotor winding by the flux density time fundamental wave and time harmonics of the stator give rise to flux density waves of the rotor which can be expressed by the following Fourier series:

$$b_\lambda(x, t) = \sum_\lambda B_\lambda \cos (\lambda p x - \omega_\lambda t - \psi_\lambda), \qquad (3.51)$$

where

$$\lambda = \frac{gS_2}{p} + 1,$$

$$\omega_\lambda = \omega_1 \left[\frac{gS_2}{p} (1-s) + \nu \right].$$

The amplitude can be obtained from eqns (3.14), (3.17) and (3.49). The flux density space harmonics due to rotor eccentricity are found to be:

$$b_{\lambda e}(x, t) = \sum_{\lambda e} B_{\lambda e} \cos [(\lambda p \pm 1)x - \omega_{\lambda e} t - \psi_{\lambda e}], \qquad (3.52)$$

where

$$\omega_{\lambda e} = \omega_1 \left[\frac{gS_2}{p} (1-s) + \nu \pm (1-s)p^{-1} \right].$$

The amplitude can be determined by the procedure set out in [29].

On the basis of the equality of orders, the flux density waves detailed above can be grouped as follows:

$$b(x, t) = \sum_\nu b_{f\nu} + \sum_\mu b_\mu + \sum_\lambda b_\lambda + \sum_{\lambda e} b_{\lambda e}. \qquad (3.53)$$

The force waves can be calculated in a similar way as in Section 3.1.3. Noting all the possible component squares and mixed products, then comparing the set of force waves obtained with the corresponding set generated in the case of purely sinusoidal feed, we can conclude that

(1) no new mode number is found, so the set of exciting force mode numbers has not increased;

(2) for a given, already existing mode number the frequency composition of the set of forces has become richer.

On the basis of our second finding, we can anticipate that we may have an increased number of potential coincidences owing to the increased set of exciting force frequencies produced by the harmonic content of the supply, which in turn can contribute to the increase of noise of electromagnetic origin.

Simplifications concerning force mode numbers and frequencies set out in Section 3.1.3 still apply, but apart from the mixed product $b_\mu b_\lambda$ which is danger= ous in terms of noise generation, the following terms are also critical:

$$b_\nu^2 \text{ (order } 2p \text{, frequency } 2\nu f_1)$$

and

$$b_\nu b_{\nu''} \quad \text{(order 0 or } 2p \text{, frequency } f_1 \, (\nu' \pm \nu'')).$$

where ν' and ν'' — the orders of time harmonics for different values of k.

In inverter-fed asynchronous motors parasitic oscillating torque components are produced, since the supply high time-harmonic content. These parasite torques are in general much greater than the oscillating torques produced by space harmonics. The order of the space fundamental of any time harmonic is p, so the condition of torque generation, i.e., the identical pole number, is given. As that the order of time harmonics is $\nu = 1 + 6k$, the frequency of torque oscilla- tions is $6kf_1$ (where f_1 is the alternating frequency of the supply voltage fed to the motor by the inverter). Most inverters incorporate an intermediate d.c. circuit between the power rectifier and the converter as shown in Fig. 3.7. The rectified voltage is not smooth, so current time harmonics are also present in the inter=

Mains supply

$$\sim U_{sup}, \, f_{sup}$$

Rectifier

$$i_d(t) = I_e + \sum_{\tau=2}^{\infty} I_{e\tau} \cos(\tau \, \omega_{sup} t + \frac{\beta}{\tau})$$
$$\tau = 2, 4, 6 \ldots$$

Inverter

$$\sim U_1, \, \sim f_1$$
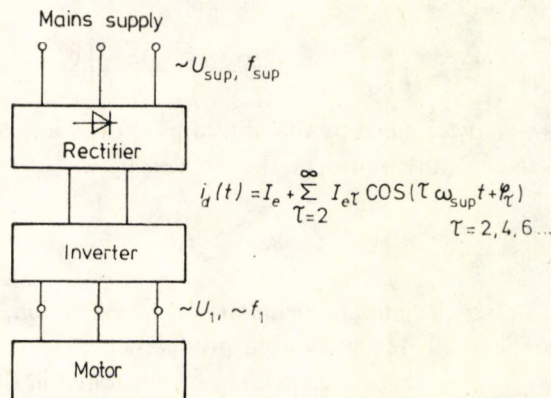
Motor

Fig. 3.7. Time harmonic currents in the intermediate d.c. circuit

mediate d.c. circuit, which, in turn, create new torque oscillations in the asynchronous motor, substantially interfering with the smooth running of the motor. The amplitudes and frequencies of torque oscillations produced in inverter applications are compiled in Table 3.4, following [97].

When the first inverter and antiductor drives appeared in industry, they caused a lot of problems in terms of noise, vibrations, additional losses and torque oscillations. At low speed, the noises and vibrations of mechanical and aerodyna=

Table 3.4. Torque oscillations with inverter supply

The torque oscillation's	
peak value	frequency
$1.83pL_m I_{d0} \hat{I}_{d\tau} \dfrac{1}{s\omega_1 T_{r0} + \dfrac{1}{s\omega_1 T_{r0}}}$	τf_{sup}
$\dfrac{\hat{U}_1^2}{\omega_1^2} \dfrac{1}{L_l} \left(\dfrac{1}{(6k-1)^2} - \dfrac{1}{(6k+1)^2} \right)$	$6kf_1$
$\dfrac{\hat{U}_1^2}{\omega_1^2} \dfrac{1}{L_l} \left(\dfrac{1}{(6k-1)^2} - \dfrac{1}{(6k+1)^2} \right) \dfrac{\hat{I}_{d\tau}}{2I_{d0}}$	$6kf_1 - \tau f_{sup}$

where p is, the number of pole pairs of the motor,

L_m is the magnetizing inductivity of the motor, $L_m = X_m / \omega_1$,

L_l is the leakage inductivity of the motor

$$L_l = (X_{ls} + X'_{lr})/\omega_1,$$

I_{d0} is the direct current flowing in the intermediate direct current circuit,

$\hat{I}_{d\tau}$ is the peak value of the τth harmonic current in time of the current flowing in the intermediate direct current circuit,

s is the slip,

ω_1 is the angular frequency of the fundamental harmonic voltage on the motor,

$\hat{U}_1$ the peak value of the fundamental harmonic voltage on the motor,

$$T_{r0} = \frac{L_m + L'_{lr}}{R'_r},$$

R'_r is the rotor circuit resistance of the motor in primary terms,

τ is the order of the harmonic current in time caused by the rectifier in the intermediate direct current circuit ($\tau = 2, 4, 6, \ldots$),

$k = \pm 1, \pm 2, \pm 3, \ldots$

mic origins decreased sharply, while those of electromagnetic origin increased because of the large amplitudes of low-order time harmonics in the supply, which, in many cases, fell in the range of the voltage time fundamental amplitude. The force components b_ν^2 and $b_{\nu'}b_{\nu''}$ mentioned above could cause up to 10 to 15 dB increase in the A-weighted sound pressure level and up to 200 percent increase in vibration velocity in the low-speed range, compared with other configurations without time harmonics, under the same load conditions. When the speed increased, the increase in noise of electromagnetic origin due to the solid

state power supply became less and less apparent, because it was suppressed by the rapidly growing mechanical and aerodynamic noise.

The above shortcomings in the low-speed range could be overcome as a result of the development in power electronics. To eliminate the lowest-order time harmonics ($|v| = 5, 7, 11, 13, \ldots$), the three phases are modulated in symmetrical cycles (PWM inverters). The optimal switching time is precalculated in order to get rid of the unwanted low-order harmonics and to be stored in the memory. These programs in memory must be changed to match the frequency of the time fundamental so that the number of commutations is constant. This optimized inverter control could eliminate the low-order harmonics in the low-speed range, although it is not the best solution as far as the additional losses are concerned. Now the harmonics produced by the modulation replace the previous low-order harmonics, being responsible for a substantial part of the voltage amplitude with quite high orders, i. e., $v = 35$ or more. The frequency of these voltage harmonics is very high (vf_1) and, as we see in Fig. 3.7, even these high-level voltage harmonics only produce relatively low-level currents in the stator windings, with frequency vf_1. Consequently, the amplitude of flux density time harmonics is reduced considerably. The 10 to 15 dB increase in A-weighted sound pressure level experienced before could be reduced to 4...5 dB in the low-speed range. One can find articles in the literature where it is recommended to avoid rotor slot skewing when solid-state power supply systems are to be used, in order to minimize additional losses. This restriction, however, leads into a wrong direction the designer of electrical machines, since, as we will see, skewing is an important means of noise and vibration reduction.

3.3 Single-phase asynchronous motor

The motor in common household appliances is, in most cases the simplest transformer of electrical energy, a single-phase asynchronous motor. For starting, an auxiliary phase is used, and exciting force waves rotating in the positive (i.e., corresponding to the sense of mechanical rotation of the rotor) and negative directions are produced under steady-state running conditions, regardless of whether the auxiliary phase is switched off following acceleration or not. The ratio of these contra-rotating force waves depends on the load, the stator winding arrangement and the degree of asymmetry. The construction of the machine is similar to that of the squirrel-cage three-phase motors, so the permeance waves are the same as discussed above. The generating process of flux density waves and the calculation of deformational force waves are also similar, therefore we simply point out the differences here.

If we look at the orders of the m. m. f. harmonics of a three-phase ($m=3$) asynchronous motor ($\mu=2mg+1$, where $g=0, \pm1, \pm2, \ldots$), we already see harmonics rotating backward, such as those with orders -5 and -11. Since the motor concerned is a single-phase system that can be broken down to a two-phase system of contra-rotating symmetrical fields, the order of stator m. m. f. harmonics is $\mu=4g+1$. This means that the harmonic orders will take the values of each odd number. For example, the μ values of positive-sequence m. m. f. waves rotating at a frequency of $+\omega_1$ will be $1, -3, +5, -7, \ldots$.

As the space angular frequency of the m. m. f. harmonic is $\omega_1/p\mu$, the positive-sequence m. m. f. fundamental rotates in the same direction as the rotor, the third harmonic in the opposite direction, backwards, etc. The angular frequency of the negative-sequence m. m. f. fundamental is $-\omega_1$, so the fundamental rotates in the negative direction at an angular frequency of $-\omega_1/p$, the third harmonic in the positive direction at $-\omega_1/(-3p)$ (this is the reason why when looking from the stationary coordinate system we see m. m. f. harmonics of any odd number rotating in both directions). The situation is similar for slot harmonics of order $\mu_s= =g'S_1+2g+1$.

The order and angular frequency of squirrel-cage rotor flux density space harmonics are $\lambda=g'S_2\pm2g+1$ and $\omega_\lambda=\omega_1[gS_2(1-s)/p\pm1]$, respectively (these equations assume sinusoidal supply free from time harmonics).

Homopolar fluxes, of course, may be produced in single phase asynchronous motors as well. The frequencies of the corresponding flux density waves are f_1, sf_1 and $(2-s)f_1$. We may have radial tensile stress waves at frequencies of $2sf_1$, $(1\pm s)f_1$, $2(1-s)f_1$, $(3-s)f_1$, $2f_1$ and $2(2-s)f_1$.

Regarding the noise of electromagnetic origin in single-phase asynchronous motors, we should point out that the direct airborne noise radiation is seldom of importance. There are two reasons. Firstly the resonance frequencies of single-phase motors are quite high owing to small motor sizes, and therefore the resonant frequencies are seldom within the audible range. Secondly owing to the small size, single phase motors are poor sound radiators.

3.4 Synchronous machines

3.4.1 The noise of synchronous machines

Among the electrical energy conversion devices, synchronous machines are available in the widest power range. We can find them in power plants as giant generators, but also in delicate instruments as drives. Nowadays they are used typically in the very high (say, several hundred MW) or very low (micro) power

ranges. Small and medium size machines are used mostly in applications where special requirements for speed control (speed stability) must be met.

Advantages: fewer stray losses, better efficiency at high power, less sensitive to supply variations. Drawbacks: relatively larger size at small and medium power, the need for an exciter or starter and regulator, higher level of maintenance. The listed characteristics, in fact, determine the application features of synchronous machines.

The present level of solid-state technology, the modern systems of supply frequency variation and the development of permanent-magnet rotors tend to extend the field of applications.

From the noise and vibration point of view,

(a) in high-power synchronous generators the noise and vibration of mechanical origin (e.g., dynamic imbalance, ventilation, bearings) substantially exceed the level of magnetic noise and vibration;

(b) the power of micro machines is very low, the machines are placed inside much larger equipment, and therefore they cannot be considered as serious noise sources. Their mechanical natural frequencies are very high and they are very poor sound radiators, both resulting from their small dimensions.

The construction and winding arrangement of stators in synchronous machines are very similar to those in asynchronous machines. The constructional design of rotors, however, varies over a very wide scale from excited cylindical rotors to gear-like rotors without excitation of medium-frequency generators. Noise analyses are generally based on the results obtained for asynchronous machines: first the stator flux density fundamentals and harmonics are determined, then the frequencies of the expected force waves [110]. A simplified analysis of the stator and rotor field [73] presents a basis for the noise calculations of synchronous machines. Detailed and in-depth analyses have been published about the electromechanical and mechanical properties of turbogenerators [6].

3.4.2 The radial components of the air gap field; force waves

There is one basic difference between the air gap flux density build-up of synchronous and asynchronous machines. The m.m.f. established by the currents passing through the stator windings of synchronous machines does not induce voltage in the conductors (field coil, starter and damper cage) under steady-state running conditions. The rotor gives rise to its own m. m. f. fundamental and space harmonics owing to its d.c. excitation. These m. m. f. waves induce voltage in the stator winding, which drives currents in the circuit closed through the supply network. The stator m. m. f. waves are given by eqns (3.2) and (3.3).

The rotor m. m. f. fundamental is given by:

$$\bar{F}_{m_{2p}} = F_{m_{2p}} e^{j(px - \omega_1 t - \varphi_k)} \tag{3.54}$$

where

— for a cylindrical rotor:
$F_{m_{2p}} = S_2^2 I_e / 4p.$
$S_2 =$ rotor slot number,
$I_e =$ excitation current,
— for salient pole rotors, F_{m2p} can be determined by the Fourier series of the spatial force distribution,
— φ_k depends on the phase angle of the no-load current (load angle).

The rotor m. m. f. space harmonic is

$$\bar{F}_{m_2}(x, t) = \sum_{\lambda} F_{m_\lambda} e^{j(\lambda px - \omega_1 t - \psi_k)} \tag{3.55}$$

where $\lambda = 2g - 1$ $(g = 1, 2, 3)$.

The flux density wave of sinusoidal space distribution to be produced by the rotor can be generated by most constructions, and therefore it is essential to analyse the m. m. f. wave that corresponds to the individual arrangement. The air gap flux density wave can be calculated from $\bar{F}(x, t)$ comprising the rotor and stator m. m. f. and from the permeance wave $\bar{G}_m(x, t)$. The construction of the permeance wave is identical with that shown in Section 3.1. Applying the appropriate approximations, the components of $\bar{G}_m - \bar{G}_{m_0}, \bar{G}_{m_1}, \bar{G}_{m_2}, \bar{G}_{m_{sat}}$ — can be determined. In the calculation of k_{c2}, we have already taken into consideration the specialities relevant to the different rotor constructions, which are most important factors in $\bar{G}_{m_2}$, the component that takes care of rotor geometry. The modelling of the salient pole rotors as rotors with slot number of $S_2 = 2p$ (large slots) gives a good opportunity for approximation, although this approximation does not replace the Fourier analysis of the concrete permeance distribution. In addition, this model is not suitable for taking into account the non-circular pole arc present to promote the establishment of sinusoidal air gap flux density. The term due to eccentricity can be neglected in the permeance wave expression for synchronous machines, because the potential eccentricity has only a minute effect on the relatively wide air gap.

$\bar{G}_{m_{sat}}$ represents the effect of saturation. We note again that owing to the wider air gap, the effect of saturation is smaller than in asynchronous motors.

The air gap flux density fundamental is given by:

$$\bar{B}_p(x, t) = [\bar{F}_{m_{1p}}(x, t) + \bar{F}_{m_{2p}}(x, t)] G_{m_0}, \tag{3.56}$$

while the winding harmonics are found to be:

$$\bar{B}_w(x, t) = [\bar{F}_{m_1}(x, t) + \bar{F}_{m_2}(x, t)]G_{m_0}. \tag{3.57}$$

In the calculation of slot and saturation harmonics, the same procedure may be followed as in Section 3.1. If the radial components of the air gap flux density are known, the radial force waves can be determined.

3.5 Transformers

Transformers, as electric power transforming devices, are noise sources just as complex as the common electrical machine, discussed in Section 2.1. There are noise sources of electromagnetic origin in power transformers, too, namely the motion of the core of the transformer caused by magnetostriction, the electromagnetic forces, and also noises of aerodynamic and mechanical origin, such as the forced draught system and oil pumps. Magnetic forces are produced in the transformer winding and in the core where the magnetic flux passes from one lamination to another. This latter phenomenon is prominent when the magnetic permeability of parallel laminations is different and when gaps are present at the fitting of core limb and yoke laminations. It is very hard to estimate these forces, and the calculation of the noise produced by them is even harder. The general principle is again valid, that is, considerable noise is produced when the frequency of one of the exciting forces equals the mechanical natural frequency of one of the transformer elements of reasonable radiating capability. According to the literature [89], the noise of electromagnetic origin is about 5 to 15 dB less than the magnetostrictive noise produced in the transformer core. The noise produced by magnetic forces is important only in choke-coils that accommodate an air gap in their construction. Between the two iron surfaces meeting the air gap, alternating magnetic forces act at twice the supply frequency.

Noises of mechanical and aerodynamic origin will be discussed in Chapters 8 and 9, since their character is the same as that of noises of similar origin in rotating electrical machines.

3.5.1 The magnetostrictive effect

The dominant effect that determines the noise of transformers is the elastic deformation of core laminations due to magnetostriction. This elastic deformation manifests itself as oscillatory motion owing to the sinusoidal variation of the inducing flux density with time. The vibrational energy is partly emitted to the surroundings by the iron core through direct radiation. The remaining part, and

the more important part in terms of transformer noise, is transmitted through the oil and the structural elements holding the iron core to the transformer's oil container, which is a good sound radiator, especially in the case when the natural frequency of the container or one of the elements rigidly coupled to it is equal to the frequency of the magnetostrictive motion.

When a ferromagnetic body is placed in an alternating magnetic field, its shape and dimensions change. This phenomenon is called magnetostriction. Magnetostriction is simply the internal deformation of the material, which depends on how easily the magnetic domains can change their position under the influence of a magnetic field. Although this deformation is really minute, it can still cause considerable noise. The specific magnetostrictive elongation is called the magnetostriction factor and is expressed as $\varepsilon = \Delta l / l_i$, where l_i is the initial length and Δl is the elongation due to the change in the magnetic field.
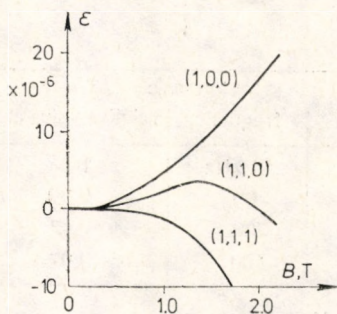
Fig. 3.8. The magnetostriction factor versus the flux density in the three principal directions of an iron monocrystal
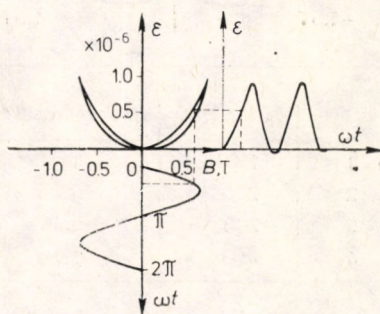
Fig. 3.9. The instantaneous value of the magnetostriction factor as a function of time for ideal iron under the influence of a sinusoidal flux density variation with time

The magnetostriction factor depends on numerous parameters. Figure 3.8 illustrates the variation of ε with flux density in three space directions (the directions are defined by the lines drawn through the origin and coordinates 1, 0, 0; 1, 1, 0 and 1, 1, 1), in an iron monocrystal.

In the core of the transformer, the flux density varies sinusoidally. The instantaneous value of the specific elongation, ε, can be determined as shown in Fig. 3.9. If the function $\varepsilon(B)$ is parabolic, then the magnetostrictive deformation is sinusoidal with twice the frequency of flux density variation.

For real iron materials, the curve $\varepsilon(B)$ is not exactly parabolic, therefore the time function of the magnetostriction factor includes harmonics with frequencies that are the whole number multiples of twice the supply frequency. Figure 3.10

shows the curve $\varepsilon(B)$ for a transformer core lamination with the peak value of the alternating flux density $B_{max}=1.5$ T. In the attached table we list the values of harmonic deformations relative to the fundamental. The problem is complicated by the fact that different curves belong to different flux densities in the same material. According to the experimental results, the material shown in Fig. 3.10 behaves as shown in Fig. 3.11 when subjected to a flux density of $B_{max}=1.8$ T.
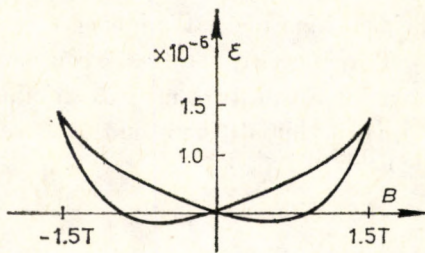
Harmonic		
order	frequency	relative value of ε
$n=1$	100 Hz	1
2	200	0.38
3	300	0.14
4	400	0.28

Harmonic		
order	frequency	relative value of ε
$n=1$	100 Hz	1
2	200	0.89
3	300	0.47
4	400	0.07

Fig. 3.10. The instantaneous value of the magnetostriction factor versus time for ideal iron under the influence of a sinusoidal flux density variation with time. $B_{max}=1.5$ T

Fig. 3.11. The instantaneous value of the magnetostriction factor versus time for ideal iron under the influence of a sinusoidal flux density variation with time. $B_{max}=1.8$ T

Looking at the table, we can see that the relative values of elongation harmonics increased considerably. The magnetostrictive deformation increases substantially with flux density, and consequently the noise of saturated transformer cores will also increase.

Foster and Reiplinger [27] conducted a very interesting experiment to determine how important is the role of magnetostrictive elongation harmonics in noise generation. First they determined the magnitude of magnetostriction factor harmonics for each harmonic frequency in a given iron material, then they measured the noise component of corresponding frequency, L_n, in decibels. As in the case of other mechanical noise sources, the resultant noise of transformers is measured by an A-weighting filter, so they weighted each noise component according to the frequency response of the A-weighting filter. (The A-weighting filter networks will be discussed in Chapter 13 in detail.) The measured values are shown in

Table 3.5. The participation of magnetostrictive elongation harmonics in noise [26]© 1981 IEEE

Frequency, Hz	Order					
	$n=1$ 100	$n=2$ 200	$n=3$ 300	$n=4$ 400	$n=5$ 500	$n=6$ 600
$\varepsilon_n 10^6$	1.35	0.368	0.0885	0.0147	0.0117	0.015
L_n, dB	81.8	76.5	67.7	54.5	54.5	58.1
L_n, dB(A)	62.7	65.7	61.2	49.7	51.3	56.2

The unweighted resultant sound pressure level is $L=83$ dB.

The A-weighted sound pressure level is $L_A=69$ dB.

where $\varepsilon_n=$ the peak value of the nth harmonic of the magnetostriction factor,

L_n, dB $=$ the sound pressure level produced by the nth magnetostriction harmonic,

L_n, dB(A) $=$ the sound pressure level produced by the nth magnetostriction harmonic, corrected by an A-weighting filter.

Table 3.5. It can be seen that the harmonics of ε drop sharply with increasing order, but this trend is not so striking in the sound pressure levels produced by the individual harmonics. The 100 Hz noise component seems to be dominant. We have quite a different picture, if we consider the A-weighting filter that simulates the frequency response of the human ear. In the third row of the table we see the sound pressure level components in A-weighting. Thus it shows that the magnitudes of noise components are comparable up to quite high orders, which means that the magnetostrictive deformation harmonics are important noise sources. The A-weighted sound pressure level is primarily determined by the harmonics.

3.5.2 Factors which modify the effect of magnetostriction

There are several factors that affect the magnetostrictive deformation of transformer core laminations. We saw before that the magnitude of flux density affects the value of ε and even its harmonic content.

In our discussion, as generally accepted in the literature, we illustrate the effects of the individual factors with the aid of magnetostriction curves recorded by d.c. magnetization.

One of the first findings was that alloying with silicon (i.e., silicon-irons) has a considerable effect on magnetostrictive deformation. Curves (a), (b) and (c) in Fig. 3.12 illustrate the variation of specific magnetostrictive elongation with flux density for hot-rolled iron material of 2.4, 4 and 6 percent silicon content, respectively. We see that magnetostriction can almost be eliminated in hot-rolled sheet

iron by increasing the silicon content of the metal, as illustrated by curve (*c*) in Fig. 3.12. Unfortunately, Si-alloying substantially deteriorates the machinability of sheet materials, so this method is not feasible in practice.
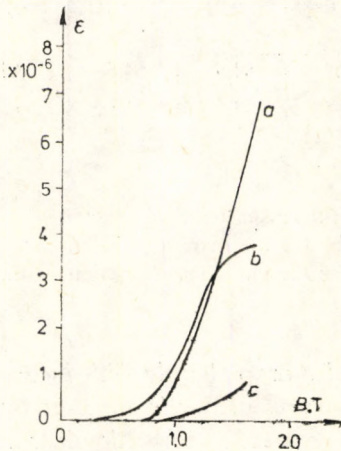
Fig. 3.12. The magnetostriction factor of sheet materials versus flux density: *a* — hot-rolled 2.4 percent Si, *b* — hot-rolled 4 percent Si, *c* — hot-rolled 6 percent Si
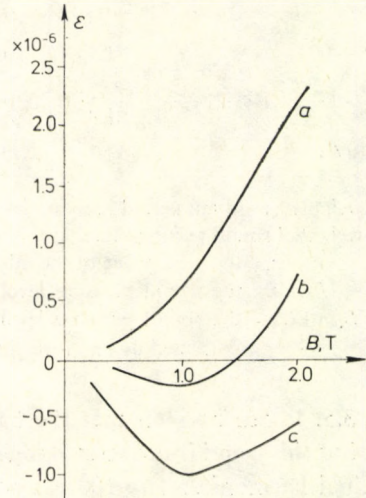
Fig. 3.13. The magnetostriction factor of plate steel M5X versus flux density for various stress relieving temperatures: [26] *a* — stress relieving at 780°C, *b* — stress relieving at 820°C, *c* — stress relieving at 850°C
(© 1981 IEEE)

   The specific magnetostrictive elongation of cold-rolled sheet iron is generally smaller than that of hot-rolled materials. Care must be taken when the laminations are cut and built into the core, because not only the specific iron loss, but also the magnetostriction factor of cold-rolled plate steel, vary with the orientation of the flux with respect to the direction of rolling. Cold-rolled plates are very sensitive to any kind of treatment. According to Foster and Reiplinger [27], the post-roll stress-relieving heat treatment temperature decisively affects the value of the magnetostriction factor. Figure 3.13 shows the specific elongation curves of plate steel M5X for 5-minute heat treatment at various temperatures. The heat treatment was followed by slow cooling in each case. By increasing the temperature, the curve could be shifted completely to the negative quadrant of elongation. The usual heat treatment temperature of 800 to 820°C proved to be very good in practice.
   The experiments conducted by the two above authors revealed that the slightest external mechanical impact could fully offset the magnetostriction-factor-decreasing

effect of heat treatment. They dropped an object of 330 g weight from a height of 20 mm onto a properly heat-treated sample plate of slightly negative magnetostric‐ tive properties, with a contact area of 5 mm radius. After five to six drops, the elongation increased to an extent equivalent to a 30-degree decrease in heat treating temperature. A similar effect can be achieved by static pressure exerted in the direction of rolling.

3.5.3 Predicting the magnetic noise of transformers

The magnetic noise of transformer cores was calculated for years on the basis of specific magnetostrictive elongation curves obtained by d.c. magnetization, measured on plate samples. However, the predicted figures were frequently found to deviate significantly from the values determined by noise measurement. The reason was that in determining the magnetostriction factor by d.c. magnetization, they did not take into account the harmonic elongation components that exist in reality, and the imponderable mechanical impacts that the plate material had been subjected to during the manufacturing process. The latter problem is very hard to control, but for the former, namely that how to calculate with the elongation harmonics, Reiplinger and Stelter suggest a sensible procedure [91].

From their experiments, they claim that more accurate noise prediction is possible if we use the measurable mechanical vibration velocity $v = d\varepsilon/dt$ of the plate sample instead of the magnetostriction factor obtained by d.c. magnetization in our calculations. As the transformer noise is measured in units of A-weighted sound pressure level, we also measure the vibration velocity in A-weighting. Now the measured v_A values reflect the effects of elongation harmonics as well. If we relate the value of v_A to the unit plate length, l_0 we then obtain a parameter
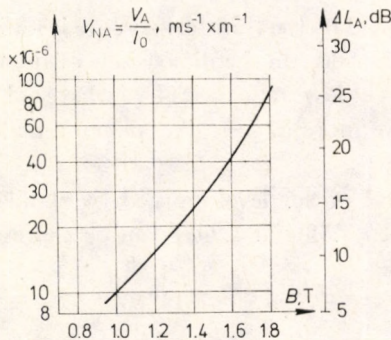
Fig. 3.14. The variation of the A-weighted vibration velocity and A-weighted sound pressure level with flux density

v_{NA}, which is characteristic of the plate material in terms of noise generation. Figure 3.14 shows the variation of v_{NA} with flux density for a plate material, Hi–B. The vertical scale ΔL_A on the right side of the figure directly shows the change of sound pressure level caused by a change of ΔB in the flux density. The A-weighted sound pressure level to be measured on the surface of a laminated iron core of length l can be written in terms of v_A as:

$$L_A = k_1 + 20 \log \left(\frac{v_A}{v_0} \frac{l}{l_0} \right), \tag{3.58}$$

where $v_0 = 1$ m s^{-1} and $l_0 = 1$ m,
    k_1 — empirical constant,
    v_A — measured vibration velocity in A-weighting,
    l — length of flux path in the iron core.

The constant k_1 allows for the non-uniform flux density across the cross-sectional area of the iron core and the cross fluxes of flux transitions at the lamination junctions in the core corners. These secondary effects can be considered as constant for a given core design.

If we consider the approved laws of growth and rations which express the relations between transformer sizes, mass and power, we can determine the A-weighted sound power level emitted by the transformer core in terms of the vibration velocity v_A measured on the sample made of the lamination material, using the following formula:

$$L_{WA} = k_2 + 20 \log \frac{v_A}{v_0} + \frac{20}{3} \log \frac{m}{m_0}, \tag{3.59}$$

where m — mass of transformer core,
    $m_0 = 1$ kg,
    k_2 — a constant characteristic of the given core design.

The sound power generated by the transformer core is radiated to the environment with an efficiency that depends on the dimensions of the transformer tank. Small tanks are poor radiators at low frequencies (see what said about σ in Chapter 1), while large tanks behave more or less like plane radiators with high efficiency ($\sigma = 1$).

The A-weighted sound power level emitted by standard power transformers with flux density between 1.65 and 1.75 T can be expressed with good approximation as:

$$L_{WA} = 20 \log (P/P_0) + 55, \tag{3.60}$$

where P — the rated power of the transformer in MVA,
    $P_0 = 1$ MVA.

Potentiometer range: __50__ dB Rectifier: __r.m.s.__ Lower lim. freq: __50__ Hz Writing speed: __315__ mm s^{-1} Paper speed: ____ mm s^{-1}

$\overline{L}_A$ = 59.6 dB

L_{WA} = 71.5 dB

Multiply frequency scale by: __1__   Zero level: __20 dB__

A B C Linear
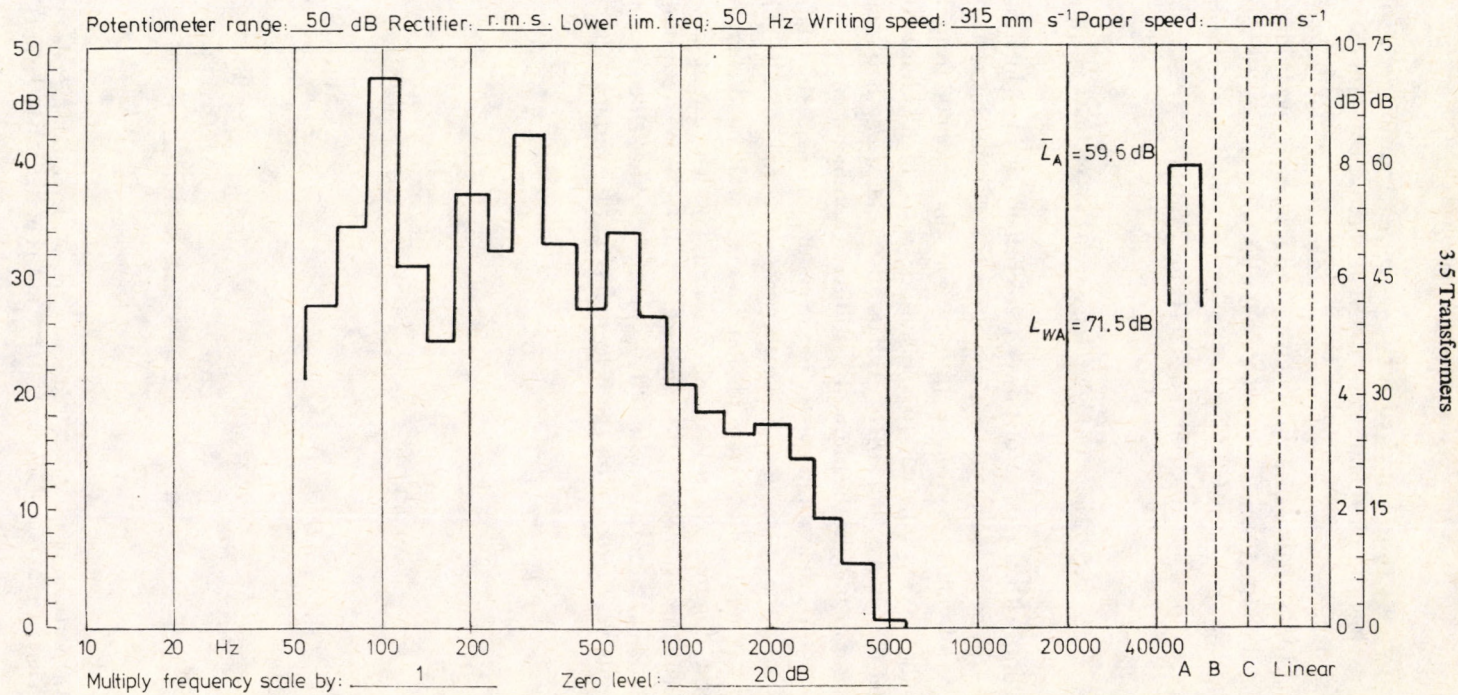
Fig. 3.15. The one-third-octave-band frequency spectrum of the sound pressure level of the oil
transformer NA 400/10 (10.5/0.4 kV, 400 kV)

A similar formula can be derived for lower power transformers, with different factor for the logarithmic quantity and different additive constant characteristic of the given design.

Figure 3.15 shows the one-third–octave–band frequency spectrum of the sound pressure level emitted by a 10.5/0.4 kV, 400 kVA oil transformer, measured at a distance of 1 m.

The expected peaks at 100, 200 and 300 Hz are evident.

3.5.4 Noise of high voltage transmission lines

In connection with the noise of power transformers, it is of interest to discuss here briefly the noise generated by high voltage transmission lines.

The noise of a.c. high voltage transmission lines results from the corona discharge that occurs adjacent to the surface of the high-voltage conductor. It depends on the number and size of strands, the field strength on the surface of the conductor or bundle, the physical condition of conductor surfaces and the age of the conductor surfaces and the age of the conductor. Also, the relative position and distance of the phases and the weather may effect the noise magnitude.

The noise of high voltage transmission lines is of wide band character, ranging from several hundred Hz to several thousand Hz. The use of an A-weighting network in the measurement proves to be favourable again. According to American calculations and experimental data [63], the A-weighted sound pressure level depends very strongly on the field strength at the surface of the conductor,
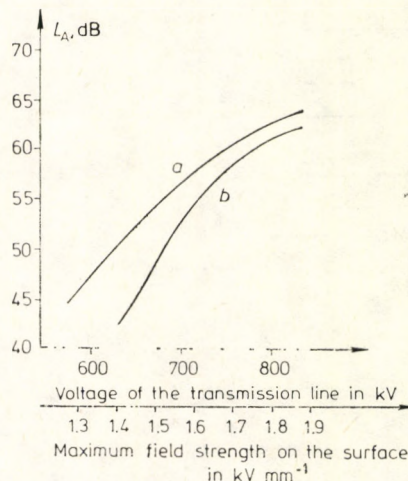
Fig. 3.16. The variation of the A-weighted sound pressure level with the rated voltage of the transmission line: a — in rain of 2.5 mm h^{-1}, b — in rain of 0.25 mm h^{-1} [62]. (© 1983 IEEE)

as shown in Fig. 3.16. A 40 percent increase in field strength (from 1.3 kV mm^{-1}) to 1.8 kV mm^{-1}) results in a 15 dB increase in noise. The difference between the two curves shows that rain is the particular weather factor to which special attention must be paid. Laboratory experiments were conducted to determine the relationship between transmission line noise and the quantity of rain. The results are illustrated in Fig. 3.17. The correlation between the A-weighted sound
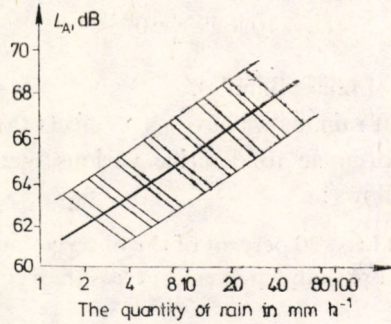
Fig. 3.17. The variation of the A-weighted sound pressure level with the quantity of rain
[62]. (© 1983 IEEE)

pressure level and the quantity of rain is apparent, though the dependence is not too strong. If the amount of rain increases at a rate of 30 times (from 2 mm h^{-1} to 60 mm h^{-1}), the noise increases only by 6 dB.

The subjective judgement of transmission line noises in terms of spectral characteristics depends on the distance from the transmission line. It is well known that absorption in air varies with frequency, and therefore the damping of high-frequency components is stronger than that of low-frequency ones with distance. The law of distance discussed in Chapter 1 (i.e., 6 dB decrease with double the distance) does not apply here owing to the environmental background noise.

In the case of d.c. high voltage transmission lines, we find that only the positive conductor emits noise and it is not dependent on rain.

There are empirical formulae for the calculation of the A-weighted sound pressure level emitted by a high voltage transmission line. The expression of A-weighted sound pressure level includes four functions with the following variables:

g — field strength on the surface of the bundle conductor in kV cm^{-1},
n — number of strands per phase,
d — diameter of strands in cm,
D — distance of observation point from transmission line, in m.

Also included are five empirical constants, k, k_1, k_2, k_3 and k_4, and, finally, the reference level L_0 in A-weighting. The general formula published by different

authors in different countries for the sound pressure level in A-weighting for one phase is written as:

$$L_{Aj}=k_1 f_1(g)+k_2 f_2(n)+k_3 f_3(d)+k_4 f_4(D)+L_0+k. \tag{3.61}$$

The resultant A-weighted sound pressure level of a three-phase transmission system can be expressed as the sum of the sound pressure levels for each phase:

$$L_A=10 \log \sum_{j=1}^{m} 10^{0.1 L_{Aj}}, \tag{3.62}$$

where m is the number of phase bundles.

In view of the fact that rain, as we have seen, affects the noise level, experts set up various empirical formulae to describe various meteorological conditions. Three of them are as follows:

$L_{A, 50}$ — it is raining at least 50 percent of the observation time,

$L_{A, 5}$ — it is raining more than 5 percent but less than 50 percent of the observation time,

$L_{A, max}$ — this is the maximum sound pressure level in A-weighting, measured during pouring rain.

Now we review the formulae that give results closest to the measured values, as confirmed by experience. In each case, we indicate the source.

The A-weighted sound pressure level of one phase of an a.c. power transmission line is given as:

$$L_{A, 50}=120 \log (g)+k_2 \log (n)+55 \log (d)-11.4 \log (D)+L_0, \tag{3.63}$$

(Bonneville Power Plant Trust, USA)

where $k_2=26.4$ and $L_0=-128.4$ for $n \geq 3$,
$\qquad k_2=0$ and $L_0=-115.4$ for $n<3$.

Application range:

$$230<U_n<1500 \text{ kV},$$

$$n \leq 16,$$

$$2 \leq d \leq 6.5.$$

$$L_{A, 5}=-665g^{-1}+20 \log (n)+44 \log (d)-10 \log(D)-0.02D+k'+k''. \tag{3.64}$$

(General Electric, U.S.A.)

where $L_0=75.2$ and $k'=0$ for $n<3$,
$\qquad L_0=67.9$ and $k'=[22.9(n-1)d/B]$ for $n \geq 3$.

B — the diameter of the phase bundle in cm,

$k''=7.5$ for $n=1$,

$k''=2.6$ for $n=2$,

$k''=0$ for $n=3$.

Application range:

$$230 < U_n < 1500 \text{ kV},$$

$$1 \leq n \leq 16,$$

$$2 \leq d \leq 6.$$

$$L_{A,\,max} = 2g + 18 \log(n) + 45 \log(d) - 10 \log(D) - 0.3. \qquad (3.65)$$

(FGH, Federal Republic of Germany)

Application range:

$$n \geq 6,$$

$$2 \geq d \geq 6.$$

The A-weighted sound pressure level produced by one positive-polarity bundle of a d.c. power transmission line is found to be:

$$L_{A,\,50} = 86 \log(g) + k_2 \log(n) + 40 \log(d) - 11.4 \log(D) + L_0, \qquad (3.66)$$

(Bonneville Power Plant Trust, U.S.A.)

where $k_2 = 25.6$ and $L_0 = -100.6$ for $n \geq 3$,

$\quad\quad\; k_2 = 0$ and $L_0 = -93.4$ for $n < 3$.

$$L_{A,\,max} = 1.4 \log(g) + 10 \log(n) + 40 \log(d) - 10 \log(D) - 1. \qquad (3.67)$$

(FGH, Federal Republic of Germany)

Application range:

$$2 \leq n \leq 5,$$

$$2 \leq d \leq 4.$$

3.6 Direct current machines

The electromechanical energy conversion in a d.c. machine is accomplished through the interaction of magnetic fields generated by the currents flowing in the excitation coils wound on the salient pole of the stator and in the armature current carriers and the currents themselves. The armature and its wires lying in its slots rotate in the magnetic field established by the poles.

The circumferential distribution of the radial component of the flux density in the air gap below the pole (pole shoe), the so-called field curve, is shown in Fig. 3.18.
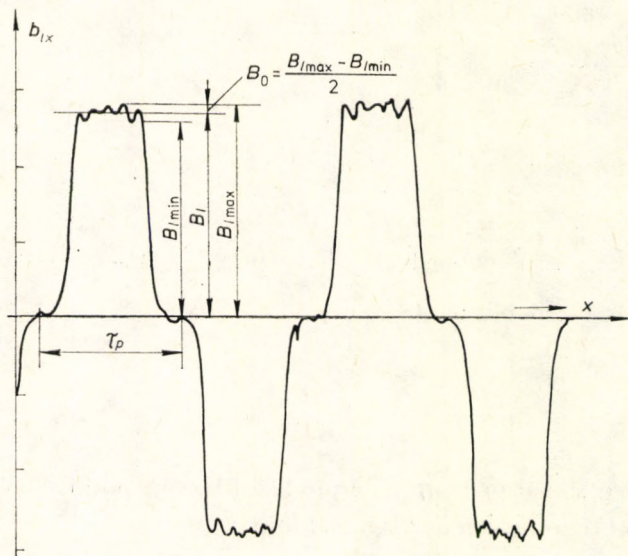
Fig. 3.18. The circumferential distribution of flux density in a compensated d.c. machine, measured on a four-pole machine with rated output of 5 kW

Owing to the rotor slots, the effective air gap length changes to $\delta_i = k_c \delta_g$, where δ_g is the geometrical air gap length and k_c is the Carter factor. The effect of the varying reluctance is noticeable on the field curve.

The shape of the field curve shown in Fig. 3.18 is independent of the load for a properly compensated d.c. machine. On this basis, assuming that the air gap flux density is zero outside the boundaries of the pole shoes, the distribution of air gap flux density below the pole shoe and along the circumference can be approximated by the constant and the first harmonic term of the Fourier series of the periodic circumferential distribution function, as:

$$b_{lx} = B_l + B_0 \cos \frac{2\pi}{t_p} x,$$

where t_p — tooth pitch,
$\quad x$ — space coordinate round the circumference.

Since the rotational speed of the armature is n, then for a two-pole machine the radial flux density may be expressed as:

$$b_{lx} = B_l \left[1 + \frac{B_0}{B_l} \cos \left(\frac{2\pi}{t_p} x - \omega t \right) \right], \qquad (3.68)$$

where $\omega = 2\pi n$.

The armature excitation modifies the field curve, if the machine is uncompensated. In order to keep down the costs and machine sizes, the commutation is improved primarily by utilizing interpoles in small d.c. machines. The field distortion still impairs commutation and decreases the effective flux. The flux of the interpole hardly influences the flux of the main poles. In d.c. motors without compensating coil, the field distribution under load is different from that shown in Fig. 3.18. The valid expression is:

$$b_{lx} = B_l \left[\Gamma(x) + \frac{B_0}{B_l} \cos\left(\frac{2\pi}{t_p} x - \omega t \right) \right]. \tag{3.69}$$

The function $\Gamma(x)$ can be determined from the circumferential distribution of flux density and depends on the armature-reaction and the degree of saturation. For an unsaturated machine, its value is 1 and eqn. (3.69) takes the form of eqn. (3.68).

The force acting on a unit pole surface area is found to be:

$$p(x, t) = \frac{B_l^2}{2\mu_0} \left[\Gamma^2(x) + 2\frac{B_0}{B_l} \Gamma(x) \cos\left(\frac{2\pi}{t_p} x - \omega t \right) + \left(\frac{B_0}{B_l} \right)^2 \cos^2\left(\frac{2\pi}{t_p} x - \omega t \right) \right]. \tag{3.70}$$

The term multiplied by $(B_0/B_l)^2$ may be neglected due to its low amplitude, so we arrive at the following formula expressing the radial force:

$$p(t) = l_i \int_{-b_i/2}^{+b_i/2} p(x, t)\, dx = \frac{B_l^2}{2\mu_0} l_i \int_{-b_i/2}^{+b_i/2} \left[\Gamma^2(x) + 2\frac{B_0}{B_l} \Gamma(x) \cos\left(\frac{2\pi}{t_p} x - \omega t \right) \right] dx, \tag{3.71}$$

where b_i — the ideal pole arc and,
$\quad\quad l_i$ — the ideal iron length in the axial direction.

Integrating for no-load condition (or for compensated machine), we get the force acting on one pole:

$$p(t) = l_i \frac{B_l^2}{2\mu_0} \int_{-b_i/2}^{+b_i/2} \left[1 + 2\frac{B_0}{B_l} \cos\left(\frac{2\pi}{t_p} x - \omega t \right) \right] dx =$$

$$= \frac{b_i l_i}{2\mu_0} B_l^2 + \frac{l_i t_p}{2\mu_0 \pi} B_0 B_l \left[\sin\left(\frac{\pi}{t_p} b_i + \omega t \right) + \sin\left(\frac{\pi}{t_p} b_i - \omega t \right) \right]. \tag{3.72}$$

According to eqn. (3.72), a constant pull is acting on the pole and, through it, on the yoke, and also a forward and a backward rotating force wave of angular frequency ω are present, with sinusoidal circumferential distribution. If this frequency is identical with one of the natural frequencies of the d.c. machine, then

resonance may occur, and chances are that it will, because d.c. motors are typically used in wide speed range, so the value of ω also varies over a wide range. The risk of resonance is further enhanced by the higher harmonics of the Fourier expansion of the flux density distribution, eqn. (3.69).

In the d.c. machines of today, noises of mechanical and aerodynamic origin dominate, and the importance of noises and vibrations of electromagnetic origin is less prominent.

4. VIBRATION OF ROTATING ELECTRICAL MACHINES

In Chapter 3, we determined the radial force waves acting on the rotating electrical machine, which were found to be waves of different mode numbers and different distribution in the air gap round the periphery. These waves propagate with different angular velocities round the rotor in the same or opposite sense as the rotor, acting on both stator and rotor. With the exception of the bending force wave of mode number $r = 1$, all exciting forces result in a more significant deformation of the stator.

For $r = 1$, the rotor seems to be more flexible. Bending forces of mode number $r = 1$ present the greatest problem in high-power rotating machines with flexible rotor and large bearing span. (A rotor is said to be flexible if its first critical speed is below or just above the rotational speed of the rotor.) The calculation of critical speeds (natural frequencies) for such machines is feasible by the section matrix method run on digital computers. The details of this method will not be presented here, but we give an approximative formula for the determination of the first critical rotational frequency of the commonest low- and medium-power machines.

Any force wave of frequency f_r and mode number r gives rise to a set of vibrations of order j and frequency f_r in the rotating electrical machine. (The standard vibration calculation methods, like the one set out in [53], simplified the procedure by attributing only one deformational force wave to each exciting force wave, with identical frequency f_r and mode number $r(r=j)$.). The instantaneous value of the deformational wave is shown in Fig. 4.1 for various vibrational mode numbers. The magnitudes of vibration components depend on the mechanical vibrational characteristics of the machine in terms of its eigenfunction, on the magnitude of the exciting force, the difference between the frequency f_r of the exciting force and the natural frequencies F_j of the machine, and on the damping conditions within the machine.

If the frequency f_r of the exciting force is close to or equal to any of the natural frequencies F_j of the machine, then resonance occurs, which results in dangerous deformations and vibrations and a substantial increase in noise. The
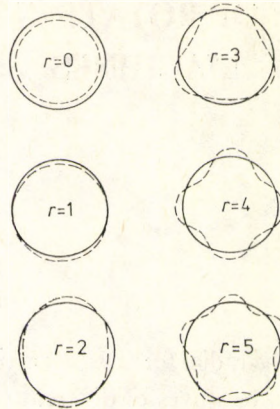
Fig. 4.1. Deformational waves of various mode numbers

r.m.s. value of the vibrational velocity produced by a force wave with amplitude P_r, frequency f_r and mode number r is given as:

$$v_{fr} = \sqrt{2}\,\pi f_r \sum_j H_j P_r, \tag{4.1}$$

where H_j — the system function of the electrical machine as a mechanical vibrating system.

The crucial step in the calculation of the system function is the determination of the correct value of the mechanical natural frequency.

More than one hundred years ago, the first calculations were accomplished for a freely vibrating homogeneous ring. Later they introduced additional masses to take the effect of teeth and winding into account. In view of the weak damping of low-frequency mechanical vibrations, they neglected the effects of damping on the natural frequency. They also neglected the effects of the housing, end shields and foot, the tangential forces and rotary inertia.

Jordan *et al.* [56] already introduced in their calculations the effects of shear and rotary inertia. The results were acceptable for medium-power machines. Lübcke improved on the thin ring theory, but his modifications were gained only experimentally, and thus they were not directly applicable to other designs.

Erdélyi [25] applied the double-ring method to medium size machines. The model of two thin rings joined by key bars, however, gave results close to the measured data only when the ratio of the radial thickness of the core to the mean radius of the core was less than 0.2.

Ellison and Yang [23] improved on Erdélyi's method. They investigated the natural frequencies of a stator consisting of a thin frame and a thick laminated core loaded with teeth and windings, solidly coupled at key bars, taking into account

the effects of deformation, shear and rotary inertia. They based their calculation on Lagrange equations written and solved in matrix form.

All of the above methods considered the machine stator as a cylindrical ring with an infinite number of symmetry axes. However, it was found in practice and confirmed by experiments of the German Hübner and the Russian Medvedjev and also by Hungarian experiments that the position of support and airducts, etc. strongly modify the calculation procedures used before to determine the natural frequencies. The finite element method gives correct results but requires large-capacity and fast computers. Our discussion is limited to simple methods that can be used in manual calculations or require at a maximum personal computers as aids.

For a rough estimation of the mechanical natural frequencies of a.c. rotating machines, the formulae of Frohne [29] may be used, who assumed an ideally symmetrical stator. It is worth noting that the vibrating capability of the machine improves with increasing size, and the mechanical natural frequencies become lower, so the natural frequencies or higher mode number appear within the audible range.

4.1 Vibration calculation for radially symmetrical a.c. machines

The system function H_j introduced in eqn. (4.1), which represents the relationship between the force acting on the system and the vibration deformation excited by it, is split into two components, as commonly found in the literature. One of them, H_{js}, contains the geometrical dimensions of the machine, the quality of the material and the mode number j. This component provides the deformation for the case where the mode number of the exciting force, r, equals j and the frequency would be $f_r = 0$, i.e., the deforming force will not vary in time. The second component, H_{jn} depends on the difference between f_r and the mechanical natural frequency F_j, characteristic of the vibration mode, $r = j$, and on the internal damping conditions. This latter component is sometimes referred to as the magnification factor. The two components of the system function H_j are shown in Table 4.1, together with the formula of the natural frequency corresponding to the individual vibration modes.

The main source of the damping D is the friction on the contacting surfaces of the winding and the laminated core. The theoretical determination of damping is extremely complex, and it is therefore derived experimentally with the help of the half-energy points. The vibrational displacement is plotted versus the excitation force frequency for mode number j, maintaining a constant force amplitude. This

Table 4.1. The system function of small and medium-sized a.c. machines

Mode number	H_{js}, the static component of the system function	H_{jm}, the magnification factor	F_j, the mechanical resonance frequency
$r=0$	$\dfrac{R_s R_{my}}{E\,h_y}$	$\dfrac{1}{\sqrt{\left[1-\left(\dfrac{f_0}{F_0}\right)^2\right]^2+\left[2D_{s0}\dfrac{f_0}{F_0}\right]^2}}$	$F_0=\dfrac{83\,750}{R_{my}\sqrt{\varDelta}}$
$r=1$	$\dfrac{4R_r l_r l_b^3}{3d^4 E}$	$\dfrac{1}{\sqrt{\left[1-\left(\dfrac{f_1}{F_1}\right)^2\right]^2+\left[2D_{r1}\dfrac{f_1}{F_1}\right]^2}}$	$F_1=\sqrt{\dfrac{3}{16\pi}\dfrac{Ed^4}{M_2 l_t^3}}$
$r=2$	$\dfrac{12R_s R_{my}^3}{E(j^2-1)^2 h_y^3}$	$\dfrac{1}{\sqrt{\left[1-\left(\dfrac{f_r}{F_j}\right)^2\right]^2+\left[2D_{sj}\dfrac{f_r}{F_j}\right]^2}}$	$F_j=F_0\sqrt{\dfrac{B}{2A}\left(1\pm\sqrt{1-\dfrac{4AC}{B^2}}\right)}$

where R_s = stator bore radius,
R_{my} = stator yoke mean radius,
h_y = stator yoke height,
E = the modulus of elasticity for iron,
R_r = outside radius of rotor core,
l_r = length of rotor core,
l_b = bearing distance,
d = shaft diameter,
D_s = stator internal damping,
D_r = rotor internal damping,
G_{t1} = stator teeth weight,
G_{w1} = stator winding weight,

G_{y1} = stator yoke weight.
j = mode number

$$\varDelta=1+\frac{G_{t1}+G_{w1}}{G_{y1}}$$

$$A=1+\frac{h_y^2}{12R_{my}^2}\left[j^2\left(3+\frac{\varDelta_m}{\varDelta}\right)-3\right]$$

$$B=\frac{h_y^2}{12R_{my}^2}(j^2-1)\left[j^2\left(4+\frac{\varDelta_m}{\varDelta}\right)+3\right]+(j^2+1)$$

$$C=\frac{h_y^2}{12R_{my}^2}j^2(j^2-1)^2$$

$$\varDelta_m=1+\frac{S_1}{2\pi}\frac{l_t b_t}{R_{my}h_y^3}(4l_t^2+6l_t h_y+3h_y^2)$$

l_t = stator tooth length,
b_t = mean width of stator tooth,
S_1 = stator slot number,

$$M_2=2\pi10^3[l_r(4R_r^2-d^2)+l_b d^2]$$

(All quantities of length dimension in m)

curve, on a different scale, is also the curve of the magnification factor (see Fig. 4.2). The damping factor D for the vibration conditions having mode number j is found to be:

$$D_j = \frac{f_{0.707}}{2F_j} = \frac{f_2 - f_1}{2F_j}.$$ (4.2)
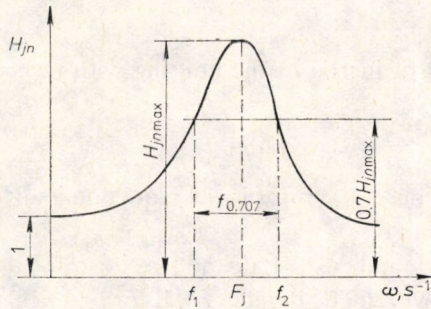
Fig. 4.2. The frequency-dependency of the magnification factor

For asynchronous machines, the value of D is normally in the range of 0.01 to 0.04, independently of the mode number. The value of D is strongly dependent on the advancement in the assembly of the machine.

4.2 Vibration of d.c. machine stators

The magnetic noise and vibration of d.c. machines are generally less important than those of mechanical origin. However, care must be taken to keep the frequency of the force acting on the machine apart from the natural frequency of the mechanical system comprising the yoke, the main poles and the interpoles. In case of coincidence, the resonance produced will substantially amplify the amplitude of vibrations. The natural frequency of the housing may be expressed as:

$$F_h = \frac{1}{2\pi\sqrt{mX}},$$ (4.3)

where m — the equivalent mass,

$\quad\quad X$ — the specific deformation dependent on the mode number of the vibration.

When the mode number is zero, $r = 0$, then:

$$X_0 = \frac{R}{2\pi ES},$$

where E — the modulus of elasticity,

   S — the cross-sectional area of the housing,

   R — the mean radius of the housing.

For a vibration of mode number $r=2$,

$$X_r=\frac{R^3\varrho^2}{2\pi EI},$$

where I — the moment of inertia of the housing with respect to the shaft and is given as:

$$\varrho=(r\sqrt{r^2+1})^{-1}. \tag{4.4}$$

For $r=1$, the deformation of the rotor is the more dominant as we saw in the case of asynchronous machines.

If forces with mode number $r\neq 1$ do not excite resonance, it is sufficient to calculate the vibration with mode number $r=1$, for practical purposes.

4.3 Determining the mechanical resonance frequency by measurement

As we saw in the previous chapter, the resonance frequency can be calculated only for models which neglect certain factors. The simpler the model and the easier the calculation, the less correct the result will be. If, in turn, the model and the mathematical tools are more complex, then we need sophisticated computer programs, tedious preparatory work and costly computer time, and still we would know the resonance frequencies for one model only!

The resonant frequencies of a complex, real system should be determined by measurement, but no exact procedure exists for this purpose at present. To get a correct result by measurement, we would need an excitation system that could produce a rotating radial directional travelling force wave with sinusoidal peripheral distribution, variable mode number and constant amplitude independent of the frequency. In such a case, the resonant frequencies could be measured directly by means of sensors located at the periphery of the machine. Nevertheless, such a system does not exist, and if the excitation is not the same as in reality, it is doubtful that the measurement yields correct results.

The literature and the experts who work in this field suggest various approxima=tive methods. These methods differ in the mode of excitation.

(a) Stationary excitation with sinusoidal distribution in space and sinusoidal variation time. It can be generated by the appropriate connection of the stator

winding. Its major drawback is that only one mode number, twice the pole pair number of the machine, can be set ($r=2p$).

(b) Travelling wave of sinusoidal alternation in space and of sinusoidal variation in time. It can be generated by a three-phase variable-frequency supply connected to the complete three-phase winding system. Its major drawbacks are that only the case of $r=p$ can be examined and a three-phase generator of power identical with the no-load power of the machine tested is required, and, apart from the tested fundamental, all the winding, slotting, eccentricity, etc. harmonics are present.

The common advantage of methods (a) and (b) is the sinusoidal distribution of the exciting force in space and sinusoidal variation of time round the periphery, while the common drawbacks are the limited mode numbers that can be tested and the difficult realisation of the measurement.

(c) Point-like excitation with sinusoidally time-varying signal. If we can place any number of, say, electrodynamic exciting elements over the periphery, fed by a proper variable-frequency supply that allows adequate timing for each element, then this is the best method, although the circumferential distribution of the force wave is not sinusoidal. Its disadvantage is its being very costly as a special supply system is required.

(d) The point-like pulse excitation is the simplest method in terms of execution, which, being quick and easy, is its main advantage. Its major drawback is the fact that the generated excitation differs considerably from the theoretically required configuration. Further, the difficulties shift from the field of measuring techniques to the field of data evaluation. Owing to the fact that this is the only method whose execution is generally feasible in view of the commonly available technical apparatus, we briefly outline its theory.

The electrical machine as a system capable of vibrating can be considered as a mechanical four-terminal network (see Section 5.2 for more detail), where the input and output terminals correspond to the excitation and sensing, respectively. The input signal is the force, the sensed signal, the vibration. The response to a general excitation is called vibration acceleration and is expressed as:

$$a(t)= \int_{-\infty}^{t} f(\tau)h(t-\tau)\,\mathrm{d}\tau, \tag{4.5}$$

where $f(\tau)$ — the excitation function,
        $h(t-\tau)$ — the weighting function.

In our case, the excitation is pulse-like, a mechanical impact, modelled by a Dirac delta function, δ.

Accordingly, the vibration acceleration $a(t)$ is identical with the weighting function $h(t)$. Because of the difficulties of analysis in the time domain and because of the aim, we study the phenomenon in the frequency domain. As the energy represented by $f(t)$ is finite, its absolute value is also integrable, so the Fourier transform of $a(t)$ exists and is written in the form:

$$A(\omega) = \int_{-\infty}^{\infty} a(t)e^{-j\omega t}\, dt. \qquad (4.6)$$

The function $A(\omega)$ is directly measurable by means of a frequency analyser. The input is the single impact force, and the output is the resultant set of decaying free oscillations. As the decay time is short, the standard analysing methods cannot be applied.

It is known that if we make a pulse function periodic, its spectrum becomes a line spectrum in such a way that the spacing of the lines is equal to the inverse value of the cycle time, while their magnitude is determined by the original amplitude spectrum of the single pulse as the envelope curve. Depending on the bandwidth used in the analysis, we get either the lines of the "lined" spectrum or the envelope curve. By carefully selecting the bandwidth and the integration time, the spectrum of the original pulse can be determined.

Each component of the spectrum obtained represents one of the resonance frequencies of the machine in much higher numbers than we would expect on the basis of resonance frequency calculations for the individual machine components (e.g., stator, rotor, end shields, etc.). The measurement indicates not only the resonance natural frequencies of the individual parts but also the frequencies introduced by the assembly process, called coupling frequencies, which may create a real resonance danger situation in the assembled machine. One shortcoming of this method is that it is very hard to associate the obtained resonance frequencies with the individual vibration modes.

When a variable-frequency inverter is used as the power supply, the local vibration maxima may be observed by continuously changing the supply frequency, the resonance phenomena thus providing a tool to determine the mechanical resonance frequencies and internal damping conditions of the assembled asynchronous motor by measurement in the frequency range of interest in terms of noise and vibration.

The precondition of the appearance of local maxima in the curve of vibration velocity measured on the surface of the asynchronous machine versus the supply frequency, i.e., in the continuous function $v(f_1)$, is the coincidence of the exciting force frequency with one of the mechanical resonance frequencies of the motor. By measuring in the ± 30 percent neighbourhood of the frequency f_1 that produced

the local maximum, i.e., measuring the vibrations while the supply frequency is "tuned" and recording the spectrum by letting the vibration signal through a narrow-band, continuously tunable filter, the mechanical resonance frequency involved in the resonance may be determined from the set of spectra obtained with an accuracy dependent on the accuracy of the frequency analyser used for the measurements. The rate of change of the resonance-inducing exciting force component with respect to f_1 in the close neighbourhood of the resonant frequency allows the determination of vibration damping inside the assembled motor with the aid of the half-energy points.

5. GENERATION OF AIRBORNE NOISE
IN ELECTRICAL MACHINES

5.1 The radiation factor of a real machine

In Section 1.3, where we discussed the theoretical acoustical terms and concepts, we introduced the radiation factor, σ, as a measure of efficiency of energy transformation (from vibrational energy to sound energy) for a radiator with vibration velocity v. We saw that even for the simplest geometrical shapes, i.e., for spherical and infinite cylindrical radiators, the formulae of σ are very complex and complicated, and therefore, in practice, we use nomograms instead (see the curves of Figs 1.4 and 1.5).

In reality, the shape of electrical machines is more complex than the ideal geometrical shapes, so their radiation properties are studied on various simplified models. Alger considered the machine as a cylinder of infinite length (the corresponding set of curves σ is shown in Fig. 1.4). This model, however, gave acceptable results only for the middle section, even for machines with large l/D ratio (l is the length, D is the diameter of the machine), where the end effects due to the finite length of the machine are negligible. The Czech Narolski also gave his vote to the cylindrical radiator model [82]. Jordan gave preference to the spherical model (see the curves in Fig. 1.5). In England, Ellison, Moore and Yang investigated by calculation and experiment the variation of the relative radiated sound power factor for various real machine proportions to determine which model is most appropriate in the individual cases. The results of their investigation were published by Yang in 1975 [143].

When the machine is bounded by large plane surfaces (as in the case of rectangular parallelepiped figure so common today), it is a good approximation to assume the machine as a plane radiator.

In the literature on small- and medium-sized machines, we frequently find contradicting standpoints as outlined above. In the following, we try to review that changes in the value of σ result when different radiator models are used to simulate the common machine forms. We consider the diameter D of the cylinder accommodating the machine as the most characteristic dimension concerned. The vibration produced by the force wave that deforms the machine gives rise to deflections which travel round this cylindrical surface. This dimension corresponds
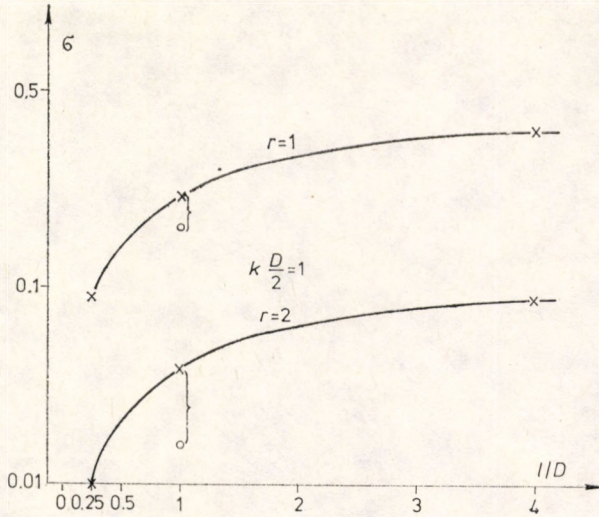
Fig. 5.1. The radiation factor for cylindrical radiators of various l/D ratio, where $kD/2=1$

to the diameter of the spherical or cylindrical radiator. Therefore, instead of kr indicated over the horizontal axis of Figs 1.4 and 1.5, we write $kD/2$. Let us look at Fig. 5.1 and see how the value of σ changes for $kD/2=1$ (where $k=2\pi f/c$). The top curve gives the values of σ for the deformational waves of mode number $r=1$ for a cylindrical radiator of finite length or for real machines of different l/D ratio. The bottom curve belongs to mode number $r=2$. Under each curve we indicated by a small circle the value of σ for the spherical radiator at $l/D=1$, since this cylindrical radiator shape is the closest approximation of the spherical radiator. Now let us see how the value of σ changes in Figs 5.2 to 5.4 for $kD/2=2$, 5 and 10. Note that for higher values of kD the relative radiated sound power is independent of the ratio l/D, disregarding the mode number. This suggests that at higher frequencies and for large machines it is immaterial which model is used for the calculation of the airborne noise. At lower frequencies and for small machines, however, there are significant differences between the values of σ obtained by different model radiators.

The airborne sound power emitted by an electrical machine with r.m.s. vibration velocity v can be determined from eqn. (1.22), if we have decided which model radiator to substitute for the machine. Apart from the model selection, we can make a general statement that small machines (with small value D) are poor sound radiators, while large machines are good ones. From experiments conducted in Hungary, one may conclude that the sound radiating capability of the housing of fully enclosed low and medium power motors is only slightly affected by the ribs on the surface.
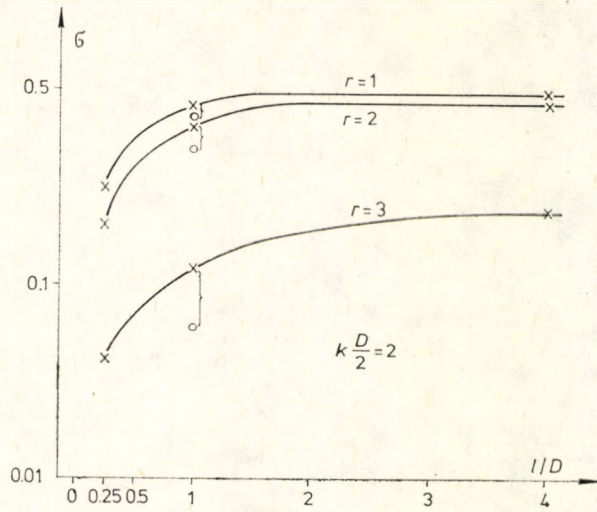
Fig. 5.2. The radiation factor for cylindrical radiators of various l/D ratio, where $kD/2=2$
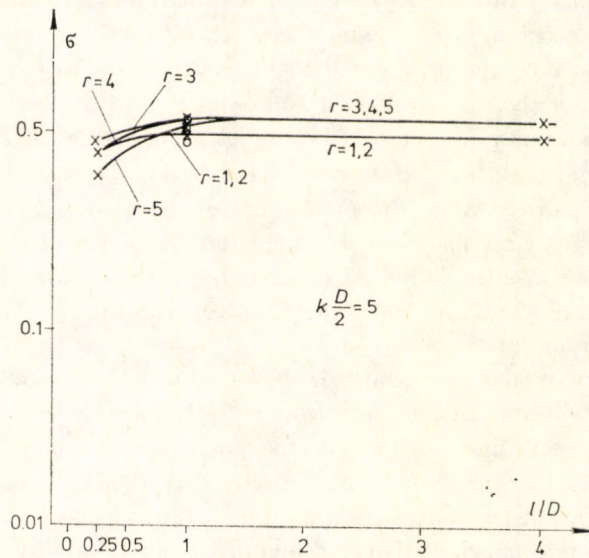
Fig. 5.3. The radiation factor for cyclindrical radiators of various l/D ratio, where $kD/2=5$
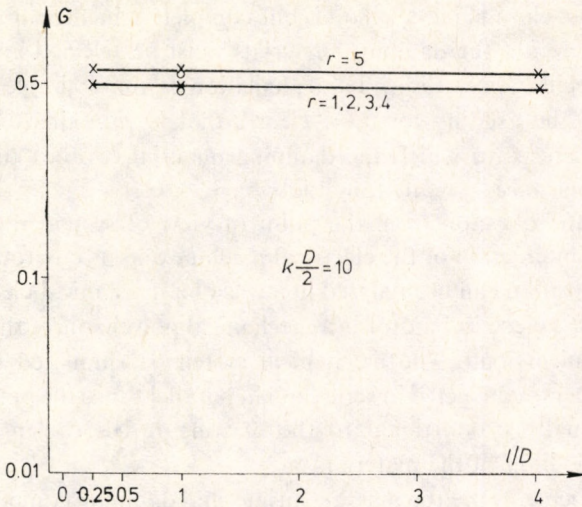
Fig. 5.4. The radiation factor for cylindrical radiators of various l/D ratio, where $kD/2 = 10$

5.2 Calculation of structure-borne sound transmission and emission

The electrical machine, together with its environment (e.g., machine base plate foundation) can be considered as a single mechanical vibrating system. This complex system can be analysed only in a complex way that takes the whole system into account. As a first approximation it is easier, and—in many cases—sufficient, to determine the resonant frequencies of each element separately (e.g., the electrical machine, the foundation, etc.) and compare them with the frequencies of the exciting forces, analysing their relative position. If any coincidence or tight closeness is found, then we may expect dangerous vibrations to occur. In certain complicated cases, we may have to refine the calculations, taking into account the coupling between subsystems. In the case of rigid coupling between the machine and its environment it can happen that the environment modifies the resonance frequencies of the stator of asynchronous machines as if reacting to it. This can explain the fact that a vibrationless machine set up on a foundation classified as non-dangerous still can give rise to strong vibrations. To avoid the flow of vibrational energy to the surroundings, the machines are mounted on vibration absorbing materials. The application of these materials requires careful consideration, because over-looking certain points might lead to disappointment. Ideal, "omnipotent" damping material does not exist. The damping material is just as frequency-dependent as, say, an electrical oscillatory circuit. It can be an excellent absorber for a given

frequency and its close neighbourhood, but completely inefficient at more remote frequencies. Therefore the damping materials must be selected and dimensioned for a given specific application. The calculation is quite simple if the spectral composition of the exciting force is "clear", that is, contains only one or two dominant frequencies to which the damping material can be "tuned". In other cases, the designer faces a really tough job.

Considering the question from the point of view of system theory, the inter-connection and interaction of the electrical machine and its environment, and also the resultant vibration can be analysed in terms of a mechanical-electrical analogy. In this system, the electrical motor is a mechanical power source that works on an external mechanical load. The mechanical system is simulated by a model of discrete components connected in series and in parallel, since the potential displace-ments are normally proportional to the exciting forces causing them to stay within the elastic limit of the material.

The discrete elements are the masses, springs and damping components involved in the vibration. The constituents and the configuration of the system do not change in time, and consequently the set of differential equations that describes the behaviour of this invariant system comprises equations of constant coefficients.

One of the most important characteristics of a mechanical power source is its output impedance [19], denoted Z_m. Also important are the output force, F_r, which can be measured at the output of the rigidly fixed, "blocked" power source (as output we mean the interface between the power source and the environment), and the "free" vibration velocity, v_f, which is measured at the output with the vibrating system suspended on a soft spring. The resonant frequency of the composite system comprising the suspension spring and the power source must be tuned far below the lowest-frequency force component of the power source to ensure unhindered vibration generation in all directions of space.

The relationship of the three characteristic parameters can be expressed as:

$$Z_m = \frac{F_r}{v_f}.\tag{5.1}$$

The values of F_r and v_f should be measured at the output of the mechanical power source in the three main directions of space. These directions are the radial, axial and transversal directions with respect to the electrical machine.

Across the terminals a and a' shown in Fig. 5.5, the electrical machine is substi-tuted by a power source with internal impedance in terms of vibration. Moving away from the source, each mechanical element in the row can be substituted for by a passive quadrupole. Since the deflections induced by the vibration do not exceed the elastic limit, these passive elements are linear in nature. Thus we arrive at the well known tandem connection of four-terminal networks. In order to be
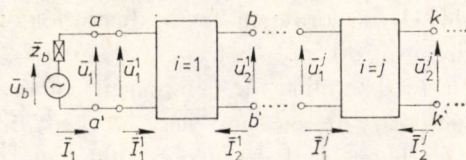
Fig. 5.5. The linear model of the asynchronous machine and its surrounding in vibration theory

able to use the established methods and symbols of electrical network analysis first we have to change over from the mechanical system to an electrical system.

If we compare the general equation of motion for a one-dimensional damped mechanical oscillating system (5.2) with the equation of a circuit comprising R, L and C components and connected to an a.c. power supply (5.3), then the formal analogy between the equations suggests analogy between the related phenomena as well. In this case, if we find the solution of the differential equation for one of the systems, then we have the solution for the other system:

$$m\frac{d^2y}{dt^2}+k\frac{dy}{dt}+\frac{y}{c}=F_0\cos\omega t, \tag{5.2}$$

$$L\frac{d^2Q}{dt^2}+R\frac{dQ}{dt}+\frac{Q}{C}=U_0\cos\omega t, \quad\text{and}\quad i=\frac{dQ}{dt}. \tag{5.3}$$

In our case, the most suitable corresponding mechanical and electrical parameter pairs are the following:

$$\begin{aligned} &F\sim U \quad k\sim R \\ &v\sim I \quad\quad c\sim C \quad Z_e\sim Z_m=\frac{F}{v}. \\ &m\sim L \quad y\sim Q \end{aligned}$$

The basic limitation of the model shown in Fig. 5.5 is that it applies only to one frequency and one direction. In reality, the vibration comprises many components of different frequencies.

In most practical cases it is enough to set up the model discussed above for one or two dominant components. The limination regarding the direction may be resolved by making an equivalent circuit for each of the three main directions. Determining the exciting components of the active two-terminal network, i.e., the exciting forces of the electrical machine, knowing the passive mechanical elements and applying the theory of cascade quadrupoles, the vibration velocity can be calculated for any point in the surroundings of the electrical machine. As is well known, the matrix form of the fundamental equation is written as:

$$\begin{bmatrix} U_1 \\ I_1 \end{bmatrix}=\begin{bmatrix} A_{11} & -A_{12} \\ A_{21} & -A_{22} \end{bmatrix}\begin{bmatrix} U_2 \\ I_2 \end{bmatrix}, \tag{5.4}$$

where the so-called chain parameters $A_{i,j}$ can be found in published parameter

tables (see for example [33]), according to the configuration of the passive quadru-
pole (*T*-network, π-circuit or other).

In order to be able to determine the components of the circuit diagram by
measurement, it is necessary to measure the "blocked" force and the "free"
vibration velocity at each terminal denoted by different letters, such as *a–a'*,
b–b', ..., *k–k'*, ... (see Fig. 5.5). From the results, the internal impedance of the
active two-pole and the elements of the passive four-poles can be determined.
Since the impedances of the two-pole and four-pole networks are complex quan-
tities, then in contrast with the usual procedure, it is not enough to measure the
r.m.s. value of the force and the vibration velocity, but the phase angle of the
measured quantities must also be recorded.

Using the model discussed, the vibrational energy at any point of the surround-
ings of the electrical machine can be determined from the vibration velocity and
the vibrating mass. From energy considerations, the airborne sound produced by
the vibration can be calculated as outlined before.

6. THE EFFECT OF CHANGES IN RUNNING CONDITION ON THE NOISE OF ROTATING ELECTRICAL MACHINES

6.1 General interpretation of the concept of load

No-load operation of electrical machines is rare and, apart from laboratory testing, they almost never run uncoupled. The primary function of the machines is to transform electrical power into mechanical rotational energy or vice versa, while they are in constant mechanical connection with the environment and the load. The size and type of load and the nature of interaction with the environment strongly affect the vibroacustical behaviour of the electrical machine. Our present discussion focuses on the commonest rotating machine, the asynchronous motor.

First of all, let us consider what happens when the load is increased from no-load to the rated load. According to the classification of literature normally applied, all three kinds of noise appear in the no-load operation, namely noises of electromagnetic, aerodynamic and mechanical origin. The magnitude and frequency of noises of mechanical and aerodynamic origin are normally proportional to the speed, so they do not vary too much with load in the case of asynchronous motors owing to their tight speed characteristic. Hovever, we may have quite considerable changes in noise of electromagnetic origin. As is well known, the interaction of flux density harmonics in the air gap gives rise to exciting force harmonics. The loading directly alters the magnitude and phase angle of the current flowing in the conductors and the slip. Owing to these direct, primary changes, the magnitude and frequency of the exciting force will change, too, while the main flux and the leakage reactances are modified as a consequence of saturation. The mechanical connection with the environment affects the resonance frequencies, and through them the so-called magnification factor characteristic of the vibration generation process in the motor. Also, as a result of the latter factor, the noise radiating capability of the asynchronous motor is affected. Considering that only a part of the changing parameters tends to increase the noise, the other part may increase or decrease it alike, so we cannot state in general that loading increases noise. The sense and magnitude of change must be determined for each dominant noise component of electromagnetic origin in each case separately, and only on this basis can we conclude whether the noise changes on loading and, if it does, in what sense and by how much. There is not

much coverage on the subject in the literature and if it is mentioned at all, only general observations are communicated. In 1970, in a public debate published in the Proceedings of the IEE, Hore in [105] stressed the importance of noise measurement under load conditions. From empirical facts, he suggests measurements to be conducted in the acoustical near field.

In the same publication, Stephen sets out that there is not much difference between the sound power emitted by small machines under no-load and load conditions. This empirical observation might be backed by theoretical considerations on the basis that the mechanical resonance frequencies of small-power small-sized machines are generally higher than the exciting force frequencies and, apart from this, they are poor radiators because of their small size, therefore the difference between the no-load and the rated current is not substantial. Based on his measurements, Brozek [12] found considerable increase in noise on loading in high-power motors. The mechanical resonance frequencies of large machines—he explained—are relatively low, so the odds of coincidence with exciting force frequencies are better, and also the larger machines are better radiators and the no-load current is much less than the rated current. The power machines of today with high power output exhibit an opposite trend. The intensive utilization of active materials has raised the cooling requirements considerably, and consequently noises of aerodynamic origin have become dominant almost independently of the pole number. These noises are almost insensitive to load size.

Japanese researchers [61] used a theoretical approach to the problem of noise variation with load and published formulae to determine the variations in electromagnetic force wave magnitudes. Unfortunately their calculation was limited to a specific motor, so the results cannot be generalized.

The analysis of noise variation with load arose as a problem to be solved because the users are subject to noise exposure during the normal, loaded operation of the machine, and the relevant safety regulations give limit values to this noise. In most cases, however, the standard noise measurements are carried out under no-load conditions, because it is very hard to simulate the "field" load conditions in the laboratory, or the special acoustical testing room with the shaft led through its wall in a sound-insulating manner is not available.

The change in operating conditions due to loading and the consequent change in noise can be investigated in a broader sense. Abrupt changes in operating conditions, the transient conditions, might have important vibroacoustical consequences. In the tool engineering industry the main problem results from the fact that modern machine tools use different asynchronous motors for each work element, therefore the different modes of operation—starting, idling, braking, reversing, etc.—frequently follow in succession, so the transient operation is more typical of these machines than the steady-state running. The amplitudes and

frequencies of electromagnetic exciting forces and also the indirectly changing parameters may vary over wide range. Since these electrical motors form a part of the complex machine tool and therefore the vibration of the latter as a complete system must be investigated, it is essential to know the resonance frequencies of the motor and the machine tool, and also the coupling frequencies of the composite system. Many machine tool designers are of the opinion that owing to the high number of mechanical resonance frequencies and the variation of exciting force frequencies over a wide range, the transient resonance in machine tools is inherent and inevitable. Thus they suggest design of the control system of automatic precision machine tools so that starting, braking and reversing of motors serving the auxiliary motions are avoided during the period the workpiece is worked on.

Special problems arise in connection with the asynchronous machines equipped with a pole changing switch, used in elevator drives. These machines normally incorporate two stator windings of different pole number. When the elevator cage approaches the selected landing, the low-pole-number winding is switched off and the high-pole-number winding is switched on, decelerating the motion in the generator braking mode of the asynchronous machine. The elevator arrives at the landing at a low speed, when the mechanical brake is activated and stops the cage. In the transient operation during starting and switch-over, the electromagnetic force frequencies often pass through the resonance frequencies of the asynchronous machine, causing the motor to race.

6.2 Calculating the noise variation on loading the asynchronous motor

The noisiness of asynchronous motors is measured in no-load condition, with the motor isolated from its surroundings (no structure-borne sound generation!). One of the components of the emitted sound power level is $L_{W,r,0}$. When the load is coupled to the asynchronous motor (structure-borne sound generation to be avoided again), the emitted sound power level at rated load is $L_{W,r,l}$. Now the change in sound power level induced by the application of load can be expressed for the given noise component as:

$$\Delta L_{W,r} = 10 \log \frac{P_{fr,l}}{P_{fr,0}}. \tag{6.1}$$

Substituting the formulae discussed in Chapters 3, 4 and 5, we get:

$$\Delta L_{W,r} = 10 \log \frac{B_{\mu,l}^2 B_{\lambda,l}^2 f_{r,l}^2 H_{jn,l}^2 \sigma_l}{B_{\mu,0}^2 B_{\lambda,0}^2 f_{r,0}^2 H_{jn,0}^2 \sigma_0}. \tag{6.2}$$

In the following sections, we examine for what reason, to what extent and in what senses the individual factors in eqn. (6.2) change:

$$\Delta L_{W,r} = 10 \log \frac{B_{\mu,l}^2}{B_{\mu,0}^2} + 10 \log \frac{B_{\lambda,l}^2}{B_{\lambda,0}^2} + 10 \log \frac{f_{r,l}^2}{f_{r,0}^2} + 10 \log \frac{H_{jn,l}^2}{H_{jn,0}^2} + 10 \log \frac{\sigma_l}{\sigma_0}.$$

Assigning serial numbers to the terms, respectively

$$\Delta I_{W,r} = \Delta L_1 + \Delta L_2 + \Delta L_3 + \Delta L_4 + \Delta L_5.$$

6.2.1 Variation of stator flux density harmonics

One of the components participating in the generating process of force waves, important with respect to noise and vibration, is always the stator flux density harmonic. This can be the stator winding harmonic itself or, when the so-called slotting permeance harmonic of the same order exists, their vectorial sum, taking the correct phase angles into account. In no-load operation, the amplitudes of the stator slot harmonics are normally much higher than those of winding harmonics, and so the slot harmonic dominates in no-load noise. The amplitude of the slot harmonic is independent of the load, while, on the contrary, the amplitude of the winding harmonic is proportional to the stator current. For squirrel-cage asynchronous motors operating in the low and medium power range, the value of the ratio $I_{1,l}/I_{1,0}$ is about 2 to 3. Accordingly, the change in in sound power level defined by eqn. (6.2), caused, in the case of winding harmonics, by the increase in stator current, can be as high as $\Delta L_1 = +9$ dB. If the slot plus winding harmonic plays the dominant role in no-load noise generation, then this increase is much less, since the slot harmonic dominant in no-load operation is independent of the load. The load-dependent change in the amplitude of the slot harmonic can result in considerable change in noise, only if the effective slot width changes due to tooth saturation, and therefore the Carter factor also changes.

6.2.2 Variation of rotor flux density harmonics

The other flux density components of importance in the generating process of electromagnetic force waves dangerous with respect to noise are the rotor flux density harmonics, which may originate from eccentricity, saturation or winding plus slotting. (While we are talking about squirrel-cage machines, each slotting harmonic has a corresponding winding harmonic of the same order. These rotor

harmonics must be summed as vectors, takint phase angles into account.) The above details on the slot harmonics apply here as well, namely they can be considered independent of load. The amplitude of rotor winding harmonics increases by a factor of

$$\frac{I_{1,l}\cos\varphi_{1,l}}{I_{1,0}\cos\varphi_{1,0}}$$

as a result of loading. For the machines concerned, taking the highest possible value of the above ratio, form eqn. (6.2) we get a possible change of $\Delta L_2 = +16$ dB in sound pressure level. Since the slot harmonic is still same, the value of ΔL_2 is smaller in reality, probably $+7$ dB. The amplitudes of rotor harmonics due to eccentricity vary only slightly with loading, and this variation may be neglected because of the logarithmic scale.

The ratio of the amplitudes of saturation rotor harmonics for the loaded and the no-load case is about 0.8 for small and medium power machines, which corresponds to a sound power level change of $\Delta L_2 = -1.0$ dB.

6.2.3 Variation of exciting force frequency

As discussed in Chapter 3, the electromagnetic components that change on loading are given by the products of stator rotor flux density harmonics.

The slip of asynchronous motors also increases on loading, and consequently the frequency of exciting forces decreases by:

$$\Delta f_r = f_1 \frac{gS_2}{p} \Delta s. \tag{6.3}$$

The value of Δs is normally from 3 to 5 percent. Table 6.1 shows typical Δf_r values for $S_2 = 28$ and different pole pair numbers. The magnitude of frequency variation in relative units is given by:

$$\frac{f_{r,0} - \Delta f_r}{f_{r,0}}.$$

The value of this quotient is higher for machines with lower frequency and lower pole number.

Table 6.1. The values of Δf_r for low-order harmonics, Hz

$\|g\|$ \ p	1	2	3	4
1	42	21	14	10.5
2	84	42	28	21
3	126	63	42	31.5

6.2.4 Variation of the magnification factor

The second term of the system function discussed in Chapter 4, denoted H_{jn}, is called the magnification factor:

$$H_{jn}=\frac{1}{\sqrt{\left[1-\left(\frac{f_r}{F_j}\right)^2\right]^2+\left[2D_j\frac{f_r}{F_j}\right]^2}} .$$

The magnification factor comprises three parameters. D is the damping factor whose main source is the friction in the winding and within the core laminations. F_j is the mechanical natural frequency and f_r is the frequency of the exciting force. The maximum expected relative frequency variation is about 5 percent. If we want to estimate the effect of magnification factor variation on the emitted sound power level variation, then we take the 5 percent change with respect to the maximum value of the magnification factor, i.e., $f_{r,0}=F_j$.

Based on eqn. (6.2), the change in sound power level due to the change in magnification factor as a result of slip variation on loading, can be expressed as:

$$\Delta L_4=10\log\frac{H_{jn,1}^2}{H_{jn,0}^2} .$$

Taking $D=0.01$ and a 5 percent variation in f_r, the maximum change is given as $\Delta L_{4\max}=14.5$ dB. The sense depends on the value of $f_{r,0}$ with respect to F_j. If $f_{r,0}>F_j$, then the noise increases, and if $f_{r,0}<F_j$, then it decreases. Of course, a variation of that magnitude is not too common. In Fig. 6.1, the variation of sound pressure level is plotted versus $\Delta f_r/f_r$, in dB (at $D=0.01$).

So far we assumed that the mechanical resonance frequency of asynchronous motors is independent of load. This is true, if the noise measurement for the load and the no-load operation is done at the same level of assembly and machine mounting. In practice, however, the situation is different. The no-load noise measurement is done on a non-rigid, soft-elastic set-up of the free-standing machine, applying the assumptions set out in Chapter 4 and widely used in the literature for the calculation of resonance frequencies. The assumptions of importance in our discussion were as follows:

— The asynchronous motor is perfectly cylindrical with infinite number of symmetry planes.

— Only the lowest of the infinite number of resonance frequencies that belong to each vibration mode should be considered, because the others are outside the audible range.

The truth of the latter hypothesis is confirmed by the values found in practice, but
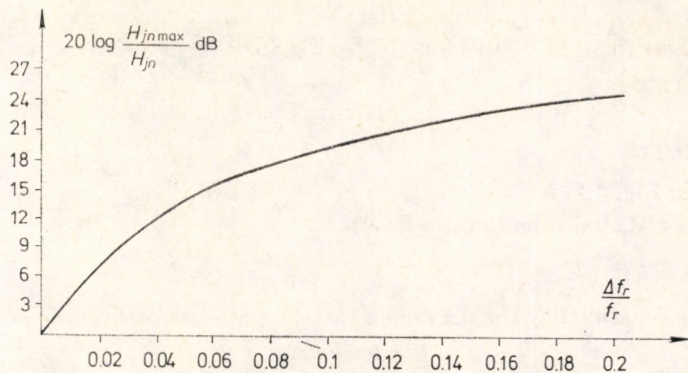
Fig. 6.1. The variation of the magnification factor with change of frequency

the former immediately proves wrong when the feet of the machine are rigidly fixed to the foundation. Doing this deteriorates the perfectly symmetrical cylindrical shape, while the rigidity of fixation and the position of the feet, characterized by the so-called foot angle (the central angle in the machine cross section corre- sponding to the radii belonging to the feet), considerably affect the mechanical re- sonance frequencies.

Thus in our case, and as found in practice, the third parameter of the magnifica- tion factor, namely the mechanical resonance frequency, also changes, although not directly as a result of loading, but between the no-load and load noise measure- ments. The value of the mechanical resonance frequency calculated by taking the foot angle into account may differ by a maximum of 10 percent from the value calculated for the symmetrical cylinder. If this change is considered together with the typical change in exciting force in calculating the magnification factor varia- tion, we find that the variation of the magnification factor estimated at $\Delta L_{4\,max} = $ $= 25$ dB can occur. This detuning of natural frequencies due to fixation and the resultant effects on noise are seldom taken into consideration in the preliminary noise calculations because of their specific, uncertain nature.

6.2.5 Change in the radiation factor

The sound radiation factor covered in Chapters 1 and 5 depends on the machine size (the diameter D of the spherical sound radiator) and the vibration frequency f_r. If the value of k is so high—large machine size and high frequency for a given mode number—that we are on the plateau section of the curve σ, then the change in f_r due to loading does not result in any change of σ, that is, the emitted sound power level remains the same. If, however, the size of the machine or the

value of f_r is so small that we are on the slope section of the curve σ for the given mode number, then ΔL_5 can be as high as 3.8 dB in negative sense for just the largest decrease in f_r:

$$\Delta L_5 = 10 \log \frac{\sigma_l}{\sigma_0} = -3.8 \text{ dB}.$$

As we see in Fig. 1.5, for a decrease in f_r, ΔL_5 is always negative, i.e., it tends to decrease the radiated sound power level.

6.2.6 Estimating the maximum variation of electromagnetic noise due to loading

In the previous sections, we investigated by factors how a component of the sound power level changes with the load. In Table 6.2, are listed the expected maximum and minimum values of ΔL.

Table 6.2. The extreme values of sound power level changes due to loading

Origin	Factor	Maximum value dB	Minimum value dB
B_μ	ΔL_1	$+9$	0
B_λ	ΔL_2	$+7$	0
f_r	ΔL_3	0	-0.5
H_{jn}	ΔL_4	$+20$	-20
σ	ΔL_5	0	-3.8
Resultant	ΔL_{Wr}	$+36$	-24.3

From the bottom row of the table, we can deduce that the noise component of electromagnetic origin may increase by 36 dB or decrease by 24.3 dB on loading in extreme cases, i.e., $-24.3 \leqq \Delta L_{W,r} \leqq +36$ dB. This does not mean, however, that the A-weighted power level of the asynchronous motor would change the same amount. (The values $+36$ and -24.3 would be the two extreme cases imaginable, anyway.) If the noise component concerned were negligible in no-load operation, then even an increase of $+20$ dB can be negligible. Therefore the tests outlined in this chapter must be done individually by noise components, starting with the component that already dominates under no-load condition. It can happen that most of the electromagnetic noise components will increase on loading, but owing to the decrease in or constancy of dominant components, the resultant sound pressure level might remain unchanged or even decrease. Thus one cannot make any general statement regarding the sense and magnitude of motor noise variation on loading.

Special attention must be paid to the variation of the magnification factor, because it can provide the major part of the change in noise level induced by loading. If the slip-dependent frequency of the exciting force becomes equal to the mechanical resonance frequency for a load smaller than the rated load of the machine, then the highest emitted sound power level is experienced at an inter₂ mediate load value. Predicting the sound power level variation on loading, we cannot overlook the fact outlined above that the noise of the machine is a product of mechanical, aerodynamic and electromagnetic noises, and the constancy of the former two definitely moderates the effect of the variation of the electromagnetic component.

6.3 The effect of starting, reversing and pole-changing on the noise of asynchronous machines

Discussing the field analysis in Chapter 3, we saw that the frequency of force waves acting on both the stator and the rotor of the asynchronous machine is a function of slip and speed. Rearranging eqns (3.25), from the product of stator and rotor winding flux density hamonics we get force waves of frequency:

$$f_r = gS_2 n + Af_1, \tag{3.25'}$$

where $A = 0$ or 2,

n — the speed,

and from the product of stator winding and rotor saturation flux density harmonics we obtain force waves of frequency:

$$f_r = gS_2 n + Af_1, \tag{3.25b'}$$

where $A = 2$ or 4,

and from the product of stator winding, rotor dynamic and eccentricity flux density waves we have force waves of frequency:

$$f_r = (gS_2 \pm 1)n + Af_1, \tag{3.25a'}$$

where $A = 0$ or 2.

The force wave frequencies obtained, as we see, are directly proportional to the speed, so they give a line in the $f_r - n$ coordinate system, the so-called sound line. When the machine does not rotate, forces with frequency Af_1 are produced, and during acceleration the sound line ascends with a slope of gS_2 or $gS_2 + 1$. Two of these lines belonging to $g = +1$ are shown in Fig. 6.2 (see eqn. (3.25')) in the top right (positive–positive) quadrant. If in the speed range of 0 to n_{nom}, f_r becomes temporarily equal to one of the resonance frequencies F_j, then transient resonance
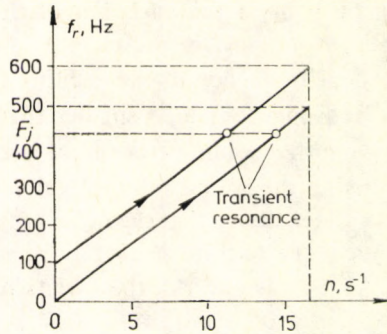
Fig. 6.2. The sound line for the acceleration of a six-pole asynchronous motor ($S_2 = 30$)

occurs, and the vibration and noise increase considerably. This resonance cannot develop completely in rapidly accelerating machines owing to the short time available, but it can give rise to serious problems in slow motors.

In reversing mode, the frequency of the first two force waves practically varies within the same range as mentioned in the starting case. The only difference is that there is the possibility of having transient resonance twice, if we find any resonance frequency F_j within the range.

The frequency equations derived from eqns (3.25) also apply in the case of phase changing. Consequently, the f_r variation range of the phase changing action is always within the frequency range of small pole-number starting.

In the analysis of transient noise, we may generally apply the simplifying assumption (as in the previous reasoning) that the electrical transients, because of their much smaller time constant, have died away by the time the mechanical transients arise. If more precise analysis is required and we cannot accept the separation of electrical and mechanical transients, then the differential equations describing the process can be solved only by numerical analysis. The measurement of transient noise and vibration phenomena is also a difficult task, but we will return to this subject in more depth in Chapters 14 to 16.

7. DESIGN CONSIDERATIONS TO REDUCE NOISE AND VIBRATION OF ELECTROMAGNETIC ORIGIN

The struggle against noise starts right at the design stage and cannot be separated from the struggle against vibration. As we saw in Chapter 2, the causes of noise and vibration were the same, so if we can get rid of the causes or at least reduce the vibrating tendency of the mechanical system of the electrical machine, than we also reduce the noise and vibration considerably.

7.1 Reducing the flux density in rotating machines

We saw in Chapter 3 that the radial magnetic force wave is proportional to the square of the flux density in the air gap. According to Chapter 4, the vibration velocity of electromagnetic origin varies directly with the exciting force. The vibration of electromagnetic origin is governed by the square law in terms of flux density. As we showed early on, in Chapter 1, the airborne sound power emitted by a vibrating body is proportional to the kinetic energy, that is, to the square of the vibration velocity, and thus the airborne sound power varies as the fourth power of the flux density, so the first possibility of noise reduction is automatically presented: we should reduce the flux density. If the airborne sound power P corresponds to the air gap flux density B, then, reducing flux density to the cth, the new flux density of $B'=B/c$ would give rise to a sound power of $P'=P/c^4$. Calculating in levels as usual, the reduction of sound power level caused by a reduction in flux density can be found as:

$$\Delta L = -10 \log c^4. \tag{7.1}$$

There are two ways to reduce air gap flux density. If the supply voltage is given, then we can increase the number of turns in the winding at the manufacturing stage, or we can make reductions with the supply voltage at the user end. Although this might seem an easy way of reducing noise, it is very rarely applied in practice, because not only the flux density, but the output power and torque of the machine are reduced too at the same time, just like the stray losses produced by

flux density harmonics. If the deterioration of torque characteristics is tole:
rable, then one might cut back the diameter of the rotor, thus reducing flux den-
sity, extending air gap length and decreasing slot harmonics.

7.2 Selecting the right slot number and dimensioning the geometric sizes

In order to eliminate or reduce noise caused by electromagnetic origin, the first
and most important task of the designer is to determine the right stator and rotor
slot numbers, and to arrive at the proper slot number combination. By selecting
the correct slot numbers, one must above all avoid the generation of small-mode-
number force waves as outlined in Chapter 3. The mode number of the force is
given by $r = p(\mu \pm \lambda)$ (the orders μ and λ can be calculated from the equations set
forth in Section 9.1.2), and this is the parameter to be used to determine the ratio
of the stator slot number to the rotor slot number.

In the last 70 years, many engineers have tried to find the optimum slot number
combinations. New rules arose one after the other, but soon they proved to be
applicable only in specific cases and for specific machine sizes, to provide quiet
operation. In the mid-thirties, Sequenz published an almost complete list of slot
number rules [100]. Since then, most of the rules were found to be mere repetitions
of other rules rewritten in a different form and also, if all the rules were to be
observed, we would fail to find any matching combination within the bounds of
reality. When the slot numbers are selected, noise is not the only aspect that must
be taken into account. There are also the torque of the motor, the parasite torques
present during acceleration, the effects on losses and feasibility of fabrication,
which are to be considered seriously. Table 7.1 lists the most widely used slot
number rules, indicating the name of the authors. The first six rules reflect general
considerations, while the remaining eight were established specifically for the
purpose of noise reduction.

Regarding variable-speed asynchronous motor drives the literature concluded
that in the design of mass produced asynchronous motors and those to be used in
inverter drives, less attention should be paid to slot number selection, and the
skewing of slots should be avoided in order to minimise stray losses. It seems to be
worthwhile discussing this subject in a little more depth. As we saw in Section
3.1.2 covering the field analysis, the amplitudes of slot harmonics are generally
much higher than those of the other flux density harmonics, therefore in most
cases it is enough to confine our efforts on them when we try to evaluate the restric-
tion on mode numbers to yield a quiet and vibrationless machine. Realizing

Table 7.1. Summary of the main rules to select the slot numbers

Rule	Author
$S_2 \neq S_1$	Arnold-la Cour, Rummel Krondl, Aparoff
$\|S_1 - S_2\|$ to be small	Galincev, Heubach
$\|S_1 - S_2\| \leq 10$	Raskop
$S_2 < S_1$	Heubach, Linker
$S_2 < 1,4 S_1$	Krondl
$S_2 < 1.25(S_2 + 2p)$	Aparoff
$S_2 \neq 2p(6g + 1)$	Arnold-la Cour, Kade, Kron
$S_2 \neq 2p(3g + 1)$	Dreese
$\|S_2 - S_2\| \neq 1, 3, 5, \ldots$	Heubach, Raskop, Möller,
$\|S_1 - S_2\| \neq \begin{cases} 2p \\ 0 \end{cases} \pm 1, \pm 2, \ldots$	Krondl, Kron, Aparoff, Jordan, Schuisky
$\|S_1 - S_2\| \neq p$	Kron, Aparoff
$\|S_1 - S_2\| \neq 4p$	Aparoff
Should not have winding with fractional slot number	Kade
$S_1 - S_2 \neq 6p, 12p$	Nürnberg

the condition of avoiding force waves with mode number less than 6, we have to observe the following inequality:

$$r = |(g_1 S_1 + p) \pm (g_2 S_2 + p)| > 5. \tag{7.2}$$

The relation (7.2) presents a stipulation regarding the ratio of stator and rotor slot numbers. And what if we do not adhere to it? Do we necessarily have a noisy machine? No, not necessary. As we know, we get considerable noise and vibration when the exciting force frequency is close to one of the mechanical resonance frequencies of the machine. So we can accept small-mode-number exciting forces in our machine, provided that the frequencies are far from the resonance frequencies. Now let us see how the type of supply affects the ease of observation of the frequency stipulation.

For an asynchronous motor supplied directly from the mains $f_1 = 50$ Hz, the frequency of the exciting force, e.g., the frequency of steady-state flux density harmonics of winding harmonic origin, is expressed as:

$$f_{r,50} = 50 \left[\frac{g_2 S_2}{p}(1 - s) + \left\langle \begin{matrix} 2 \\ 0 \end{matrix} \right] = 50 \frac{g_2 S_2}{p} + \left\langle \begin{matrix} 100 \\ 0 \end{matrix} \right. \quad \text{Hz}, \tag{7.3}$$

where $g = 0, \pm 1, \pm 2, \ldots,$

S_2 — rotor slot number,

p — pole pair number,

s — slip.

So to avoid steady resonance, we must avoid $f_{r,50}$ to get close to any of the me‑ chanical resonance frequencies F_j. During acceleration, the frequency varies within the range 0 to $f_{r,50}$, but here only transient resonances may occur, if the function $f_r(s)$ takes the value of F_j for a short period of time. (Owing to the fast change of f_r, full resonance cannot develop in most cases, anyway.)

For machines of mains supply, we could always find a design that allowed the suppression of noise and vibration. Selecting the right slot number combination, we can more or less eliminate the small‑mode‑number forces. The only force that remains with "risky" mode number, if any, can be reduced by skewing or pitch shortening.

We saw in Section 3.2 that the inverter supply multiplies the number of exciting force frequencies, and therefore improves the chances of resonance. Despite this, some authors advise to pay less attention to slot number selection!

The experts advocate the reduction of the slot number rules and a less limited slot number selection than before, because the inverter allows the acceleration of the machine up to the rated speed by gradually increasing the supply frequency from zero to the frequency that corresponds to the rated speed, while the slip is nearly constant and maintained at a low level. Thus the seizure-causing effect of parasitic synchronous and asynchronous torques produced by the flux density space harmonics during acceleration becomes negligible.

Theoretical analyses have found, however, that the variable-frequency inverters working in the usual range 0 to 100 Hz are very dangerous from the vibro‑ acoustical point of view, because of the low, gradually changing supply frequency. In the case of the inverter supply, the exciting force frequency may cause steady resonance anywhere within the range twice the frequency range calculated from eqn. (7.3), owing to the changing supply frequency (and we have not even taken into consideration the time harmonics produced by the inverter). The precondition of quiet operation can be expressed in mathematical form as a function

$$f_r = f_1 \left[\frac{gS_2}{p}(1-s) + \binom{2}{0} \right], \tag{7.4}$$

which cannot take the value of any F_j, even though the supply frequency varies within the range $0 \leqq f_1 \leqq f_{1,\,max}$ ($f_{1,\,max}$ is usually 100 Hz).

In view of the fact that none of the supply frequencies within the range 0 to $f_{1,\,max}$ can be eliminated on grounds of noise and vibration considerations when inverter supply is used, the condition of resonance avoidance cannot be satisfied with respect to frequency. The quiet and vibrationless operation can be realized only if we prevent the generation of small‑mode‑number exciting forces by carefully selecting the stator and rotor slot numbers. Thus the correct selection of mode numbers is even more important than before.

If r_m is the smallest acceptable exciting force mode number, then the following specifications should be met in selecting the rotor slot number, taking into account the practically important force, slot and eccentricity flux density harmonics.

The effect of the first two stator slotting harmonics on the generation of exciting forces with mode numbers smaller than r_m can be eliminated by selecting S_2 to satisfy the following relations (assuming the usual relation of $S_1 > S_2$):

$$\frac{S_1 + r_m}{2} + p < S_2 < S_1 - r_m - 2p. \tag{7.5}$$

From relation (7.5), we can deduce the minimum stator slot number that can eliminate the stator slotting harmonics for a given r_m and $2p$ so as not to contribute to force harmonic generation. To satisfy (7.5), the required stator slot number is $S_1' > 4r_m + 6p$.

If the geometrical sizes of the machine would not allow so high a value of S_1 that could eliminate more than the first two stator slot harmonics from the generation of force harmonics, then a quiet motor can be designed by selecting S_2 to meet the relation (7.5), and by skewing the rotor slots by half the stator slot pitch. With this compromise, the additional losses introduced by the inverter supply can be reduced and favourable vibroacoustical parameters can be achieved. In short, the principle of correct slot number combination selection is to avoid resonance in the machine of a given geometrical construction by adjusting the mode number and frequency of the exciting force to values outside the "danger zone" of noise and vibration generation. Of course, one can avoid resonance by modifying the vibrating capability of the machine, i.e., by changing the value of resonance frequency, in other words, by detuning the system. Starting out from the equations outlined in Chapter 4 for the calculation of mechanical resonance frequencies, we can see that the resonance frequency increases considerably if the radial dimension h_y of the stator yoke is extended. The proportional decrease of machine sizes also tends to raise the resonance frequencies. This type of interference should be done with proper care though, because the increased built-in iron volume makes the machine too heavy and expensive, while decreased sizes will increase the flux density for a given flux, which equally increases the noise and iron loss in the machine, deteriorating the efficiency.

If we cannot change either the exciting force frequencies or the mechanical resonance frequencies, then we can still reduce noise by increasing the structural damping D in the magnification factor H_{jn}. For example, soaking the stator laminations of small asynchronous machines in epoxy resin will improve damping.

When the slot shape is designed, there are two things to be borne in mind. First, there is the change in thickness of the tooth left behind after the slots have been cut out. In the case of slots with parallel walls, the cross-section of the tooth changes along the height. As most part of the flux passes through the tooth, it

generates saturation at the "bottleneck" of the path, that is, at the smallest cross-sectional area zone, which give rise to so-called saturation harmonics owing to the non-linear magnetization curve of the iron.

Second, there is the effect of slot opening on the noise. The fully open slots are advantageous, because they reduce leakage paths, but they increase the excitation current and lead to considerable slot harmonic generation because of the strong fluctuation of air gap magnetic permeance, increasing noise especially in no-load operation. If the slot opening is closed or magnetic wedges are inserted, we may experience substantial improvement mainly in no-load noise. Of course, we have to pay the price with an increase in leakage flux and stray losses.

Pitch shortening mainly influences no-load noise favourably. Before we decide on the amount of pitch shortening, we must carefully analyse the excitation curve to identify the harmonics whose elimination by pitch shortening would improve the noise characteristics substantially.

7.3 Skewing the rotor slots

Another favourable measure that contributes to noise reduction is the skewing of slots.

The slots of low- and medium-power asynchronous machines have been skewed for a long time. In the course of testing the effects of skewing, it has been shown that the coupling of rotor is reduced with respect to flux density harmonics, and the short-circuit current and the torque are also reduced. If the rotor slots are skewed and the coils or bars are not correctly insulated from the laminated core, then equalizing currents flow in the core, leading to local overheating, adversely affecting even the torque characteristic. Different measures were tried to improve the insulation (burning, etching, reannealing, etc.), but these methods proved to be costly.

The skewing factor known from the literature is:

$$\xi_s = \frac{\sin(\mu pb/D)}{\mu pb/D},$$

where b – the amount of skewing round the periphery of the rotor,

   D — outside diameter of the rotor,

   p — pole pair number,

   μ — order of flux density harmonic.

The skewing modifies the radial bending displacement by a factor of ξ_s. In the case of medium and large asynchronous machines with a long rotor, torsional

vibration ($\Phi_{r,\tau}$) is experienced as well. The radial displacement $Y_{r,\text{res}}$ is the resultant of the bending and torsional displacements:

$$Y_{r,\text{res}} = \sqrt{Y_{r,s}^2 + \frac{\Phi_{r,\tau}^2 \, l_i^2}{12}}, \qquad (7.6)$$

where $Y_{r,s} = \xi_s Y_r$,

$\Phi_{r,\tau}$ — amplitude of torsional vibration angle,

l_i — rotor iron length.

Since the emitted sound power is proportional to the square of the vibration velocity, then for the case of skewing:

$$P_{r,s} = k\left(Y_{r\,s}^2 + \frac{\Phi_{r,\tau}^2 \, l_i^2}{12}\right),$$

and without skewing:

$$P_r = kY_r^2,$$

while the change in sound pressure level is found to be:

$$\Delta L = 10 \log (P_{r,s}/P_r). \qquad (7.7)$$

Thus we can have an increase or decrease in sound pressure level depending on the relation of the decrement in the radial bending displacement due to skewing, and to the increment in the displacement due to the torsional vibration. In small and medium machines the torsional vibrations are not significant, and thus the airborne noise emission can be controlled by proper skewing. Generally the stator's first slot harmonic is the most dangerous factor in force wave generation, and so the amount of skewing equals the stator slot pitch in most cases. The expected reduction in sound pressure level is:

$$\Delta L = 20 \log \xi_s. \qquad (7.8)$$

7.4 Low-noise transformer design considerations

A straightforward way to decrease the magnetostrictive noise of transformers is the decrease in flux density, as clearly inferable from Section 3.5. We saw there that an average noise reduction of 20 to 25 dB/T results from the decreasing flux density. The decrease in flux density, however, leads to an increased core size, since the mass of the iron core is inversely proportional to the flux density. Flux density reduction is a rather expensive solution, so it is applied only when we want to decrease the iron loss as well, or the other possibilities of noise reduction have all been exploited.

Another method to lower electromagnetic noise is the use of Hi–B laminations. This material has lower loss and magnetostriction factors compared with other materials for the usual flux density of 1.6 T. Another advantage is that this material is less sensitive to mechanical impact. By using laminations made of Hi–B material, a noise reduction of 4 dB can be achieved in large transformers, and 2 dB in medium ones.

Discussing the design considerations that can lead to noise reduction in trans= formers, we started from the fact that the vibration and noise emission of the core is determined by the magnitude of flux density. Large transformers are placed in a tank which plays a multiple role from the acoustical point of view. On the one hand, the tank must be an effective sound insulator to retain as much of the sound power emitted by the core as possible to control radiation to the surroundings. On the other hand, however, a part of the vibrational energy of the core passes onto the tank through the oil and the rigid fixing frame of the core, then to the mechanical elements such as radiators mounted solidly on the tank, turning them into secondary noise sources.

The sound insulating characteristics of the tank can be improved by absorbing material padding, in most cases of sandwich construction. The insulating efficiency depends on what percentage of the casing surface can be covered by the absorbing material and also on the design of the padding.

In order to eliminate structure-borne sound bridges, the transformer core as the active part of the transformer is mounted on vibration damping elements. In the course of dimensioning these damping shims, the work is complicated by the assumption that the mass of the machine mounted on the shims is much less than the mass of the foundation onto which it is fixed, and that the foundation is very rigid. In our case, these assumptions are not valid, since the transformer tank cannot be considered rigid in terms of vibration theory, and also its mass is smaller than that of the iron core.

Some transformer manufacturers place the active part in a double-walled tank. The inside tank contains the winding and the core immersed in oil. This tank is mounted on damping elements inside the other tank. The acoustical efficiency of the outside tank is improved by insulating and absorbing materials fixed to the external and internal surfaces, respectively. The latter is necessary to prevent the amplification of sound power level between the two tanks due to reflection on the smooth internal surfaces. We will reconsider this subject in more detail in Chapter 10. In all cases, in the design of the double-walled tank, care must be taken to avoid the introduction of a new structure-borne sound bridge in the system by the installation of the oil inlet to the radiator, and to control the sizes of the second tank, not to produce handling and transport difficulties.

When the noise of transformers with forced cooling is tested, we should bear in

mind that the transformer core and the cooling system produce noise in different frequency ranges. The magnetostrictive noise of the transformer core is typically in the range below 1000 Hz, while in the range above 1000 Hz aerodynamic noise of the cooling system dominates. It is well known that the damping effect of air is stronger at higher frequencies, and so first of all we have to deal with the reduction of magnetic noise, provided that the transformer is located far from residential buildings (where very strict immission standards must be adhered to), because, assuming that equal amounts of electromagnetic and aerodynamic noise power are emitted, less aerodynamic noise will reach the buildings, causing less nuisance than noise of electromagnetic origin.

Table 7.2. Summary of the constructional methods to reduce transformer noise, based on [28]

Serial number of the technical solution	Technical solution	Decrease in sound pressure level ΔL_A, dB	Possible combinations
1	Covering the transformer tank with sound absorbent lining	1–7	2.3 and 4
2	Placing the active part on vibration absorbers (damping elements)	1–2	1.3 and 4
3	Reducing flux density	$(20-25)/T$	1.2 and 4
4	Double-walled tank*	13	3 and 4

* Applicable only to transformers smaller than 100 MVA owing to the increased dimensions

The constructional methods of noise reduction in transformers are summarized in Table 7.2, indicating the achievable levels of noise reduction and the feasible combinations of the various methods.

8. MECHANICAL NOISE AND VIBRATION

In this chapter, we shall investigate only the commonest mechanical noise and vibration sources that occur in electrical machines. Regarding other sources that do not form an organic part of the electrical machine, such as gear noise, belt drive noises, etc., we refer to the literature [65].

8.1 Bearings

Bearings that allow the relative displacement of the rotor and the stator are essentially mechanical elements in electrical machines. They have different contribution to noise and vibration emission, depending on the type of machine. Their effect becomes more and more substantial with speed.

Both the basic two bearing types (sleeve and rolling) are used extensively in electrical machine manufacture. Sleeve bearings are better choice in terms of noise and vibration, because their probable sound pressure level is lower than that of rolling bearings. As they are made in small volumes, the price is relatively high. Their installation and maintenance require special care, so they are very rarely used in small or medium machines except when extremely quiet operation is needed.

The following factors affect the vibroacoustic behaviour of the sleeve bearings:

— roughness of sliding surfaces,
— lubrication conditions and their changes,
— stability and whirling of the oil film in the bearing,
— manufacturing and installation technology and its faults.

Exciting force with a given frequency is produced by

— rotor unbalance and/or eccentricity at the rotor rotational frequency:

$$f_n = n, \qquad (8.1)$$

where n — the r.p.m,
— axial grooves

$$f_{ax}=f_nN,$$ (8.2)

where N — the number of grooves,

— bearing oil film instability. Oil whirl gives rise to self-excited vibration generally with a frequency equal to the critical speed of the rotor.

Manufacturers of electrical machines mostly incorporate roller or ball bearings in their machines. The frequency of the exciting forces induced by rolling bearings can fall anywhere within quite a wide range, 10 Hz to 5000 Hz, owing to the variety of possible causes.

The following factors affect the noise (vibration) of bearings:

— the accuracy of bearing elements, namely the track geometry, dimensional discrepancies between the rolling elements (balls and rollers), sphericity of the rolling elements,
— the mechanical resonance frequency of the outer ring,
— the running speed,
— the lubrication conditions,
— installation procedure and tolerances, clearances, and the alignment of shaft, bearing and bearing block,
— the load, if it increases the load on the bearing, as in the case of belt drive and gear drive,
— the operating temperature,
— the presence of foreign materials, etc.

The nature and frequency of the listed effects can only be estimated on a statistical basis. Therefore we have to approach the problem of parameter prediction also on a statistical basis. The frequencies of the most probable components of ball bearing noise are as follows.

The unbalance and eccentricity of the inner rings and the rotor produce a discrete noise component with a frequency equal to the rotational frequency of the rotor:

$$f_{ib,\,e}=n.$$ (8.3)

The irregularities in the ball cage and the rolling elements produce noise at the frequency of the cage speed:

$$f_{bc}=\frac{r_i}{r_i+r_0}\,n,$$ (8.4)

where r_i — radius of the inner contact surface,
r_0 — radius of the outer contact surface.

The frequency of the vibration of the rolling elements due to their irregular shape, while turning about their own axis:

$$f_{re} = \frac{r_i r_0}{r_r(r_i + r_0)} n,$$ (8.5)

where r_r — radius of the rolling element.

Defective rings rise vibration at the frequency:

$$f_r = \frac{r_i}{r_i + r_0} Z_b n,$$ (8.6)

where Z_b — the number of balls.

The stiffness of the bearing varies with the relative position of the ball elements with respect to the line of load at a clearance C2 (Fig. 8.1). It results in a vibration with the frequency:

$$f_s = n \frac{r_i}{r_i + r_0} Z_b i,$$ (8.7)

where i — a positive integer.
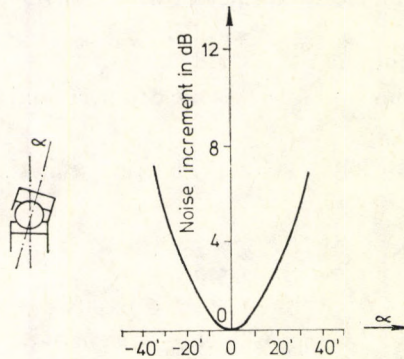
Fig. 8.1. The effect of inclined line of load on ball bearings noise

Of course, the frequencies are influenced not only by the above listed factors, but also by the surface finish and the fit between bearing and the housing. We should note that roller bearings emit more noise than ball bearings and their frequency spectrum is also wider owing to the higher probability of sliding between the rollers and the tracks.

The frequency analysis of bearing vibrations provides useful information on bearing defects, fabrication inaccuracies and installation errors. The noise increases as the second power of the misalignment. In order to diminish bearing noise a preloading spring is sometimes installed parallel to the bearing to maintain the axial position of the rotor. The optimal level of axial preload is determined by test, because a weak spring is useless and too strong a spring would shorten the lifetime of the bearing. By placing elastic inserts between the bearing and the end shield, one can limit the vibration transfer to the end shields and the housing. If the inserts

are good insulators, they then also hinder the generation of unipolar flux and, through this, the emergence of unbalanced magnetic pull. There are bearings made with plastic cages which produce less noise than bearings with metal cages. Sealed bearings are also available, and these prevent the ingress of dirt to the balls.

8.2 Brush noise

In certain types of electrical machines sliding contacts are required to establish current transfer to the rotating parts. Just like any other sliding part, the sliding contact is also a potential noise and vibration source.

The two basic systems, i.e., brush-commutator and brush-slip-ring systems, behave differently in terms of noise and vibration.

The brush-slip-ring system reacts to the forces, deformations, frictional resistances and load changes during operation in a very favourable way. The uniform radial forces exert an expanding effect on the annular slip ring, lifting it from the seat, so that the sliding surface becomes eccentric. To avoid this, slip rings are fitted prestressed on the shaft. If this prestress is larger than the centrifugal force, the ring does not become deformed and no vibration-exciting force will be produced. The intensity of noise generated by the friction between the sliding surfaces is quite low, and therefore negligible beside other machine noises. Any defect on the ring may be noticed visually. The frequency of the noise produced by eccentric slip-rings is $f_n = n$.

The brush-commutator system is more complicated and an unfavourable construction in terms of noise, one of the main noise sources in d.c. machines. The construction of the brush-commutator system, the manufacturing technology, the tolerances and the deflections under load have a determining effect on brush noise. Among the causes, the following factors should be considered:

— the brushgear design, rigidity of mounting,
— the clearance between the brush holder and the brush,
— the clearance between the brush and the commutator, the unsupported brush length,
— the brush pressure,
— the material of the brush and the commutator, the coefficient of friction between them,
— size and shape tolerances, the amount of residual unbalanced masses,
— deflections of the commutator sliding surface during rotation,
— the physical condition of the brushholder-commutator system, the defects on sliding surfaces,

— the current load and sparking of brushes,
— the surface temperature of the commutator,
— environmental effects: dust, humidity, etc.

The effect of the various factors cannot be separated because of their interrelations. The typical high-pitch brush noise is produced by friction between the brush and the sliding surface. The friction itself is a function of the condition of the film, the patina formed on the sliding surface consisting of copper oxide-graphite dust and moisture. The friction is largest on fresh, patina-free surfaces, while the brush is dusting, and a shrieking sound is heard. Patina is formed during operation under current, the colour of the sliding surface becomes bronze, the friction decreases to a minimum, and the brush sound dies away. In idle and low-current operation, the patina layer diminishes, while overload causes it to overgrow, forming an insulating layer that breaks down here and there. This process again deteriorates the frictional conditions, and the brush sound grows louder. The discrete lines in the noise frequency spectrum are found to be $f_b = iZ_{cs}f_n$, where i is a positive integer, Z_{cs} is the number of commutator segments.

As far as we know, an accurate calculating procedure to determine the sound pressure level of the emitted noise does not exist at present because of the random nature of the various interrelated causes. The magnitude of noise can be controlled by robust cast brush holders and stiff mounting brackets. Proper operation, however, depends more on building-up and maintaining the platina layer.

The application of covers to enclose the system is not effective because of ventilation. Tightly closed but easily removable covers would be required to allow proper operation and maintenance.

8.3 Rotor unbalance

8.3.1 Types, causes and modelling of residual rotor unbalance

Rotor unbalance is one of the most important causes of mechanical vibrations. If the rotor mass distribution is non-uniform, then it exerts a dynamic force on the bearings during rotation, exciting vibration with the rotational frequency due to the inertial force which varies with the square of the speed.

This adverse effect may be eliminated if we put a surplus mass in the rotational plane of the centre of gravity, on the opposite side of the existing eccentricity, which offsets the moment of the centre of gravity. This simple method, however, is only applicable to rotating parts having disk shape. The exact location of the rotational plane of the centre of gravity of cylindrical rotors is very hard to deter-

mine, and it is also very difficult, if not impossible, to place the balance weights there. In this case, we have to attach split balance weights near the bearings in the so-called balancing planes. If the ratio of the parts is not correct, only static balancing is achieved, i.e. the rotor is balanced in any angular position, but during rotation the centrifugal forces of the eccentric centre of gravity and the incorrect balance weights cause the rotor to vibrate. The basic function of modern balancing rigs is to determine the proper location and size of balance weights within the sensitivity of the rig. This process is called dynamic balancing which involves static balancing as well.

The main causes of rotor unbalance are manufacturing faults. Unbalance results from asymmetry in shape, material non-uniformities, non-observation of working tolerances, misalignment of bearings, asymmetric elastic deformations due to the centrifugal force, asymmetric thermal deflections, aerodynamic unbalance.

Rotor unbalance affects the vibroacoustical parameters of the asynchronous motor both directly and indirectly. The direct effect is purely kinematic. The unbalanced rotating mass having rotational frequency gives rise to a centrifugal force that acts on the flexible coupled system comprising the rotor and the stator, which is capable of vibrating. We have already discussed above one of the indirect effects of rotor unbalance, that is, the fluctuation of air gap permeance due to dynamic eccentricity and the resultant flux density harmonics. The frequencies of the force waves produced a fall in the range of several hundred to several thousand Hz.

The direct vibration-exciting effect of unbalance is very complex. Therefore the real problems are analysed on models. Now we shall review which models may be selected for the individual cases on the basis of the vibration generating process involved.

The most detailed physical model is the so-called continuum model. This model has been applied in the literature [141] only to the rotor to determine the critical speed by using the section matrix method, and the motion of the bearings, end shields and stator was ignored. The section matrix method requires the use of large digital computers. The accuracy of the continuum model is required in the case of large and high output machines with flexible shaft. For small asynchronous machines, however, the use of this model is not justified, because the rotational frequency of the rotor is much lower than the first critical speed of the shaft, and the exciting forces can be simulated by centrifugal forces produced by fictive unbalance concentrated in the balancing planes.

Another type of physical model is the lumped parameter linear kinematic model. Inertial masses, bodies, and springs loaded within the limit of proportionality participate in the motion. This kind of model is a very useful aid in the work of the

designer, who designs the structure and construction of the machine. This work is itemized in nature, because the parameters of the lumped parameter physical model, i.e., the masses, the spring constants of the shaft, end shields and bearings, the type and size of bearings, may be modified and altered. The designer investigates the effect of each parameter on the vibration of the machine. Since the individual phenomena are studied separately the important point is the analysis of a function that relates the residual unbalance to the radial vibration velocity with a frequency that equals the rotational frequency, excited by the unbalance and measurable on the stator. The equations that describe the properly simplified lumped parameter linear model are normally solved by digital computers. By means of the approved program once designed for the purpose, the engineer can follow up the effect of any parameter selection on the vibration of the machine, taking advantage of the speed of the computer, through the communication link between man and machine.

8.3.2 Lumped parameter linear kinematic model

The asynchronous motors are balanced in two planes, the so-called balancing planes. The location of these planes can vary depending on the construction of the rotor. In squirrel-cage motors equipped with metal fan, one of the balancing planes is the drive-side face of the rotor core, while the other is on the opposite side, the plane of the fan blades. The unbalance measured at these planes is a fictive, concentrated mass, characteristic of the amount and type of unbalance (see Fig. 8.2). Rotor unbalance may be described by three quantities, namely ΔI_1 and ΔI_2 in mm g and the angle α between the radii directed towards the two fictive masses.

To analyse the vibrations produced by the rotor unbalance in asynchronous motors, a lumped parameter linear kinematic model can be set up. The model selection is justified by the fact that only inertial masses and bodies participate in
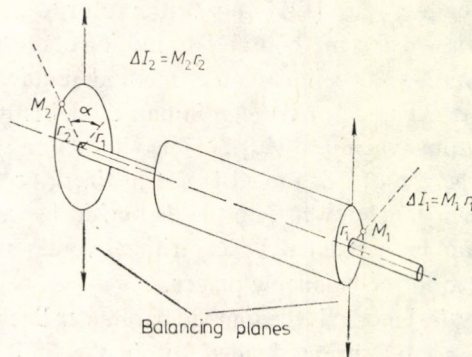
Fig. 8.2. The fictive masses of unbalance

the motion as springs loaded within their limits of proportionality. If we want to investigate vibration excited by rotor unbalance, then we investigate the asynchronous motor in itself, isolated from its surroundings by a soft spring (see Chapter 12 on vibration measurement). So we obtain the arrangement shown in Fig. 8.3. (for a squirrel-cage rotor equipped with metal fan blades).
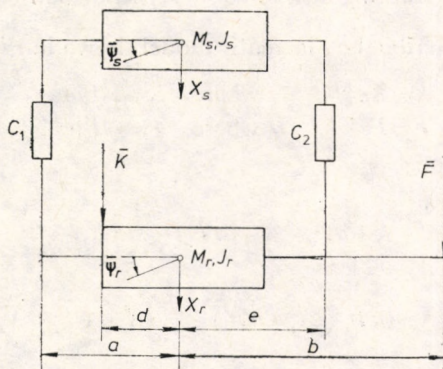
Fig. 8.3. The kinematic model comprising masses and springs to analyse the vibration inducing effect of unbalance

The stator core, the housing and the end shield, this rigidly coupled system, may be characterized by an inertial mass M_s and a moment of inertia J_s. The rotor core and shaft, also rigidly coupled, may be characterized by M_r and J_r. Weightless bars project from the masses, interconnected by springs in the plane of the bearing. These springs can be derived from shaft deflection and bearing flexibility. The shaft can be considered as a so-called rigid shaft, since the first resonance frequency of small- and medium-power asynchronous motor shaft is much higher than the operating speed of the machine. Two exciting forces act on the vibrating system shown in Fig. 8.3, the two centrifugal forces due to unbalance in the two balancing planes. The exciting force on the side opposite to the drive acts on the mass of the fan, which is negligible in comparison with M_r and M_s.

Let us briefly summarize the simplifying assumptions made during the model adaptation:

— The endshield, housing and stator core are ideally rigid, rigidly coupled with each other.

— Because of the undertuning of suspension springs, the electrical machine vibrates freely and independently of the surroundings.

— The exciting forces act in the balancing planes and are proportional to the rotor unbalance.

— The internal damping of the system is negligible.

— The spring constant of the shaft and bearings is constant and independent of load. The spring constant of the bearing may be calculated as given by Ponomar-jov [86].

— The gyroscopic torque is neglected in the equations of motion, because the rotor core is normally in the middle between the two bearings, so the rotational plane of the rotor as a rotating disk remains perpendicular to the axis of rotation.

The equations that describe the kinematic model shown in Fig. 8.3 are as follows:

$$\bar{K}=Ke^{j(\omega t+\alpha)} \quad \text{where} \quad K=\Delta I_1\omega^2, \tag{8.8a}$$
$$\bar{F}=Fe^{j\omega t} \quad \text{where} \quad F=\Delta I_2\omega^2. \tag{8.8b}$$

The equations of motion:

$$\bar{K}+\bar{F}-M_r\ddot{\bar{X}}_r-\frac{1}{c_1}(\bar{X}_r+a\bar{\Phi}_r-\bar{X}_s-a\bar{\Phi}_s)-\frac{1}{c_2}(\bar{X}_r-e\bar{\Phi}_r-\bar{X}_s+e\bar{\Phi}_s)=0, \tag{8.9}$$

$$-M_s\ddot{\bar{X}}_s+\frac{1}{c_1}(\bar{X}_r+a\bar{\Phi}_r-\bar{X}_s-a\bar{\Phi}_s)+\frac{1}{c_2}(\bar{X}_r-e\bar{\Phi}_r-\bar{X}_s+e\bar{\Phi}_s)=0, \tag{8.10}$$

$$\bar{F}b-\bar{K}d+J_r\ddot{\bar{\Phi}}_r+\frac{a}{c_1}(\bar{X}_r+a\bar{\Phi}_r-\bar{X}_s-a\bar{\Phi}_s)-\frac{e}{c_2}(\bar{X}_r-e\bar{\Phi}_r-\bar{X}_s+e\bar{\Phi}_s)=0, \tag{8.11}$$

$$J_s\ddot{\bar{\Phi}}_s-\frac{a}{c_1}(\bar{X}_r+a\bar{\Phi}_r-\bar{X}_s-a\bar{\Phi}_s)+\frac{e}{c_2}(\bar{X}_r-e\bar{\Phi}_r-\bar{X}_s+e\bar{\Phi}_s)=0. \tag{8.12}$$

In view of the symmetry, $a=e$. Introducing the following substitutions:

$$\frac{1}{c_1}+\frac{1}{c_2}=0_1 \quad \text{and} \quad \frac{1}{c_1}-\frac{1}{c_2}=0_2,$$

and trying to find the displacements due to the periodic exciting forces acting on the linear system in the form of

$$\bar{X}_r=X_re^{j(\omega t+\varrho)}, \quad \bar{\Phi}_r=\Phi_re^{j(\omega t+\beta)}, \tag{8.13}$$
$$\bar{X}_s=X_se^{j(\omega t+\delta)}, \quad \bar{\Phi}_s=\Phi_se^{j(\omega t+\gamma)},$$

after appropriate transpositions we obtain the following set of equations in matrix form:

$$\begin{bmatrix} -0_1 & -a0_2 & (0_1-M_r\omega^2) & a0_2 \\ (0_1-M_s\omega^2) & a0_2 & -0_1 & -a0_2 \\ -a0_2 & -a^20_1 & a0_2 & (a^20_1-J_r\omega^2) \\ a0_2 & (a^20_1-J_s\omega^2) & -a0_2 & -a0_1 \end{bmatrix} \begin{bmatrix} X_se^{j\delta} \\ \Phi_se^{j\gamma} \\ X_re^{j\varrho} \\ \Phi_re^{j\beta} \end{bmatrix} =$$

$$= \begin{bmatrix} Ke^{j\alpha}+F \\ 0 \\ Kde^{j\alpha}-Fb \\ 0 \end{bmatrix}. \tag{8.14}$$

Solving this linear set of equations of the first degree in four unknowns by applying Cramer's rule, we obtain:

$$X_s e^{j\sigma} = \frac{D_{xs}}{D} \quad \text{and} \quad \Phi_s e^{j\gamma} = \frac{D_{\varphi s}}{D}.$$

Now the vibration velocity component of rotational frequency due to unbalance in the drive-side bearing plane is found to be:

$$v_{y1} = \dot{\bar{X}}_s + a\dot{\bar{\Phi}}_s, \tag{8.15}$$

and in the opposite-side bearing plane:

$$v_{y2} = \dot{\bar{X}}_s - a\dot{\bar{\Phi}}_s. \tag{8.16}$$

Substituting the specific data for the given machine, the vibration velocity to be measured on the stator end shield can be determined. The determinants directly contain the material specifications and geometrical sizes of the machine, so the direct causal relationship between the electrical motor parameters and the vibration can be followed. Of course, the model discussed is only a simplified reflection of reality, since, just an example, the spring constant of a bearing is non-linear in most cases and can be determined only by complex calculation.

8.3.3 Reducing vibration by balancing

The precise balancing of the rotor can improve the performance of asynchronous machines in terms of vibrations up to a certain limit considerably, and this is favoured from both technical and economical aspects.

The production engineer is in need of a simple "handy" formula or diagram in everyday routine work to be able to instruct the worker operating the balancing machine, especially when the client specifies an upper limit for the vibration velocity as a quality requirement, giving the maximum permissible error percentage on delivery. This, of course, refers to the vibration velocity range that can be affected by balancing. The client is interested in the vibration severity controlled by the relevant standards (i. e., the highest r.m.s. vibration velocity measured at the standard measuring points discussed in detail in Chapter 12). We can instruct the balancing machine operator to go below the specified limit, ΔI_m. So the production engineer has to establish a relation between the maximum permissible unbalance—disregarding the balancing plane—and the vibration severity. This relation can only be stochastic in nature, since a physical relationship between the two variables cannot be established owing to their large "separation". The residual unbalance is directly the cause of the vibration velocity of rotational frequency. Adding to this the other components, we get a resultant vibration velocity, the largest

giving the vibration severity. This means that we need a function of given dispersion band or a mathematical model that best fits the values measured at various points on sample machines representative of the tested series manufactured in accordance with a given procedure.

From technical considerations, a causal relation exists between the maximum permissible unbalance and the vibration velocity. The determination of this relationship, the qualitative and quantitative establishment of the governing rules, would be quite beneficial in practice in that it would allow safe estimation of the maximum allowable unbalance to be observed in the manufacturing process, from the limit value specified for the vibration velocity as standard, based on technical and/or economic considerations. Of course, we could bypass the question by declaring: "Let's balance the rotor perfectly!". This instruction, however, does not make any sense from a practical point of view. On the one hand, the perfection of the balancing is limited by the limited sensitivity of the balancing rig. On the other hand, any refining costs time, energy and money. Thus the correct question is that which is the maximum acceptable residual unbalance which, if observed, ensures that the vibration severity remains safely below the specified limit value. Thus the aim is to work out a procedure on the basis of the function $v_{sev} = f(\Delta I_{max})$. Unfortunately, this function is not known in the present state of the art. To derive or assume a funtional relationship between these two physical quantities is not justified, because:

— The effect, the independent variable, ΔI_{max} is the larger of the two unbalance values measured in the balancing plane.

— The cause, the dependent variable, the vibration severity depends not only on the maximum unbalance but also on other variables and, as we stated at the beginning of this chapter, it is the result of deliberate selection.

Therefore we are searching for a stochastic relationship between the maximum unbalance and the vibration severity.

To better understand how to set up the mathematical model, we first discuss the evaluation procedure of test results.

Figure 8.4 shows a simplified sketch of the asynchronous machine as a vibrating system. As a first approximation, the whole machine is considered as an ideally rigid, inertial system excited by the centrifugal force produced by one concentrated unbalanced mass in each balancing plane:

$$\bar{F} = \Delta I_2 \omega^2 e^{j\omega t} \quad \text{and} \quad \bar{K} = \Delta I_1 \omega^2 e^{j(\omega t + a)}. \tag{8.17}$$

According to the basic rules of mechanics, the forces $\bar{F}$ and $\bar{K}$ can be transposed to the centre of mass O, establishing the vibrating force $\bar{F} + \bar{K}$. A vibrating moment of $\bar{K}0.5k - \bar{F}(0.5k + l_2 + l_v)$ is also produced. The overall inertial mass of the stator and

rotor counterbalances the former, and the polar moment of inertia of the rigid sys-
tem comprising the stator and rotor counterbalances the latter. In the subject case
of balanced series of asynchronous machines, the effect of the vibrating force has
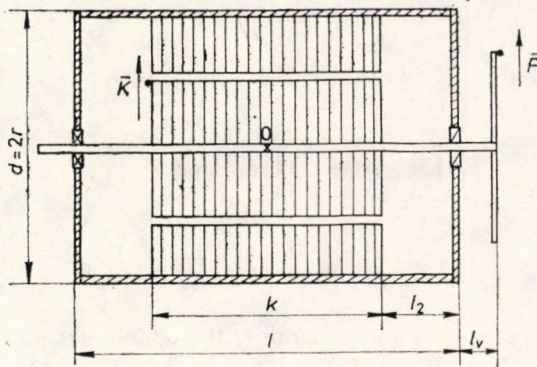
Fig. 8.4. Simplified kinematic model

been found to be smaller than that of the vibrating moment in practice, therefore
we shall neglect the effect of the vibrating force and discuss the case of pure dynamic
unbalance ($\alpha = 180°$).

As we want to establish a dimensionless relation, we introduce the following
simplifications:

$$\Delta I_1 = \Delta I_2 = \Delta I, \quad \text{so} \quad \bar{K} = -\bar{F} = \bar{P}.$$

In this case the vibrating moment is found to be $\bar{P}(k + l_2 + l_v)$. This moment is
counterbalanced by $\Theta_0 \varepsilon$, where Θ_0 is the second degree polar moment of inertia of
the rotating machine with respect to O, ε is the angular acceleration about O.
Now let us express the values of Θ_0 and ε.

Θ_0 can be expressed by the first scalar invariant I_{01} of the inertia tensor I_0. In the
coordinate systems of the principal axes, the matrix of the inertia tensor is given
by:

$$I_0 = \frac{M}{12} \begin{bmatrix} (3r^2 + k^2) & 0 & 0 \\ 0 & (3r^2 + k^2) & 0 \\ 0 & 0 & 6r^2 \end{bmatrix}. \tag{8.18}$$

$M = M_s + M_r$, where M is the total mass of the motor, while M_s and M_r are the
mass of the stator and rotor, respectively. The following equation applies:

$$I_{01} = [(3r^2 + k^2) + (3r^2 + k^2) + 6r^2], \tag{8.19}$$

therefore

$$\Theta_0 = \frac{M}{12} (6r^2 + k^2). \tag{8.20}$$

ε can be expressed by the circumferential acceleration which is the derivative of the vibration velocity measured on the end shield with respect to time:

$$\varepsilon = \frac{a}{l/2}, \quad a = \frac{dv}{dt}, \quad v(t) = \sqrt{2} v_{\mathrm{r.m.s.}} e^{j\omega t}.$$

The amplitude of the acceleration is $\sqrt{2} v_{\mathrm{r.m.s.}} \omega$, hence

$$\varepsilon = \frac{2\sqrt{2} v_{\mathrm{r.m.s.}} \omega}{l}.$$

The equation of the moment is:

$$\Delta I \omega^2 (k + l_2 + l_v) e^{j\omega t} = \frac{M}{12} (6r^2 + k^2) \frac{2\sqrt{2} v_{\mathrm{r.m.s.}} \omega}{l} e^{j\omega t}. \tag{8.21}$$

Transposing the equation and expanding the denominator on the left side by M_r/M_r, we obtain:

$$\frac{\Delta I}{M_r \left(\dfrac{M}{M_r} \sqrt{2} \dfrac{6r^2 + k^2}{6l} \right)} = \frac{v_{\mathrm{r.m.s.}}}{\omega (k + l_2 + l_v)}.$$

Both sides of the equation contain a bracketed factor in the denominator with dimension of length. Let us denote them by $k_1 l$ and $k_2 l$, respectively. Now we obtain:

$$\frac{\Delta I}{k_1 l M_r} = \frac{v_{\mathrm{r.m.s.}}}{k_2 l \omega}. \tag{8.22}$$

For machines of identical pole number and construction, the ratio k_1/k_2 is constant, so we obtain the following dimensionless relation between vibration velocity and unbalance:

$$\frac{v_{\mathrm{r.m.s.}}}{\omega l} \sim \frac{\Delta I}{M_r l}. \tag{8.23}$$

Another advantage of this dimensionless expression of unbalance is that it includes the quantity $e = \Delta I / M_r$, known as specific unbalance in the literature, which is an important factor in specifying the manufacturing procedure.

Now let us return to the original question of the relation between the significant vibration velocity and the maximum imbalance. Let $x = \dfrac{\Delta I_{\max}}{M_r l}$ and $\dfrac{v_{\max}}{\omega l} = y$, indicating the direction of the cause and effect relationship, and, to keep the physical meaning constantly in mind, we shall denote x as unbalance and y as vibration velocity. Figure 8.5 shows the results of measurements of this kind, indicating the corresponding $x-y$ values for all nine standard four pole machine sizes. The set of points obtained shows a kind of homogeneity and is suitable for the approximation with a single mathematical model.

Also, if we examine carefully the distribution of the points, we see that it implies certain order over the plane, and is readily suitable for approximation by a curve or a function. The correlation is reasonably good. Having small
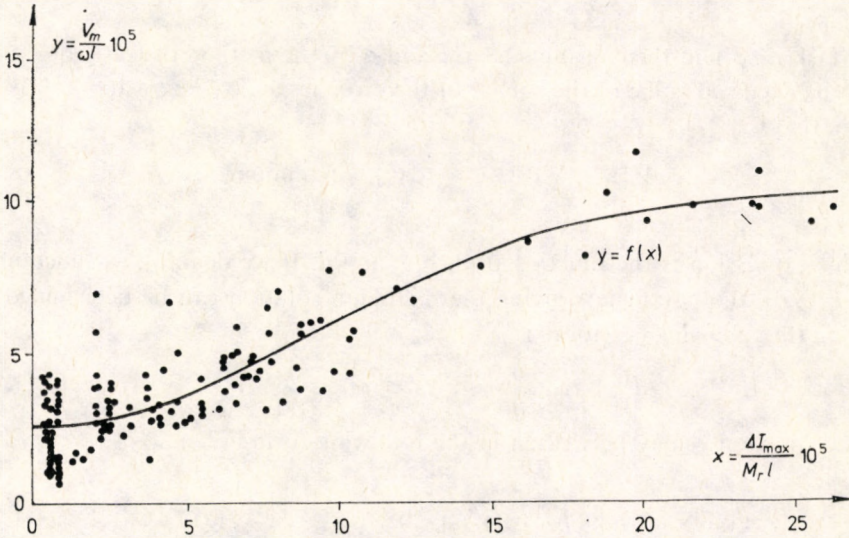
Fig. 8.5. Specific vibration velocity as a function of specific unbalance

unbalance, the set of points tends to congregate; this range corresponds to the machines with precisely balanced rotor. If we extrapolate zero unbalance, we see that the curve intercepts the y axis at a definite value. This is expected on a technical basis, since, as we said before, there are other vibration components of other origin with frequencies close to the rotational frequency. We can also see that a sort of saturation is reached when the value of the maximum specific unbalance is increased.

Simply connecting the points or arbitrarily fitting a curve to them is a rather rough method. As we know from mathematics, we always find a so-called inter-polation polynomial of degree $(n-1)$ that fits all the n points concerned. The deter-mination of this polynomial, however, is quite laborious and unnecessary. First, it would result in a function that depends on the number of measuring points, and secondly, it would take the measured values as accurate values, though we know that we have a measurement error in terms of both x and y.

Therefore we should find an empirical function fitting our measured data by means of regression analysis. The aim of regression analysis is the quantitative and qualitative assessment of relations between different quantities. The technique applied is called the method of least squares. The results are then analysed by

statistical test [138]. Looking at the cluster of points shown in Fig. 8.5, a third-degree function seems to be the most appropriate approximation.

The general form of the function in question:

$$y = a + bx + cx^2 + dx^3. \tag{8.24}$$

Our task is to find the constants a, b, c and d by the method of least squares so that the expected value of the square of the error $y - a - bx - cx^2 - dx^3$ is a minimum, that is,

$$M\{y - a - bx - cx^2 - dx^3\}^2 = \text{minimum}, \tag{8.25}$$

equation stands.

This expression is the function of a, b, c and d. If we denote this function as $g(a, b, c, d)$, the parameters giving the minimum solution can be determined by solving the following equations:

$$\frac{\partial g}{\partial a} = 0, \quad \frac{\partial g}{\partial b} = 0, \quad \frac{\partial g}{\partial c} = 0, \quad \frac{\partial g}{\partial d} = 0.$$

The function g may be written in the following form:

$$g(a, b, c, d) = \int_{-\infty}^{\infty} \int_{-\infty}^{\infty} (y - a - bx - cx^2 - dx^3)^2 f(xy) \, dx \, dy, \tag{8.26}$$

where $f(xy)$ is the common probability density function of the random variable pair x, y. After differentiation and reduction, we obtain the following linear set of equations for the unknown parameters a, b, c and d:

$$\begin{bmatrix} 1 & M\{x\} & M\{x^2\} & M\{x^3\} \\ M\{x\} & M\{x^2\} & M\{x^3\} & M\{x^4\} \\ M\{x^2\} & M\{x^3\} & M\{x^4\} & M\{x^5\} \\ M\{x^3\} & M\{x^4\} & M\{x^5\} & M\{x^6\} \end{bmatrix} \begin{bmatrix} a \\ b \\ c \\ d \end{bmatrix} = \begin{bmatrix} M\{y\} \\ M\{xy\} \\ M\{x^2y\} \\ M\{x^3y\} \end{bmatrix}. \tag{8.27}$$

In general form:

$$\int_{-\infty}^{\infty} \int_{-\infty}^{\infty} x^k f(xy) \, dx \, dy = M\{x^k\}, \tag{8.28}$$

where $M\{x^k\}$ is the expected value of the random variable x^k, and $k = 1, 2, 3, 4, 5, 6$:

$$\int_{-\infty}^{\infty} \int_{-\infty}^{\infty} x^l y f(xy) \, dx \, dy = M\{x^l y\}, \tag{8.29}$$

where $M\{x^l y\}$ is the expected value of the combined moment $x^l y$, and $l = 0, 1, 2, 3$.

As we do not know the common density function of the random variable pair x, y, we can only estimate the coefficients of the regression equation from the sample. We have at our disposal the observed discrete values (X_i, Y_i) regarding the continuous random variable pair (x, y), so we obtain the following normal equation system:

$$\begin{bmatrix} n & \Sigma(X) & \Sigma(X^2) & \Sigma(X^3) \\ \Sigma(X) & \Sigma(X^2) & \Sigma(X^3) & \Sigma(X^4) \\ \Sigma(X^2) & \Sigma(X^3) & \Sigma(X^4) & \Sigma(X^5) \\ \Sigma(X^3) & \Sigma(X^4) & \Sigma(X^5) & \Sigma(X^6) \end{bmatrix} \begin{bmatrix} a \\ b \\ c \\ d \end{bmatrix} = \begin{bmatrix} \Sigma(Y) \\ \Sigma(XY) \\ \Sigma(X^2Y) \\ \Sigma(X^3Y) \end{bmatrix}. \tag{8.30}$$

The unknown variables of this set of equations, i.e., the coefficients of the third-degree regression function, may be expressed by Cramer's rule as:

$$a = \frac{D_a}{D_e}, \quad b = \frac{D_b}{D_e}, \quad c = \frac{D_c}{D_e}, \quad d = \frac{D_d}{D_e}.$$

The deviation of the calculated value Y_{ei} at a given point, X_i, from the measured value Y_i is given by the residual as:

$$z_i = Y_i - Y_{ei}.$$

The variance $\hat{S}_z^2$ is the estimated variation of Y_e about the empirical function:

$$\hat{S}_z^2 = \hat{S}_{yx}^2 = \frac{\sum_i (z_i^2)}{n - m}. \tag{8.31}$$

The degrees of freedom are found in the denominator which is simply the number of elements in the sample reduced by the number of constants in the regression equation. The estimated variation of the estimated regression equation practically means that 68 percent of the measured Y values fall within the range $Y_e \pm \hat{S}_{yx}$, and nearly 95 percent within the range $Y_e \pm 2\hat{S}_{yx}$.

However, we do not yet have the answer to the question of the strength of the dependence of the dependent variable on the independent variable. This dependence is characterized by the correlation factor, defined as:

$$r_{yx} = \frac{\sum_i (Y - \bar{Y})(X_i - \bar{X})}{n S_y S_x} \tag{8.32}$$

or rewritten as:

$$r_{yx} = \sqrt{1 - \frac{\sum_i (Y_i - Y_{ei})^2}{\sum_i (Y_i - \bar{Y})^2}}, \tag{8.33}$$

where $\bar{Y}$ is the arithmetic mean value of the sample. Several authors suggest

that the square of the correlation factor, the so-called determinational index, is a better measure of the closeness of the correlation:

$$d_{yx} = r_{yx}^2. \tag{8.34}$$

For the production engineer, the model obtained allows quick determination of the balancing limit to be specified for the worker operating the balancing machine.

The question the technologist must ask is what acceptable unbalance ΔI_{max} should be specified for the balancing work in order to control vibration velocity below v_{max} with a safety of p percent.

Further, the model allows the determination of the minimum vibration velocity together with its dispersing band for each standard machine size, which can be achieved by balancing, and also the residual imbalance level that is worth achieving by balancing. As the shape of the curve suggests, we can determine a reasonable unbalance level. We could reduce vibration by going below this level, but the required amount of time and cost is not in proportion to the gained improvement. We note that this mathematical model applies only to a given technology, materials and machine design. If any of these changes, the model must be set up again to reflect the new conditions, or in other words, the mathematical model should be "maintained" on a continuous basis.

9. NOISE OF AERODYNAMIC ORIGIN

The major part of the sound power emitted by low-power high-speed machines (such as two-pole asynchronous motors) and medium and large rotating electrical machines is noise of aerodynamic origin. In the noise of power transformers, that produced by the external forced cooling system can be predominant as well. For at least 50 percent of machines running today, noises of fluid flow origin are the greatest. This situation is the result of two factors. First, the increased utilization of active parts in the machine resulted in increased machine losses, and consequently the cooling intensity had to be improved. Secondly, engineers have achieved significant results in reducing noises of various origins.

The cooling air in power machines either circulates in a closed internal circuit, transferring the heat to water or ambient air in a heat exchanger, or exits to the ambient after warming up, letting the fresh cool air flow in from the outside environment. In either system, the air flow is driven by a fan or group of fans. During its passage, the direction and rate of air flow changes continuously owing to deflections and friction on the walls, so that the air pressure steadily decreases. This pressure drop is compensated by the fans. The capacity of the fan is determined by the amount of heat to be transported (required volume flow rate) and the pressure boost required to maintain the flow. Experience proves that obstacles placed in the air stream produce sound, therefore the basic source of aerodynamic noise is the fan itself. Based on the spectral distribution of the fan noise, we talk about broad-band noise and siren noise.

The sound power that gives rise to the broad-band noise is continuously distributed over the frequency range of 100 Hz to 10.000 Hz. Broad-band noise is caused by turbulence and separation of the flow (vortex and separation noise). These noises are inherent in the operation of the fan and cannot be eliminated but at best reduced to a reasonable and acceptable level.

Siren noise is characteristically tonal and certainly an unpleasant sensation of hearing. It is produced when a stationary object is placed near the rotating impeller, building up a vortex field around it. From the frequency of the pure tone, the noise source can be identified in many cases. At present, no exact calculation

procedure exists to predict the magnitude of siren noise. Siren noise may be eliminated by increasing the distance between the impeller and the stationary obstacle.

9.1 Broad-band noise

9.1.1 Theoretical background of broad-band noise generation

We talk about flow-induced noise when certain flow parameters, like velocity v or pressure p, fluctuate in time in a section of the flow space, and this fluctuation propagates at the speed of sound.

The cause of the noise produced by an air stream injected into a medium at rest is the fact that the kinetic energy of the air stream is consumed by the friction along the periphery of the stream, slowing down the flow. Now the fluctuations in velocity, pressure and tangential stress within this space section generate sound which is radiated to the surroundings. The varying direction of air flow, aiming at the fan blades or aerofoil, gives rise to a fluctuating pressure on the surface. This way the surface of the obstacle becomes a sound source fed by the kinetic energy of the flow.

The theory of flow-induced noise is based on the laws of fluid mechanics, in particular, on the non-homogeneous wave equation (derived from the continuity equation and the equation of motion), since the homogeneous wave equation of classical physics governs only the propagation of sound. The non-homogeneous second-order linear differential equation, apart from representing all classical acoustical phenomena (sound diffraction, dispersion, etc.), takes into account the tangential stresses, rates and pressure fluctuations in the stream and on bounding solid surfaces, involved in the flow process. Integrating the equation, we arrive at the so-called Kirchhoff's formula [112], which allows the computation of the sound pressure, provided that the flow parameters representing the inhomogeneity of the equation are known. This last criterion is very rarely met, and so the theory set up by Lighthill in 1952 has very seldom yielded correct quantitative results. Nonetheless, the theory contributed a technique of immense importance to the technical world, albeit only of qualitative nature.

Each term of the Kirchhoff integral may be substituted for by the known quantities of classical acoustics, namely by monopoles, dipoles and quadrupoles, respectively, whose strengths are determined by the actual flow conditions. Now the propagation pattern can be computed using methods of classical acoustics for the system of singularities representing the true flow regime.

A monopole arises when a varying mass flow appears in the space at rest or leaves it. A pulsating sphere, for example, represents a monopole. A monopole
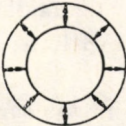
can replace any throbbing air stream, like the exhaust gas. The finite number of fan blades may produce a similar pulsating volumetric flow.

When forces that vary in time act on a medium, we talk about a dipole. These forces may arise as a product of vibrating boundary walls, but also from pressure fluctuation of the flow over wall surfaces. A vibrating solid sphere may be considered as a dipole radiator. A dipole can be derived from the concept of two monopole spheres pulsating in a push-pull fashion, at infinitesimal separation. The blades of the fan, for example, can be considered as dipole-like radiators.

Quadrupoles are generated when the normal and tangential stresses in the flow vary in time. A quadrupole can be derived from two dipoles. An unbounded turbulent flow or the whirling of the central stream may be considered as a quadrupole-like radiation.

For compact sound sources $l \ll \lambda$, where l is the overall measurement of the sound radiator and λ is the wavelength, in the acoustical far field where the sound pressure and the particle velocity excited by the sound are in phase, the power laws compiled in Table 9.1 apply. These laws govern the dependence of the radiated sound power P on the parameters of flow and geometry. These power laws can be derived from the Kirchhoff integrals, so they are not purely empirical relationships but are based on theory. The laws use three typical parameters: velocity, v, characteristic of the flow; the so-called Mach number, which is the ratio of the above velocity to the speed of sound, c, that is, $\mathrm{Ma} = v/c$; and the characteristic geometric size of the coherent radiator, l, ϱ is the density of the medium and L_W is the radiated sound power level.

Table 9.1. Power laws in flow acoustics

Pole number	Model	Sound power, W Sound power level, dB	Acoustic efficiency
Monopole		$P_M \sim \varrho \dfrac{v^4}{c} l^2 = \varrho v^3 l^2\, \mathrm{Ma}$ $L_{W,M} = L_{W,jM} + 20 \log l + 40 \log v$	$\eta_M \sim \mathrm{Ma}$
Dipole		$P_D \sim \varrho \dfrac{v^6}{c^3} l^2 = \varrho v^3 l^2\, \mathrm{Ma}^3$ $L_{W,D} = L_{W,jD} + 20 \log l + 60 \log v$	$\eta_D \sim \mathrm{Ma}^3$
Quadrupole		$P_Q \sim \varrho \dfrac{v^8}{c^5} l^2 = \varrho v^3 l^2\, \mathrm{Ma}^5$ $L_{W,Q} = L_{W,jQ} + 20 \log l + 80 \log v$	$\eta_Q \sim \mathrm{Ma}^5$

For a cooling system of large electrical motors, the Mach number is small (Ma < 0.3), and so only monopoles and dipoles play important role.

The power functions give information about ratios only. The quantity $L_{W,j}$ is characteristic of a given fan design, in most cases determined experimentally.

In principle, the power functions allow noise diagnosis, since the source and pole number of the noise can be determined by altering the flow rate (this can be achieved by controlling the speed of the fan) and measuring the resultant sound power. Unfortunately, reality is a little more complicated, because $L_{W,j}$ can also depend on the speed, since, for example, the Reynolds number involved is a function of flow rate. Therefore it can occur that instead of the expected sixth power we measure the fifth, fourth power for fans whose noise is typically dipole in nature because of blade force fluctuation. The situation is further complicated by the fact that a dipole placed inside a tube behaves like a monopole, and a quadrupole, like a dipole. However, this occurs only under well defined conditions, so in general we can say that the power laws outlined provide only indications.

Measurements reveal that the noise spectrum emitted by fans is continuous with superimposed peaks of pure sounds here and there. A certain pressure distribution pattern can be measured on any fan blade, whether it is of a radial-flow or an axial-flow type. This pressure distribution pattern depends on the direction of the fluid stream and on the size of the blade. If this direction or strength changes or fluctuates, then a dipole-like sound source will be produced. There can be various reasons for changes in direction or strength. The stream itself can be strongly turbulent, which means that the flow rate inside the stream fluctuates about a constant mean value. This fluctuation is stochastic, the response is poorer to high-frequency (fast) changes owing to the inertia of the flow. Therefore pressure distribution cannot strictly follow the excitation, and the spectrum consequently tails off for high frequencies. As the vortex sizes cannot grow infinitely in the turbulent flow, the spectrum tails off in the direction of low frequencies as well. Strong turbulence can result in an increase of 10 to 15 dB in the sound power.

The turbulent flow should not be mixed up with the separation flow which contains large vortices (vortex shedding). Owing to the positive pressure gradient being built up along solid walls or in the trail of obstacles in the air flow, vortex shedding develops, since the flow pattern cannot follow the gradient. The prevailing large vortices give rise to substantial low-frequency excitation which makes the machine "growl" and "hammer". Vortex shedding may occur in radial-flow machines across the face of large wheels, induced by poor intake conditions, incorrect inlet box design or through "stalled" blades (i.e., too large attack angle). The latter is a result of a poor fluid mechanical design, e.g., in the case of incorrectly calculated radial blading or a blading used in reversing mode, or

under operating conditions when the actual volume flow rate is well below or above the design value.

Even the smoothest and most precise inflow pattern gives rise to a certain broad-band spectrum. The reason is the so-called trail noise. When the split streams flowing along the two sides of the blade meet behind the blade, the mixing boundary layers give rise to a vortex trail as shown in Fig. 9.1. The drifting vortices induce
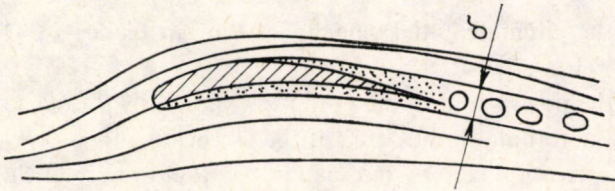
Fig. 9.1. Stationary obstacle in the way of flow

circulation and pressure disturbances on the blade, manifesting a dipole sound source. Removal of this trail by suction or by eliminating the boundary layers through cleaning is still beyond today's technology.

9.1.2 The sound power level of the fan

The complicated theories of flow acoustics proved to be excellent means for practical purposes, but there is still no reliable procedure at our disposal for the exact calculation of fan noise. We do have, however, an approved empirical formula, which is suitable for practical applications:

$$L_W = (40 \pm 4) + 10 \log \frac{\dot{V}}{\dot{V}_0} + 20 \log \frac{\Delta p_t}{\Delta p_{t,0}}, \tag{9.1}$$

where $\dot{V}$ is the volumetric flow in $m^3 \, s^{-1}$, Δp_t is the total pressure increment produced in Pa, $\dot{V}_0 = 1 \, m^3 \, s^{-1}$, $\Delta p_{t,0} = 1$ Pa. The ± 4 dB in the constant term indicates the spreading range of the formula. The correctness of the formula can be proved on an exact theoretical basis for axial fans without guide vanes. The important point of the formula is that the minimum value of the radiated sound power depends on the volume flow rate (delivered volume) and, in particular, on the total pressure increment produced. We should note, however, that we may get results 3 to 5 dB higher by measurement, compared with those yielded by the formula, if the actual volume flow rate differs by ± 50 percent from the design value. If strong pure tone components are present in the spectrum, then the formula may underestimate the real sound power level by 8 to 10 dB.

To sum it up, the formula gives only the minimum level to which the produced noise can be brought down, and highlights the fact that we can reduce the noise considerably by reducing the losses (Δp_t) in the flow circuit. In the Slavonic literature, Gorodeckij, Pazout and Zavadil used the following formula to calculate the 1-meter sound pressure level [150]:

$$L_p = 10\beta \log \frac{v}{v_0} + 10 \log \frac{D_t b_t}{S_0} + \sum_{i=1}^{8} K_i, \tag{9.2}$$

where v — the circumferential velocity of the fan blade; $v_0 = 1$ m s^{-1}; $S_0 = 1$ m^2,

β — the power used in the power law, normally $\beta = 6$ is taken,

$D_t b_t$ — the trailing surface area of the fan blade,

K_i — correction factors that take into account the following:

— volume flow rate,
— geometric sizes of the fan blade, and their ratios,
— number of blades of the fan wheel,
— sound absorption of the fan enclosure,
— inherent error of the measuring method, etc.

In order to improve the accuracy of eqn. (9.2), we can approximate the dependence of power β on the peripheral speed and the changing importance of the individual acoustic singularities in the process, as

$$\beta = \frac{6}{5} v^{2/5}, \tag{9.3}$$

on the basis of regression analysis of measured data.

At first sight, eqn. (9.2) seems to imply that the noise produced by the fan depends mostly on the peripheral speed. However, this is only apparent. A given cooling function can be realized with different peripheral speeds (a given amount of heat to be transported corresponds to a concrete $\dot{V} - \Delta p_t$ value pair). If the peripheral speed is increased by increasing the diameter of the fan, then it is true that the first term of eqn. (9.2) increases, but in this case a much smaller b_2 is required to solve the same cooling problem, so the second term decreases just as several correction factors (K), and therefore the radiated sound power remains almost the same.

9.1.3 Predicting the spectral composition of broad-band noise

The formula (9.1) gives the unweighted total sound power level radiated in the whole frequency range. The spectral distribution depends on the fan type. For preliminary calculation purposes we achieve acceptable results, if the octave-band

sound power level is determined by using different correction factors for each octave band in order to correct the value of sound power level calculated from eqn. (9.1). The correction factors (ΔL_{oct}) are given in Table 9.2 for a 400 mm diameter opening (the one closer to the fan, normal suction). If the diameter is increased, the low-frequency components grow. If the diameter is decreased, the low frequency components diminish.

Table 9.2. The values of ΔL_{oct} for different centre frequencies, in dB

	f_k, Hz							
	63	125	250	500	1000	2000	4000	8000
Straight-blade radial-flow fan	13	10	13	13.5	15	20	23	26
Backward-curved-blade radial-flow fan	14	11	11	11.5	13	16	19	22
Axial-flow fan	17	14	9	7.5	8	11	16	18

$L_{W \cdot oct} = L_W - \Delta L_{oct}$.

In many cases it may be necessary to predict the probable A-weighted sound pressure level in the vicinity of the motor. To accomplish this task, first the octave-band sound power levels should be calculated from the total sound power level determined by eqn. (9.1) After that the octave-band unweighted sound pressure levels L_i should be computed from the distance of the observation point. Now the L_i values should be corrected according to the damping characteristic of the A-weighting filter and summed, just as in eqn. (9.4):

$$L_A = 10 \log \sum_{i=1}^{n} 10^{0.1(L_i - K_{Ai})}, \qquad (9.4)$$

where L_A — the A-weighted sound pressure level at the observation point,
L_i — the octave-band sound pressure levels at the observation point,
n — the number of octave bands,
K_{Ai} — the damping of the A-weighting filter in the ith octave band.

9.1.4 Cooling system and noise. Noise reduction through design

Almost all low-power asynchronous motors are equipped with straight radial fan blades in order to allow operation in both rotational directions. These blades are unsatisfactory from the point of view of aerodynamics, and are noisy, so it is very hard to reduce their noise. There is no generally approved method to cure

the problem. The sound power emitted by medium-sized and large asynchronous motors depends strongly on the design of the ventilation system, so we will discuss this subject in a little more detail. The commonest ventilation systems and the main aerodynamic noise sources are shown in Fig. 9.2.
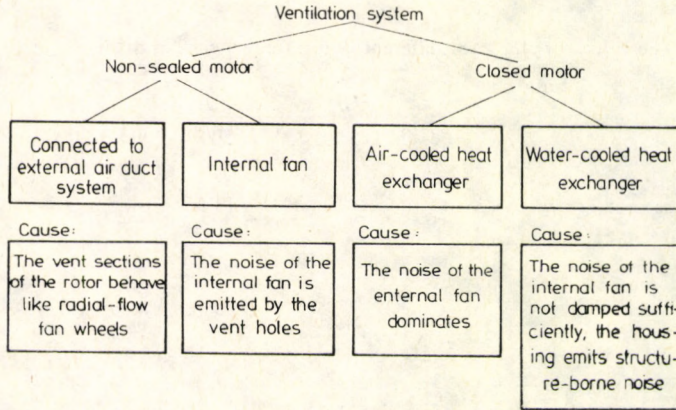
Fig. 9.2. Relationship between the ventilation system and the causes of noise

There are two main flow paths of the cooling air inside the electrical machine. One of them leads through the winding heads and the air duct between the stator core and the housing. This route is characterized by a relatively small pressure drop and high volume flow rate. The other path leads through the vent sections between the lamination packs of the rotor, the air gap and the vent sections of the stator. This route is characterized by a large pressure drop and a relatively low volume flow rate. The cooling air streams passing through the two different routes coalesce and exit to the atmosphere or enter the heat exchanger and in closed machines start the flow circulation again. In short machines, the internal ventilation system is located on one side, while in long machines, on both sides. The two-sided ventilation is better, because the temperature distribution within the active part of the machine is more uniform, the volume of air fed to each fan is smaller by 50 percent, and the total pressure drop to be maintained, Δp_t, is reduced by almost 50 percent. The acoustical consequence is a 4 to 5 dB reduction in aerodynamic noise, as obtained from eqn. (9.1). The flow of the internal cooling air is maintained by radial-flow fans in small machines, and by axial-flow fans in large machines. The stator and rotor vent sections and their radial spacer bars behave as a poor efficiency fan.

Closed machines that employ an air-cooled heat exchanger are equipped mostly with a radial-flow outer fan wheel, but sometimes with an axial-flow type. Figures 9.3a and b and 9.4a show examples of the three commonest constructions

(a)

(b)
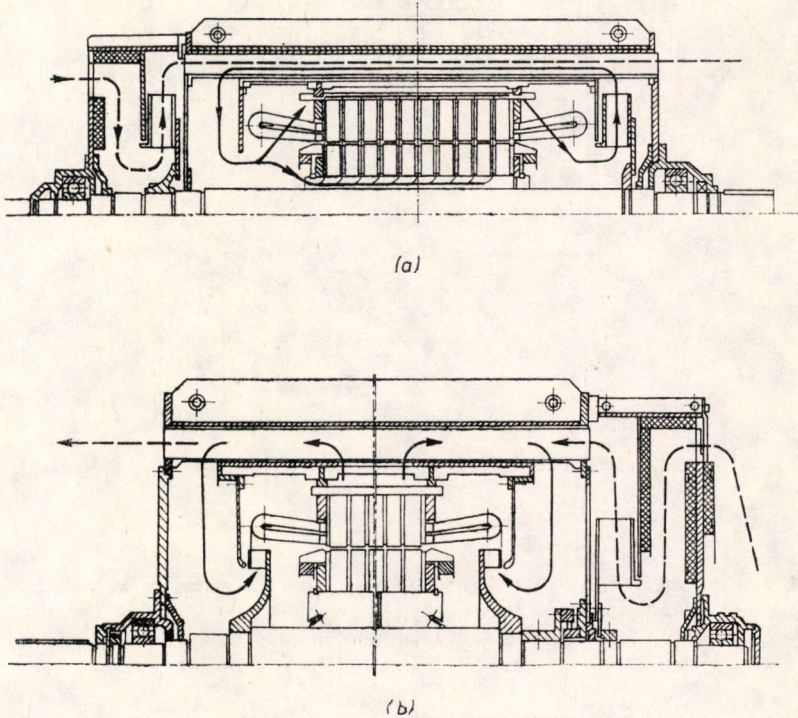
Fig. 9.3. The cooling system of totally enclosed asynchronous machines with air-cooled heat exchanger and radial-flow internal fan: (a) one-side cooling, (b) two-side cooling

for closed machines. As shown in Fig. 9.4b, it is possible to mount the axial fan system on a tube which separates the air passing through the vent section from the air cooling the winding head. The two parallel flow routes incorporate a fan that is more suitable for the aerodynamic situation.

One straightforward way of reducing noise by design is to take advantage of the inherent noise level difference between the various protection grades of rotating electrical machines and the corresponding cooling systems. For a given speed and output, the quietest machines are, of course, the totally enclosed machines equipped with a water–air heat exchanger. The first example of deliberate utilization of selected cooling methods for the reduction of noise was set by SKF, when they equipped their totally enclosed asynchronous motors of 132 mm axial height with a liquid surface cooling system (water or oil). This way
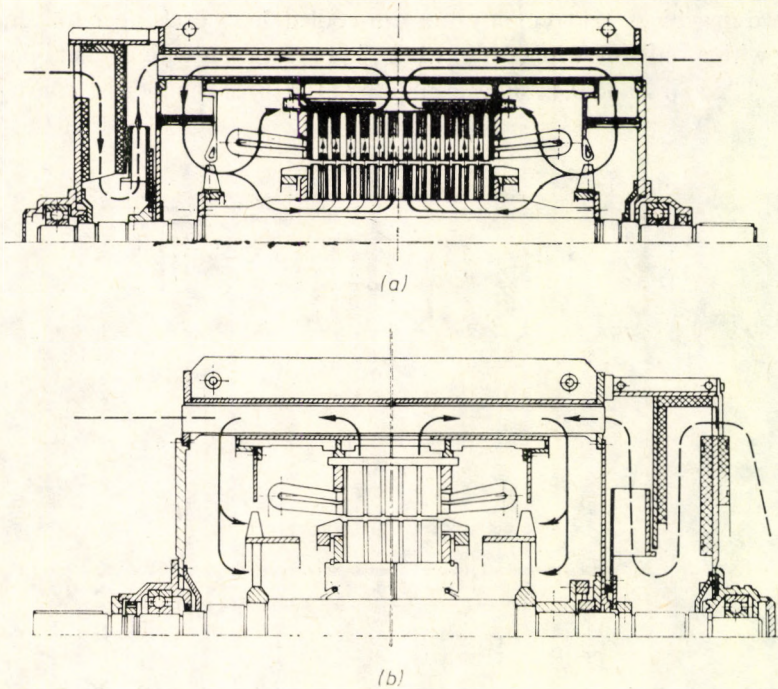
Fig. 9.4. The cooling system of totally enclosed asynchronous machines with air-cooled heat exchanger and axial-flow internal fan: (a) two-side cooling with axial-flow fan, (b) two-side cooling with axial-flow fan on tube

they could decrease the noise of two-pole asynchronous motors fed from a 100 Hz supply by 35 dB.

The noise of totally enclosed high-power 50 Hz asynchronous motors could be reduced by 17 dB just by replacing the air-cooled heat exchanger with a water-cooled design.

Surprising reduction may be achieved in the ventilation noise of electrical machines at the installation site by connecting the machine into the closed external ventilation duct. In this case, the fan of the motor becomes unnecessary, of course. A solution similar in principle was adopted by English ventilation system manufacturers, who removed the fan, which was a poor design from an aerodynamic point of view, from the electrical machine, and rerouted the air flow driven by an aerodynamically optimized driven fan wheel so that it cooled the electrical machine as well.

It is no coincidence that the small two-pole motors available on the world

market are very similar with respect to noise quality—there are no prominently quiet machines.

The rotational sense of medium-sized and large motors is normally given, and they can therefore be equipped with unidirectional fan blades. The noise level of backward-curved blades is lower, but the pressure produced by them is also lower. If the pressure is not enough, then we must be satisfied with fans of small angle of attack but of radial outflow. The noise of the latter, however, is larger than the noise of that with backward-curved blades. According to the experience of ASEA, 8 to 10 dB noise reduction is feasible in the case of two-pole machines, if unidirectional fans with backward-curved blades are used, with correct aerodynamic design.

The transfer from radial-flow fans to axial-flow types can result in a noise reduction of 4 dB. However, this change in design is feasible only if the lower pressure produced by the axial-flow fan is sufficient for the required air flow.

In the case of custom-built or small-series electrical motors, mostly in the medium and high output range, we frequently encounter the task of machine noise reduction, mostly of aerodynamic origin, without changing the design of the machine. In such a case, we first have to see whether the machine has some thermal margin or not. If not, then we can only adopt the secondary noise reducing procedures set out in Chapter 10.

In many cases, the loading test carried out on the completed machine reveals that there is still a thermal margin in the machine. In such a case, it is worthwhile checking the cooling system of the completed machine by calculation, taking into consideration the actual characteristics of the machine. The measurement of the actual losses provides accurate information on the amount of heat to be transported. On this basis, we can calculate the required volume flow rate which is normally lower than the nominal value. The total pressure increment decreases with decrease in volume flow rate squared. Both of these changes tend to reduce noise. The smaller fan that corresponds to the new values of volume flow rate and total pressure may be made in most cases easily by machining down the diameter of the original fan. The amount of diameter reduction is closely proportional to the ratio of the original volume flow rate to the new value. The reduction is limited by the fact that the length of the blades decrease faster than proportionally to the diameter. The achievable decrease in sound power is given by $\triangle L_W = 50 \cdot \log (D_{k,\text{new}}/D_{k,\text{old}})$. We should bear in mind, however, the thermal effect of such a noise reduction. With the same ambient temperature the air temperature at the outlet of the cooling system will be higher. If the air temperature increment at the outlet is $\triangle t$, then the same parameter inside the machine is only $\triangle t/2$.

9.2 Pure-tone ventilation noise, the siren effect

A pure tone is produced if a periodic disturbance of the inflow acts on the fan, or if air leaving the blade hits a stationary obstacle near the fan. The resultant sound A phenomenon is mostly the product of the interaction between the equispaced blades of the fan and the stationary obstacles. Owing to the tonal character of the produced sound, the phenomenon is called siren effect. As the frequency of the pure tone is given by:

$$f=N_b n, \qquad\qquad (9.5)$$

where N_b is the number of blades and n is the rotational speed, this component and its harmonics can be readily identified in the noise spectrum of the machine.

If more than one stationary obstacle exist near the rotating fan, experience shows that each one behaves like an individual sound source. The magnitude of the pure sound produced is strongly affected by the distance of the stationary obstacle from the rotating fan and the angle of attack of the flow with respect to the boundary surfaces of the stationary obstacle.

The following formula is widely used in the literature as an empirical inequality to be observed if we want to avoid the appearance of pure-tone components in the ventilation noise spectrum:

$$\delta \ge \frac{v^2}{30}, \qquad\qquad (9.6)$$

where δ is the distance of the stationary obstacle from the rotating fan in mm and v is the peripheral speed of the blade in m s^{-1}.

If the shape and speed of the blade and the size and profile of the stationary obstacle is constant, then the experimentally determined sound pressure level established by the fan varies with the distance δ as shown in Fig. 9.5. If we sub-
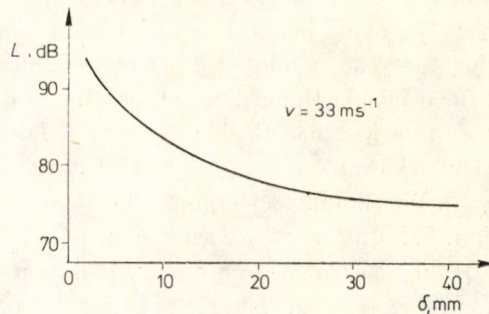
Fig. 9.5. The variation of the sound pressure level produced by the fan in terms of δ, when a pure-tone component is also present

stitute the values given for the measuring equipment described in [93] into eqn. (9.6), the minimum value of δ is found to be 37 mm. This corresponds with the observation that at such a distance the pure-tone component diminishes and the broad-band noise of the fan at around 75 dB becomes independent of the value of δ. We can also see that the pure-tone component may decrease considerably at a distance of one third of the value calculated from eqn. (9.6) for δ. In certain cases, however, the installation space of the electrical motor is so limited (as in the case of traction motors) that there is no way to increase the dimensions and hence δ.

BBC engineers solved this problem by changing the profile of the obstacle with constant distance δ [85]. They experimentally determined the most favourable shape that gave rise to the lowest sound pressure level. This solution took advantage of the fact that by modifying the profile of the obstacle they also modified the angle of attack of the air flow with respect to the obstacle, thus finding the acoustical optimum in a hit and miss fashion.

As we have seen, evenly spaced blades are required to produce pure-tone noise. This fact readily suggests the other method of pure-tone ventilation noise reduction, namely the use of unevenly pitched blades.

Based on experiments, the following formula has been found for the determination of uneven pitch angles:

$$\alpha_i = \frac{360}{N_b + g\beta \cos\left[\dfrac{2\pi g}{N_b}(i-0.5)\right]} , \tag{9.7}$$

where α_i — the central angle between the ith and $(i+1)$th blades, in degrees,
$\quad N_b$ — the number of blades,
$\quad g$ — 1 or 2,
$\quad \beta$ — the degree of non-uniformity in the blade spacing, $0 < \beta < 1$.

The sum of these blade pitch angles, $\Sigma\alpha_i$, must of course be 360°. For this reason, the values α_i obtained by eqn. (9.7) must be adjusted by a factor of $360/\Sigma\alpha_i$.

The stator and rotor cores of large rotating machines incorporate radial vent sections to provide adequate heat transport to prevent heat build-up between lamination packs due to iron loss and coil losses in coils axially bridging the vent sections. The width of the vent section is maintained by means of spacer bars. The rotor itself, with its vent sections, spacer bars and coil bars, behaves like a fan. If the rotor is axially positioned so that its vent sections face the vent sections in the stator, then the siren effect may arise in the machine. In this case, the stator spacer bars, the stator winding and the key bars serve as stationary obstacles.

Experiments were conducted to determine the effect of the relative axial position of stator and rotor vent sections on noise generation within these sections. It was

found that as far as the siren effect was concerned, the worst case resulted when the vent sections were positioned face to face. When the rotor vent section was shifted in an axial direction, the pure-tone component decreased and, consequently, the A-weighted sound pressure level also decreased. Unless the vent sections do not "see" each other, we always have a prominent pure-tone component in the noise spectrum. By mismatching the axial position of vent sections, the noise can be reduced by as much as 10 dB.

In view of the fact that the noise produced by vent sections arises inside the machine, it can seriously effect the emitted sound power only if the machine it not closed. In the case of totally enclosed machines, the sound insulating effec of the enclosure is strong enough to suppress the internal noise considerably, so it cannot become predominant in the measured noise.

In non-sealed motors, there is usually sufficient free space to place absorbing materials inside the housing and route the air flow through them to allow properly damped sound power enter the acoustic space surrounding the machine. If this damping is not adequate, then the secondary noise reducing procedures described in Chapter 10 must be used.

10. SECONDARY NOISE REDUCING MEASURES

The technical measures aimed at noise reduction comprise the so-called primary and secondary solutions. Primary solutions are those which modify the active noise source itself. We have discussed these solutions in detail in the previous chapters, when we talked about design considerations regarding the reduction of noises of electromagnetic origin, or about rotor balancing and then the various ventilation systems. These primary measures, almost without exception, can be implemented only at the manufacturing factory, mostly in the design or assembly stage. The only exceptions are the several aftermeasures, though considered primary, such as operating the asynchronous machine at reduced supply voltage, extending the air gap length by cutting the rotor diameter, or replacing the bearing or fan wheel.

It follows by logic from the above that secondary intervention does not modify the design of the electrical machine but rather applies additional noise reducing elements, e.g., an enclosure, insulating panels, etc., in order to reduce the measurable sound pressure level in the vicinity of the machine. In other words, the complex system comprising the electrical machine and the additional noise reducing elements, emits less sound power to the surroundings than the initial machine alone.

The vibration absorbing foundation is also considered to be secondary intervention, although the situation here is a little different. Normally the noise reducing measures reduce the airborne sound power emitted by the electrical machine. In the course of the standard noise measurement, usually for small and medium-sized machines, we prevent the vibrational energy of the machine being transmitted to the surroundings, so we measure only airborne sound power, since structure-borne sound cannot be transmitted there. When the machine is set up on its foundation, structure-borne sound bridges are produced, so it is possible that a part of the vibrational energy transferred to the environment is transformed into airborne sound, increasing the sound pressure level measured in the vicinity of the machine. If we eliminate the sound bridges by means of vibration absorbing materials, then we do not actually decrease the sound power emitted directly by

the electrical machine, but rather reset the measured level to the level emitted directly by the machine.

We have to be very careful in applying either primary or secondary noise reducing measures. We should constantly bear in mind that any interference with the electrical machine as a system will have some consequence. If we decrease fan noise by decreasing the diameter of the fan, we inevitably raise the temperature inside the machine. If we decrease flux density, we also decrease the rated output, etc. Also, we should not forget that the secondary measure of putting an enclosure around the machine will deteriorate the conditions of ventilation within the machine. Before the noise reducing measures are implemented, the technical and economic consequences of these measures should be thoroughly considered and reviewed.

The two most important types of secondary measure aimed at reducing ventilation noise are noise damping and the use of enclosures. The enclosure can be a shell-type arrangement mounted on the surface of the machine (mostly on the plane boundary surfaces of large machines) or a separate housing at a certain distance from the machine. Secondary noise reducing measures are usually used on high-power, large-sized machines, and only rarely on small and medium-sized machines.

10.1 Reducing ventilation noise by damping elements

If the external cooling air of non-sealed machines or those equipped with air-cooled heat exchanger is routed through properly configured noise damping elements at the inlet and outlet, the noise can be reduced quite effectively, by up to 15 or 20 dB, and the costs involved are generally much lower than those of building an enclosure for the machine. In the literature [9], noise dampers are divided into two basic groups, namely, reactive and absorptive noise dampers.

The acoustical efficiency of reactive dampers is mostly determined by their geometric arrangement and shape. Reactive dampers are the chambers, resonance devices, pipes, branches, ducts and their various combinations. These elements introduce mismatches in the flow path of the acoustical energy, so a part of the energy flow is reflected back towards the noise source or tends to create strong pressure fluctuations in the chamber through multiple reflections. The reactive dampers can reduce noise considerably, even with few sound absorbers. Nonetheless, reactive dampers are relatively seldom used for noise damping of electrical machines.

The acoustical efficiency of absorptive dampers is defined by the sound absorbing materials placed in the flow ducts. These materials absorb a part of the sound

energy flowing in the duct, transforming it into frictional and thermal energy. An absorbing material is characterized by its acoustic absorption coefficient α and its specific flow resistance, r_{sf}:

$$\alpha = \frac{\text{sound energy absorbed and transmitted}}{\text{incident sound energy}},$$

$$r_{sf} = \frac{\Delta p}{cd}, \tag{10.1}$$

where Δp — sound pressure drop across the absorbing material of thickness d,
$\quad c$ — speed of sound in the absorbing material,
$\quad d$ — thickness of the absorbing material.

One of the most commonly used damping devices is the absorbent-plate silencer.

A wide range of silencers designed for ventilation systems which are to be installed in the air duct, is available commercially. Their damping effect is based on absorption. The silencers are generally 1 m long pieces with square-section connecting port, but cylindrical, straight and 90° elbow sections are also available. The various forms are common in that they are most efficient in the medium-frequency ranges of $f_k = 500$ to 2000 Hz where their damping effect can reach 30 dB. At low frequencies ($f_k = 63$ Hz) only a few decibels may be expected, but, fortunately, the code requirements in most cases specify the reduction of the A-weighted noise level and the importance of low sounds is negligible in this respect.

If the suction of the built-in fan opens to the ambient, then the silencer should be mounted on the inlet port. This may, however, increase the length of the machine unacceptedly and therefore the insertion of an elbow might be necessary (Fig. 10.1). When selecting the connecting cross-section, we should take care not to reduce the free flow area compared with the original suction port of the machine. As for most silencers, the ratio of the clear opening to the contact surface area is 50 percent (or only 33 percent), the connecting port cross-sectional area should be at least twice that of the inlet port.
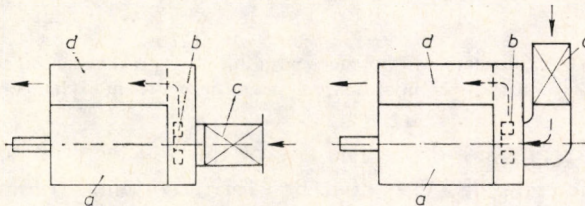
Fig. 10.1. Silencer on the suction side: a — motor, b — fan, c — silencer, d — heat exchanger

Downstream of the heat exchanger, at the air outlet, normally less damping is required, so those types with large clear openings are also acceptable. Drive-side installations frequently give rise to problems because of the driven machine. In such cases, the use of 90° or 180° change in direction is almost inevitable (Fig. 10.2). It can be a good solution to split the air flow and route the two branches separately.
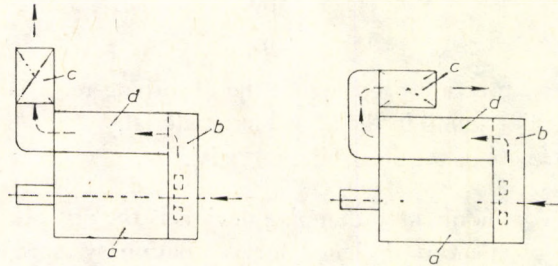
Fig. 10.2. Silencer on the discharge side: *a* — motor, *b* — fan, *c* — silencer, *d* — heat exchanger

If the cooling air enters the fan section on the drive side, the situation could be truly complicated owing to the lack of elbow room. From the point of view of fan operation, it is essential that the flow in the inlet path is even and smooth. This requires a lower flow rate, that is, larger clear opening, upstream of the suction port. This can be achieved by an inlet box which covers the clutch. In this configuration, the silencers are positioned on the two sides of the motor, as shown in Fig. 10.3.
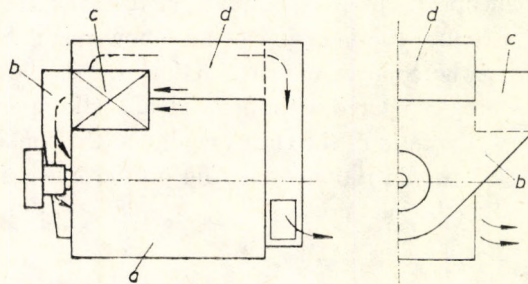
Fig. 10.3. Silencers on both sides with inlet box on the suction side: *a* — motor, *b* — inlet box, *c* — silencer, *d* — heat exchanger

Silencers cause pressure drop. The size of this loss may be determined from design data. The computation is done first for the original volume flow rate, $\dot{V}$, that corresponds to the conditions without silencers. Following the installation of the silencers, the originally required total pressure boost of Δp_t should be

increased to Δp_t^*. Now we have a new working point in the fan characteristic at a lower volume flow rate. We must check whether or not this decrease in volume flow rate gives rise to unacceptable heat build-up inside the machine. To compute the resultant drop in noise level, we have to know the original octave-band noise spectrum measured without the silencers in position. Then we deduct the damping specified by the manufacturer of the silencer for the corresponding medium-frequencies from each octave-band level and immediately add the correction necessary due to the change in working point of the fan, which can be determined from eqn. (10.2):

$$\Delta L = 10 \log \frac{\dot{V}^*}{\dot{V}} + 20 \log \frac{\Delta p_t^*}{\Delta p_t}, \quad \text{dB.} \tag{10.2}$$

Since $\dot{V}$ decreases and Δp_t increases, the sign of this correction term can turn out to be positive or negative.

Now the weighted noise level can be computed from the corrected octave-band levels according to eqn. (9.4). The size or installation circumstances may demand that one-off silencer designs be applied. The operation of these custom-made silencers that match the specifications of the given motor is also based on sound absorption. The correct solution is to line the internal surface of the air duct wherever possible with absorbing material. Of course, this must be done so that the clear opening is not reduced substantially along the flow path, for the increased flow rate could give rise to sounds when hitting mounting ribs, grids or other structural elements, and the flow losses would grow strongly as well. If possible, we should avoid flow speed higher than 15 ms^{-1}.

In custom-made sound damping devices, the flow (and the fan noise) passes between parallel sound absorbing links. Their thickness should be at least 80 to 100 mm, and the same values apply to the width of the channel between them. In sections normally shorter than 1 m, the damping is proportional to the length, measured in the direction of sound propagation. Nevertheless, sections shorter than 0.5 m should not be used.

The sound absorbing enclosure itself should be commercial product, if possible. It is beneficial if the volume mass is small, typically less than 100 kg m^{-3}. Surfaces in contact with the flow should be protected against dusting out. The utilization of glass-fibre-lined commercial sheets is expedient. The plastic and, especially, aluminium foil covering layer strongly lowers the sound absorbing efficiency. The absorbing sheets may be glued to metal surfaces. The mechanical strength may be improved by anchor pins piercing through and holding down the absorbing material to the metal surface to be lined.

When custom-made damper designs are used, the additional pressure drop that arises along the air flow path should be calculated for each section, using the

original (measured or computed) volume flow rate $\dot{V}$ in the calculation to find the corresponding total pressure boost Δp^* required, which is higher than the original value. The intercept of the new loss curve and the fan characteristic gives the new, reduced volume flow rate, $\dot{V}^*$. Its acceptability must be checked with respect to the heating of the machine. Figures 9.3 and 9.4 show custom-designed noise damping elements.

The calculation of expected damping is rather uncertain. In the case of parallel absorbing links, we may use the available measured data on commercial dampers of similar size. If the length is different, we use a correction factor proportional to the length.

The approximate estimation of damping due to absorbent lining of air duct sections is possible. If we have a section of this kind, i.e., a straight piece of air duct with length 800 to 1000 mm and a maximum width of 300 mm, about 12 dB may be assumed in the medium-frequency bands ($f_k = 500$ to 2000 Hz), 6 dB at $f_k = 4000$ Hz, and we neglect the damping of the other bands.

If we sum the damping values calculated for each frequency-band according to the above procedure, subtract the sum from the spectrum expected without dampers but corrected as required to take the shift of working point into account, we then obtain the expected octave-band spectrum from which the weighted noise level can be computed.

10.2 Enclosures

If the sound energy propagating in air impinges on a solid surface, i.e., on a wall, it is partially reflected, partially absorbed or spreads in the wall as structure-borne sound, and a substantial part passes along on the other side of the wall as airborne sound. The sound power entering the wall, P_1, the exiting airborne sound power, P_2, and the transmission loss of the wall, R, are interrelated as:

$$R = 10 \log \frac{P_1}{P_2} = 10 \log \frac{1}{\tau}, \quad \text{dB}, \tag{10.3}$$

where τ — the acoustic transmission factor, $\tau = P_2/P_1$.

From the sound pressure difference between the two sides of the wall, $(p_1 - p_2)$, and the wall vibration velocity c_w due to the airborne sound, the so-called wall impedance is found to be:

$$Z_W = \frac{p_1 - p_2}{c_W}; \tag{10.4}$$

For an infinite, homogeneous, plane surface:

$$Z_W = \frac{B(k^4 \sin^4 \vartheta - k_B^4)}{j2\pi f}, \tag{10.5}$$

where B is the stiffness factor

$$B=\frac{E_W}{(1-\mu^2)}\frac{h^3}{12},$$

where E_W— the modulus of elasticity,
          h— the thickness of the wall,
          μ— Poisson's ratio (between 0.3 and 0.4),
          k and k_B—the wave numbers in air and in the wall, respectively:

$$k=\frac{2\pi f}{a},$$

$$k_B=\sqrt{2\pi f}\sqrt[4]{\frac{M}{B}},$$

where M is the so-called sheet mass of the wall, that is, $M=\varrho_w h$ where ϱ_w is the density of the wall material.

If ϑ is the angle of incidence made with the normal to the wall, then the transmission loss is given as:

$$R=20\log\left(1+\frac{Z_W}{\varrho c}\cos\vartheta\right),\tag{10.6}$$

where $\varrho c=408$ N s m^{-3}, the characteristic impedance of air. From the above we may deduce that the transmission loss of the wall depends on the sheet mass M and stiffness B of the wall, and on the angle of incidence and the frequency of the sound.

From the above equations, it follows that in the case of $k^4\sin^4\vartheta-k_B^4=0$, the wall impedance Z_W and the transmission loss R of the wall are also zero. In reality, we have some transmission loss due to the internal damping of the wall, but, especially in the case of metallic materials, there is a steep fall in the transmission loss–frequency curve (about 10 to 20 dB) (Fig. 10.4). Assuming a diffuse sound space, the coincidence frequency is given by:

$$f_C=\frac{a^2}{1.8h}\sqrt{\frac{\varrho_W}{E_W}}.\tag{10.7}$$

As a good approximation (h in mm, f in Hz):

— for steel, aluminium and glass $hf_C=12\,000,$
— for concrete $hf_C=16\,000,$
— for brick $hf_C=30\,000.$

Below the coincidence frequency, i.e., $k<k_B$, we may assume that:

$$Z_W\approx j2\pi fM,\tag{10.8}$$
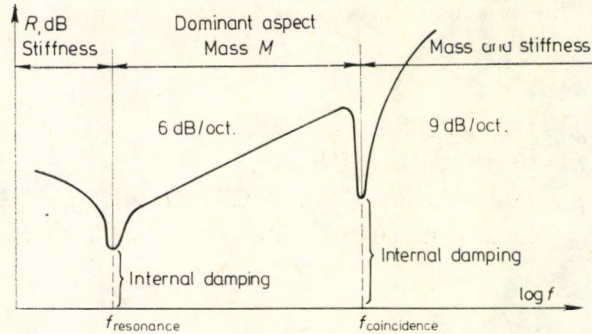
Fig. 10.4. The transmission loss of a wall

so the transmission loss in the wall is found to be:

$$R = 20 \log \left(1 + j \frac{\pi f M}{\varrho c} \cos \vartheta \right) \quad \text{dB}. \tag{10.9}$$

In practice, the 1 in the argument is negligible compared with the imaginary term, and by comparing the calculated values and the values found by measurement in the diffuse sound space, we arrive at the following formula that has proved very useful in practical application:

$$R = 20 \log \frac{\pi f M}{\varrho c} - 5 \quad \text{dB}. \tag{10.10}$$

We see that doubling the sheet mass, i.e., the wall thickness of a given material, results in an increase of 6 dB in the transmission loss. In the transmission loss–frequency curve, the same relationship is found in terms of frequency (Fig. 10.4).

For walls of finite dimensions, the internal damping of the wall becomes worse, so the transmission loss found above can be considered as a maximum. For steel plates where $h = 1$ to 5 mm,

$$R_{max} = 20 \log f + 20 \log h - 27.5 \quad \text{dB},$$

applies, provided that $\eta \approx 1000 \left(\frac{h}{l} \right)^2$, where η is the loss factor of the steel plate

and $2l$ is the minimum distance of the plates, e.g., the distance between the reinforcing ribs. The minimum transmission loss without internal damping is given as:

$$R_{min} = 15 \log f + 5 \log h + 10 \log l - 12 \quad \text{dB}.$$

The above discussion indicates that the maximum achievable improvement in transmission loss by the application of absorbent lining is:

$$\Delta R = R_{max} - R_{min}.$$

At frequencies higher than the coincidence frequency, again assuming a diffuse sound space:

$$R_{f>f_c} = 20 \log \frac{\pi f M}{\varrho c} + 10 \log \frac{f}{f_c} + 10 \log \frac{2\eta}{\pi}. \tag{10.11}$$

As we see, this expression contains the third power of the frequency, that is, by doubling the frequency, we may expect 9 dB increase in transmission loss. Since the transmission loss also depends on the method applied to fix the plates in position, we may expect different transmission losses for different methods of fixing the same plates.

The lower limit of the frequency range, where the sheet mass M predominates in the determination of the transmission loss, is the resonant frequency f_r which corresponds to the natural frequency of the plate (Fig. 10.4). Within this range, the transmission loss is solely determined by the internal damping of the wall.

In the frequency range below the natural frequency of the plate, the transmission loss is determined by the stiffness of the plate. It is obvious that the value of the resonant frequency is of great importance: if the damping range falls within the range of sheet mass dominance, then a resonant frequency as low as possible is preferable, but if we want to damp low frequencies, then the stiffness of the wall should be predominant, so the resonant frequency should be "tuned" higher. This is noteworthy because, owing to the limited design possibilities, only the requirements on mass or stiffness can be economically met, that is, we cannot improve on both parameters without unacceptedly raising the costs.

A plate of given sides a and b and thickness h may vibrate in various modes. The frequency is the lowest when the vibration nodes are at the corners of the plate. In this case, the resonance frequency f_r is found to be:

$$f_{1,1} = 0.48 \sqrt{\frac{E}{\varrho_W}} \, h \left(\frac{1}{a^2} + \frac{1}{b^2} \right), \quad \text{Hz.} \tag{10.12}$$

Thus, if we want to increase the natural frequency, then we have to select a material with high $\sqrt{E/\varrho_W}$ value, that is, the propagation speed of longitudinal waves is high in the material.

The above facts clearly prove that the transmission loss is a combined function of the sheet mass, material and design. Proper selection of the various parameters is possible only on the basis of the frequency range to be damped.

The transmission loss in the high-frequency range ($f > 1000$ Hz) can also be improved by placing absorbent material on rigid wall. The transmission loss of a 300 mm thick absorbent layer with a sheet mass of only 3 kg m^{-2} is about 60 dB at 1000 Hz. This level of damping could be achieved with a wall of fifty times that thickness and a sheet mass of 150 kg m^{-2}. At 250 Hz, however, the absorbent layer yields a transmission loss of only 10 dB, while the other gives 42 dB.

To improve the transmission loss in the low-frequency range, the absorbent layer is covered with a membrane, which can be a thin metal foil, asphalt paper or lead vinyl plastic layer. The aim is to form a layer as thin as possible but with considerable sheet mass. A layer like this is most efficient in the frequency range 200 to 500 Hz, but also affects the damping characteristics at higher frequencies (Fig. 10.5).
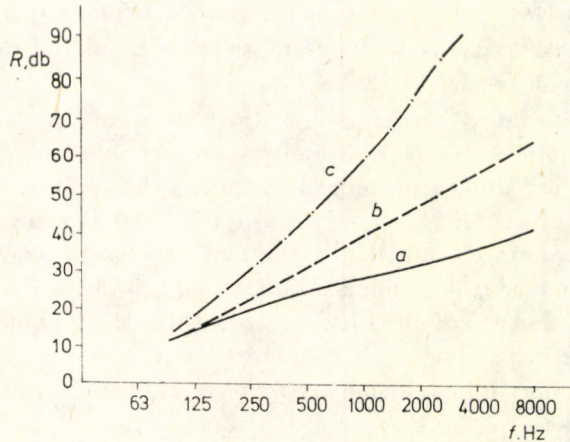
Fig. 10.5. The transmission loss of a laminated structure: a — $h=1.3$ mm aluminium, b — same as (a) plus 50 mm fine fiber glass layer, c — same as (a) plus 75 mm fine fiber glass layer $+h=1$ mm aluminium sheet (membrane)

10.3 Secondary methods to reduce transformer noise

In order to decrease transformer noise, normally a constructional solution is applied at the installation site. If the noise is to be reduced only in one direction and the facility to be protected is more remote than 100 m and 8 dB reduction is sufficient, then it is enough to erect a brick or panel wall between the transformer and the facility to be protected. As shown in Fig. 10.6, this wall is built at a distance of 1 m from the transformer to allow access to the transformer for maintenance and inspection purposes.
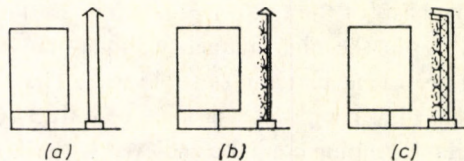
Fig. 10.6. Various noise screening walls: (a) simple solid wall, (b) sound absorbing wall made from absorbent blocks, (c) solid wall with absorbent block lining

If adequate absorbent materials are used as illustrated in Figs 10.6b and c, the noise reducing effect can be as high as 10 to 12 dB.

The height of the wall is a very important factor in determining the amount of noise reduction that can be achieved. Figure 10.7 illustrates how the amount of
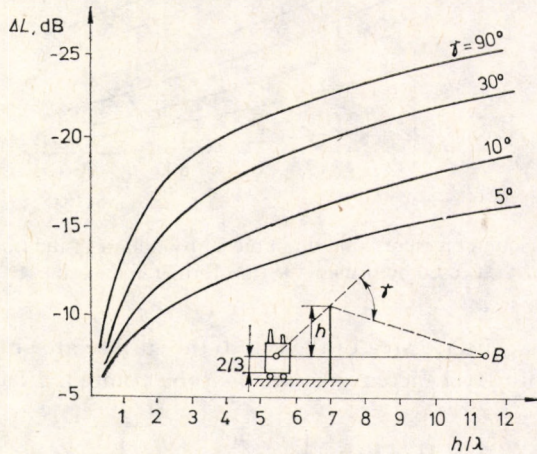
Fig. 10.7. Decrease in sound pressure level due to the noise screening wall:
h — height of the wall with respect to the observation level,
λ — wavelength of sound, f — frequency, γ — sound diffraction angle, B — observer

noise reduction, ΔL, varies with the height of the wall, h, at the observation point B positioned at two third the transformer height (the height of the wall is measured with respect to the level of the observation point). The parameter of the set of curves shown is the diffraction angle, γ, which increases with increasing h. It can be seen that for a given geometric configuration the amount of noise reduction achievable by means of a screening wall decreases with decreasing frequency. Further reduction is feasible, if the wall is covered with absorbent lining and the cooling system is set up separately with separate damping measures. This way the noise reduction can reach 20 dB.

If the noise must be reduced considerably in all directions in the transformer's surroundings uniformly, then walls are erected on all sides of the transformer and the unit is covered with a roof as well. This solution is quite efficient but gives rise to other types of technical problems. The walls of this outside housing should be at least 1 m from the transformer to facilitate access. If the internal surface of this transformer chamber or cell is smooth and reflects sound, then the sound pressure level will be higher in the space between the transformer and the cell owing to the internal multiple reflections, than in the same place but before the walls were erected. This build-up in sound pressure level is given in Fig. 10.8 in terms of the
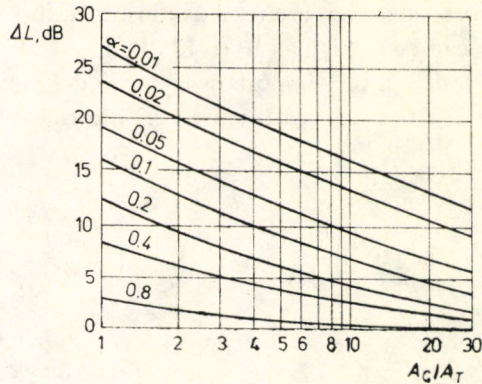
Fig. 10.8. Sound pressure build-up in the surroundings of the transformer
caused by placing the transformer in the cell

ratio of the internal surface area of the cell to the surface area of the transformer. The sound pressure level increment, ΔL, may be computed from the following expression:

$$\Delta L = 10 \log \left(1 + \frac{4(1-\alpha)A_T}{A_C} \right), \qquad (10.13)$$

where α — the average sound absorption coefficient of the inner surface of the cell,

A_T — the surface area of the transformer,

A_C — the surface area of the boundary surfaces of the cell.

Since the transmission loss of the cell walls must now be subtracted from the increased internal sound pressure level, the inner surfaces of the cell should be lined with sound absorbent materials. Further, we should not forget about the disposal of heat due to transformer losses, i.e., an adequate cooling system should be provided. It is easier to set up the cooling system at a certain distance from the transformer, that is, outside the cell, because in this case noise reduction is accomplished by noise reduction of the fan and only the ductwork transporting the cooling medium must be erected in a vibration fashion. If, however, the transformer and the cooling system form an integral unit, then the cell must be designed so that the necessary air flow is led in and out through proper noise damping elements. It should be noted that the totally closed cell design requires the use of really large high-voltage bushings. In spite of these, this solution is the most efficient, since up to 35 dB noise reduction is possible, but, of course, it is most costly at the same time. The erection costs of noise screening walls and cells may be reduced by using prefabricated wall panels.

It is useless to say that any after-measures in noise reduction are expensive.

Table 10.1. Posterior noise reducing methods and their costs for a 400/120 kV
power transformer not equipped with forced cooling system,
with rated output of 350 MVA

Serial number	The technical solution of noise reduction	Reduction in A-weighted sound power level in dB	Percent noise reduction costs related to the cost of the standard design
1	Optimal noise screening cell	20	6.9
2	Same as 1 except for no screening at the bushings	18	6.6
3	Same as 2 except that the cover plate is not covered by absorbent lining either	14	5.7
4	Same as 3 except that the narrow side the transformer is not covered by absorbent lining either	8	5.0

According to a feasibility study conducted in FRG [89], the efficiency and cost of
added noise reducing measures varies as shown in Table 10.1, for a given flux
density and design.

If in the example illustrated in Table 10.1 not only a screening cell is used to
cover the transformer casing but also the flux density is decreased simultaneously
and the laminations are made of Hi–B sheets, then, plotting the costs of noise
reduction against the decrease in iron loss due to the decreased flux density, i.e.,
against improvement in efficiency, we arrive at a truly informative diagram (Fig.
10.9) The horizontal axis indicates the relative incremental cost ΔK. (By definition,
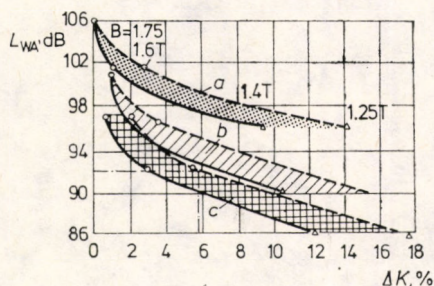
Fig. 10.9. Reduction of the noise of a 400/120 kV
transformer with rated output of 350 MVA, not equipped
with cooling system, as a function of the resultant incremental cost:
a — standard design, *b* — case covered with absorbent lining,
c — the same as (*b*), but Hi–B laminations used

ΔK= resultant incremental cost/normal design cost). Two curves correspond to each design type, including normal design. The values of the dashed curve were determined by attributing an investment cost decrement of £300 to each decremental kilowatt of iron loss reduced by the decreased flux density. This decrement represents a decrease in power requirement from the power plant. The solid lines were drawn by taking £100 for the above parameter. If, for example, Hi-B laminations are used, the walls of the cell are covered with absorbent lining, and we want to realize a noise reduction of 14 dB, then (assuming an investment cost decrement of (200£/kW), we find the corresponding flux density value as 1.58 T which corresponds to an overall cost increment of 5.8 percent. Of course, an economic feasibility study should be made for each individual case, because the circumstances may not be the same in all respects. When analysing the economic ramifications of noise reduction, we should bear in mind that the concrete cost of noise reduction is charged to the investing company, while the recurrent operating cost savings due to the reduced losses appear in the balance of the operating organization.

B. EXPERIMENTAL INVESTIGATION
OF NOISE AND VIBRATION PHENOMENA

11. MEASURING NOISE AND VIBRATION PHENOMENA

11.1 General features

The measuring process comprises a series of different activities. First we set the target of the measurement, then we work out the most appropriate procedure and select adequate measuring tools, and only at this point are we ready to start the measurement itself. The final phase is the processing of the results obtained. The determination of the measuring procedure and the selection of measuring tools may involve making some necessary preliminary measurements.

It is certain that the measurement itself requires the least time in the process outlined, although it is still generally believed that the measurement is the heart of the measuring process, and therefore usually insufficient time is allotted for preparation and evaluation. In such cases, the measurement is generally faulty, but this might not become apparent at all owing to the perfunctory evaluation. We should constantly bear in mind that even results obtained with up-to-date techniques and computerized instruments must be evaluated and processed to determine if they are faulty or not.

Setting the target of measurement tends to cause problems of increasing importance. This target is frequently set by an engineer who is expert in measuring techniques, rather than an expert in the object to be measured. In other words, if we want to identify operating troubles on the basis of the noise spectrum of an electric motor, then only engineers who know the operation of electric motors can set the targets of measurement. Now, it is true that their requests must be translated into the language of measurement techniques and, in turn, the results must be converted into the language they understand, otherwise the costly measurements turn out to be useless.

To sum up, measuring activities require the cooperation of an interdisciplinary team. In this team, the experts of measuring instruments and procedures are permanent members, while the engineers setting the target and evaluating the results change as the object of measurement changes. The two former functions, i.e., the procedure and the equipment, are normally not separated, although the jobs of the two engineers are completely different. The first selects the procedure that best matches the target, based on an estimation of the physical properties

the signals to be measured might reveal, or on actual preliminary measurements of these properties. It is the engineers' responsibility to determine the limits of applicability of the procedure selected, and to carry out the preliminary error analysis. It is a frequently overlooked fact that the measuring procedure itself has an inherent error and this absolute error limit cannot be improved even by the best instruments available of the subject kind. The only way to improve on such a limit is to select another procedure with lower inherent error. It is also the job of the first engineer to make preliminary evaluation of the results obtained and to check the accuracy of the estimated error. The second engineer selects the measuring instrument or system to meet the accuracy and functional requirements set out in the procedure. The engineer is the one who sets up the measurement, checks if the selected instruments comply with the specifications and makes sure that the whole measuring system operates as required.

Of course, the functions and responsibilities outlined above cannot be separated categorically. To be able to carry out their work successfully, the members of the team should know and understand each other's work.

In the case of vibroacoustic measurements, the well-known triad of questions arises: what to measure, how to measure and by what means? To answer these questions correctly, first we have to see the purpose of the measurement clearly. We can talk about informative research and qualification measurements according to standards, and within each group we have accurate, technical and indicative types according to the accuracy level of the measurement. In the case of the latter standard qualification measurements, most standards clearly specify which physical quantities to measure, while the available equipment and the local circumstances normally determine the procedure to be applied, the instruments to be used and the accuracy to be obtained with the available instruments. In the case of measure= ments of other purposes, the decisions are made by the engineer carrying out the measurement. Before he tries to answer the questions of how and by what means, he must examine the character of the physical quantity to be measured. The choices are as follows:

— single non-repeatable,
— single repeatable,
— periodic single,
— deterministically repetitive single,
— continuous phenomenon.

On the basis of time response, the phenomena can be constant or variable. The variation can be small, large, slow, fast or pulsed.

When the phenomenon to be measured has been properly assessed, we have to set up an adequate measuring system. The measuring system can be a special

configuration of general-purpose or universal instruments or a single-purpose equipment. The signals flowing in the system can be analogue, digital or subject to multiple conversions during processing. The conditions under which the measurement is to be carried out also affect the configuration of the measuring system. From this aspect, we may have laboratory measurements, factory measurements and special field measurements.

The selection of a proper measuring system for vibroacoustical measurements requires a thorough preliminary survey that takes many factors and aspects into account. Among the listed factors, we have mandatory ones which are technically essential for the accomplishment of the measurement. Another factor is economic in nature and serves to find the optimum of technical and economical aspects of the measurement. This is the point where numerous other considerations must be assessed with care. Our decision may be influenced by the available level of instrumentation, that is, we need only several supplementary items to be added to the existing equipment in order to be able to carry out the measurement concerned, or we have to equip the laboratory with brand-new instruments or units. When substantial investment is involved, we depend on the available financial resources (investment capital).

The measuring instruments or their components may be connected in various configurations. There are two basic groups into which these configurations can be divided. The first contains the direct measuring techniques or, using a widely known computer term, on-line systems. These systems are characterized by a continuous signal flow between the primary detecting element and the displaying instrument, so the function of measurement and data processing are integral parts of the system. In most current cases, such a system comprises direct reading analogue or digital instruments, but it can be realized by on-line computers as well. The second group contains the indirect measuring techniques or, again using a computer term, off-line systems. In these systems, the signal flow is broken by an analogue or digital storage facility (memory unit) placed between the primary detecting element and the displaying unit. This storage separates the actual measuring from processing, in both time and space.

Many factors determine which measuring technique to use. One of them may be the existing conditions at the research centre where the measurements are to be carried out, the other is the ever present economic factor, since if the data processing system is much faster than the measuring part of the system because of the microprocessor or computer used, then more measuring units may be connected to the data processing unit. In such systems, the application of indirect configurations is, of course, the most appropriate choice. The third factor could be the target or purpose of the measurement. Now let us discuss in more detail the relationships which can be established between the fields or purposes of the

measurement and the direct or indirect types of measuring technique to be applied.

The direct measuring technique provides the real-time value of the vibroacous-tical signal being measured. This feature may be necessary in the following tests or fields of research:

(1) Medical or physiological examinations
In most cases, the doctor or physiologist conducting the examination must see the immediate response of the patient to various vibroacoustical stimuli. It is necessary to see the values of the vibroacoustical parameters and their effect simultaneously. The researcher must sense the immediate physiological or psy-chological responses induced by the individual parameters. The observations involved can be deduced from the words or behaviour of the patient, which can hardly be recorded by means of objective measuring instruments. Of course, the physiological effects that can be measured must be measured and recorded, but this work expectedly falls within the scope of indirect measuring techniques.

(2) Safety hazard tests on the installation site
Instruments should indicate immediately if there is any hazard that could be directly or indirectly harmful to humans. This hazard can be either noise or vibration.

(3) Preliminary checks
Preliminary checks made by direct reading instruments serve to determine if there is any harmful noise or vibration that warrants a detailed investigation to be initiated and carried out by means of indirect types of measuring technique.

(4) Comparative tests
These tests involve real-time comparison of test items at different locations or within the same area.

The instruments used for the above purposes should be portable with simple operation. The present state of microprocessor technology makes this objective feasible. It is a basic requirement that these instruments must display the value of the quantities concerned without delay, and therefore the built-in microprocessor calculates and displays the measured values straight away or stores them tem-porarily to allow recording at the end of the measurement.

The basic function of direct measurement is the quick determination of the most important, decisive characteristics of vibroacoustical phenomena.

Indirect measuring techniques are used mostly in the following fields:

(1) Physiological examination of hazardous noises and vibrations are harmful to human beings. As we outlined above, doctors frequently need a direct type of measuring instrument that displays the measured values at once, because this is the only way to identify the physiological and psychological effects. In addition, however, it is interesting to determine the effects of various noise and vibration

parameters or their changes on the human constitution, e.g. in terms of the following physiological parameters and their changes: blood pressure, pulse rate, blood-sugar level, vasoconstriction, skin contraction, perspiration, certain reflex responses, etc. The main characteristics should be stored for the time of the measurement and further for future use. The time required to process the physiological data and to convert them to proper electrical signals is usually so long that it does not allow real-time display, and so provision must be made for storage and computer processing of the corresponding values of noise, vibration and physiological parameters.

(2) It is worthwhile preparing computer programs for analysing relations between the vibroacoustic parameters, and their changes, and the physiological effects induced by them. It is also worthwhile plotting the results in a diagram to facilitate comprehension. This kind of data processing requires an indirect method.

(3) The use of indirect measuring techniques is beneficial when the test must be repeated a large number of time in order that statistically correct results be obtained. On the one hand, the same individual must be subjected to the test of noise and vibration effects in different parts of the day or under different external influence (e.g., weather fronts). On the other hand, many individuals must be subjected to the same test and the correct resultant of the physiological reactions must be determined. This requires computerized data processing, which means an indirect method.

(4) The main target of vibroacoustic testing is not only the determination of the effects of noise and vibration, but also their elimination. Physiological examinations reveal the harmful vibroacoustic parameters. Then we have to analyse the noises and vibrations for the physical phenomena that give rise to them. On the basis of this analysis, the sources can be identified, at least partially. Since the tests require detailed analysis, high-capacity computers should be used. The analysis of the measured and stored signals is done by off-line processing with special computer programs.

The measuring system to be used for vibroacoustic measurements must satisfy the following functional requirements:

— sensing and signal conversion,
— signal shaping, with single or double integration, if necessary, amplification,
— spectral information on the signal,
— magnitude information on the signal,
— signal recording.

The last four requirements refer to the processing phase and their order of sequence may change depending on the nature of the measuring system.

11.2 Development of noise and vibration measuring systems

First of all simple noise and vibration measuring instruments appeared, which generally characterized the physical quantity to be measured with a single value, and they were used for the measurement of weighted levels. During development, various supplementary units were added to the basic noise measuring instrument to allow the accomplishment of sophisticated functions, like spectrum analysis. The birth of microprocessors and digital techniques resulted in certain standardization trends which culminated in the appearance of ultraspecialized instruments. However, this was not the end. The everyday reality proved to be far more complicated than could be handled by a single instrument, however marvellous it was. The next stage and, at the same time, the present stage of development is the application of general-purpose elements, memory units and computers to provide new measuring functions. The instrument of the future is again a compact unit, but owing to the simplified design and operation of microprocessor-based computers and memory units, these compact instruments can combine the advantages of a measuring instrument and a sophisticated computer system so that the resultant intelligent instrument is easily reprogrammable for a given task, matching the actual requirements with surprising versatility.

When setting up a vibration or noise measuring system, we should always bear in mind that the terminal point in terms of evaluation and interpretation is the user, who is a human being. Human sense organs, the eyes, the ears and the brain, are capable of receiving only a limited amount of data at a limited rate. In the beginning, the information rate of measuring instruments lay far behind human capability, in terms of both quantity and rate. Today, if we collect all the data and information provided by the measuring systems, we are simply unable to understand and use them. Think of a moderately sophisticated and moderately fast real-time analyser which measures 40 spectra each second. If we store this information in some memory device on mass storage media and slowly read the data for evaluation, the time required for processing is incredibly long. Users of the up-to-date powerful and fast instruments frequently encounter a situation when most of the information gained from the instrument is lost, owing to the substantial difference between the conprehensive capability of the human brain and the information rate of modern devices. In such a situation, expertise and self-control are essential traits allowing the selection of the most important information types, ignoring all the rest.

A further step in the development process is seen when the designers of a complicated measuring system incorporate several data processing and evaluating programs in the system as integral parts, providing for data selection and reduction. This way, a kind of balance can be achieved between the human comprehen-

sion rate and the information rate of the measuring system. At this point, however, we face one of today's gravest problems. Operators of the measuring equipment become mechanical figures pushing buttons just as they were trained to do, since the data processing and evaluation is done by the built-in programs of the equipment, so the complete noise and vibration measuring technique is in the hands of instrument manufacturing brain trusts. This danger might be avoided if future development takes the direction of versatile programmable microprocessor-based measuring systems, as mentioned above.

11.3 The sensor used for vibration measurement

For machine vibration measurement, purely mechanical instruments were used in the past. These instruments measured the vibrational displacement. Owing to their nature, they could measure only small-amplitude low-frequency vibrations, and also reacted on the system to be measured because of their considerable mass. As the development of measuring technique made it possible, these instruments went out of fashion.

According to the requirements of the modern measuring technique and, in particular, the modern signal processing technique, we try to convert the mechanical signal into an electrical signal as soon as possible also in the field of vibration measurement, since there has been an immense development in the measuring technique of electrical signals for several decades. We intend to use such sensing element in which the mechanical-electrical transducer is an integral part.

As is well known, the vibrating body is in motion. As motion in general is essentially a relative phenomenon, the sensing of motion must be essentially relative as well. Depending on the reference to which the motion of the machine or machine part to be measured is related, we have two different measuring methods.

In the non-contact vibration measurement, the sensor is fixed to a body considered motionless in the surroundings of the vibrating machine. If the distance between this "fixed" vibration detecting element and the vibrating body changes, it is considered to be due to the motion of the vibrating body. This hypothesis, on which the non-contact vibration measurement is based, readily implies one very serious deficiency of this method, namely, it is impossible to find an absolutely motionless point close to the vibrating machine to be tested. In certain cases, however, the non-contact method is the only applicable way to measure vibration. (We discuss this in detail in Section 12.3.) Furthermore, this method is used when direct contact should be avoided for whatever reason (e.g., safety, technical, or because of the small mass of the object being measured).

There are two kinds of non-contact transducer in general use: electrodynamic and capacitive transducers. Their other deficiency, apart from that mentioned above, is that they are extremely sensitive to the surface finish, material and paint coat of the vibrating body, and also to magnetic disturbances and changes in air permittivity. Also, the relationship between the output signal of these transducers and the displacement of the vibrating body is non-linear. We should note that the non-contact transducers sense displacement, so the other two vibration characteristics, namely, the vibration velocity and the vibration acceleration cannot in practice be measured with them. Although in theory it is possible to produce signals proportional to the vibration velocity and acceleration, by determining the first and second derivatives of the time function of displacement with respect to time, unfortunately the signal noise and fluctuation content of the measured signal would turn out to be misleading because of the derivation—but would even get special emphasis. (This error does not manifest itself when the signal is integrated.)

The second group of vibration-measuring transducers includes the so-called contact transducers. In this case, the transducer is directly and rigidly fixed to the vibrating body. The commonest type of contact transducer, the piezoelectric transducer, consists of three basic parts. One part, which is normally called the housing and is hollow, is rigidly fixed to the vibrating body in order to follow its movements in all respects. An inertial mass m is placed within the housing, coupled with a piezoelectric crystal in compression or shear. There is no direct mechanical coupling between the inertial mass and the housing. If the vibratory motion of the vibrating body and the housing attached to it is characterized by an acceleration a, then the inertial mass m exerts a force of magnitude ma on the crystal which gives rise to a piezoelectric signal proportional to the force and the acceleration, the mass m being constant. This type of sensor is also called an absolute vibration sensor. This signal, which is proportional to the vibration acceleration, can be integrated once or twice by means of simple circuits to produce a signal proportional to the vibration velocity or vibration displacement, respectively. Another advantage of these piezoelectric acceleration sensors is their low mass. Their sensitivity allows their application in the range from several mm s^{-2} to several ten thousand m s^{-2}, and their frequency response is linear over a wide range, constant in time and insensitive to environmental effects.

Figure 11.1 illustrates the construction of two different kinds of piezoelectric accelerometer sensor. The classic design is the compression type (b), while in the other solution a shearing force acts on the crystal (a). The latter called "Delta Sheer" can be much more sensitive than the compression type.

The housing of the accelerometer, the piezoelectric element, the inertial mass and the other ancillary parts constitute a vibratory system characterized by
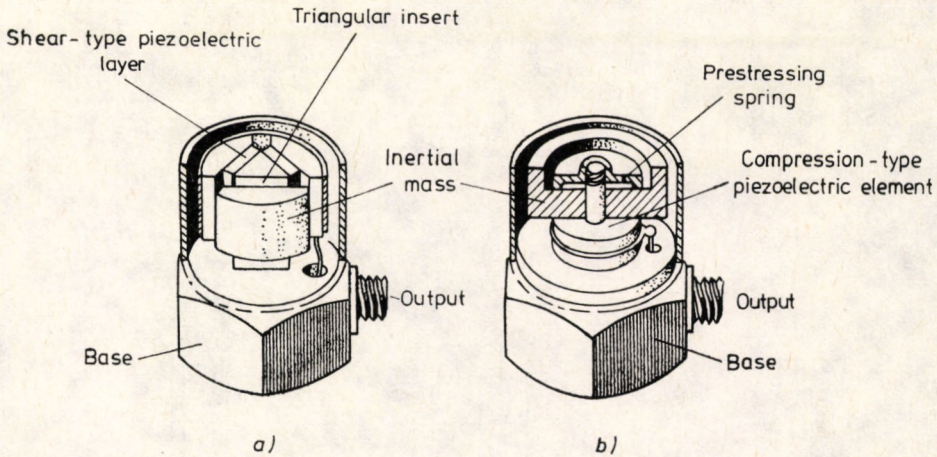
Fig. 11.1. Two types of general-purpose accelerometers: (a) shear-type, **(b)** compression type

a mechanical natural frequency. If the frequency of the measured vibration is equal or close to this natural frequency, then the output signal of the accelerometer is not proportional to the exciting vibration because of the resonance that develops. Figure 11.2 shows the typical frequency response of a piezoelectric accelerometer. The curve clearly shows the frequency range where the sensitivity is constant. The upper limit of this range is at one third the natural frequency f_{res} of the sensor. The typical natural frequency of standard accelerometer is about 25 kHz.
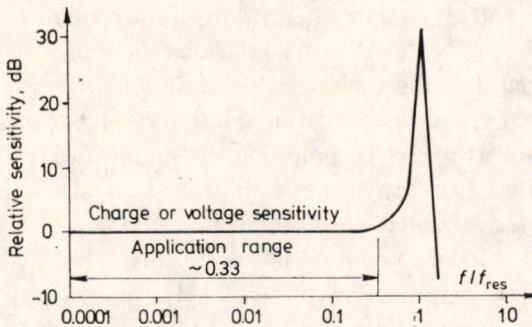
Fig. 11.2. The frequency response of the sensitivity of piezoelectric accelerometers

The piezoelectric accelerometer should be brought into contact with the vibrating body. There are various methods of fixation, which are illustrated in Fig. 11.3. The best is that which employs a stud bolt. Beeswax or even epoxy resin gluing is also very good. The quality of fixation depends on how much the fixation
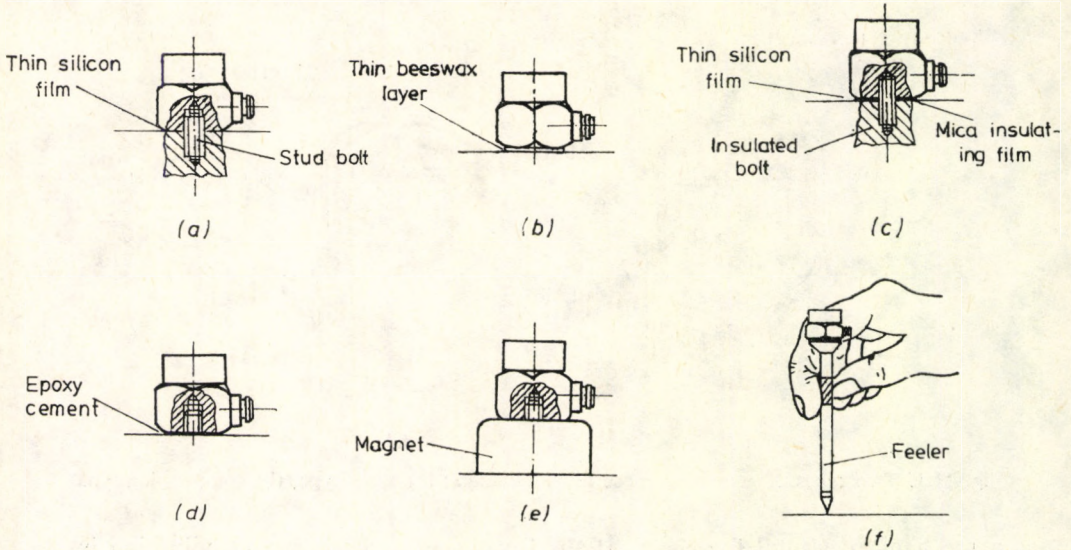
Fig. 11.3. Methods of fixation for accelerometers. The ratio of the mechanical natural frequency f'_{res} of the system comprising the fixing element and the accelerometer to the natural frequency f_{res} of the transducer in the various cases:

fixation	a	b	c	d	e	f
f'_{res}/f_{res}	1.0	0.98	0.96	0.95	0.28	0.07

modifies the natural frequency of the transducer. The methods of fixation shown in Figs 11.3a, b, c and d do not alter the operating frequency range of the transducer in practice. A fast method for attaching the sensor to bodies made of magnetizable material, like most electrical machines, is the magnetic mounting shown in Fig. 11.3e. Of course, this latter solution does not provide a mechanical coupling as good as a bolted mounting, so the operating frequency range of the sensor is reduced to less than one third. For standard transducers, this range still gives a relatively high cut-off frequency (about 2 to 3 kHz) that meets the requirements of standard vibration measurements.

Feeler mounting is acceptable only up to 600 Hz. When the measuring system is set up, due attention must be paid to avoid the formation of a ground loop through the sensor housing and the ground wire of the signal cable, since the ground current flowing through the instrument would invalidate the results of the measurement. A good solution is the application of an insulated bolt and an insulating disk under the sensor, as shown in Fig. 11.3c.

Care must be taken to ensure that the mass of the transducer used for the measurement is much smaller than that of the body measured, otherwise the

mass of the transducer would influence the results by modifying the amplitude and frequency of the vibration. If the mass of the accelerometer exceeds 10 percent of the mass of the body to be tested, then the correction shown below should be applied to the measured value of vibration acceleration and frequency, as given by eqns (11.1) and (11.2), respectively, to obtain true figures by spectrum analysis of the measured signal:

$$a_s = a_m \frac{m_s + m_a}{m_s},$$ (11.1)

where a_m — the measured vibration acceleration together with the accelerometer attached to the body,

a_s — the true vibration acceleration of the tested body without the accelerometer,

m_a — the mass of the accelerometer,

m_s — the mass of the tested body,

$$f_s = f_m \sqrt{\frac{m + m_a}{m_s}},$$ (11.2)

where f_m — the frequency of the signal measured by the accelerometer,

f_s — the vibrational frequency of the body without the accelerometer.

Now we arrived at the point where we can stop talking about the special characteristic of the vibration measurement and start to apply general methods of electrical signal processing.

The output signal of the piezoelectric crystal, that is, the potential difference across the crystal armatures, is directly proportional to the acceleration of the transducer housing and, consequently, to that of the vibrating body. This signal, however, is very small, and so it must be amplified. There are two general types of pre-amplifier used for this purpose. The output voltage of voltage amplifiers is proportional to the input voltage. Their construction is simple, and they are relatively cheap, but, especially at low frequencies, they are very sensitive to the resistance and capacitance of the cable connecting the sensor with the pre-amplifier.

The other type is called a charge amplifier. Here the output voltage is proportional to the charge on the sensor. This pre-amplifier is more expensive than the other type, but it is insensitive to the cable impedance, so we can use longer cables to connect the sensor with the amplifier and the pre-amplifier may be located further away from the vibrating body tested. At the same time, the pre-amplifier serves as an impedance transformer, matching the sensor with the instrument following the amplifier. Figure 11.4 shows the equivalent circuit to the system comprising the accelerometer, signal cable and charge amplifier.

The old, mainly mechanical engineering, standards specified the measurement
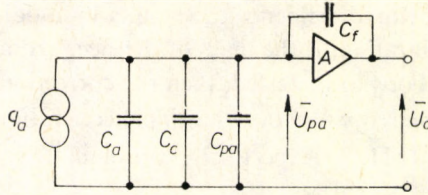
Fig. 11.4. Equivalent circuit of the accelerometer, the cable
and the charge amplifier: U_0 — output voltage of the pre-amplifier,
q_a — accumulated charge, A — gain, U_{pa} — input voltage
of the pre-amplifier, C_a — capacitance of the accelerometer,
C_c — capacitance of the connecting cable, C_{pa} — input capacitance
of the pre-amplifier, C_f — feedback capacitance

of vibrational displacement (or, incorrectly used the word, amplitude) within the
scope of possibilities provided by the available, purely mechanical, instruments
of those days. Recently, vibration of the machine has been characterized by the
vibration velocity or its r.m.s. value. The national and international standards
effective today equally follow this principle, basically for the following reasons:

— From the three vibration characteristics, acceleration, velocity and displace-
ment, the vibration velocity is related linearly to the subjective sensation of vi-
bration intensity, independently of frequency.

— It is the vibration velocity with which the kinetic energy of the vibrating
body is in closest relation. A given energy content corresponds to a given vibration
velocity, while the acceleration signal enhances the importance of high-frequency
components and the displacement signal, the low-frequency ones (Fig. 11.5).

— The vibration velocity that corresponds to a given vibrational energy is not
dependent on the frequency. This means that if we set a limit to the vibrational

Fig. 11.5. The interrelations of vibration acceleration,
velocity and displacement as a function of frequency

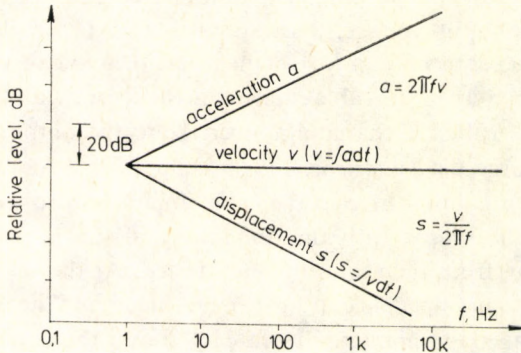energy, we also set a limit to the vibration velocity owing to the unique relationship between vibrational energy and velocity.

— The vibration components commonest in electrical machines and other rotating equipment can be studied on the basis of the spectrum analysis of vibration velocity, since this choice provides the best opportunities for taking advantage of the dynamics of sensitivity that characterize the measuring system, over the widest frequency range.

11.4 The sensor used in noise measurement

In the previous section, discussing vibration measurement, we stated that only the transducer, usually accelerometer, is a special element connected with the vibration measurement. All the other components (e.g., amplifier, filter, r.m.s. circuit, indicating instrument, memory, etc.) are general electrical signal con ditioning and processing elements. If we compare the measuring systems used for vibration and noise measuring, we find that the only substantial difference is between the sensors used. In noise measurements today, a condenser micro= phone will be used, and the frequency range of the filters is naturally different, because the acoustic frequency range of interest is not the same for noise mea= surements as for mechanical vibration measurements. Even this latter difference is eliminated when the structure-borne noise is measured by means of a vibration pick up.

In modern noise measuring instruments condenser microphones are employed because of their numerous advantages. The transfer characteristics of condenser microphones are constant over a relatively wide frequency and dynamic range. These features are retained for a long time and are relatively insensitive to environ= mental interferences like humidity, magnetic field, etc. Calibration is easy, the size of the microphones is small. The construction of condenser microphones is shown in Fig. 11.6. The microphone contains two armatures, one of them is a diaphragm, the other is rigidly fixed in the housing, providing a capacitor structure. If this capacitor is charged, any deformation of the diaphragm will result in a change of voltage owing to the change of capacitance. As we see, the consender microphones require a bias voltage for their operation, supplied by the pre= amplifier.

The commonest standard microphone diameters are $1''$, $1/2''$, $1/4''$ or $1/8''$. As the diameter decreases, so does the conversion sensitivity (mV/Pa), but the working frequency range in turn increases.

The frequency range of $1''$ microphones is the audible range (with upper cut=off frequency of about 20 kHz), which is appropriate for the analysis of steady=state
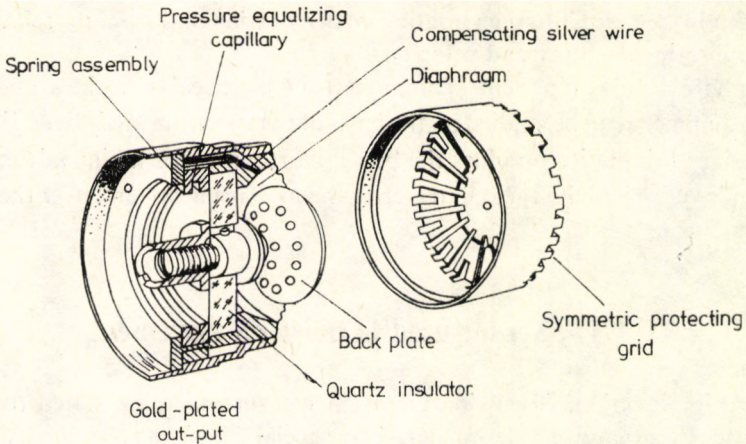
Fig. 11.6. The construction of a condenser microphone

noises. If, however, we want to study transient or, by any chance, pulsed noises, then we have to raise the upper limiting frequency further to allow high slew rates (which means high frequency) to follow the pressure pulses closely. The working frequency range of 1/8″ microphones can be as high as 140 kHz. We should note that consender microphones measure pressure, which is a scalar quantity.

11.5 Analogue methods of spectrum analysis

11.5.1 Weighting filters

The means of presenting information related to the frequency characteristics of vibroacoustic signals can be defined by taking many aspects into consideration. First we need to consider the purpose of the measurement. If the vibration measurement is aimed at the standard qualification of the machine in terms of vibrations or at testing the machine for certain characteristics, then we present the required information in the form of a single value. The standards relevant to vibration measurements of machines accept the resultant r.m.s. vibration velocity of components within the frequency range 10 to 1000 Hz as a single-value characteristic. This value is produced by allowing the electrical signal, which is proportional to the vibration velocity, through a wide-band filter of lower and upper cut-off frequencies of 10 Hz and 1000 Hz, respectively. Thus the components within the transmission band of the filter are not attenuated in practice, with a tolerance specified for the vibration measuring instrument by the relevant standards, while

the components outside the range limited by the cut-off frequencies are attenuated with a slope also specified by standards.

As accepted internationally, the so-called A-weighting filter is used for testing electrical machines and other mechanical noise sources. This weighting filter (normally placed between the pre-amplifier and the final amplifier of the measuring system) simulates the average frequency response of the human ear in the neighbourhood of the commonest sound pressure levels of 60 to 90 dB. The A-weighting network is a band-pass filter with cut-off frequencies (that correspond to an attenuation of 3 dB) in the neighbourhood of 700 Hz and 10.000 Hz. The use of A-weighting filters is beneficial in allowing quick determination of the single value that represents the noise level, in most cases in close correspondence with the subjective human sensation of hearing. It is disadvantageous, however, that the results may differ from the human ear response at low and high sound pressure levels and we do not obtain any information on the individual noise components and their frequencies. From a noise nuisance point of view, it is not the same when the given sound pressure level in A-weighting is the resultant of broad-band hissing noise or we hear a pure tone at a well defined frequency. In many cases, the spectrum analysis is beneficial even in qualification type of measurements, while definitely, essential in research.

The frequency response of A-weighting filters is illustrated in Fig. 11.7 together with the frequency response of so-called B-weighting and C-weighting filters. The sensitivity of the human ear improves at lower frequencies at higher sound pressure levels, so the B-weighting and C-weighting filters better simulate the human hearing in this range. To allow comparison, the relevant standards specify the use of A-weighting filters at all sound pressure levels for the testing of mechanical noise sources.
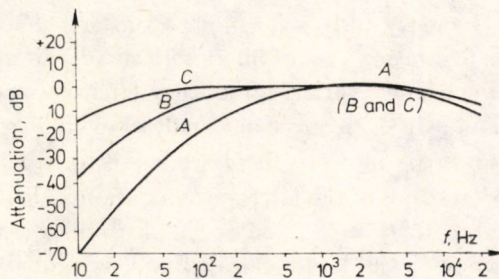

Fig. 11. 7. Frequency response of weighting filter attenuations

11.5.2 Band filters

We are frequently eager to know what components make up the vibration or noise of the machine tested. In such a case, a spectrum analysis is carried out. The objective of this analysis is to determine the frequency and amplitude of each component. In the past, and in many cases even today, an analogue frequency analyser is used as part of the measuring system. The electrical signal, which is proportional to the vibration or noise, passes through a filter system. Each band=pass filter within this system (Fig. 11.8) is characterized by an upper and a lower
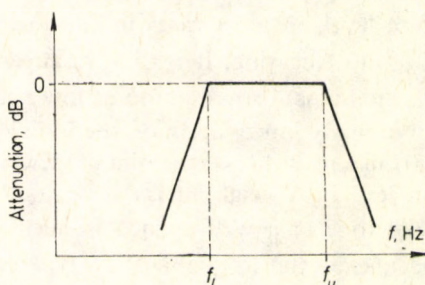
Fig. 11.8. The typical frequency response of band-pass filters

cut=off frequency (f_u and f_l, respectively) limiting the pass=band, where the signal passes through practically unaltered, while for components with frequencies below f_l or above f_u the attenuation is strong. The centre frequency f_c is defined as the geometric mean of the upper and lower cut=off frequencies, that is, $f_c = \sqrt{f_l f_u}$.

In industrial practice, the constant percentage or constant relative bandwidth analysis is used most frequently. This means that the following relationship applies to any ith band: $f_{u,i}/f_{l,i} = $ constant. Constant percentage analysis is feasible in two ways: first, using a set of filters with standardized centre frequencies $f_{c,i}$ or, secondly, using a single variable-frequency filter whose centre frequency f_c can be tuned continuously. The spectrum analyser with fixed centre frequency contains as many band-pass filters as there are bands to be used in the measure= ment. The transmission bands of the filters cover continuously the whole frequency range to be analysed, with $f_{l,i} = f_{u,i-1}$. For simple applications, the ratio of the upper cut-off frequency to the lower cut-off frequency equals 2 for each band, that is, $f_{u,i}/f_{l,i} = 2 = f_{c,i}/f_{c,i-1}$. This analysis is called octave=band analysis. A more detailed picture of the spectrum is obtained from the one-third=octave= band analysis, where $f_{u,i}/f_{l,i} = \sqrt[3]{2} = f_{c,i}/f_{c,i-1}$.

The band centre frequencies are specified by international standards. The constant percentage fixed-centre=frequency filters normally satisfy the analysis

requirements of factory measurements, although the bandwidth of the in=
dividual filters increases with increasing frequency, the discrete frequencies of
vibration components of electrical machines are also becoming more and more
separated as the frequency increases. The absolute bandwidth that increases with
increasing frequency at the same time facilitates the economic execution of the
measurement, since the analyser quickly runs through the high-frequency range
that contains only a few components. The frequency spectrum obtained by fixed=
centre-frequency constant-bandwidth frequency analysis looks like a histogram in
that we cannot separate the individual components, if any, within a given band,
because the measurement made through a given band-pass filter yields the resultant
r.m.s. value of vibration components within the frequency range $f_{l,\,i}$ to $f_{u,\,i}$.

The international standards specify the following centre frequencies for octave=
band analysis: 16, 31.5, 63, 125, 250, 500, 1000, 2000, 4000, 8000 Hz. For one-third=
octave-band analysis, the standardized centre frequencies are 10, 12.5, 16, 20, 25,
31.5, 40, 50, 63, 80, 100, 125, 160, 200, 250, 315, 400, 500, 630, 800, 1000, 1250,
1600, 2000, 2500, 3150, 4000, 5000, 6300, 8000, 10 000 Hz. In the case of octave=
band filters, the upper and lower cut-off frequencies may be obtained by multiply=
ing and dividing the band centre frequency f_c by $\sqrt{2}$, respectively. For one-third=
octave=band analysis, the factor to be used is $\sqrt[6]{2}$.

The constant percentage filters with continuously variable centre frequency
provide a more accurate picture of the dominant vibration components, their
frequencies and magnitude. The highest usual value of f_u/f_l is 1.23 (which means
that the resolution of the one-third-octave-band analysis is 23 percent), and drops
as low as 1.01 (1 percent) in the case of precision filters. This resolution is sufficient
even for the most delicate operating requirements. The frequency spectrum drawn
by a constant percentage filter with continuously variable centre frequency is a
continuous curve with local maxima and minima, where the loci of maxima give
the frequencies of the individual vibration components, while the peak values give
the magnitudes. A flat peak and the moderate slope of rising and falling edges
indicate that the resolution is not enough, and more than one components are
merged into a single local maximum.

If the bandwidth is decreased too much, the analysis time becomes unacceptably
long, despite the more accurate results yielded. On the one hand, the drawing
and reading of the numerous components take too much time, and on the other
hand, the filters themselves pose a new problem. When the signal to be analysed
is applied to a filter network, it takes a certain time before the steady=state condition
is achieved in the network. This is called the response time of the filter, and we
must ensure that the signal is applied to the filter for at least this long. The response
time increases proportionally with the decreasing bandwidth of the band-pass

filter. The accuracy of the measurement is acceptable, if the following relation is observed:

$$(f_u - f_l)T \geq K, \tag{11.3}$$

where T is the time during which the signal is applied to a given filter. For harmonic signals, $K = 1$, for combined signals, $3 \leq K \leq 10$, depending on the analysis method and the applied trigonometric function. Higher values of K correspond to more accurate results. When deterministic signals are tested, the test time should be at least 3 to 5 times the cycle time of the lowest-frequency component tested.

If more accurate analysis is required than that provided by a factory test, and it is necessary to separate components that are very close to each other, then a constant absolute bandwidth (or heterodyne) analyser should be used with continuously variable centre frequency. In this case $f_{u,i} - f_{l,i} = \text{constant}$. The results obtained are accurate, but the measuring time increases considerably.

Above all, there is one thing we must be cautious with when using the analogue analysers discussed above. The spectrum obtained by analysis of the noise or vibration signal reflects reality only if the signal is continuous in time with constant magnitude. Otherwise, in view of the essentially finite speed of the analysis, it is not the same signal that is applied to the input of the individual filters owing to the changes in the signal, and consequently the various components of the spectrum correspond to different signals. This problem can be solved only with digital technology that cuts analysis time substantially.

11.5.3 The realization of an analogue frequency analysis

The classic method of determining the components of an electrical signal is leading the signal through filters with various pass-bands and measuring or recording the output signals. The result is the amplitude distribution of the tested signal as a function of frequency, or the power spectrum, if a squaring circuit is incorporated in the instrument. The frequencies of the band-pass filters may be determined by one of the following methods.

When the signal is switched from filter to filter of different fixed band centre frequency and the output signals are evaluated and recorded individually, the method is called step-by-step filter switching. The resolution achieved with this method is practically the one-third-octave-band level, because the increase in the number of filters applied means a more expensive instrument and the analysis time would be unacceptably long.

The tuned filter method is used mostly for narrow-band analysis so that the signal is fed to the input of the filter and the components are measured and

recorded at the output by continuously tuning the filter over the selected frequency range (e.g., one decade). The filter itself can be the constant percentage or constant absolute bandwidth type.

The two former methods are suitable only for analysing signals that are constant in time, since if the signal changed, we would measure different signals at different frequencies. In real-time parallel analysis, the signal to be measured is fed simul= taneously to the input of all filters with centre frequencies of interest, and the output signals are also read and recorded simultaneously. This is one of the fast analysis methods. From our previous discussion, we see that this method is suitable only for one-third-octave-band analysis at reasonable costs.
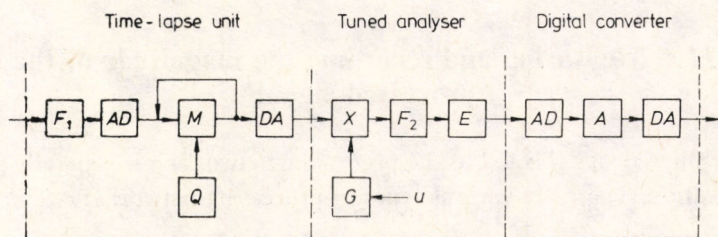
Fig. 11.9. Real-time parallel analyser: F_1 — low-pass filter, AD — analogue-to-digital converter, M — recirculation memory, Q — clock, DA — digital-to-analogue converter, G — voltage-controlled generator, X — mixer, F_2 — filter, E — measuring instrument, A — averaging network

The time-lapse method (Fig. 11.9). From eqn. (11.3), we see that T can be reduced only if the bandwidth is increased without impairing the selectivity (re= solution) of the measurement. These limitations can be circumvented by recording first the signal to be measured, then playing it back N times faster and applying this time-lapsed signal to the input of appropriate filters. Now the individual components will appear at frequencies N times higher, and T can be reduced by a factor of N by increasing the bandwidth by the same factor, while the original selectivity is maintained. Recording and playback is feasible with a magnetic tape unit, but the maximum speeding is only of the order of ten. A much better solution arises when the signal to be tested or its time sample is stored in a digital memory unit, because we can retrieve it at a rate of several thousand times the original speed.

Let us consider the special case when the factor of speeding equals the number of components to be identified. From the relation

$$T \frac{1}{N} N(f_u - f_l) \geqslant K,$$

we find that the bandwidth has increased by a factor of N, while T has decreased by the same factor. This means that the time required to complete the analysis of

N components equals the time required to measure only one component of the original signal without the time-lapse effect. If the time of recording is longer than T, then, by applying two memory units, the signal or the samples taken from the signal may be analysed continuously. The sampling frequency, f_s, of course, should match these requirements as well. The other condition to be observed in selecting f_s is the well-known rule, namely that f_s should be at least three times the frequency of the highest-frequency component to be analysed. In the commonest practical solutions, the time-lapsed signal is reconverted to an analogue signal to be analysed by the tuned filter method, tuning the filter centre frequency synchronously with the rate of playback.

11.6 Measuring and recording the magnitude of the processed signal

Before the filtered signal is fed to the processing network, it is generally subjected to amplification. There are various types of processing networks:

— r.m.s. circuit,
— averaging circuit,
— peak value indicator,
— pulse indicator,
— equivalent value calculator.*

The processing network is usually followed by an indicating instrument to facilitate the reading of the measured vibration value on a linear or logarithmic scale.

---

* Note: For signals of long duration and changing magnitude, a so-called equivalent value is defined as in eqn. (11.4), which is simply the effective value taken for the long duration. (Note that the integration time in eqns (1.6) and (1.8) was equal to the cycle time.)
For vibration velocity:

$$v_{eq} = \sqrt{\frac{1}{\tau} \int_0^\tau v^2(t)\, dt}, \tag{11.4a}$$

where τ is the total measuring time and $v(t)$ is time function of the mean vibration velocity.
For sound pressure level:

$$L_{eq} = 10 \log \left(\frac{1}{\tau} \int_0^\tau 10^{0.1 L_t}\, dt \right), \tag{11.4b}$$

where $L(t)$ is the time function of the sound pressure level.

The signal may be recorded at the end of the measuring system after processing, but also right after the sensor, following the first amplification. The signal recording at the end of the measuring system can be performed in many ways:

— manually, after visual reading,
— by means of a graphic level recorder,
— by digital or analogue memory.

Signal recording with a recorder usually means the application of a direct recorder working on the compensation principle. Here the paper feed rate is synchronized with the stepping rate or tuning rate of the filters by means of a flexible shaft or with electric pulses, and thus the spectrum is drawn directly on the paper scaled to frequency.

If it is expected that further processing will be required at a later date and at a different location, then the processed signal is stored in memory. This can be analogue equipment like a high-quality high-dynamic precision tape-recorder, or digital equipment or even punch tape following the conversion of the processed signal by means of an analogue digital converter. When the signal is stored, care must be taken to save all the important characteristic information of the measurement in a clear-cut manner, including the measuring range, the parameters measured, the identification of the object measured, etc.

In many cases, the measuring system cannot be set up completely at the site of the measurement. The reasons can be technical, economical or other. In such cases, the measured signal is stored in a memory unit before processing, which takes place later, perhaps at a different place.

11.7 Frequency analysis by digital procedure

Time-lapse analysis is intermediate between analogue and digital analysers. Here the digital samples of the signal are speeded up, but the actual analysis is solved by tuned heterodyne filters. The application of digital filters and fast Fourier transformation (FFT) allowed the development of a new generation of analysers with fast operating and complex signal processing capability.

11.7.1 Real-time one-third-octave-band analysis

The application of digital filters allowed the construction of high-speed real-time analysers. A real-time analyser continuously samples the vibroacoustic signal to be tested through an analogue-to-digital converter. The series of samples obtained is

analysed by digital filters and the spectrum components identified by the analysis are averaged. The main advantages of analysers based on digital filters over ana-logue analysers are the following: an increase of about 10 dB in the dynamic range, high speed, linear averaging facility, considerable decrease in peak factor sensitivity owing to the digital r.m.s. circuit. Although digital band-pass filters with narrower bandwidth may be built, these instruments frequently determine only one-third-octave-band components in order to be able to compare the results with spectra obtained by other methods (e.g., analogue procedure) and to comply with certain code regulations. For similar reasons, the frequency scale of the spectrum is logarithmic. This method is not too suitable for the analysis of short signals. Furthermore, care must be taken to select the right averaging time, which can be varied over a very wide range, especially in relation to the measuring accuracy of low-frequency components.

11.7.2 Narrow-band analysis with FFT

The FFT-based narrow-band analysers generally determine 400 different spectrum components of constant bandwidth. The minimum length of the time signal that can be analysed and the largest frequency component, f_{max}, are closely related, since the analysis is carried out on a specified number of time samples, normally $1024(=1\,K)$. The sampling frequency, f_s, in accordance with the theory of sampling, is at least twice, or more exactly $1024/400=2.56$ times the frequency of the highest component. The frequency spacing of the individual components is given by $f_s/[2.56\times400]=f_s/1024$, which gives the frequency of the lowest component as well. The minimum length of the time signal, T_l that can be analysed is simply determined in the following manner:

$$T_l=\frac{1}{f_s}\,1024=\frac{1}{2.56f_{max}}\,2.56\times400=\frac{400}{f_{max}}\,.$$

Since the fast Fourier transformation (FFT) is applicable only to signals with zero leading and trailing end values, then, if this restriction is not a natural characteristic of the tested signal, the time samples must be weighted with the Gaussian or Hanning time window prior to processing. When transient signals are tested, we may omit the application of the weighting function in many cases, but then the whole signal must pass during the sampling.

Most FFT analysers can display the time function of the recorded signal on the screen, so we can ensure that the required condition is met (although the value of f_{max} will be small, if the signal to be tested is long). This contradiction may be resolved by an external memory that allows the reading and testing of the signal

in sections up to the required f_{max} (in such a case the weighting functions might be needed). The r.m.s. values of the individual components are also produced digitally in FFT analysers, which reduces the peak value dependency substantially. Owing to the fact that linear averaging is also possible, which leaves the final value of the evaluation constant, it is possible to determine the resultant of spectrum components of signals analysed in sections.

11.7.3 High-resolution analysis with FFT

The operating principle of high-resolution analysers is basically identical to that of narrow-band analysers, but their memory capacity is ten times larger than that of the latter (i.e., 10 K words). When the 10 K time samples are analysed in ten 1 K sections, the whole spectrum is broken down into 4000 components. Only 400 discrete spectrum lines can be displayed on the screen simultaneously, but any 40-component part of the spectrum can be produced at a resolution of 400 lines, when tenfold frequency compression is used (ZOOM-FFT). A "sliding" time window (constant or Hanning-weighted) allows the generation of a 400-line spectrum of any part of 1 K of the signal. This time window is continuously moved over the total 10 K of the time sample (8 selectable scanning speeds) while the individual sections are displayed continuously on the screen. When the scanning is completed, the linearly summed 400-component spectrum is also at our disposal. This operation allows determination of the time function of any selected spectrum component. Some of the analysers can process the time samples not only as a function of time, but also as a function of an external control signal. This allows the generation of the individual components in terms of any external control signal.

11.7.4 Dual-channel FFT analysers

Two-channel analysers operate in a dual processing mode, repeatedly evaluating the complex frequency spectra of signals applied to the input of the instrument and determining the relationship of the two signals from various aspects. These instruments generally comprise all the modes and facilities of high-resolution FFT analysers with the addition of higher accuracy and speed, and additional features regarding practically all parameters. The facility of dual processing provides for the determination of a diversity of relationships between the signals fed to the two channels or by parallel connection of the two channels (i.e. by multiple processing of a given signal). The functions include signal enhancement (the

elimination of background noise from the time signal), envelope curve display, trajectory and transfer function generation, coherence identification. This multitude of applications in function analysis allows the use of these instruments in every field of vibroacoustics.

An unquestionable advantage of digital frequency analysers is the high measuring speed. This feature, however, gives rise to an unexpected problem. A digital frequency analyser can be compared to an infinitely quick and accurate snapshot. A snapshot, however, grasps only an instant of life, not necessarily the most characteristic. The vibration of our machines can be uncertain, fluctuating. The digital analyser catches a glimpse of the phenomenon. On the other hand, analogue analysers owing to their slowness can average out minor changes. To retain the advantages of digital analysers but, at the same time, to reduce their deficiencies, sampling and analysis must be done continuously, as though to filming. This way, however, such an enormous mass of data is produced that on-line computer control and processing or built-in microprocessor are required to record and present them.

12. VIBRATION MEASUREMENTS ON ELECTRICAL MACHINES UNDER STEADY-STATE OPERATING CONDITIONS

12.1 Basic regulations on standard vibration measurement and the evaluation of results

12.1.1 Contact vibration measurement

In contact vibration measurement, the absolute vibration of the machine surface is measured by a contact sensor. Usually, the piezoelectric accelerometer discussed in Section 11.3 is used and the signal proportional to the vibration velocity is obtained by integrating the output signal proportional to the vibration acceleration. We can say that the value of vibration velocity to be measured is a two-fold effective value. First we generate the effective value of the individual harmonic vibration components as given by eqn. (12.1):

$$v_{ie} = \sqrt{\frac{1}{T} \int_0^T v_i^2(t)\, dt},\qquad(12.1)$$

where v_{ie} — the effective value of the ith harmonic vibration component,
$v_i(t)$ — the instantaneous value of the ith harmonic vibration component,
t — time,
T — the duration of effective value generation.

And then we use the resultant r.m.s. value of harmonic components falling within the range 10 Hz to 1000 Hz, found as:

$$v_{r.m.s.} = \sqrt{\sum_{i=1}^n v_{ie}^2},\qquad(12.2)$$

where $v_{r.m.s.}$ — the resultant r.m.s. vibration velocity,
i — the ith component of harmonic vibration within the frequency range 10 Hz to 1000 Hz,
n — the number of such components.

The r.m.s. value given by eqn. (12.2) is produced by means of a band-pass filter with cut-off frequencies of $f_l = 10$ Hz and $f_u = 1000$ Hz.

The product standards strive emphatically to isolate the machine mechanically from its environment and to ensure the reproducibility of the measurement by specifying the measuring conditions. It is obvious that these conditions are achieved

in a variety of ways and to various degrees for different machine sizes. In the case of small and medium-sized machines, flexible mounting receives priority, isolating the machine from its surroundings by means of undertuned springs. For large machines, completely rigid mounting is better. Rigid mounting should be applied, of course, for small machines as well, if the vibration of a machine line is measured. In the case of flexible mounting, proper undertuning must be checked. The spring-mounted machine or a machine placed on a flexible baseplate forming a vibrating system should have a resonance frequency lower than one quarter the number of revolutions of the rotating machine per second. This requirement is met if the static deformation of the elastic element remains within the range given by eqn. (12.3):

$$0.5l \geq \delta \geq \frac{4200}{n^2}, \tag{12.3}$$

where l — the unloaded length of the elastic element, mm,

δ — the permanent change in length of the elastic element due to the weight of the machine, mm,

n — the r.p.m. of the machine tested in s^{-1}.

The relevant product standards strictly specify the operating conditions during vibration measurement. For asynchronous motors, the vibration measurement is normally carried out under no-load condition, with the rated supply.

The number and location of measuring points are dependent on the type and design of the machine, but in general the points with high dynamic requirements should be selected, where the vibration is transferred to the surroundings. In the case of rotating electrical machines, important measuring points are the bearing planes and the points where the machine is coupled to its surroundings. Vibration is measured in three mutually orthogonal x, y and z directions, as shown in Fig. 12.1, where the z axis always corresponds to the axis of rotation of the machine.
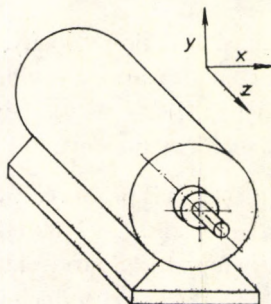
Fig. 12.1. The principal directions of vibration measurement

No international standard exists for the vibration measurement of transformers. In view of the fact that the architects want to know the vibrations generated and passed on by the transformer for the calculation of structure-borne sounds produced by the transformer, the same principles as discussed for the vibration of rotating machines must be applied for vibration measurements of transformers. The points where the vibration is transferred should be selected as measuring points.

Regarding emission standards relevant to vibration measurements, we should mention two problems related to the question of structure-borne sound discussed in Section 5.2. To determine the contribution to structure-borne sound generation of the electrical machine that serves as a power source and energy transformer in the mechanical unit, it is not sufficient to know the vibration velocity in the frequency range 10 Hz to 1000 Hz, but we must expand the measurement to higher frequencies. For calculation of structure-borne sound generation, the acting forces should be measured as well, in order to be able to treat the electrical machine as a two-pole, a power source with internal impedance, applying Thevenin's theorem on the basis of the mechanical-electrical analogy.

12.1.2 Evaluating the results of vibration measurements

From the point of view of the quality of vibration the qualification of the electric machine as a product is a typically single value qualification. This qualification is based on the vibration severity. The vibration severity of the machine is the maximum r.m.s. vibration velocity measured at selected measuring points. The various vibration grades are set out in standards based on international agreements (Table 12.1) so that an increase of 4 dB in vibration severity level within each grade corresponds to an absolute increase of 60 percent.

The various quality grades of rotating machines of different size and type are determined on the basis of Table 12.1, selecting limit values from there. This was the may we complied Table 12.2, which shows the vibrational quality grades of electrical rotating machines with rated speed of 600 min^{-1} to 6000 min^{-1} and axial height of 50 to 400 mm.

Table 12.1. The limit values of vibration quality grades

Vibration quality grade		
Symbol	Limit values, mm s^{-1}	
	lower	upper
0.11		0.112
0.18	0.112	0.18
0.28	0.18	0.28
0.45	0.28	0.45
0.71	0.45	0.71
1.12	0.71	1.12
1.8	1.12	1.8
2.8	1.8	2.8
4.5	2.8	4.5
7.1	4.5	7.1
11.2	7.1	11.2
18	11.2	18
28	18	28
45	28	45
71	45	71

Table 12.2. The vibration quality grades of small- and medium-sized electrical rotating machines (as per ISO 2373)

Vibration quality grade	Nominal speed n, s^{-1}		Axial height, mm		
			$56 \leq h \leq 132$	$132 < h \leq 225$	$225 < h \leq 400$
	over	up to	h, the permissible vibration severity in mm s^{-1}		
N, Normal	10	60	1.8	2.8	4.5
R, Reduced vibration	10	30	0.71	1.12	1.8
	30	60	1.12	1.8	2.8
S, Special	10	30	0.45	0.71	1.12
	30	60	0.71	1.12	1.8

12.2 Vibration measurement of rotating machine parts

The vibration measurement standards applied in everyday practice refer to the testing of mechanical vibrations measurable on the machine surface by contact transducers. However, we frequently encounter the situation, especially in large machines, when the bearing housing and the bearing bracket are rigidly mounted separately from the machine body. Consequently the mechanical vibration measurement on the surface of the bearing housing does not provide in-depth information on the vibration of the rotor (shaft). In such a case, the direct measurement of the vibration of the rotating part (shaft) by means of a non-contact transducer is equally important in analytical, diagnostic and safety testing. As we saw in Section 11.3, non-contact transducers measure displacement, so the characteristic quantity in the vibration of rotating shafts is always the vibrational displacement. The output signal of the non-contact transducer is a relative quantity that gives the instantaneous position of the surface element of the shaft with respect to a stationary rigid bracket mounted on the bearing housing, or to the bearing housing itself. Of course, we can determine the absolute displacement of the rotating shaft by simultaneously measuring the relative displacement of the shaft with respect to the rigid clamping device mounted on the machine body (or bearing bracket) by means of a non-contact transducer and the absolute displacement of the clamping device with respect to the reference inertial system by means of, say, a contact transducer, such as a piezoelectric accelerometer. Double integration of the signal of the piezoelectric accelerometer and subtraction from the signal of the non-contact sensor, gives the absolute vibrational displacement of the rotating shaft.

The vibration measurement of the rotating shaft should be done generally in the frequency range mentioned in Section 12.1. We should remember, however, that many ultra-high power machines (like hydrogenerators) operate at low speed, and the measuring frequency range must include the rotational frequency of the shaft. The measured vibrational displacement values are highly dependent on the rigidity and design of the non-contact transducer clamping device, and therefore, in most cases, only the shaft vibration values taken by using the same clamping device can be compared directly.

It is advisable to measure the vibration of rotating shafts in two mutually perpendicular directions, i.e., vertically and horizontally. The measuring arrangement shown in Fig. 12.2 allows measurement of both the absolute and relative shaft displacement. When only the non-contact sensor, denoted $E1$, are clamped in the clamping device, B, then the relative displacement is measured. If, however, the absolute vibration sensors, denoted $E2$, are also put in position and the measuring and processing instrument, M, calculates the difference between the two
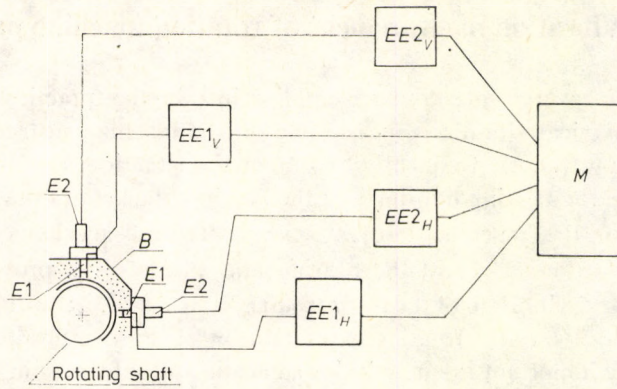
Fig. 12.2. Arrangement for simultaneous measuring of absolute and relative shaft displacement
$E1$ — non-contact sensor, $EE1$ — pre-amplifier, $E2$ — accelerometer, $EE2$ — pre-amplifier
and integrator, M — measuring and evaluating instrument, B — clamping device rigidly fixed to
the machine housing [168]

different kinds of vibration signal, then the absolute vibrational displacement of
the rotating shaft is obtained.

Figure 12.3 shows the trajectory of the rotating shaft centre in a plane per-
pendicular to the shaft. If we assume, as is justified in most cases, that the cross-
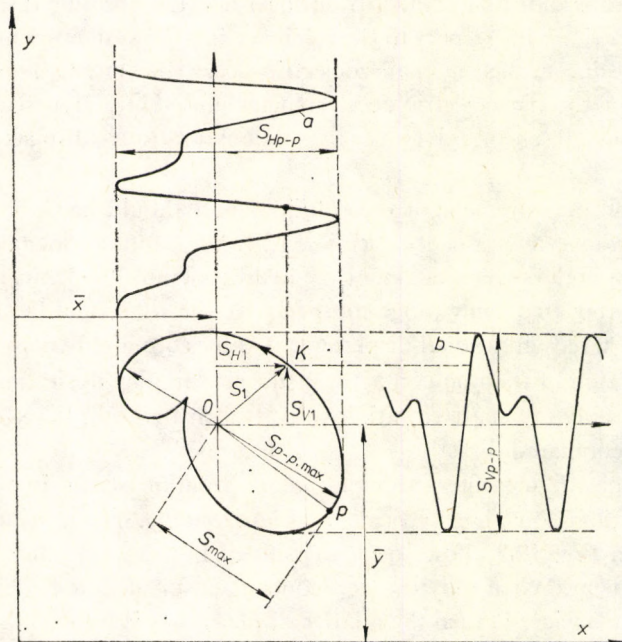

Fig. 12.3. The trajectory of the rotating shaft centre: a — time function of the horizontal sensor,
b — time function of the vertical sensor [168]

section of the shaft is circular, then Fig. 12.3 also shows the trajectory of a surface element while the shaft turns under the sensor. If the instantaneous coordinates of the shaft centre, K, are $x(t)$ and $y(t)$ in the horizontal and vertical directions, respectively, then the integrated mean position of the shaft centre with respect to time, i.e., the coordinates of the origin O are given by:

$$\bar{x} = \frac{1}{t_2 - t_1} \int_{t_1}^{t_2} x(t)\, dt, \tag{12.4}$$

$$\bar{y} = \frac{1}{t_2 - t_1} \int_{t_1}^{t_2} y(t)\, dt. \tag{12.5}$$

The displacement with respect to origin O is indicated by the rectangular coordinates $S_{H,1}$ and $S_{V,1}$, while the distance is given by S_1:

$$S_1^2 = S_{H,1}^2 + S_{V,1}^2.$$

Figure 12.3 also shows the measurable time functions of vibrational displacement that correspond to the given shaft centre trajectory, in both vertical and horizontal directions. The peak-to-peak values, $S_{H,p-p}$ and $S_{V,p-p}$, can be read off from the time functions of vibrational displacement.

The maximum peak-to-peak value, $S_{p-p,\,max}$, should be considered as being characteristic of the shaft vibration, which is found to be the longest chord drawn inside the trajectory of the shaft centre. The correct value of $S_{p-p,\,max}$ can be determined by measurement only if the rigid clamping device that holds the vibration sensor can be adjusted concentrically about the shaft centre. In such a case, the clamping device should be moved slowly until one of the sensors gives a maximum signal, that is, the signal decreases if we turn the device any further. However, the position of the clamping device is fixed in most designs. In this latter, more typical, case, the value of $S_{p-p,\,max}$ may be computed from the peak-to-peak values measured in the vertical and horizontal directions, using formula (12.6) as a good approximation:

$$S_{p-p,\,max} = \frac{(S_{V,p-p} \text{ or } S_{H,p-p}) + \sqrt{(S_{V,p-p})^2 + (S_{H,p-p})^2}}{2}. \tag{12.6}$$

In the first bracketed term of the numerator, the larger value of $S_{V,p-p}$ and $S_{H,p-p}$ should be used. Code ISO/DIS 7919 defines the value of the largest unidirectional shaft centre displacement, S_{max}. By definition:

$$S_{max} = [S_1(t)]_{max}. \tag{12.7}$$

In most cases, we know only $S_{V, p-p}$ or $S_{H, p-p}$, so the value of S_{max} may be approximated as:

$$S_{max} = 0.5 S_{p-p, max}, \tag{12.8}$$

which gives the correct value only if the time function of the vibrational displacement of the shaft is a single sinusoidal wave.

Also, the above mentioned standard sets out certain instructions regarding the evaluation of the shaft vibration measurement results. If the absolute displacement of the sensor clamping device (the output signals of EE2 in Fig. 12.2) is smaller than 20 percent of the output signal of the pre-amplifier EE1 that measures the relative shaft displacement, then the qualification in terms of vibrations may be carried out on the basis of the relative shaft displacement. In any other case, the absolute shaft displacement must be used for this purpose.
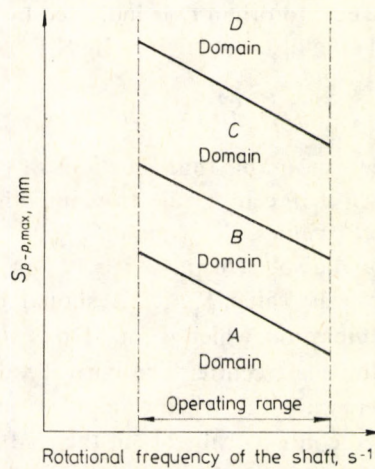

Fig. 12.4. The quality grade domains of shaft displacement [168]

The domains shown in Fig. 12.4 may be used for the purpose of qualification. The x axis indicates the rotational frequency of the shaft, the y axis, $S_{p-p, max}$. The boundaries of vibrational quality grades (domains) are lines sloping towards higher rotational frequencies, which correspond to the same kinetic energy levels at different frequencies. The individual domains correspond to the following grades:

Domain A — generally the vibration of newly assembled perfect shafts.

Domain B — the vibration measurement period should be decreased, short runs of operation with frequent checks are acceptable.

Domain C — maintenance should be scheduled and carried out.

Domain D — dangerous operation, the machine must be stopped immediately.

The available experimental data are not sufficient yet to establish clear-cut standards for the grade limits. The discussed standardization of the measuring method and the spreading measurements of rotating shafts will sooner or later allow the code regulation of permissible vibration levels. Meanwhile, limit values may be worked out for the commonest machine types.

13. NOISE MEASUREMENTS ON ELECTRICAL MACHINES UNDER STEADY-STATE OPERATING CONDITIONS

13.1 General noise measuring considerations

Let us consider a sound source away from any reflecting surfaces or other sound sources. Enclosing this source within an optional closed surface, the sound power radiated by the sound source is given by:

$$P = \oint_S \bar{I} \, d\bar{S}, \qquad (13.1)$$

if the energy absorption in the space is neglected,

where P — sound power,

$\bar{I}$ — vector of intensity,

S — the closed surface that encloses the sound source,

$d\bar{S}$ — vector of surface element.

On the right-hand side of eqn. (13.1), we have the expression of the energy passing through the closed surface S that bounds volume V. The rate of change of this quantity is identical with the change of energy within the space per unit time. Rewriting eqn. (13.1) with this approach we obtain:

$$P = -\frac{\partial}{\partial t} \int_V w \, dV, \qquad (13.2)$$

where w — the specific sound energy per unit volume,

V — the volume including the sound source, enclosed by the surface S,

t — time.

The intensity may be expressed as the average of the product of the speed of sound and the sound pressure:

$$\bar{I} = \overline{p\bar{v}}, \qquad (13.3)$$

where p — sound pressure,

$\bar{v}$ — speed vector of sound propagation.

Therefore:

$$P = \oint_S \overline{p\bar{v}} \, d\bar{S}. \qquad (13.4)$$

The energy transport through the surface S is characterized by the vector $p\bar{v}$. This vector is analogous with the electrotechnical Poynting vector. According to this definition the surface element and the intensity have vector interpretation, and the normal of the surface and the direction of energy flow need not necessarily be parallel, but if the intensity and the surface element are interpreted as scalars, this requirement is essential.

13.2 The acoustical characteristics of noise sources

The sound power emitted by electrical machines may vary over an extremely wide range (think of the difference between the noise of a tape recorder motor and the noise of a turbogenerator), and therefore the sound power levels introduced in Chapter 1 are used in the noise analysis of electrical machines as well. As we deduced there, on certain simplifying assumptions there is a close relationship between the sound power level and the sound pressure level detectable at a point of the acoustic space surrounding the machine. The value of the sound pressure level depends on the sound power emitted by the sound source, the directivity of the sound source, the distance of the sensing point from the sound source, the type of the sound source, the homogeneity of the sound space, the acoustic characteristics of the testing room, the magnitude of background noise and the volume of the reverberation space.

The question of which acoustic parameter should be accepted to characterize the sound source was raised at an early date. In view of the fact that the available measuring systems allowed direct measurement of sound pressure level, the noise testing procedures and specifications of the past accepted the average sound pressure level measured at a given distance from the machine as the acoustic parameter that characterized the sound source. Knowing, however, that neither the sound source, nor the acoustic space surrounding it is ideal, a tolerance band was included to allow for various interferences, specifying the permissible deviation from ideal conditions. The engineer who used acoustic parameters in acoustic design work, say, took the sound power level emitted by the noise source as the initial design parameter and determined the sound power level of the machine from the average sound pressure level specified for the machine and the index of the measuring surface. The value L_W so calculated was quite uncertain, since the engineer knew from the noise testing certificate of the machine only that the conditions of noise measurement had complied with the tolerances set out in the noise measuring standards. To what extent, it was not known. Consequently the uncertainty of the computed sound power level was rather high.

Over recent decades, the noise testing procedures and standards widely accepted

and specified the use of the sound power level emitted by the machine as the characteristic acoustic parameter of the noise source. This practice is advantageous from many aspects:

— It provides directly usable acoustical data for the user or operator of the machine.

— The task of the person who carries out the noise measurement is not only to ensure that the noise measuring conditions comply with the requirements, but also to correct the measured acoustic parameters to the extent required by the degree of compliance. In this way, the measured and calculated sound power level emitted by the machine are much more accurate and reliable than before.

From the above discussion, it is understandable that the sound pressure level of the machine is considered to be the most important acoustic parameter of the machine as a noise source, and this is the parameter to be determined by measurement.

13.3 Basic methods of sound power level determination

Around the sound source placed in a closed space, two different types of sound field may be established depending on which energy component is dominant in determining the magnitude of energy density. In the space close to the sound source the direct sound energy is predominant, while further away, the reflected sound energy is stronger. The space where the sound pressure level is determined only by the parameters of the sound source is called the direct field, while that where the reflected sound waves dominate is called diffuse field. We must not confuse the direct field with the near field, the diffuse field with the far field. The near field/far field classification is based on the relative phase position of the p and v (i.e., if they are in phase or not). There are two basic methods of determining the sound power level depending on whether the measurement is carried out in the direct field or in the diffuse field. In practice, we always try to select measuring points so that the sound energy component to be measured is predominant at the selected points over the other component. There is not available a measuring instrument suitable for direct measuring of sound power, and therefore the determination of sound power is reduced to the measurement of sound pressure level. The basic difference between sound pressure measurements conducted in the direct field and in the diffuse field is that in the former we want to determine the intensity, whilst in the latter, the energy density from the sound pressure.

In the direct field, we generally assume that the relationship between the pressure and the particle velocity of the sound wave may be expressed as $/\bar{v}/=p/(\varrho c)$, so

that the intensity may be determined as $I=p^2/(\varrho c)$. This simple formula is based on the following assumptions as simplifications:

— The intensity vector and the normal of the measuring surface are pointing in the same direction.
— The pressure and the velocity waves are in phase.
— The sound pressure levels measured at a finite number of measuring points refer to measuring surface elements of identical size and are truly representative of the individual surface elements.

One promising alternative for direct field measurement is the direct measuring of intensity.

As we have seen the sound power output of a machine can be expressed as in Eq. (13.1).

Sound intensity, defined as the average rate of sound energy across a unit area, can be expressed as in Eq. (13.3). A single microphone can measure pressure, this is not a problem, but measuring particle velocity is not as simple. The particle velocity can be related to the pressure gradient with the linearized Euler equation:

$$\bar{v}=-\frac{1}{\varrho}\int \frac{\partial \bar{p}}{\partial r}\,\mathrm{d}t,$$

where ϱ is the density of the air. Euler's equation is essentially Newton's second law applied to a fluid. The pressure gradient is a continuous function, that is, a smoothly changing curve. With two closely spaced microphones it is possible to obtain a straight line approximation to the pressure gradient by taking the difference in pressure (p_B-p_A) and dividing by the distance Δr between them.

$$v=-\frac{1}{\varrho}\int \frac{p_B-p_A}{\Delta r}\,\mathrm{d}t.$$

The average pressure can be expressed as

$$p=\frac{p_B+p_A}{2},$$

or the sound intensity:

$$I=-\frac{p_B+p_A}{2\varrho\Delta r}\int (p_B-p_A)\,\mathrm{d}t.$$

The accuracy of the procedure applying two pressure microphones (intensity probe) is strongly dependent on the distance between the two microphones.

The direct measurement of intensity is feasible by means of digital analysers applying Fast Fourier Transformation. This method relates the intensity to the imaginary part of the cross spectrum of the two sound pressure signals:

$$I=-\frac{1}{\varrho\omega\Delta r}\,\mathrm{Im}G_{AB},$$

where ω is the angular frequency, $\mathrm{Im}G_{AB}$ is the imaginary part of the cross spectrum. The formulation of the intensity expressed by the average pressure and by the cross spectrum are equivalent, both give the sound intensity.

The sound power level radiated by the electrical machine can be determined as follows:

$$L_W = 10 \log \frac{1}{n} \sum_{i=1}^{n} 10^{0.1 L_{Ii}} + 10 \log \frac{S}{S_0},$$

where L_W — the sound power level,

   L_{Ii} — the measured sound intensity level in the ith measuring point,
   n — the number of the measuring points,
   S — the area of the measuring surface, $S_0 = 1$ m^2.

For reverberation zone measurements, the sound source should be located in order to allow the establishment of a sound field that can be considered as diffuse at the place of measurement, at a certain distance from the sound source and the walls of the room. The energy density of this diffuse sound field may be determined by measuring the sound pressure at various points of the space. The sound power is calculated from the energy density. As there is no transducer that can measure particle velocity correctly, pressure microphones are used also for this purpose. The energy density actually measured is not the total energy density but only the density of potential energy. When the sound power level is determined, we implicitly assume that the total energy density is twice the density of potential energy. This means that the density of potential energy is equal to the density of kinetic energy at any point of the space. In reality, however, this is true only for the averages taken for the whole of the diffuse field. From the sound pressure level averaged for the whole of the diffuse field, the sound power level is given as:

$$L_W = \bar{L} + 10 \log \frac{V}{V_0} - 10 \log \frac{T}{T_0} - 14, \qquad (13.5)$$

where $\bar{L}$ — sound pressure level averaged for the whole of the diffuse field,

   V — volume of the room; $V_0 = 1$ m^3,
   T — reverberation time; $T_0 = 1$ s.

As seen, the accuracy of a diffuse field measurement depends partially on the accuracy of the average sound pressure calculated from the sound pressure levels for the whole of the diffuse field, i.e., on how the mean value of the discrete sample approximates the expected value of the continuous lot, and partially on the accuracy of the measured reverberation time. (The latter can be different for different frequencies, therefore when the average T is used, as generally accepted in practice, the error in the measurement of noises with dominant pure-tone component can be significant.)

The comparison theorem is frequently used in the case of both direct field and diffuse field measurements. In this method, the sound power level of a so-called reference sound source with known sound power level is measured under the same conditions as the tested noise source. Comparing the known sound power level with the levels measured during the comparative test, we can identify the deviations due to local acoustic conditions and use them to correct the results obtained for the noise source by measurement.

If we consider methods of sound power level determination, we deduce that the intensity measurements did not yet come into general use. The diffuse field measurements can be accomplished also very rarely since a special acoustic laboratory is required to produce the diffuse field, and this is very costly. The remaining are direct field measurements whose accuracy depends on the acoustic conditions in the test room. For accurate measurements, a completely free sound space, in many cases an anechoic chamber (i.e., an acoustic laboratory with non-reflecting walls), is required, which is also very costly and seldom available. Of practical importance are the technical and informative direct field measurements (discussed in detail in Section 13.5), especially in the semi-anechoic field over a reflecting plane. Placing the machine to be tested on a reflecting plane, we can exploit the theory of acoustic reflection.

13.4 Determining the sound power level in direct sound field

For a perfect ideal case, small and medium-sized electrical machines can be considered as point sound sources that generate spherical sound field described in detail in the literature. The ideal acoustic environment may be identified with the free sound field where only the sound waves emitted by the sound source are present without reflecting surfaces and, consequently, without reverberation field or any sound of other origin, that is, the background noise level is considered to be zero. In such a case, the sound pressure level in a spherical sound field at a distance d from the sound source emitting sound power P or sound power level L_W is found to be:

$$L = L_W + 10 \log \frac{S_0}{4d^2\pi}, \tag{13.6}$$

or in the free sound field over a reflecting plane

$$L = L_W + 10 \log \frac{S_0}{2d^2\pi},$$

where $S_0 = 1$ m²,

　　　d — the distance of the measuring point from the point sound source.

As can be seen from eqn. (13.6), in an ideal case it is sufficient to measure one sound pressure level at one distance, and then the value of L_W can be readily calculated. In reality, however, electrical machines are not ideal point sources producing spherical radiation, and we cannot carry out the noise measurement under ideal acoustic environment.

In the following, we investigate step-by-step what problems are to be encountered, which procedure is used in practice, what is the inherent error in this procedure, and how we can take into account, reduce or eliminate this inherent error.

13.4.1 The finite element error

The noise measuring points are positioned over a measuring surface with area S which encloses the machine. Different standards specify different shapes for the measuring surface, like a hemisphere, a prism or a complex surface placed on a rigid floor. The distribution and density of the measuring points are determined by the geometrical dimensions of the machine to be tested and the difference of sound pressure levels measured at adjacent measuring points. If the number of measuring points were infinite, then we could find the exact value of the emitted sound power using the following formula:

$$P=\oint_S \frac{p^2}{\varrho c}\, dS, \qquad (13.7)$$

where ϱ — the density of the acoustic medium,
c — the speed of sound in that medium.

For technical reasons, the number of measuring points is finite, and consequently the integration is replaced by summation. We assume that the individual measuring points correspond to surface elements of roughly equal size and that the directivity of the machine as a sound source is such that the intensity values characterized by the measured sound pressure levels at the measuring points, as elements of a population, exhibit a normal distribution and the expected value of the normal distribution are equal to the average intensity. Then, in the standard procedure, the sound power level is computed from the average of intensities (called average sound pressure level, see Chapter 1) based on the measured sound pressure levels:

$$L_W=\bar{L}-10\log\frac{S_0}{S}, \qquad (13.8)$$

where

$$\bar{L}=10\log\frac{1}{n}\sum_{i=1}^{n}10^{0.1L_i}, \qquad (13.9)$$

when $L_{i,\,max} - L_{i,\,min} \geq 5$ dB. If $L_{i,\,max} - L_{i,\,min} < 5$ dB, a simpler formula may be used:

$$\bar{L} = \frac{1}{n} \sum_{i=1}^{n} L_i. \tag{13.10}$$

Measuring practice proves, however, that the use of the average value for the estimation of the expected value of the population is not accurate enough. Let us illustrate the possible magnitude of this error. The intensity values calculated from the measured sound pressure levels, L_i, constitute an infinite population of normal (Gaussian) distribution. The assumption of the normal nature of this continuous distribution is justified, since the number of noise components directly produced by the noise causes is high and they can be considered as independent elementary random variables. The resultant intensity is produced as the sum of these elementary random variables. The fluctuation in the component random variables is random and small in comparison with the fluctuation of the resultant random variables, so in view of the central-limit theorem, the distribution of the resultant intensity as a random variable will be very close to normal.

In everyday practice, of course, if samples are taken, sound pressure level measurements with finite number of elements can be realised. The mean value of the discrete variables $p_i^2/p_0^2 = 10^{0.1 L_i}$, which are proportional to the intensity and are computed from the sound pressure levels measured at the measuring points, will deviate from the expected value of the continuous variables. According to the well-known relation of mathematical statistics, the deviation of the expected value from the mean value follows the Student distribution of $(n-1)$ degrees of freedom for a given confidence level:

$$M\left(\frac{p_i^2}{p_0^2}\right) - \overline{\left(\frac{p_i^2}{p_0^2}\right)} = \frac{t\sigma}{\sqrt{n-1}}, \tag{13.11}$$

where t is the variable of the Student distribution of $(n-1)$ degrees of freedom,

$$\overline{\left(\frac{p_i^2}{p_0^2}\right)} = \frac{1}{n} \sum_{i=1}^{n} 10^{0.1 L_i} = 10^{0.1 \bar{L}}, \tag{13.9a}$$

$$\sigma^2 = \frac{1}{n} \sum_{i=1}^{n} \left[\left(\frac{p_i^2}{p_0^2}\right) - \overline{\left(\frac{p_i^2}{p_0^2}\right)}\right]^2, \tag{13.12}$$

where n is the number of measuring points.

The error in the determination of the sound power level due to the finite number of measuring points is simply the difference between the upper limit of the true sound power level at confidence level $\alpha\%$ and the sound power level calculated from the results of n sound pressure level measurements:

$$\Delta L_1 = L_{W,\text{ true}} - L_{W,\text{measured}},\tag{13.13}$$

where

$$L_{W,\text{ true}} = 10 \log M \left(\frac{p_i^2}{p_0^2}\right) + 10 \log \frac{S}{S_0},\tag{13.8a}$$

$$L_{W,\text{ measured}} = \bar{L} + 10 \log \frac{S}{S_0}.\tag{13.8b}$$

Substituting the true and measured values of the sound power level into eqn. (13.13):

$$\Delta L_1 = 10 \log M \left\{\frac{p_i^2}{p_0^2}\right\} - \bar{L} = 10 \log \frac{M\left\{\dfrac{p_i^2}{p_0^2}\right\}}{\left(\dfrac{p_i^2}{p_0^2}\right)}.\tag{13.14}$$

Equation (13.11) may be rewritten as:

$$\frac{M\left\{\dfrac{p_i^2}{p_0^2}\right\}}{\left(\dfrac{p_i^2}{p_0^2}\right)} = 1 + \frac{t\sigma}{\sqrt{n-1}}\ \frac{1}{\left(\dfrac{p_i^2}{p_0^2}\right)},\tag{13.11a}$$

and substituted into eqn. (13.14) to obtain the so-called finite element error of the measuring method as:

$$\Delta L_1 = 10 \log \left[1 + \frac{t\sigma}{\sqrt{n-1}}\ \frac{1}{\left(\dfrac{p_i^2}{p_0^2}\right)}\right].\tag{13.15}$$

According to experiments published in the literature [134], the following empirical relationship has been found between the standard deviation σ, the average sound intensity and the range R of the n sound pressure level measurements:

$$\sigma = 0.087 R^{0.82} \overline{\left(\frac{p_i^2}{p_0^2}\right)},\tag{13.16}$$

where $R = L_{\text{max}} - L_{\text{min}}$.

Substituting eqn. (13.16) into eqn. (13.15), we arrive at the finite element error of power level determination for a finite n measuring points:

$$\varDelta L_1 = 10 \log \left[1 + \frac{0.087 t R^{0.82}}{\sqrt{n-1}} \right]; \qquad (13.17)$$

As we see, the error is always positive, that is, the sound power level is underestimated by the measurement.

The graphical representation of eqn. (13.17) is shown in Fig. 13.1 [23] for a confidence level of 97.5 percent. Six different spreads were taken as parameters of the graph in the range from 2 to 25 inclusive.
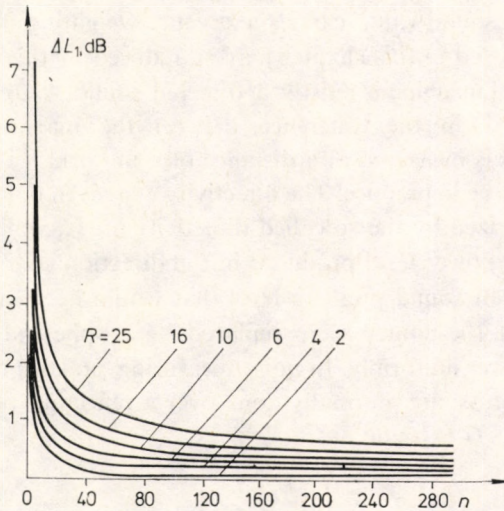

Fig. 13.1. The error of sound power level determination with n measuring points and a spread of R for 97.5 percent confidence level

In the course of deducing eqn. (13.7) we made no stipulation whatever in our discussion for the shape of the measuring surface, and therefore eqn. (13.17) applies generally to any standard measuring surface and gives an estimation of the error. This equation is also suitable for the determination of the minimum number of measuring points required for a given level of acceptable uncertainty ($\alpha\%$) and accuracy of sound power level determination specified in advance in dB.

According to the recommendations of the international standard ISO 3745, the measurement satisfies the requirements for accurate measurements, if the value of the spread, i.e., the difference between the measured maximum and minimum sound pressure levels in dB, is smaller than the number of measuring points, provided the sound pressure level measurement is carried out at the suggested ten measuring points with discrete microphone arrangement. As shown in

Fig. 13.1, for ten measuring points and $R=10$ dB the finite element error exceeds 1.5 dB.

The international standard recommendation ISO 1680/2 relevant to the noise measuring methods of large electrical rotating machines sets out an interesting method that is easy to handle in practice. This method adds another measuring point to the measuring points specified by ISO standards, located near the one at which the highest level is being measured. If L_{max} is measured at, say, measuring point no. 5, then the standard suggests another measurement at a distance of 20 to 30 cm from that point at the same elevation. In doing so the location having the highest sound value carries a greater weighting in the calculations, and the error discussed in this chapter may be reduced by this simple method.

The real electrical machine is mostly a directed sound source. A sound source is called directed when the difference between the maximum and minimum sound pressure levels measured at a distance of a uniform d is larger than 5 dB, which is generally true in practice. The directivity at a given point of the measuring surface is characterized by the so-called directivity index, which is the difference between the sound power level produced in the direction concerned by the noise source and the mean sound pressure level that would be measured at the same measuring point if the source were replaced by a spherical radiator emitting identical sound power uniformly. In noise measuring practice of electrical machines, the measurements are normally done over a reflecting plane in which case the directivity index G is found as:

$$G=L_i-\bar{L}+3, \tag{13.18}$$

while the directivity factor D is given by:

$$D=10^{0.1G}. \tag{13.19}$$

Among others, it is the very directivity of the electrical machine which is responsible for the fact that the sound pressure levels measured at the individual measuring points do not correctly represent the measuring surface elements that correspond to them.

13.4.2 Background noise correction

In this section, we investigate the error caused by the presence of background noise, i.e., the sound pressure level produced by foreign noise sources, in the measurement of symmetric spherical sound radiators in a free acoustic field. In routine noise measurement practice, the sound pressure level reading, L', obtained during the measurement of the machine noise is the resultant of the sound pressure

level emitted by the machine and the background noise L_n. When the machine is switched off, we measure the background noise L_n. L is obtained by subtracting L_n from L', that is:

$$L = 10 \log (10^{0.1L'} - 10^{0.1L}).\qquad(13.20)$$

In view of the arithmetics of levels, when $L' - L_n > 10$ dB, the maximum error is 0.4 dB if $L' = L$ is taken.
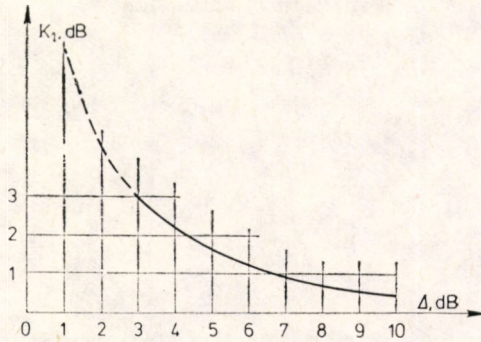

Fig. 13.2. The background noise correction term K_1

To facilitate calculation, eqn. (13.20) may be rewritten by factoring out the first term of the argument and introducing the increment $\Delta = L' - L_n$ that can be measured. We can define a correction term K_1 (Fig. 13.2) as:

$$L = L' - K_1,\qquad(13.21)$$

where

$$K_1 = 10 \log \frac{10^{0.1\Delta}}{10^{0.1\Delta} - 1}.$$

13.4.3 The near field error

The noise measurement of electrical machines cannot always be carried out in a noiseless environment, so we may be forced to reduce the measuring distance d. Of course, this results in an increase in the value of Δ. In other words, the direct sound pressure level emitted by the sound source is much higher than the background noise due to other sources and the sound pressure level of reflected waves. The sound power level may be determined from eqns (13.8) and (13.9). In each concrete case, however, we must make sure that the assumptions on which eqns (13.8) and (13.9) are based are justified. When we substitute eqn. (13.7) for the

sound power expression (13.4), it is assumed that the pressure and velocity waves
are in phase and the intensity vector is parallel to the normal vector of the
measuring surface element $\mathrm{d}\bar{S}$. It is far from being certain in the near field of the
machine that these assumptions are correct. Hübner [47], [50], Yang [146] and
others have investigated this question in detail and gave the curves shown in
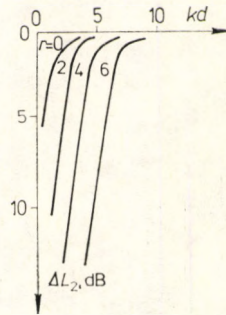Fig. 13.3 as a graphic representation of the near field error:

Fig. 13.3. The near field error versus kd. where $k=2\pi f/c$ (wave number), for spherical radiators of
different mode numbers (r). d is the distance of the measuring point from the radiator

$$\Delta L_2 = 10 \log \frac{\oint\limits_S \overline{p\bar{v}}\,\overline{\mathrm{d}S}}{\oint\limits_S \frac{p^2}{\varrho c}\,\mathrm{d}S}, \tag{13.22}$$

for a spherical radiator. As we see, the magnitude of the near field error is a
function of three parameters, namely, the mode number of the radiator (deflection
mode number R), the wave number k (and, through it, the frequency) and the
measuring distance d. For a measuring distance of 1 m and $R\leqslant6$, which is typical
in the noise of electrical machines, the near field error is smaller than 1 dB below
400 Hz. For a measuring distance of 0.25 m, i.e., in the near field, assuming that
the dominant vibration mode number of the radiating motor is 6, the near field
error drops below 1 dB only for frequencies over 1600 Hz. For the noise component
with frequency twice the supply frequency, frequently encountered in asynchronous
machines, and mode number $R=2$ (two-pole machines), the near field error can
be as high as -15 dB at a distance of 0.25 m, but only -5 dB at a distance of 1 m.
Note that the near field error mostly impairs measurement of low-frequency
components. The situation is slightly improved by the fact that the A-weighting
filter strongly attenuates the low-frequency components (e.g., 100 Hz, where the
attenuation of the A-weighting network is 19 dB). Most standards intend to

avoid the near field error by specifying a measuring distance of 1 m, which can be reduced only in very special cases. The phase error part of the near field error, which is due to the phase difference between the pressure and velocity waves, may be eliminated by means of a two-microphone intensity meter.

The other part of the near field error, the normality error, reduces to zero if the sound source is an ideal spherical radiator and the sound waves propagate in the form of expanding spherical surfaces, and the spherical measuring surface is concentric with the sound source. From the different measuring surface shapes, for a given number of measuring points, the spherical surface is more accurate in the case of point sources, while in the case of a sound source with finite dimensions, complex (conform) measuring surfaces are better. According to experiments and theoretical calculations, the normality part of the near field error can be as high as 1 dB for a rectangular prism-shaped measuring surface, a shape beneficial in terms of the easy and quick execution of the noise measurement, since the intensity vector and the normal of the measuring surface are not parallel along the edges and at the corners of the rectangular prism, i.e., at the measuring points located there. In practice, however, a near field error of 1 dB is never experienced with a rectangular prism-shaped measuring surface, because the other component of the near field error, namely the phase error, is reduced at the measuring points along the edges or at the corners of the measuring surface since they are more than 1 m distant. Considering that the finite element error ΔL_1 discussed above may be considerably higher than the near field error ΔL_2 in the neighbourhood of 8 to 10 measuring points applied in practice (see Fig. 13.1), increasing the number of measuring points is much more important than the shape of the measuring surface in the reduction of methodological errors (i.e., ΔL_1 and ΔL_2), aimed at improved accuracy in noise measurement.

According to theoretical calculations and experience, there is higher accuracy with sound power level measurement by means of a rectangular prism-shaped measuring surface having supplementary measuring points added to the specified main measuring points, than those having the main measuring points positioned on complex measuring surfaces of a theoretically better fit. In many cases, despite the higher number of measuring points, the rectangular prism-shaped measuring surface is quicker and simpler (and therefore cheaper) to use than other measuring surfaces.

In noise measuring practice, we may encounter other situations that result in near field error. If the machine to be tested is set up at a fixed location and there is an immovable landmark or object in the close vicinity (i.e., within 3 meters), then an eccentrical measuring surface must be employed around the noise source. This means that the noise source gets very close to certain parts of the measuring surface, so the measuring points located there are in the near acoustic field. From

calculations by Hübner [47], the near field error ΔL_2 varies with the eccentricity of the measuring surface as shown in Fig. 13.4 for spherical radiators of mode numbers $R=0$ and $R=1$. The error of the zero-mode-number radiator is independent of wave number k and distance d, while that of the radiator with mode number 1 is strongly dependent on wave number and radius d of the spherical measuring surface.
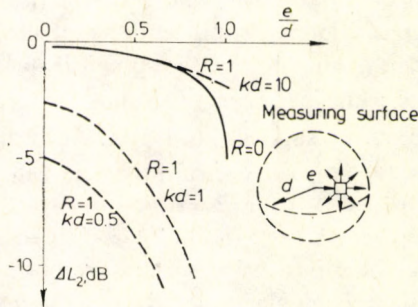

Fig. 13.4. Measuring error due to eccentrical noise source location

13.4.4 Correction according to the reverberation sound field

As we have seen, the microphone is placed in the direct sound field for the noise measurement of electrical machines. Unfortunately, only direct sound field in an acoustic laboratory or in an anechoic chamber can be considered "pure", i.e., free from reflected sound waves at the measuring points. In reality, however, we always have some sound waves reflected by the walls of the room or by other objects in the room.

At a measuring point at a distance of d from the sound source, the sound pressure level is given by eqn. (1.49) as:

$$L'=L_W+10 \log \left(\frac{S_0}{S}+\frac{4}{R}\right). \tag{13.23}$$

In the usual sound fields, workshops, etc. found in practice, the room constant R may be well replaced by the absorption factor A. The absorption factor is:

$$A=\bar{a}S_t,$$

where $\bar{a}$ — the mean absorption coefficient of the internal wall surfaces of the testing room (for workshops the typical value lies in the range 0.05 to 0.1),

  S_t — the total surface area of the testing room.

If $\bar{a}$ and S_t are known, the absorption factor A may be computed, just as by measuring the reverberation time and applying the following formula:

$$A = \beta \frac{V}{T},\qquad (13.24)$$

where $\beta = 0.164\ \mathrm{m^{-1}\,s}$,

V — the volume of the testing room,

T — the reverberation time (i.e., the time required for a 60 dB drop in sound pressure level after the sound source is switched off).

Rearranging eqn. (13.23), we arrive at the sound pressure level increment (let us call it correction term K_2) that increases the sound pressure level L to be measured in free sound field, so we have to correct the obtained result by this term:

$$L' = L_W + 10 \log \frac{S_0}{S} + 10 \log \left(1 + \frac{4/S_0}{A/S}\right) = 1 + K_2,$$

where

$$K_2 = 10 \log \left(1 + \frac{4/S_0}{A/S}\right),\qquad (13.25)$$

that is,

$$L = L' - K_2.\qquad (13.25)$$

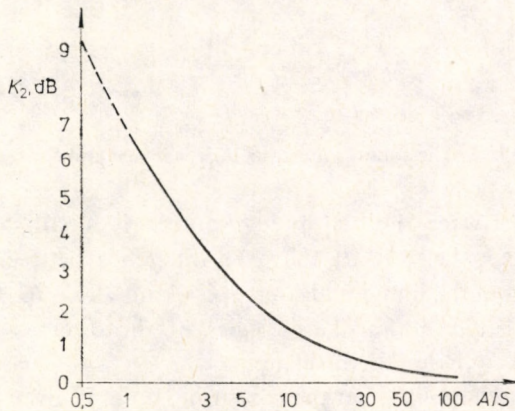The correction term K_2 may be represented graphically in terms of A/S (see Fig. 13.5).

Fig. 13.5. The correction term K_2 to take the reverberation field into account

13.4.5 The reflection error

The assumption of a hemispherical symmetry of the acoustic field in the testing rooms with solid floor used in practice would be justified only if the sound source were an acoustic sound source positioned symmetrically to the horizontal plane

passing through the centre point of the electrical machine, and this plane were identical with the solid floor. In reality, however, the machine is placed on the reflecting plane, so the machine is completely above this plane, and therefore the microphone at the measuring point senses not only the sound waves emitted directly by the machine, but also the waves reflected from the reflecting plane with shifted phase. This phenomenon is the source of an other type of error, as shown below.

By placing the sound source at a height h over a solid foundation (like concrete), the measured noise will be the sum of the direct noise and the noise reflected from the foundation. The solid foundation reflects the incident sound waves without changing the phase angle of the pressure wave, and consequently it can be replaced by an image source that emits a sound with identical amplitude and phase to that emitted by the original source. This image source is located below the boundary plane of the foundation at the same distance as the original source is located over the boundary plane (Fig. 13.6).
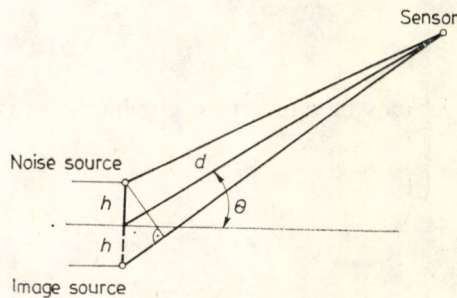

Fig. 13.6. The sound source, its mirror image and the sensor

If the distance between the two point sources is small compared with the distance of the sensor (i.e., $2h \ll d$), then the difference between distances of the measuring point from the individual sources is about $2h \sin \theta$.

The difference between the phase angles of the direct and reflected waves is $\Delta\Theta = 4h\pi \sin \Theta/\lambda$ (where λ is wavelength).

The total pressure amplitude at the measuring point is given by:

$$\hat{p}(t) = \sqrt{2}p_1 \left[\cos \omega t + \cos \left(\omega t + \frac{4\pi h \sin \theta}{\lambda} \right) \right], \tag{13.26}$$

where p_1 is the r.m.s. pressure that would be measured at the given point without any reflection from the floor. Applying the well-known trigonometric relationship:

$$\hat{p}(t) = 2\sqrt{2}p_1 \cos \left(\omega t + \frac{2\pi h \sin \theta}{\lambda} \right) \cos \frac{2\pi h \sin \theta}{\lambda}. \tag{13.27}$$

The r.m.s. value of the pressure at a point of the hemisphere surface, if the centre of the sphere is midway between the source and its mirror image, is given by $2p_1 \cos \dfrac{2\pi h \sin \theta}{\lambda}$. The average value of the r.m.s. sound pressure levels, which can be obtained by measuring the pressure at n points over the hemispherical surface is found to be:

$$\bar{L}' = 10 \log \left[\frac{\overline{p_i^2}}{p_0^2} \right] \left(\frac{4}{n} \sum_{i=1}^{n} \cos^2 \frac{2\pi h \sin \theta_i}{\lambda} \right) = \bar{L}_1 + 10 \log \left(\frac{4}{n} \sum_{i=1}^{n} \cos^2 \frac{2\pi h \sin \theta_i}{\lambda} \right),$$

where

$$\bar{L}_1 = 10 \log \left[\frac{\overline{p_1^2}}{p_0^2} \right].$$

The sound power emitted by the source spherically may be determined from the mean sound pressure level as:

$$L_{W1} = \bar{L}_1 + 10 \log (4d^2\pi). \tag{13.28}$$

Similarly, the sound power level obtained by measurements over the surface of the hemisphere placed on a foundation is given by:

$$L_W = \bar{L}_1 + 10 \log \left(\frac{4}{n} \sum_{i=1}^{n} \cos^2 \frac{2\pi h \sin \theta_i}{4} \right) + 10 \log (2d^2\pi). \tag{13.29}$$

So the sound power level determined in the hemispherical field over the solid foundation differs from the level obtained in a free spherical field by:

$$\Delta L_3 = L_W - L_{W1} = 10 \log \left(\frac{2}{n} \sum_{i=1}^{n} \cos^2 \frac{2\pi h \sin \theta_i}{\lambda} \right). \tag{13.30}$$

If the number of measuring points is very high, the summation transforms into an integral, so the above difference may be expressed by the following approximation:

$$\Delta L_3 = 10 \log \left(1 + \frac{c}{4\pi\gamma} \sin \frac{4\pi\gamma}{c} \right), \tag{13.31}$$

where c—the speed of sound in the acoustic medium,
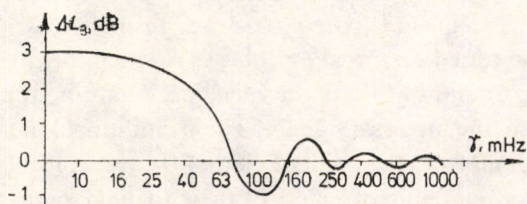$\gamma = hf$.

Fig. 13.7. The error caused by sound reflected from the rigid floor

As shown in Fig. 13.7, for $h=0.25$ m we may expect an error higher than 0.5 dB for frequencies below 640 Hz. Most standards attempt to eliminate this source of error by specifying that the machine to be measured must be as close to the rigid reflecting floor as possible. This condition, however, cannot be satisfied in the case of skid-mounted or platform-mounted machines.

13.5 Main specifications and methods of rotating machine noise measurements

13.5.1 The standard noise measurements in direct sound field

In noise measuring practice of electrical machines, the most frequently encountered situation is the measurement in the direct sound field. The accuracy of these measurements is mostly technical or informative. Considering that numerous standards relate to this subject, with a little care and goodwill we can always find the standard relevant to a given acoustic situation, allowing the accomplishment of the measurement under specified conditions. Since the standards concerned have a common measuring principle and differ only in the values of acoustical environmental parameters that affect the accuracy of the measurement, we will discuss the subject of standard noise measurement through a measuring algorithm based on the common principle. The details can be found in the relevant standards.

(a) Setting up the machine. The objective is to determine the airborne sound power level, and consequently the machine should be set up so that it does not transmit any structure-borne sound to the surroundings thus generating secondary sound radiators. The machine to be tested should be placed on a rigid floor as a sound reflecting plane, as close as possible to this reflecting plane. There should not be any reflecting wall or other object on either side near or above the machine. Considering the usual 1 m measuring distance, it is recommended not to have any object within a 3 m surroundings of the tested machine.

(b) Operating condition. In principle, the objective is to determine the sound power level radiated by the electrical machine under rated operating conditions, that is, rated supply, frequency, speed and load. In many cases this task is very hard to solve. If the tested electrical machine is a generator, then we cannot live without the driving motor, while if the machine is motor, then we need some machine to provide the necessary load. These additional machines are noise sources themselves, and from the point of view of the tested machine they manifest themselves as background noise. Because of their spatial closeness, however, these background noises are very hard to separate. Most electrical rotating machines

tested are electrical motors, which can run in themselves under no-load condition. An aspect that deserves some consideration is that the load dependency of electrical rotating machine noise is not unambiguous as we proved for asynchronous motors in Chapter 6. The effort to simplify the accomplishment of the measurement as much as possible and the consideration that the noise measurement of electrical motors aims at the qualification of the motor as a product anyway, made the writers of the standards accept an allowance of no-load noise measurements in the case of motors. Noise measurement under load is discussed in the next section.

(c) Noise measuring instruments and the measuring system must be calibrated as specified in the relevant standard or instrument manual. We must make sure that the environmental interferences (e.g., electromagnetic field, temperature, humidity, wind, etc.) do not exceed permissible levels.

(d) Selecting the measuring surface and the measuring points. The small electrical rotating machines in most cases can be considered to be a point source or a spherical source. In the case of medium-sized and large electrical rotating machines, we can use a rectangular prism as enveloping surface with one of its sides on the reflecting plane, while the other five sides touch the noise radiating surface of the machine. The measuring surface is set up at a distance d from the enveloping sphere or prism surface. The usual value of d is 1 m, since this normally gets us out of the acoustic near field of the machine but the effect of reflected sound waves is still weak.

If for safety or other reasons the value of d is increased, we may find ourselves in a difficult situation because of the background noise or the reflected sound field. As for the shape of the measuring surface, we can usually choose from several possibilities. For testing small electrical machines, the best choice is a hemispherical surface with a radius not smaller than twice the largest linear dimension of the tested machine (i.e., $r \geq 2l_{max}$). When the noise of a medium-sized or large electrical machine is measured, although we may use the hemispherical surface here as well it is best to use a complex measuring surface or a rectangular prism-shaped measuring surface. The shape of the conform measuring surface and the distribution of measuring points over it are illustrated in Fig. 13.8. The characteristic dimensions of the measuring surface can be found from the following equations:

$$a = 0.5l_1 + d,$$

$$b = 0.5l_2 + d,$$

$$c = l_3 + d, \tag{13.32}$$

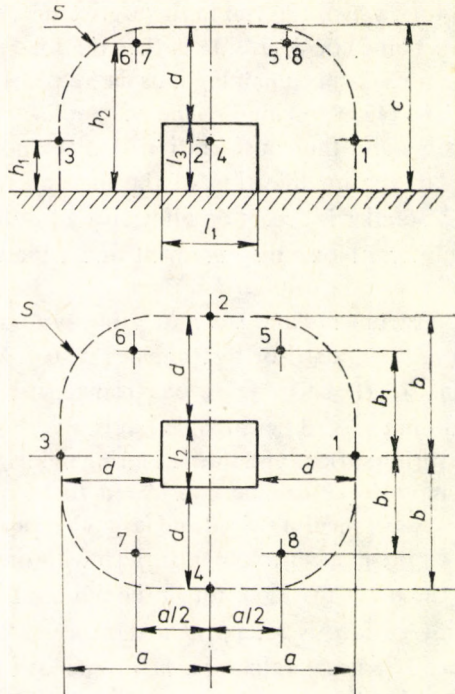where l_1, l_2 and l_3 are the overall dimensions of the rectangular prism enveloping

Fig. 13.8. The conform measuring surface and the measuring points [156]: S — measuring surface, 1 to 8 — key measuring points, l_1, l_2 and l_3 — dimensions of the rectangular paralelepiped that encloses the machine, d — measuring distance

the machine. The other dimensions indicated in Fig. 13.8 may be computed from the following set of equations:

$$h_1=0.25(b+c-d), \quad b_1=0.5(b+c-d),$$

$$h_2=0.75(b+c-d). \tag{13.33}$$

The measuring points over a hemispherical surface should be located also as shown in Fig. 13.8, but in this case $a=b=c=d=r$.

The shape of the conform measuring surface ensures relatively well that all the measuring points are at a distance d from the noise source. We can select a measuring surface of rectangular prism shape (Fig. 13.9). The advantage of this measuring surface is that it allows easy location of the measuring point coordinates. Its disadvantage is that the corner points are at a distance larger than d, and therefore the effect of reflected waves and the background noise is more substantial at these points. In turn, it is beneficial in the reduced near field error. Rectangular prism-shaped measuring surfaces are used mostly for testing large noise sources, where

the condition of $d \geq 2l_{max}$ cannot be satisfied owing to the background noise, and the reflected sound field and a reasonable, say $d=1$ m, selection results in a relation of $d \leq 1.5l_{max}$. The height of the bottom measuring plane is $h=0.5c$ in this case. (Dimensions a, b and c are obtained from eqn. (13.32).) It is true for both measuring surfaces first that the so-called key measuring points should be located. If the spread of the measured values, i.e., the difference between the maximum and minimum sound pressure levels measured, is larger than 8 dB, then
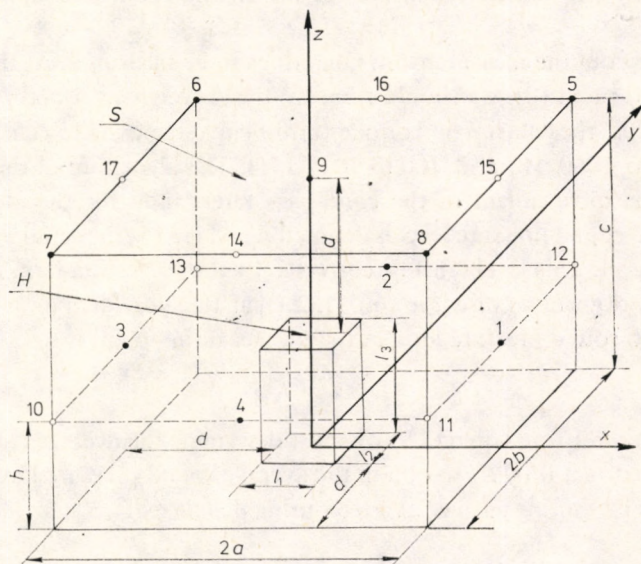

Fig. 13. 9. Rectangular paralelepiped measuring surface and measuring points.

The coordinates of the key measuring points [156]

Serial no.	X	Y	Z
1	a	0	h
2	0	b	h
3	$-a$	0	h
4	0	$-b$	h
5	a	b	c
6	$-a$	b	c
7	$-a$	$-b$	c
8	a	$-b$	c
9	0	0	c

S — measuring surface, H — the rectangular paralelepiped that encloses the machine, 1 to 9 — key measuring points, 10 to 17 — supplementary measuring points, l_1, l_2 and l_3 — dimensions of the rectangular paralelepiped that encloses the machine, d — measuring distance

additional measuring points must be selected in between the main measuring points in order to decrease the finite element error ΔL_1. The accuracy of the sound power level determination can always be improved by increasing the number of measuring points.

(e) Checking the acoustical conditions by measurement. The background noise must be measured at the measuring points in the same frequency range as the measurement under point (f) is to be done. We have to measure the reverberation time in order to be able to determine the value of the correction term K_2 from the known volume and boundary surfaces of the testing room (see eqns (13.24) and (13.25)).

(f) Carrying out the measurement. Quantities to be measured. At the measuring points located point (d), we should measure the A-weighted sound pressure level and, as required, the octave-band or one-third-octave-band in the centre frequency ranges 125 to 8000 Hz and 100 to 10 000 Hz. The algorithm of the subsequent calculations is independent of the band-pass filters used for the measurements. The measured sound pressure level is denoted L_i', where i is the serial number of the measuring point. This level must be corrected by the correction term K_1 that takes care of the background noise [see eqn. (13.21)] at the individual measuring points. The corrected sound pressure level at the ith measuring point is

$$L_i = L_i' - K_1.$$

(g) Evaluation. From eqn. (13.9) we must determine the average sound pressure level $\bar{L}$, then correct it by K_2 to obtain the average sound pressure level L_m characteristic of the measuring surface at a measuring distance of d:

$$L_m = \bar{L} - K_2.$$

The sound power level emitted by the electrical machine is obtained from the average surface sound pressure level corrected by the measuring surface, regardless of the type of band-pass filter used:

$$L_W = L_m + 10 \log \frac{S}{S_0}.$$

The measuring surface S is computed from the eqns (10.39) depending on the shape of the measuring surface:

$$S = 2\pi r^2 \quad \text{for hemispherical surface,}$$

$$S = 4(ab + ac + bc)\frac{a+b+c}{a+b+c+2d} \quad \text{for conform surface,}$$

$$S = 4(ab + ac + bc) \quad \text{for rectangular prism-shaped surface.} \qquad (13.34)$$

Now we can determine the directivity index G and the directivity factor D.

(h) Measurement record. All the information on the machine to be measured and on the circumstances of the measurement, as well as the measured and evaluated noise data should be entered into the measurement record. One of the most important items of data is the A-weighted sound power level L_{WA}, since this parameter serves as a basis for the qualification of the electrical rotating machine as an industrial product.

13.5.2 Measuring the noise of large, immovable machines

In industrial practice of noise measurement, we frequently encounter the difficulty of measuring on large noise sources that cannot be moved. These machines cannot be transported to an acoustic laboratory for the measurements and the classic method of substitution, i.e., the application of a comparative sound source, cannot be used either because of the difference in sizes or the immovability. In such situations, in situ noise measurement must be done, but under such circumstances the acoustic conditions specified in the standard series ISO 3741 through 3746 cannot be satisfied. The answer is found in ISO 3747—this standard substantially expands the circle of noise measuring possibilities by carefully applying the concept of comparative or reference sound sources. It is worthwhile discussing this method in a little more detail, but, of course, only the part that differs from the measuring method described in Section 13.5.1.

The measuring surface should be located around the noise source. The recommended measuring distance is $d=1$ m. Over the measuring surface, n measuring points should be selected. At these points we should measure the background noise levels $L_{l,n}$ with the machine switched off. Then we calculate the average background noise level, $\bar{L}_n$. After the machine has been switched on, the sound pressure level $L'_{i,F}$ is measured at each measuring point.

The values of $L'_{i,F}$ must be corrected in terms of the background noise by an amount that depends on the difference between the average background noise and the individual $L'_{i,F}$ to obtain the values of $L_{i,F}$. Now the reference sound source is to be used, which emits a reference sound power level $L_{W,\,ref}$ (calibrated in an acoustic laboratory), in m operating positions. These operating positions are located along the sides of the motor (side-by-side procedure) or on the top of the motor (superpositional procedure). For each reference source position, we should measure the sound pressure level at each measuring point to obtain the levels $L'_{i,j,\,ref}$ (where i is the subscript indicating the measuring point and j is the subscript indicating the operating position of the reference sound source). Of course, for the time of this measurement the motor is switched off. Each value of $L'_{i\,j,\,ref}$ is to be corrected for background noise, and thus we obtain the values of $L_{l,j,\,ref}$.

The sound pressure levels measured for the different positions of the reference sound source are averaged at each measuring point:

$$L_{i,\,\text{ref}} = 10 \log \frac{1}{m} \sum_{j=1}^{m} 10^{0.1 L_{ij,\,\text{ref}}}. \tag{13.35}$$

Knowing the geometric configuration of the measuring points (i.e., their distance from the operating positions of the reference sound source), we can calculate the values of $L_{i,\,j,\,\text{ref},\,c}$ from $L_{W,\,\text{ref}}$ for each measuring point, then average these values for each measuring point:

$$L_{i,\,\text{ref},\,c} = 10 \log \frac{1}{m} \sum_{j=1}^{m} 10^{0.1 L_{ij,\,\text{ref}\,c}}. \tag{13.36}$$

Now the correction terms that take into account the acoustic conditions must be determined for each measuring point:

$$K_{2i} = L_{i,\,\text{ref}} - L_{i,\,\text{ref},\,c}. \tag{13.37}$$

The average of these correction terms is K_2. Now we are ready to compute the sound pressure level averaged over the measuring surface and corrected for the acoustic environment:

$$\bar{L} = 10 \log \left(\frac{1}{n} \sum_{i=1}^{n} 10^{0.1 L_i} \right) - K_2. \tag{13.38}$$

Finally, corrected for the measuring surface, the sound power level emitted by the motor is found as:

$$L_W = \bar{L} + 10 \log (S/S_0), \tag{13.39}$$

where $S_0 = 1 \ \text{m}^2$.

If the spectral characteristics of the motor noise and the reference sound source noise are similar, the algorithm is directly applicable to the sound pressure levels measured through an A-weighting filter to determine the A-weighted sound power level. If, however, the spectral characteristics are different, the procedure discussed should be applied to the octave-band sound power levels, and the A-weighted sound power level can only be calculated from the octave-band sound power levels at the end, taking into account the A-weighting curve.

13.5.3 Individual noise measurement on mass-produced electrical machines

In accordance with the valid regulations, the manufacturers of electrical machinery determine—mostly by measurements of technical accuracy—the sound pressure level and, on this basis, the noise quality grade of their product, within the frame of the standard type testing. For this standard testing, they do not deem it necessary

to build their own acoustic laboratory, which would be a considerable investment, but rather send their machines outside to be noise-tested. This way, of course, it is not possible to check every machine. Individual noise measurement is not a common practice even in factories which have their own acoustic laboratory, since labora: tory testing cannot be matched to the process flow of the assembly-line type of production. Although individual noise measurement is not specified by the standards as mandatory for mass-produced motors, it would have numerous advantages. First, we could monitor the noise quality of the motors on a continuous basis, issuing a noise quality certificate to each motor that would enhance the confidence in the quality of the product. Secondly, continuous individual noise measurements would reveal the majority of adverse manufacturing deviations including defects that would otherwise be discovered only by the user during operation, leading to premature breakdown.

In fact, noise measurements require the realization of very stringent acoustic conditions, as discussed in this chapter. The accomplishment of vibration measure: ments is much easier. As proved in Chapter 2, there is a rather tight casual rela- tionship between vibration and noise. The classification illustrated in Fig. 2.2 shows that most noise phenomena are preceded by mechanical vibrations measurable on the external surface of the machine, so in the case of machines where vibration: induced noises prevail (most noises of electromagnetic or mechanical origin), the connection between vibration and noise is very close.

Summing up the physical processes reviewed in Chapters 1 and 5, we may deduce that the relationship between the vibration of the electrical rotating machine and the sound energy due to the radiation of vibrational energy can be described by a system function $\bar{\mathbf{H}}^*$. Mathematically, this means a matrix equation:

$$\bar{\mathbf{P}} = \varrho c \bar{\mathbf{H}}^* \mathbf{v}^2, \tag{13.40}$$

where the elements of the column vector $\bar{\mathbf{P}}$ are the sound power components characterized by their frequency and magnitude, the elements of $\bar{\mathbf{v}}^2$ are the vibra: tion velocity squares proportional to the vibrational energy components character- ized by their vibrational mode number and magnitude, and $\bar{\mathbf{H}}^*$ comprises the acoustic energy conversion efficiency elements which depend on the mode number, frequency and the shape and dimensions of the machine. (ϱ is the density of air, c is the speed of sound in air.) Any element of $\bar{\mathbf{H}}^*$ is found as:

$$\mathbf{H}_j^* = \sigma_{r_j, f_{rj}} S_m, \tag{13.41}$$

where $\sigma_{r_j, f_{rj}, D}$ — the radiation factor for a given characteristic machine size D, vibration mode number R and vibration frequency f_r,

S_m — the radiating surface of the machine.

The elements H_j^* of the system function are unique and constant for a given machine type size unless the design changes. Using the usual reference values:

$$P_0 = \varrho_0 c_0 S_0 v_0^2 10^{-12}, \tag{13.42}$$

where $P_0 = 10^{-12}$ W, $\varrho_0 = 1$ kg m^{-3}, $c_0 = 1$ m s^{-1}, $S_0 = 1$ m^2, $v_0 = 1$ m s^{-1}, then dividing eqn. (13.40) by eqn. (13.42) and introducing the usual levels, the sound power level emitted by the electrical machine is given by:

$$L_W = \bar{L}_v + 10 \log \frac{\overline{H^*}}{S_0} + 146, \tag{13.43}$$

where

$$\bar{L}_v = 10 \log \frac{1}{n} \sum_{i=1}^{n} \frac{v_i^2}{v_0^2},$$

and n is the number of vibration measuring points and $\bar{H}^*$ is the average value of the system function. Considering that the theoretical determination of the radiation factor contained in $\bar{H}^*$, and of the radiating surface is difficult owing to the complicated shape of the machine and its being a complex sound source, it is practical to define the radiation parameter of the machine as:

$$R_s = 10 \log (\overline{H^*}/S_0). \tag{13.44}$$

This parameter can be determined during a standard type measurement in the acoustic laboratory by measuring the vibration velocity and the sound power level through the same filter. Knowing R_s and applying eqn. (13.43), for the future it is enough to measure only the mechanical vibrations on the machine surface. This measurement is easy, quick and cheap, and does not require an acoustic laboratory to be built in every machine works. Also, it conveniently fits into the manufacturing process and allows individual noise measurement.

The method discussed is suitable for the noise testing of synchronous or asynchronous machines with four or more poles, and also for the determination of the A-weighted sound power level.

13.5.4 Noise qualification of electrical rotating machines as per IEC Publication 34–9

The basis for noise qualification is the characteristic A-weighted sound power level L_{WA}, which can be determined by measurement as discussed in Section 13.5.1. Based on their L_{WA}-value, the electrical rotating machines can be classified in five quality grades, numbered from 0 to 4. According to IEC Publication 34-9, the A-weighted sound power level of Class 1 machines with IP 44 protection must not

exceed the value specified in Table 13.1. The maximum permissible A-weighted sound power levels of Class 2, 3 and 4 machines are at least 5, 10 or 15 dB lower than the value permitted for Class 1 machines, respectively. In the case of Class 0 machines, the permissible value of L_{WA} is higher than those shown in Table 13.1. A similar table can be found for machines with IP 22 protection in the standard.

Table 13.1. The permissible A-weighted sound power level of Class 1 machines of IP 44 protection (as per IEC 34–9)

Rated output, kW (kVA)	L_{WA}, dB					
	Rated speed, s^{-1}					
	to 16	from 16 to 22	from 22 to 31.66	from 31.66 to 39.33	from 39.33 to 52.5	from 52.5 to 62.5
Up to 1.1	71	74	78	81	84	88
From 1.1 to 2.2	74	78	82	85	88	91
From 2.2 to 5.5	78	82	86	90	93	95
From 5.5 to 11	82	85	90	93	97	98
From 11 to 22	86	88	94	97	100	100
From 22 to 37	90	91	98	100	102	102
From 37 to 55	93	94	100	102	104	104
From 55 to 110	96	98	103	104	106	106
From 110 to 220	99	102	106	107	109	110
From 220 to 630	102	105	108	109	111	113
From 630 to 1100	105	108	111	111	112	116
From 1100 to 2500	107	110	113	113	113	118
From 2500 to 6300	109	112	115	115	115	120

The values published in ST CEV 1348 (see Appendix (A 1.1)), are basically similar to those specified by IEC 34-9.

As we see, the permissible A-weighted sound power level increases with increasing power. If we happen to compare the maximum permissible values specified by the standards with the noise characteristics of the standard series machines made by leading manufacturers and available in the world market, we find that the noise quality of standard series machines of low power and low speed is about Class 3, which means that the standard for small machines is rather lax. As we approach higher powers, the gap between the world standard and permissible values closes up. In the case of rotating machines with power about 100 kW, even products of leading manufacturers hardly meet the standards specified for Class 1. In this power range, we have to struggle hard for each dB of noise reduction. Manufacturers who supply machines with noise quality higher than the international standard may charge extra for the quality. In many cases, where this

quality is required for a given motor application, even this high cost is acceptable to the customer just to obtain the right quality. The various laws and regulations of environmental protection also tend to back this tendency.

13.6 Noise measurement of asynchronous motors under load

The conditions of noise testing can generally be classified in two groups. The first group includes those general conditions that must be guaranteed in any noise measurement:

— The noise measurement should be carried out in the far field of the sound source, where the sound pressure and the velocity are in phase.

— The noise measurement should be done in free acoustic field where no reflected waves coming from nearby reflecting surfaces are present. Figure 1.7 shows a typical example of how the sound pressure level varies with distance d from the sound source. As the above conditions are generally met at a measuring distance of $d=1$ m, the noise measurements are normally carried out at that measuring distance:

— The sound pressure level caused by other sound sources, i.e., the background noise, should be much lower than the sound pressure level of the machine to be tested. If the difference exceeds 10 dB, the effect of background noise on the accuracy of the noise measurement is negligible.

— The noise measurement is aimed at the determination of the airborne sound power level emitted by the motor, and consequently we have to avoid the generation of structure-borne noise by the electrical motor tested.

The above general conditions can be generally met in no-load noise measurements. However, human protection against noise pollution requires the vibro-acoustic behaviour of machines under operating conditions to be tested, since during routine work, personnel are close to loaded machines. The specifications and standards relevant to the qualification noise measurements of electrical motors accept the determination of the airborne sound power on the basis of no-load measurements, but only on an undefined condition that the no-load noise level does not differ substantially from the level under load. But how should we know in advance if we have not measured both levels? This uncertainty of the noise measuring procedures results from the fact that the earlier theoretical works did not clarify properly enough the sense and amount of change caused by loading in the noise of asynchronous motors in comparison with the no-load noise level.

In order to be clear in advance if the no-load noise measurement is sufficient, without the need to carry out the noise measurement under load, we must add the

measurement of airborne sound power by origin (in the frequency-bands used in the no-load measurement) to the standard type no-load noise measurement (by which the sound power level $L'_{W,0}$ can be determined).

This is done in two steps in practice. First we separate the airborne sound power $L_{W,v}$ of the ventilation system by reducing the volume of the forced external cooling air to zero (then we measure L'_W). By gradually decreasing the supply voltage, we must plot the curve of L'_W versus U_{mains}. Extrapolating this curve to zero voltage, we can separate the sound power levels of mechanical and electromagnetic origin $L_{W,m}$ and $L_{W,em}$, respectively. If the relation

$$10 \log (10^{0.1 L_{W,m}} + 10^{0.1 L_{W,v}}) - L_{W,em} > 8 \quad \text{dB} \tag{13.45}$$

holds, then the result of the no-load noise measurement may be accepted as characteristic of the motor and the noise qualification must be done on this basis. If, however, the above inequality does not hold, then noise measurement under load must be performed as well. When we want to measure the noise of loaded asynchronous motors, we have to face two immense difficulties.

The first is airborne noise produced by the loading machine, with magnitude of the order of the sound pressure level of the tested motor, which must be considered as background noise. In order to distinguish this background noise, which is an integral part of the noise measurement from the background noise of other origin that may be turned off or eliminated, the former, produced by the loading machine, is called internal, and the latter external background noise.

As mentioned before, the sound pressure level of the loading machine is sensed by a microphone placed at a distance $d=1$ m from the asynchronous machine tested, as for the sound pressure level of the machine tested. The separation of these two levels is not usually possible, either on the basis of magnitude, or on the basis of frequency composition.

The second problem is that the loading machine is connected by a clutch mechanism to the asynchronous motor, and these two machines are mounted on a platform. As we have seen, this is another source of error. There are several methods of separating the sound pressure level of the loading machine.

(a) The loading machine is placed in an acoustically separate air space. In this case only the electrical motor to be tested is in the noise testing room (acoustic laboratory, anechoic chamber), and the loading engine is located in another room. The air spaces of the two machines are separated by a wall of good sound-isolating characteristics, through which the drive shaft is led in an acoustically sealed manner. Structure-borne noise coming in through the shaft does not normally give rise to considerable airborne noise, for the flexible couplings installed because of the length of the shaft substantially damp structure-borne noise. In

this case, it is possible to measure the noise of the electrical machine under load directly, and to determine the sound power level emitted under load, also directly.

(b) The noise of the loading machine may be separated in such a way that the loading machine is covered with a sound-isolating enclosure. Of course, the shaft going through the enclosure wall must be carefully sealed acoustically. A well designed sound-isolating enclosure may reduce the sound pressure level produced by the loading machine by 10 to 20 dB, locating it far away from the sound pressure level of the machine to be tested. However, the enclosure may give rise to cooling problems for the loading machine. This solution also allows direct noise measurement under load.

(c) The procedure described in Section 13.5.4 is also suitable for the measurement of noise changes due to loading, mostly of electromagnetic origin, since noise changes of electromagnetic origin always accompany changes in vibration.

(d) The solutions discussed above reduced the effect of background noise level in the sound field around the microphone in such a way that they reduced the background noise level itself to get far from the sound pressure level to be measured. However, the difference between the two levels can also be increased by increasing the sound pressure level of the motor at the microphone. This can be achieved by reducing the measuring distance d. This, however, can take us to the acoustic near field of the sound radiating machine, increasing the near field error. Thus a near field measurement could be suitable for the direct determination of the sound power level under load owing to the relative reduction of background noise level, but, in turn, it gives rise to a considerable error of different magnitude for each component, depending on the mode number, frequency and measuring distance.

(e) If the implementation of the perfect solution described in point (a) is not possible or there are problems with the application of the method outlined under point (b), then we have to carry out the measurement in the near field, but we must make an effort to reduce the measuring error due to the near field. This can be done in the following way. We determine the sound power level under load in two steps. First we measure the sound power level of the idling asynchronous motor under adequate acoustic conditions in the free acoustic field and determine the no-load radiated sound power level $L_{W, 0}$. Then we couple the motor and the loading machine together and measure the sound pressure level $L''_{p, 0}$ in the near field, with the loading machine unexcited. Now, by the proper excitation of the loading machine, we set the rated load of the asynchronous machine and measure the average value of the sound pressure level $L''_{p, l}$ at the same measuring point in the near field. From the two latter values, we obtain the loading correction term, ΔL_l:

$$\Delta L_l = L''_{p, l} - \bar{L}''_{p, 0}. \tag{13.46}$$

Adding this term to $L_{W,0}$, we get the sound power level radiated under load:

$$L_{W,l} = L_{W,0} + \Delta L_l, \qquad (13.47)$$

since the subtraction of eqn. (13.46) eliminates the near field error mentioned under point (d). At $\Delta L_l < 1$, $L_{W,0}$ should be accepted as characteristic acoustic parameter of the machine, while in the case of $\Delta L_l \geq 1$, $L_{W,l}$ should be used to determine the noise quality grade of the machine.

13.7 Special regulations on transformer noise measurements

As in the case of rotating machines earlier, the determination of the A-weighted sound pressure level was set as an aim of transformer noise measurements. More recent international standards, however, changed here as well to the determination of the A-weighted power level. In the following, the measuring procedures are discussed mostly according to IEC 551. The steps of A-weighted power level determination are the same as for rotating machines. We must measure the sound pressure level at the measuring points over a measuring surface enclosing the transformer. These levels are averaged and corrected for background noise and for the acoustic properties of the environment, then ten times the logarithm of the measuring surface area is added to obtain the required result. So why and how is noise measurement of transformers different from that of rotating machines?

There is no difference in the measurement of low-power transformers, but the weight, size, electrical power and supply requirement of high-power transformers do not normally allow the transformer to be moved to a special acoustic environment for noise measurement. We might use the solution described in Section 13.5.2, but experts involved in transformer noise problems prefer the acoustic near field using a microphone, being aware of the increased uncertainty of the measurement. The relevant standards specify a measuring distance of 0.3 m. To reduce the near field error, the number of measuring points must be increased. If the transformer is equipped with a forced draught cooling system, then the measuring distance should be 2 m because of the high air flow rate. This, of course, brings out the consequence that the discussed formulae cannot be used for the calculation of the measuring surface. The following empirical expressions should be used for the determination of the measuring surface:

For a measuring distance of 0.3 m:

$$S = 1.25 l_3 l_m. \qquad (13.48a)$$

For a measuring distance of 2 m:

$$S=\frac{3}{4\pi}\,l_m^2. \tag{13.48b}$$

where l_3 — the height of the enclosing prism of the transformer,
l_m — the length of the measuring line consisting of the measuring points.

Now we shall discuss in a little more detail how the measuring surface and the measuring points are selected for noise testing of large transformers. Here we must differentiate between the measurements of self-cooled and forced-draught transformers.

Self-cooling means that only gravity flow is used for cooling. In this case the sound radiating surface is identical with the surface of the transformer tank. The upper limit is the top plate of the transformer tank, the lower limit is the bottom plate of the casing, while the side plates are the sides of the tank or the enveloping surfaces fitted to any element rigidly fixed to them, that takes an active part in the radiation process. From the point of view of noise radiation, we may ignore the bushings, the oil reservoir and the skid and caster system under the baseplate of the transformer tank. The measuring line runs at a distance of 0.3 m from the transformer tank, its height is $l_3/2$, provided that $l_3 \leqq 2.5\,\text{m}$. When $l_3 > 2.5\,\text{m}$, then two measuring lines should be used at heights of $l_3/3$ and $2l_3/3$. Each measuring line should comprise at least six equispaced measuring points. The space between two adjacent measuring points is a maximum of 1 m.

Transformers equipped with forced draught cooling are classified in two groups depending on the location of the cooling system. When the cooling system is directly mounted on the transformer or is set up at a distance of less than 3 m from the transformer, then they are considered to be a single radiating unit. The radiating surface is considered as a rectangular prism enveloping the transformer and the cooling system together. This prism is surrounded by the measuring surface at a measuring distance of 0.3 m when the cooling system is not running and at a distance of 2 m when it is running (the transformer, of course, is excited in both cases). The number of measuring lines and measuring points should be selected just as we did in the case of self-cooled transformer measurement.

If the forced draught cooling system is set up at a distance of more than 3 m from the transformer, then it is handled as a separate sound source (it can normally be operated independently of the transformer). First, the transformer noise is measured at a distance of 0.3 m as if it were a self-cooled type, with the cooling system turned off, and then the transformer is switched off and the noise of the cooling system is measured in operation at a measuring distance of 2 m. If the height of the cooling system, l_3, is not over 4 m, then only one measuring line is taken at half height, otherwise two, at one third and two third of the height are

used. At any point in the surroundings of the transformer, the expected value of sound power level in normal operation is the resultant of the sound pressure levels emitted by the two noise sources.

The transformer is frequently the only fixed noise source of a residential area and therefore it is frequently of interest to predetermine the sound pressure level at a considerable distance from it. As discussed in Chapter 1, the sound pressure level at an observation point at a distance R from the noise source is found to be:

$$L_{(R)} = L_W - 20 \log \frac{R}{R_0} - 8, \tag{13.49}$$

where L_W — the sound power level of the transformer and $R_0 = 1$ m.
This expression, however, gives a correct result only if:

— The experimentally determined value of the transformer sound power level L_W does not contain any substantial error,
— the propagation of sound in the space is uniform,
— the transformer is the only noise source in the vicinity of the observation point.

Numerous publications deal with the question of why the experimentally determined sound pressure levels at a distance of R differ from the values obtained from eqn. (13.49). The reasons for this difference are the following:

— The accuracy of the experimental determination of the transformer sound power level is adversely affected by the near field error.
— The sound propagation in the space is not uniform because of buildings, landmarks, etc.—which may serve as reflecting surfaces—hinder the building-up of a uniform propagation pattern.
— The strength and direction of wind which is always present in an open space influence the propagation of sound.
— The damping effect of air varies for noise components of different frequency, and therefore it can alter the character of the noise spectrum.
— At the observation point the magnitude and spectral composition of the background noise may be different from that at the time of the transformer measurement, so it may occur that it conceals the sound pressure level produced by the transformer in a certain part of the audible range.
As we see, the arguments are abundant to explain why the results of a noise measurement conducted, say, in an apartment house 100 m away from the transformer differ from the results calculated from eqn. (13.49). This underlines the importance of the fact that the consideration of the local acoustic conditions is essential in any noise testing activity.

14. MEASUREMENT OF THE TRANSIENT NOISE PHENOMENA

14.1 The concept of fast-changing short-duration noise phenomena

The definition used in practice is that steady noise occurs where the maximum change in sound pressure level during the testing time is below 5 dB. If the magnitude of change is higher than 5 dB, we talk about variable noise. It is usual to classify the variable noises as follows:

— irregular noises, where the level changes are random and irregular in time,
— fluctuating noises, where the changes exhibit certain regularity,
— intermittent noises, where we have two or more clearly defined levels at which the noise can be considered steady.

The bursts of noise (impulsive noise) and the transient noise belong to the category of short-duration sound phenomena.

The two most important short-duration sound phenomena are the shock wave and the transient noise. A shock wave is produced when an extremely fast pressure change takes place at a point in space. This pressure change passes on in all directions, and this propagating shock wave is characterized by a very steep leading edge and a gentle trailing edge. The sudden change in pressure at the point of generation may be caused by an explosion, an electric spark, etc.

A sound impulse is a sound phenomenon that takes place in a very short time. The time limit under which the sound phenomenon may be considered to be an impulse or burst can be defined in various ways. The most straightforward definition is based on the characteristics of human hearing. As is well known, signals having a time separation below 30 to 35 ms become indistinct to the human ear, so signals with such short duration are heard as a single click. However, other definitions are also possible.

The transient noise is normally generated by applying a very short impulse or step function excitation to a dissipative system capable of vibrating. In practice, this is the case when a load is applied abruptly to an electrical motor. Of course, we could continue with other examples. If the decay time of the signal is shorter than the mentioned 30 to 35 ms, then the transient noise may be considered as impulsive or as burst of noise.

Purely transient noise is very rarely found in practice. The noise generally starts with a high-amplitude pulse and continues with a mixed decay involving several transients. In the case of bodies of poor vibrating ability of high damping, the transient part may not even appear. It can happen that the noise phenomenon includes several reflected signals following the first impulse. The problem of short-duration noise phenomena is incredibly complex, but three aspects are worth mentioning. One is the accoustic aspect. From an acoustic point of view, the phenomenon can be single, like for example a shock wave, characterized by an unambiguous length of time, but also periodic or quasi-periodic. Such phenomena are characterized by an absolute length of time during which they take place, but from an acoustic point of view a more important parameter is damping, that is, the ratio of the decay time to the cycle time. The value of this ratio determines if the transient noise is called fast-damping or slow-damping. The slower the damping of a vibration, the more applicable are the concepts and measuring procedures relevant to steady-state signals.

The other basic aspect, hearing, was mentioned before. Here we will just point out that owing to the time limit set by human hearing, slowly decaying transient noise may be heard as a pulse, while fast decaying noise appears as a complex musical sound. The total decay time of an ultrahigh-frequency damped noise can be shorter than 30 ms even though the rate of damping is quite slow. Conversely, the decay time of a fast-damping 100 Hz signal is certainly longer than 30 to 35 ms.

The third basic aspect is the measuring technique. In principle, the steady-state and non-steady-state signals must be analysed with completely different methods. Even concepts specially constructed for steady-state signals (e.g., amplitude, frequency, spectral power distribution, etc.) do not apply directly to non-steady-state signals. The usual practice, however, is to reduce the measurement of pulse signals to the measuring methods of steady-state signals. These problems will be discussed in depth in the next chapter. Here we will just deal with the following. In a given concrete case, the available instruments predetermine a boundary between the steady-state and non-steady-state sound phenomena. As a matter of fact, any transducer or instrument has its own characteristic time constant. From the point of view of the measuring system, a phenomenon is steady-state if the measuring system can follow it closely without problem. Of course, the transducers and instruments can be selected so that they can follow even the fastest changing acoustic pulse, since it is only a question of dynamic range and upper cut-off frequency. Care must be taken, however, for a measuring system set up carelessly may invalidate the results.

Thus, the determination of short-duration sound phenomena is not straightforward and clear-cut. In spite of the problems mentioned, the question should be approached from the aspect of human hearing, since in practice the impairing and

disturbing effects of noise bursts on human hearing are of interest in the majority of cases. The measuring methods should be selected to ensure the correlation between the obtained results and the sensation of our ears.

14.2 Characteristics of fast-changing short-duration noise phenomena

Sound impulses may be characterized by various quantities, depending on their type. For example, shock waves are best described by their peak amplitude and signal duration. This latter is defined as illustrated in Fig. 14.1, but sometimes the difference in time values that correspond to the 10 percent amplitude (-20 dB) is used for this purpose. The rise time is also specified. Further characteristics of the shock wave are the turnover amplitude and the integral of the square of the signal, that is, the energy of the signal.
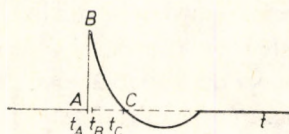
Fig. 14. 1. Characteristic parameters of a shock wave: B — peak value, $t_B - t_A$ — rise time, $t_C - t_A$ — duration (length)
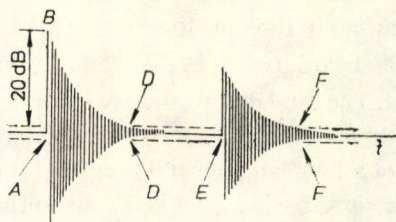
Fig. 14.2. Characteristic parameters of transients: B — peak value, $t_D - t_A$ — effective length. When two transients occur within the measuring time, their length is given by

$$(t_D - t_A) + (t_F - t_E)$$

Transient noises are not so easy to characterize. A periodic phenomenon may be described by its frequency, and the quantities introduced for shock waves can be defined for the envelope curve of the signal. In most cases, however, the transient process is extremely complex, the periodicity cannot be recognized and it can even occur that the envelope is not of a purely decaying nature. The usual definitions are illustrated in Fig. 14.2. The integral of the squared signal is used for transient signals as well, and it is usual practice to determine the spectrum or the spectral energy distribution of the signal. We may say, in general, that the characteristic quantities of pulse-type sound phenomena are connected partly with the envelope curve of the time function, partly with the spectrum of the signal. We must be careful though, since in most cases the signal is not symmetrical about the zero line, so the positive and negative envelope curves are not identical, and, also, the

spectrum of the signal is not completely clear-cut, so we must treat the calculating and measuring procedure with care.

In the course of research, various "nuisance parameters" may be defined. The analysis should start on the most unpleasant transient noises known. Examples are the pneumatic hammer and poorly damped exhaust noise, just to mention a few. It is worthwhile expanding investigations on the effects of transient noise in open and closed acoustic fields. In such cases, the values obtained from cross correlation are also of importance among the parameters.

The number of the many parameters that characterize transient noise should be practically reduced in a given test, otherwise the test becomes chaotic and confused. This reduction of the quantity of parameters is especially important in direct measurements. We must introduce equivalent parameters that correspond to identical effects. The length of pulses and the transient time durations must be described by characteristic time durations.

14.3 General considerations of transient noise measurement

It is worth investigating again what problems arise when we try to find the answers to the standard three questions, namely, what, how and by what means to measure in relation to transient noise. The practical measuring technique of transient noises is not completely developed yet, but is a field of research, so giving a clear-cut answer to these questions is very hard.

The basic consideration in any technology is the human being, and so the main task in the first group of questions is to identify the harmful transient noise parameters, to determine their quantitative and qualitative nature, and, finally, to eliminate them. It is not quite clear today which are the harmful properties of the transient noise in terms of physiology and psychology. This research is hindered by the lack of even the very basic tools of the second, "by what means" group of questions. Without the clarification of the "what" questions we could not have any progress in the field of measuring procedures that belong to the "how" group of questions. Lacking the measuring tools and procedures, we cannot identify the harmful characteristics of the transient noise, that is, what should be measured. The methods and tools, in turn, can be worked out only on the basis of what we want to measure.

The answer to the question of "what to measure" can be given only with the knowledge of the objectives of the measurement. As the number of measurable physical parameters is very high, it is reasonable to separate the measurements aimed at the harmful effects of transient noises completely from those trying to figure out the properties of the source from the characteristics of the transient

signal. In the former case, the measuring system should model the properties of the human organ of hearing, the applied time constants, rise times, dynamic ranges and cut-off frequencies should correspond to the same characteristic data of the organ of hearing. When assessing loudness, human beings integrate the signal with a time constant of about 35 ms. The measurement done with a standardized impulse time constant is therefore related to loudness. The harmfulness of a transient signal, however, is dependent on the peak value—not the peak value of the acoustic signal, but the peak value of the signal induced by it in the inner ear, which, in turn, is a function of the transient transfer characteristics of the ear-drum and the inner ear.

We must see clearly that an instrument which takes the aspects of human hearing into account is necessarily too slow to follow the transient signal closely. The measuring amplifiers classified as slow for the measurement of transient signals are not so because the manufacturer concerned cannot make a faster one, but because the design is based primarily on aspects of human hearing.

The acoustical diagnostics, which have received wider and wider application recently, necessarily demand that the original characteristics of the signal must not get distorted in the measuring system. It is increasingly clear that the measuring tools and instruments required for diagnostic purposes differ from those for assessing loudness or harmfulness. We encounter numerous measuring tasks, especially in the field of short-duration signal measurement, which cannot be accomplished by means of the standard acoustical instrument pool, or else the error is unacceptably high. The only possible solution is total separation of the two fields.

Another problem source is the fact that the tools used for the transformation, shaping, transfer and recording of acoustic signals should have quite different parameters from those used for steady-state signals. At present, we do not have these tools at our disposal and we cannot even expect the appearance of transducers, microphones and electronic units that would be equally suitable for the analysis of steady-state and transient signals. It seems more practical to separate the two fields concerning both microphones and electronics.

Further problem arises owing to the fact that the concepts used in describing the characteristics of a signal are very strongly related to steady-state or even sinusoidal signals, and therefore their application to other signal types presents difficulties. The concept of filters, for example, is distinctly connected to sinusoidal signals. It is very easy to tell what happens to a steady-state signal comprising sinusoidal components when it passes through a filter, but, in contrast, it is very hard to do the same for a short pulse or a transient signal.

It is a frequent fault that an originally mathematical concept is used outside its justified scope of validity, as in the case of fast Fourier transformation (FFT) for steady-state signals. This and numerous other examples indicate a far more general

problem which is becoming more and more important with the development of technology.

To answer the question of "by what means to measure" is at least as hard as the answer to the other questions, partly because in most cases more than one measuring system may be used for the same measuring function, and partly because the engineer is always forced to compromise in solving real measuring tasks. On one scale of the balance, there is the measuring system designed to match the given task, while on the other scale there are the available instruments and the investment budget. To reach a balance of the two sides normally requires serious engineering consideration.

For measuring transient noise phenomena, analogue and digital measuring instruments, memories and even computers are all equally used.

14.4 Measuring systems

In a wider sense, the functional units of the measuring system are generally the following: measuring network, system controller, algorithm (preparations for the measurement, selecting the required instruments, working out the measuring procedure, etc.) and data processor. As we see, man plays an important role in such a measuring system, especially in relation to the algorithm. In a narrow sense, more common in everyday use, a measuring system is a set of tools, comprising data supplying instruments, value generating instruments, display units, signal generators, signal sources, controllers and auxiliary elements, this set serving the purpose of a concrete, well defined measuring function.

The measuring system and the object of testing may be connected with the lines of action of sensing, stimulus, reference input and control loop. Through the stimulus-reference signal-control connection, the measuring system influences the object of testing. These may not be present in the individual cases, but the sensing element is an essential part of any measuring system.

The measuring system design may be modular or integrated. The modular measuring system is made up from separate units which are suitable for a specific but general measuring function, i.e., these component units can be used independently for certain measuring tasks and can be put together in various configurations or combinations. The integrated measuring system, in turn, is a single-purpose instrument tailored to a concrete measuring function. The data-supplying instrument (sensing element), in the field of acoustics, means microphones and accelerometers (together with their accessories). These units produce the signals for the other elements of the system in a form that allows the separation of the

information on the magnitude of the measured quantity in a way that can be processed.

The characteristic numerical values are produced in the value generating components of the instruments (r.m.s. circuit, averaging circuit, etc.). The numerical value of the measured quantity is displayed by the data display of the instrument or the measuring system, i.e., indicating instrument, level recorder, X-Y recorder, for the user, or output in an intelligible form for the connected system component.

The data may be displayed in analogue (dial instrument, curve register), or digital (digital display, printer) form.

14.4.1 Analogue measuring systems

Analogue measuring systems are normally of a "daisy-chain" configuration, which, in the case of complex measurements may be closed through the object of testing. The elements of the chain are generally distinct units and their operation may be followed by eye (following the routing of the signal cables). For a closed loop or chain, a good example is provided by the determination of the frequency-dependent noise damping of a wall, which involves all the basic elements of a measuring system. Normally the question arises of how the analogue measuring system should be controlled. Selecting from several possible solutions, the Brüel and Kjaer Co., famous for their system-oriented instrument pools, solved the problem by assigning the control function to the level recorder, the last link in the logical process flow of most measuring systems. The results recorded on a pre-printed chart paper can be correct to the time or frequency scale only if the operation of the recorder mechanism is synchronized with the mechanical operation of analysers, filters, generators, etc. The mechanical control is acceptable only for rather slow operating speed and simple (i.e., direct) control configuration.

14.4.2 Digital measuring systems

As a result of the rapid development of electronics and the general requirement for high-accuracy measurements, more and faster measurements had to be and could be coordinated and accomplished. In other words, an interexcitation of requirements and possibilities took place. The digitally controlled measuring systems can be reduced to a common basic scheme, although the requirements of concrete applications may differ considerably. In this field are microprocessors of immense importance, which enhance the intelligence of measuring systems and advance the development of distributed measuring networks. "Machine-centric" measuring

systems are replaced by distributed control and hierarchic structure. One of the manifestations of the new system is the fact that certain components of the measuring system can carry out certain tasks quickly and independently, while they receive instructions for starting, analysing, reading or passing on the obtained results for further processing to other components from the system controller. While one of the instruments is working on a task, the system controller communicates with the other instruments, so the components of the system operate virtually simultaneously which highly increases the speed of accomplishing complex measuring tasks. The controller of digital systems, with limited functions, may be a component of the system, especially prepared for this purpose, nevertheless for the complex control of many instruments microprocessors are used (8 to 12 instruments can be controlled this way), which, being computers, accomplish the necessary mathematical operations as well. As we shall see in the discussion of concrete cases, the advance of digital technology in the field of transient vibro-acoustic signal processing has opened up new possibilities regarding the difficulties of processing, the amount of data taken into account, and the accuracy and presentation of the results obtained.

14.5 Problems related to the dynamic characteristics of the individual measuring system components

Several basic requirements can be established for the components of vibroacoustic measuring systems. The fulfillment of these requirements is necessary in all cases in order to ensure that the measuring system operation is up to expectation. Let us consider these requirements individually.

(a) The sensing element of the measuring system should produce an electrical signal proportional to the amount of sound or vibration applied to its input. The electrical signal should follow in time identically the time-variations of the vibro-acoustic signal.

(b) The signal shaping circuits of the measuring system should not alter the time changes of the electrical input signal. The amplitude ratio between different sections of the signal must not change even if the amplitude changes.

(c) The processing system should be capable of measuring those characteristics of any signal within the specified limits, whose determination is the objective of the evaluation process.

These requirements, of course, can be met only between certain limits and with certain accuracy. In the case of steady-state signals, the requirements outlined under (a) and (b) are automatically satisfied provided that the amplitude charac-

teristics of the applied transducers and electronic circuits are linear, and the slope of the characteristics (i.e., the sensitivity of the transducer, the gain of the amplifier, etc.) is independent of the frequency. If we specify the amplitude and frequency limits between which the linearity is guaranted with a given accuracy, then we also specify the range where the requirements of (a) and (b) are satisfied.

The fulfillment of requirement (c) must be checked within the above range. We may have different cases depending on what parameter the given measuring system measures. If we are dealing with, say, a root mean square detector, then the time constant should match the lower cut-off frequency and the dynamic range of the detector should be sufficient to sense the dynamic changes of the signals to be measured. In conclusion, we can say that as far as the requirements listed under (a), (b) and (c) are concerned, the most important thing is to ensure the linear amplitude and frequency transfer for all the components of the measuring system, when steady-state signals are measured.

When transient signals are to be measured, however, the amplitude and frequency linearity is no longer enough to satisfy requirements (a), (b) and (c). Other important parameters come into play, such as the group transit time, which is the derivate of the phase shift of the tested measuring system or circuit with respect to the angular frequency:

$$\tau = \frac{d\varphi}{d\omega}.$$

If the group transit time varies with frequency, it takes the various spectral components of the transient signal different times to pass through the measuring system.

This results in changes in length, envelope curve and spectrum of the transient signal.

When transient signals are measured, not only is the amplitude linearity important but also the slew rate of the measuring system. If a unit step function of height U is applied to the input of the system, the steady state of the output signal will be reached only after a time T. The slew rate of the system is defined as U/T. This ratio must be much higher than the slew rate of the signals to be measured, otherwise the measuring system cannot follow the changes of the signal. A good approximation of the slew rate of the measuring system is the ratio of the upper dynamic limit to the transit time. The higher the upper dynamic limit and the smaller the transit time, the higher the slew rate of the system will be.

Before we start discussing the complicated questions of transient signal analysis, let us review how the standard vibroacoustic transducers and measuring tools comply with the requirements for group transit time and slew rate.

14.5.1 The transient characteristics of vibroacoustic transducers

We can model the transient characteristics of vibroacoustic transducers quite well by considering the transducer as a simple resonant system. This notion is equally well applicable to electrostatic microphones and accelerometers, the only difference being that the electrostatic microphones are strongly damped, while the accelerometers are weakly damped systems. Let us see what the transit time characteristic of a damped vibrating system looks like. The amplitude transfer function of an attenuated oscillatory circuit is:

$$A = \frac{1}{\left[(1-\Omega^2)^2 + \dfrac{\Omega^2}{Q^2}\right]^{1/2}}, \tag{14.1}$$

where $\Omega = \dfrac{\omega}{\omega_0}$ is the frequency variable, normalized to 1 at the resonant frequency, and Q is the Q-factor (quality factor) of the system. The phase-frequency characteristic of the oscillating system is given by the function:

$$\varphi = \tan^{-1}\left(\frac{1}{Q}\frac{\Omega}{1-\Omega^2}\right). \tag{14.2}$$

From the point of view of transient transfer characteristics, the most important feature of the system is the group transit time:

$$\tau = \frac{d\varphi}{d\omega} = \frac{1}{\omega_0 Q} \frac{1+\Omega^2}{(1-\Omega^2)^2 + \dfrac{\Omega^2}{Q^2}} = \tau_0 B, \tag{14.3}$$

where

$$\tau_0 = \frac{1}{\omega_0 Q} \quad \text{and} \quad B = \frac{1+\Omega^2}{(1-\Omega^2)^2 + \dfrac{\Omega^2}{Q^2}}.$$

For good transient transfer, the transit time must be constant with respect to frequency, otherwise the sound pulse, which can be considered as a wave packet, will spread out while passing through the system.

In order to analyse the transit time characteristics, the amplitude and transit time curves of an oscillatory system with a resonance frequency of 10 kHz are illustrated in Figs (14.3) and (14.4) for various Q factors. It is apparent that the change in transit time is faster than that of the amplitude, and the initial (low-frequency) value of the transit time is smaller with higher system Q.

Now let us calculate for any Q the frequencies that correspond to a 10 percent change of transit time. Substituting $B=1.1$ and $B=0.9$ into eqn. (14.3), we readily obtain the required frequencies. The results prevail that for typical values of

Q the transit time curve may be considered linear in the frequency range up to one-third or one-fifth of the original resonant frequency.
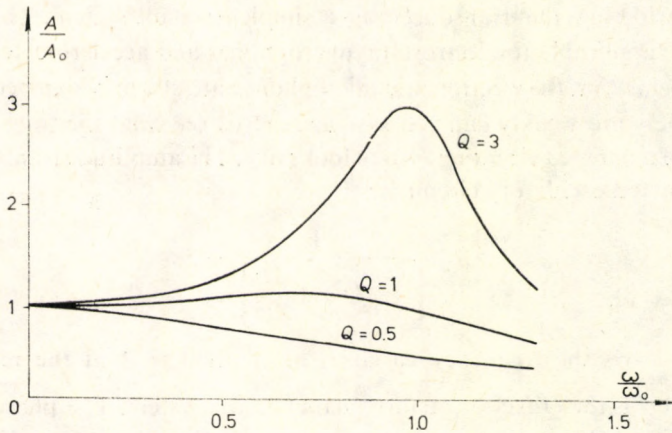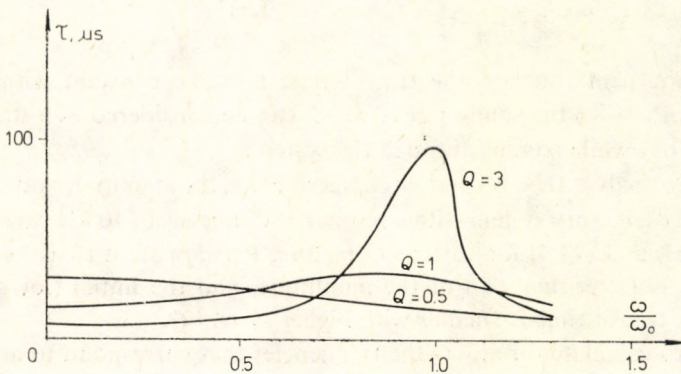

Fig. 14.3. The amplitude characteristics of a microphone with resonant frequency $f_0 = 10$ kHz for various values of Q

In the case of electrostatic microphones with small Q factor, the upper cut-off frequency is considered to be one-third of the resonant frequency, while in the case of acceleration sensors with high Q factor, it is one-fifth of the resonant frequency, for transient signals. For electrostatic microphones, the resonant frequency is rather low, and falls within the operating range specified by the manufacturer. In the case of a 1/2″ outdoor microphon, for example, the resonant frequency is about 12 kHz, but the amplitude transfer is linear up to 18 kHz. According

Fig. 14.4. The transit time characteristics of a microphone with resonant frequency $f_0 = 10$ kHz for various values of Q

to the above facts, this microphone gives reliable results only up to 4 kHz for transient measurements. The requirement of constant transit time therefore considerably reduces the frequency range of microphones.

The Q factor of accelerometers is normally in the range of about 30 to 100. The upper cut-off frequency is generally specified at one-fifth of the resonant frequency by the manufacturers. This specification is acceptable even in terms of transient tests. The slew rate of transducers may be characterized by the ratio of the upper dynamic limit to the transit time in the operating frequency range. As we have seen, the transit time at frequencies much lower than the resonant frequency can be approximated as:

$$\tau_0 = \frac{1}{\omega_0 Q} . \tag{14.4}$$

Among transducers with a given resonant frequency, those with higher Q factor have shorter transit time.

The slew rate is given by the following formula:

$$S = \frac{A_{max}}{\tau_0} = \omega_0 Q A_{max}, \tag{14.5}$$

where A_{max} denotes the maximum measurable value of the physical quantity concerned, namely, the sound pressure or the acceleration.

As we can see, the higher the Q factor of the system, the higher the slew rate. From the transient transfer point of view, transducers with sharper resonance are better than strongly damped ones. Therefore the piezoelectric accelerometer are well applicable to analysis of transient signals, provided that the highest frequency to be measured does not exceed one-fifth of the resonant frequency of the transducer. Electrostatic microphones, however, are not really suitable for measuring transient signals. Nevertheless, if we have to use them for transient measurement, we must predetermine the frequency range where the microphones can be used for that purpose. Furthermore, we have to calculate the time and the slew rate, also in advance.

As an example, for a 1″ outdoor microphone, $f_0 = 10\,\text{kHz}$, $p_{max} = 500\,\text{Pa}$ (148 dB) and Q is about 1 to 1.5. Using these data, we find that $S = 31.4$ to 47.1 Pa/μs, which corresponds to a slew rate of 1.6 to 2.4 V/μs at the input of the pre-amplifier. (The sensitivity of the microphone is 50 mV/Pa.)

Reliable signal tracing can be expected only if the slew rate of the microphone is 5 to 10 times that of the signal. Consequently, the microphone in question is suitable for the analysis of transient signals whose components have a slew rate of about 4 to 8 Pa/μs and a maximum frequency of 3.3 kHz.

The calculated slew rate is normally sufficient for transient signal measurements. In the case of shock waves, however, it can happen that the slew rate of the signal is faster than that of the microphone. In such cases, the peak value of the electrical

signal produced by the microphone is much lower than the expected value. Electric sparks, gun or pistol shots may present cases of this kind.

A bigger problem in the measurement of transient signals is posed by a frequency-limited transit time characteristic. If we want to investigate the whole audible range, we would need microphones with a resonant frequency of 50 kHz.

The selection of an adequate transducer is generally very hard. On the one hand, the transient characteristics of commercially available microphones and transducers are not indicated in the data sheets, and on the other hand, these transducers are not designed for transient measurements. Another problem is that in most cases we do not know in advance what the nature of the signal to be tested will be, so we cannot select the right transducer. If possible, we should start measuring with the fastest and highest dynamic microphone available and, provided the signal allows, we should change to one more suitable for the purpose. We have to bear in mind though that if we make the wrong choice in selecting the transducer, our measurement will be unquestionably useless.

14.5.2 The transient characteristics of measuring equipment

The instruments used in vibroacoustic measuring systems can be used only with due foresight for measuring transient signals. The condition that constant transit time is required for acceptable transient transfer applies to instruments as well, so we must determine for each instrument the frequency range where the requirement of constant transit time is met.

Wide-band measuring amplifiers are normally characterized by constant transit time, but the frequency range that can be used is somewhat narrower than the range of linear amplitude transfer. If we determine the phase-frequency characteristic of the amplifier by measurement, we can calculate the transit time characteristic from the curve obtained. In the frequency range where the phase curve is linear, the transit time is constant.

A measuring system normally comprises various filters. As far as the transient behaviour is concerned, the filters are the most critical elements of the measuring system. In particular, the narrow-band filters may give rise to problems, for the transit time of filters is not generally constant. Analogue band-pass filters, which are used in vibroacoustic application, are not designed for constant transit time, since the requirements for constant transit time and linear amplitude transfer cannot be met simultaneously in band-pass filters. The instruments incorporate filters which have been designed for optimum amplitude transfer, and the transit time may vary considerably even within the pass band and changes abruptly at the ends of the band.

The band-pass filters may be designed for constant transit time in the pass band, but then the amplitude will vary in that range. Such a filter would be inadequate for measuring constant amplitude signals. It would be practical to incorporate constant transit time filters in addition to the existing ones in vibroacoustic instruments, for it would allow the user to decide which filter to use for a particular measuring task.

Until we have this facility, we must take special care when allowing transient signals through filters. If possible, we should measure the phase characteristic of the built-in filters, then determine the transit time curves. Otherwise, we should avoid application of narrow-band filters with steep side slopes.

Other critical units in terms of the transit time are AM (amplitude modulation) and FM (frequency modulation) tape recorders. The manufacturers generally do not specify anything about the phase and transit time characteristics. This is no mere chance but arises simply because these curves are really poor. Figure 14.5 shows the transit time curves of three tape recorders which are quite popular in
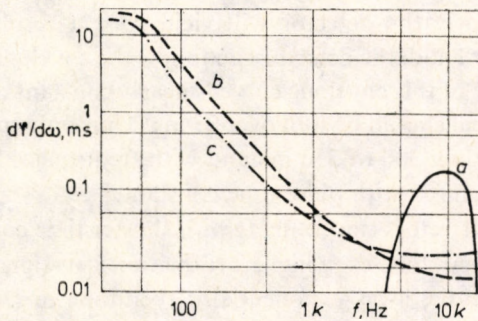
Fig. 14.5. The measured transit time curves for several tape recorders: a — A-type tape recorder, FM operation, b — A-type tape recorder, AM operation, c — B-type tape recorder, AM operation

vibroacoustic measuring systems. As we see, the transit time of AM tape recorders (b and c) falls sharply at low and medium frequencies, while that of FM tape recorders (a) varies strongly at higher frequencies.

For measuring transient signals, only those tape recorders whose transit time has been measured and accepted in advance should be used. If necessary, the transit time characteristic of the tape recorder may be corrected by means of a transit time corrector.

The slew rate of measuring instruments is generally determined by the upper dynamic limit and the upper cut-off frequency. If the amplitude and frequency of the signal fall within the appropriate ranges of the instrument, the slew rate will pose no problem. In this respect, it is enough to investigate the characteristics of

the applied detector. For the correct measurement of the peak values of transient signals, the slew rate of the peak value detector must be much higher than the slew rate of the signal (e.g., the rise time of the peak value detectors used in noise measuring instruments and measuring amplifiers nowadays is 20 μs). Since the maximum voltage of the detector is 10 V, the slew rate is 0.5 V/μs. This value is normally acceptable for measurements in the audible frequency range, but considerably lower than the typical slew rate of electrostatic microphones.

The measurement of transient signals with r.m.s. detectors also gives rise to problems. When the r.m.s. value is measured, the problem results from the averaging time constant. For steady-state signals the time constant affects only the lower cut-off frequency of the measurement, since averaging with a required accuracy necessitates that a sufficiently high number of full cycles fall within the averaging time. For transient signals, however, we must take care that the time constant is also smaller than the length of the signal. These two conditions are very hard to meet simultaneously. The standard pulse time constant is about 35 ms. For an acceptable accuracy, about ten cycles should occur during this time, and consequently the detector will yield correct results only over about 300 Hz. On the other hand, the detector can follow the envelope curve of the signal only if the amplitude of this envelope curve is nearly constant during the 35 ms, so the length of the signal should be well over 35 ms. Thus only transient signals with components longer than 300 to 350 ms and with frequencies higher than 300 Hz can be correctly measured with pulse time constant.

Of course, r.m.s. detectors can be made with shorter time constant, but then the lower cut-off frequency shifts even higher. If the transient signal is considered as a harmonic signal that dies away exponentially, then the r.m.s. detector can follow the envelope of the signal only if the inverse of the damping constant is higher than the cycle time by at least one order of magnitude. In the case of signals that die away quickly, the r.m.s. detector will inevitably distort the envelope curve.

Finally, problems may arise from the dynamic range of the measuring equipment, if it is smaller than required. When transient noise phenomenon accompanies a steady noise, and both phenomena convey useful information so that they must be measured simultaneously, it may arise that a useful dynamic range of up to or higher than 60 dB must be tested. The dynamic range of transducers, measuring amplifiers and filters is normally wide enough, but it is not certain that this covers the dynamic range of the various signal detectors and recorders. The rated dynamic range of detectors used in noise measuring instruments and measuring amplifiers does not generally exceed 50 or 60 dB and the inherent error of these detectors is very large in the lower third of the dynamic range. For this reason, we cannot measure high-intensity transient noise and low-intensity background noise in the same measuring setting.

The dynamic range of detectors is much less a problem than that of the recorders. In the specifications of commercial tape recorders, we find figures as high as 70 dB, but such levels are sometimes not valid. Generally speaking, the dynamic range of FM tape recorders is somewhat narrower than that of AM recorders.

It is no large mistake to take the dynamic range of professional FM tape recorders as 45 to 55 dB and that of AM records as 50 to 60 dB, with the lower figure considered more reliable. It is obvious that the correct recording of pulses that rise high above the background noise level is not always possible with such a dynamic range. To make matters worse, we cannot generally utilize the whole available dynamic range. It is very hard to estimate the peak value of pulsed and transient signals in advance, and the peak value of subsequent transients of the same origin may vary considerably. Therefore a safety margin of at least 10 dB should be provided in order to avoid overdrive, in other words, the dynamic range of the tape recorder, measured for steady-state signals, must be reduced by at least 10 dB for recording transient signals.

This problem arises to an increased degree in digital recording. The AD converters currently in use divide the amplitude range into equal sections, so their accuracy is higher in the upper part of the dynamic range. This upper third, however, should be the safety margin for us, which means that we cannot make use of one-third of the dynamic range of the AD converter. For this reason, the most frequently applied 8-bit AD converters are not suitable for transient signal recording. At least 12-bit resolution is necessary.

The transducers and measuring instruments used for vibroacoustic measurements must meet requirements other than the standard instruments designed for steady-state applications. At present, instruments specially designed for detecting, recording, and processing transient signals do not exist, so we have to use existing equipment for transient signal analysis. The leading manufacturers of vibroacoustic measuring equipment endeavour to produce devices which are equally suitable for steady-state and pulsed signal measurement. As we have seen, this is theoretically impossible, so even if the most up-to-date instruments are used, we have to expect poorer accuracy for transient signals than for steady-state ones. It may be that the transient signal measurement is completely wrong. Therefore trial measurements and simple calculations are highly recommended to give an idea before the actual measurement starts.

15. DIRECT MEASURING TECHNIQUES
OF TRANSIENT VIBROACOUSTIC SIGNALS

The direct and accurate measurement of short-duration transient vibroacoustic signals is highly limited by the dynamic characteristics of the individual elements of the available measuring system. The shorter the vibroacoustic phenomena to be tested, the stronger these limitations become.

Let us assume that the proper transducer and, matched with it an acceptably fast electronic measuring system, are at our disposal. Now let us investigate the possibilities of determining the characteristic quantities of the phenomena. The direct signal processing may be done by means of an analogue, digital or hybrid measuring system, the latter combining the former two, and the signals can be tested in the time, frequency or amplitude domain.

15.1 Analysing the time function of a phenomenon

15.1.1 Approximative analysis

Several time-domain parameters of transient vibroacoustic signals, e.g., the duration of the phenomenon and the maximum amplitude that appears during the phenomenon, can be determined approximately by displaying the parameter concerned on an oscilloscope of adequate parameters. Oscilloscopes built with persistent CRT or the so-called memory scopes are especially suitable for this purpose. The duration or the maximum amplitude can be read directly from the screen grating as distance (or division), provided that the deflection and the input sensitivity are properly calibrated. The process of the phenomenon, that is, the shape of the envelope curves fitted to the positive and negative local maximum values, can be displayed on the screen as well.

15.1.2 Determining the peak values

The modern sound pressure level measuring instruments normally incorporate fast-rise peak detectors, so we can determine the positive and negative peak values of the signal in the "+Peak Hold" and "−Peak Hold" settings, respectively. In this case, we must make sure that only the transient signal to be measured is applied to the input of the instrument or ensure by adequate auxiliary circuits that only one transient is fed into the measuring system (synchronizing, gating, etc.).

Since the peak detectors also have a finite slew rate, we must look through the specification of the instrument and determine the approximate value of the signal slew rate by the procedure outlined above to decide whether the instrument is suitable for the task concerned, and what the expected error is.

15.1.3 Determining the effective value

By means of a level recorder and an r.m.s. circuit, under certain conditions, we can determine the development of the effective value of the signal. If the time constant of the r.m.s. circuit is much shorter than the duration of the transient signal, we can hope to follow the changes of the effective value of the signal in time. Because of the fact that the short time constant raises the lower cut-off frequency of the measuring system, it also contributes to the distortion of the envelope curve.

The built-in r.m.s. detector of the common level recorder may be a suitable circuit for effective value generation in a.c. mode, since the minimum of its time constant can be as low as several ms, depending on the lower cut-off frequency selection. Note, however, that the recorder performs a further averaging function which depends on the magnitude of the pen deviation, so the shortest resultant time constant is about 10 ms.

15.2 Frequency analysis

The standard analogue measuring instruments are not suitable for spectral analysis of transient vibroacoustic signals, since outside the limits discussed with the effective values generating circuits above the settling time of band-pass filters, especially for low-frequency components, will further increase the minimum duration of the transient which can be tested. Therefore only approximative determination of the envelope curve fitted to components with frequencies of several kHz can be undertaken with this method.

15.2.1 Analogue parallel analysis

From the numerous important parameters that characterize transient vibro=
acoustical signals, analogue procedures allow only the determination of a limited
number. One of these procedures is analogue parallel analysis by which the maxi=
mum values at one-third-octave intervals can be determined from the transient
signal.

These analysers incorporate several tens of filters connected in parallel, and
detectors and holding circuits connected to each filter output. When using such an
analyser, we should remember that the settling time of the lowest centre frequency
filter to be used in the test, which is at least three times the inverse of the band=
width, and the time constant of the detecting, holding and displaying circuit
together determine the length of the shortest transient noise phenomenon that
can be analysed with acceptable error. With typical parameter values, assuming
that the lowest-frequency component falls within the 125 Hz one-third-octave
band, the time taken by the phenomenon should be at least 100 ms. Similar li=
mitations apply to parallel analysers built with digital filters, since these filters
simulate the operation of one-third-octave band filters.

15.2.2 The time-lapse procedure

The time-lapse method outlined in Section 11.5.3 is also suitable for spectral
analysis of transient vibroacoustical signals up to a certain frequency in the so=
called real-time mode of operation. The instruments that operate on the principle
illustrated in Fig. 11.9 can normally be used up to an upper cut-off frequency of
10 kHz.

When the analogue-to-digital converter at the input of the instrument operates
at a sampling frequency of 30 kHz, then three samples represent one cycle of the
signal at the upper cut-off frequency (if the capacity of the digital memory is 1200
words, so it is 400 cycles altogether. From the signal at the lower cut-off frequency
at least one full cycle must fit in the memory, and so this frequency is found as
10 kHz/400 = 25 Hz. As the instrument measures four hundred spectral compo=
nents (to a linear scale), the distance between two adjacent components is 25 Hz.

The signals in memory are played back 400 times faster, so the highest-frequency
component is at 4 MHz, the lowest, at 10 kHz. In the course of each play-back
the signal, following digital-to-analogue conversion, is applied to a heterodyne
filter tuned synchronously with the play-back rate. In theory, in such a way
40 ms is required to draw up a 400-line spectrum, which corresponds to the
sampling time of a 1200-word sample.

In order to ensure the continuity of signal processing, during each play-back three samples are replaced by new ones, and in this way the whole memory content is changed completely in the course of 400 play-backs. One drawback of this method is that the resultant spectral components are not derived from the same sample. The spectral components obtained during the transient process are averaged by linear or exponential weighting, so the result is the weighted average of the maxima of instantaneous values. This method can be used with acceptable error when the duration of the transient vibroacoustical signal is at least ten times the sampling time.

15.2.3 Applying the Fast Fourier Transformation

Up to a given upper cut-off frequency, the FFT-based instruments are also suitable for real-time analysis and, through that, for the spectral analysis of transient signals. Instruments working on this principle also take samples from the signal to be tested (generally 1024 samples) and determine the complex spectral components by computation from these samples. Since the inherent error of the computation method increases with increasing frequency, only the lower 400 components are used out of the possible 512 spectral components.

The sampling frequency is normally $1024/400 = 2.56$ times the frequency of the highest frequency component to be tested. The lower cut-off frequency and the distance of adjacent components is 1/400th of the upper cut-off frequency. The instrument can be considered as real-time up to an upper cut-off frequency at which the time required for the computation and display of the spectral components is shorter than the sampling time. The upper cut-off frequency of commercial instruments in the real-time mode is typically 2 to 10 kHz. This method can be considered as suitable for direct transient signal analysis if the length of the transient signal is at least ten times the sampling time.

15.3 Determining the energy of a sound phenomenon

One of the most important characteristics of a transient noise phenomenon is the energy of the signal. The direct measurement of this energy, however, is a difficult task. Informative measurements may be conducted with standard acoustical measuring instruments [104]. If a transient signal shorter than the averaging time is applied to an r.m.s. detector, the peak value of its output signal will be proportional to the energy of the transient, since the r.m.s. detector averages the square of the signal for a given averaging time and then extracts the square root of the

result. The output of the detector is normally expressed in dB. The level of the r.m.s. sound pressure is defined as:

$$L = 20 \log \frac{1}{p_0} \sqrt{\frac{1}{T} \int_t^{t+T} p^2 \, dt.} \tag{15.1}$$

The energy of the transient signal acting on the microphone:

$$W = \int \left(\int_{S_{mi}} \bar{I} \, d\bar{S} \right) dt = \frac{S_{mi}}{\varrho c} \int p^2 \, dt, \tag{15.1a}$$

where S_{mi} is the surface of the membrane of the microphone. Comparing eqns (15.1) and (15.1a) and introducing the reference power:

$$W_0 = \frac{p_0^2}{\varrho_0 c_0} S_{mi} T_0, \quad \text{(where } T_0 = 1 \text{ s),}$$

the energy level of the transient noise event is given in:

$$L_W = L + 10 \log \frac{T}{T_0} + 10 \log \frac{\varrho_0 c_0}{\varrho c}. \tag{15.2}$$

The last term of the expression is normally smaller than 0.1 dB, so we will neglect it in later discussion.

The standard value of the "Slow" time constant is 1 s, thus the correction term due to the averaging time is zero in this setting, giving:

$$L_W = L_{max}.$$

Thus if we measure transient signals shorter than 1 s with a common sound measuring instrument switched to the "Slow" setting, then the level corresponding to the maximum deflection of the pointer is a good approximation of the energy of the transient signal, expressed as level. This measuring method yields surprisingly good results, but we should take care not to overdrive the instrument during the measurement, because overdriving may give rise to considerable error in the measurement.

If the length of the transient is too slow, it may happen that the deflection of the instrument pointer is so small in the "Slow" setting that we cannot even read it. In such a case the measurement should be done with a shorter time constant. The standard value of the "Fast" time constant is, for example, 125 ms and the cor-responding correction term is −9 dB. Now, if we read the level indicated by the maximum deflection of the pointer in the "Fast" setting, the transient energy level is lower than this by 9 dB.

If we also detect the peak value of the signal L_{peak} simultaneously, we can give

a good estimate of the length of the transient signal. Let us define the effective length of the signal of the transient event, T_{ev}, as:

$$W = \frac{p_{peak}}{\varrho c} S_{mi} T_{ev}.$$ (15.3)

Applying our previous considerations, we arrive at the following expression:

$$10 \log \frac{T_{ev}}{T} = L_{max} - L_{peak}.$$ (15.4)

A great advantage of this time definition is that the length of transient signals can be measured with standard sound pressure measuring instruments. Let us assume that we obtained 89 dB for the level of the transient sound phenomenon by measurement with the "Fast" time constant, while the peak value of the same phenomenon was found to be 106 dB. Then:

$$10 \log \frac{T_{ev}}{125} = 89 - 106 = -17 \text{ dB},$$

from where:

$$T_{ev} = 2.5 \text{ ms}.$$

By simultaneously measuring the peak value and the effective value of the signal, we can thus determine the effective length and the energy of the transient phenomenon as well. These measurements can be accomplished by means of a simple portable sound pressure measuring instrument. Before starting more serious measurements, it is always advisable to carry out informative measurements with this method on the site.

No other analogue method is used for direct measurement of the energy of a signal, but the digital measuring systems can measure the energy as well by computing the integral of the squared signal from digital samples. This computation does not take too long, so it can be done in real-time. This method, however, has not come into general use, and the FFT analysers currently in use instead determine the spectral energy density of the signal. From this, the total energy may be calculated. In many cases though, we do not need the additional information provided by the spectral energy density, we want to know only the energy. In such cases the fastest result is obtained by the analogue measuring procedure outlined above.

15.4 Statistical analysis

In the measuring technology of steady-state vibroacoustic signals, measuring procedures based on amplitude statistics are widely used. The point of this method is to take samples from the signal to be measured for a given time, determine the

amplitude of these samples and then, from the stored data, the characteristic amplitude distribution for the given measuring session, through which the information on the changes of the signal with time is also saved. In the field of acoustics, the frequency distribution of sound pressure levels is normally determined. A common statistical analyser, for example, samples the output signal of the built-in logarithmic detector by means of an 8-bit AD converter. With a resolution of 0.25 dB, a dynamic range of 64 dB is provided which is easily sufficient for most acoustic measurements.

The statistical signal processing is done digitally. If the measuring equipment was designed for long-time measurements, for testing noises that do not change too fast, then the maximum sampling frequency is 10 Hz. Consequently, this instrument is not capable of measuring the amplitude distribution of short-duration signals. The unit takes a preset number of samples from the sound pressure level and divides up the measured values into 256 channels. Then it calculates the percentage of samples which fall into the individual channels. These values make up the density function of the distribution. The integrated distribution shows in turn what percentage of the samples are higher than the level indicated along the x axis (see Fig. 15.1). For example, the level L_{50} is considered as the mean value of
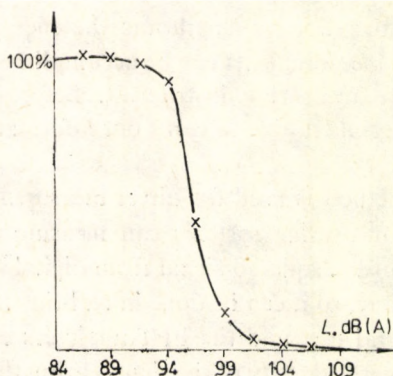
Fig. 15.1. The integrated distribution of steady-state noise:
L_{99}=90.5 dB(A), L_{90}=94 dB(A),
L_1=107 dB(A), L_{10}=99 dB(A),
L_{50}=96 dB(A), L_{eqv}=98 dB(A)

the signal, since 50 percent of the samples are higher than this level. The background noise is given by L_{99}, and the maximum signal, by L_1. The dynamic range of the signal may be obtained from the expression $\Delta L = L_{10} - L_{90}$.

The analysis of frequency distributions yields substantial new information, if the dynamic character of the signal varies considerably during the measurement, or sections of different character follow each other. This is well illustrated by the

curve shown in Fig. 15.1, which represents the pulse-like noise of a smithy. As we see, the integrated distribution of the sample, which includes many pulses, extends towards higher levels. The distribution density is obtained as the derivative of such curves. At the impulse-like noise sample, the equivalent level L_{eqv} is much higher than L_{50}, while, for example, in the case of the nearly steady noise of a compressor room, the two levels are almost identical.

The dynamic character of transient signals may vary considerably as a function of time, and it frequently happens that a new transient mixes with the former decaying signal. In any case, the analysis of the amplitude distribution is always advisable. The detector must be fast and the sampling frequency must be high enough that at least 1000 samples from the transient to be tested can be sent to the memory. From the technical point of view, the building of such an instrument is not difficult at all. If the output signal of a fast detector is applied to the input of a digital frequency analyser which is capable of computing amplitude statistics, we can easily try out this measurement. Of course, it would be practical again to analyse the amplitude distribution of the two signal halves separately.

The statistical analysis of transient signals is recommended especially when transients occur frequently in a steady noise. A mixed noise of this kind characterizes electrical rotating machines, for example. Statistical analysis of a longer signal segment reveals how the transients modify the distribution function characteristic for transient noise, we can determine the average amplitude of the transients and figure out what percentage is represented by the transients in the total energy of the mixed signal. In mixed signals most frequently encountered in practice, the transients differ considerably, thus one transient from the signal flow does not represent the other transients, and detailed analysis does not yield any useful information. Statistical analysis, in turn, can furnish characteristic results even in such cases. If, for example, the transients are produced by the strongly and quickly varying load conditions of the electrical rotating machine, the analysis of the individual transients offers information on the instantaneous load changes, while the statistical analysis of the signal is suitable for the characterization of a longer segment of operation.

Instruments capable of direct measurement of the amplitude distributions of transient signals are not commercially available yet. As we mentioned before, the sampling frequency of instruments developed for noise measuring is too low, and the digital frequency analysers can span only a very short length of time. In the case of computerized signal processing, however, it is easy to establish the possibility of statistical signal processing, and we should only connect the output of an analogue measuring amplifier equipped with a fast r.m.s. detector to the analogue input of a computer, providing for controllable sampling. The computer generates the distributions from the collected samples. Another advantage of this method

is the virtually unlimited number of samples, which allows the determination of distributions for prolonged processes. When the objective of the measurement is to determine the characteristic noise of a sound source which emits transient compo= nents as well, the most practical solution is to draw up the distribution by prolonged measurement and then, from this, to compute the peak value, mean value and equivalent level of the mixed signal.

If single transients are to be measured, the distribution can be of good use again. The starting section of transient signals normally features a small amount of phase and frequency uncertainty. If we want to determine the average characteristic of similar transients, the direct averaging of the time functions may yield erroneous results because of the above-mentioned uncertainties. The same applies to spectral averages, but the amplitude distribution is completely insensitive to phase fluctua- tions. From any number of subsequent transients, we can draw up an average dis- tribution curve that retains some characteristic information on the original signal process. If the decay is considered purely exponential, then a very simple connec- tion may be found between the envelope curve of the time function and the inte- grated distribution. Finally, reliable information can be obtained from the inte= grated distribution on the maximum amplitude, energy and decay time of the tran- sients tested. Measurement conducted this way yields correct average values.

The statistical analysis can be carried out in terms of frequency selection. If, for example, all the channel outputs of a parallel filter analyser or a digital real- time analyser are loaded into a computer, we can determine the distribution of the signal in each frequency band, so we can obtain even more information on the characteristics of transient signals. When a computerized measuring system is set up, it is always advisable to provide for statistical distribution functions. We have already pointed out that the high-speed digital measuring systems produce such a tremendous amount of information that a researcher cannot absorb it. The greatest advantage of statistical methods is the very fact that they can highly condense the mass of information supplied by the instruments and provide a single distribution from any number of individual cases. This makes the measure- ment series more lucid, and the omission of useless details aids the discovery of important relationships.

16. INDIRECT MEASURING OF TRANSIENT VIBROACOUSTIC SIGNALS

To resolve the limitations set out in the discussion of the frequency analysis in Chapter 15 and to determine further characteristics of the transient phenomenon, the signal obtained by conversion must be stored somehow in an analogue or digital way. The actual processing takes place later, perhaps at another place, in an adequate manner depending on the purpose, transforming the recorded signal into the required form, slowed down, speeded up playing back only parts of it.

16.1 Analysing the time function of the phenomenon

The signal saved in the memory might be fed into the oscilloscope in a speeded up and repeated sequence, generating a periodic signal out of the single phenomenon. Speeding up is necessary to obtain a flicker-free, virtually stationary display. The observation of the signal is especially easy when the rate of play-back is synchronized with the horizontal deflection of the oscilloscope.

Knowing the amount of speed up, the calibrated deflection and sensitivity of the oscilloscope, information can be obtained in the time and amplitude domains as well (e.g., duration, the maximum value and its approximate time coordinate, the positive and negative envelope curves fitted to the maximum values, characteristics of the process such as beat, resonance, etc.).

In order to record the signal by means of an X–Y or X–t recorder, it must be slowed down when played back from memory to an extent that the highest frequency component of the played-back signal is not over 8 to 10 Hz.

When the time base and the sensitivity are calibrated, more accurate information may be obtained from the recorded signal than above and, further, the time function of the phenomenon is presented in a form suitable for further processing and display. In the case of an X–Y recorder, instead of applying a time sweep a signal proportional to any other physical or electrical quantity (e.g., speed, torque, frequency, voltage, etc.) may be applied to the X axis in order to obtain the transient vibroacoustic signal as a function of the selected quantity.

16.2 Frequency analysis

16.2.1 Analysing the periodic signal made by repeated play-back

The transient signal is played back repeatedly and periodically with a repetition time of T_{rep}, which is longer, of course, than the length of the signal $(T_{rep} > T_E)$. In this way, an artificial periodic signal is produced, and the discrete spectrum obtained as a result of the analysis can be easily converted into a continuous spectrum. Furthermore, the power spectrum can be easily converted into an energy spectrum by multiplying by the repetition time.

To measure the energy of the periodic signal, an r.m.s. measurement should be conducted with an averaging time (T_A) several times longer than the repetition time in order to damp the fluctuation (beat), that is, $T_A \geq nT_{rep}$, where n is higher than two, but generally lower than five. This procedure is widely approved and accepted for the following reasons:

(a) Instruments used for steady-state signal analysis can be used.

(b) The result does not depend too much on bandwidth variation. For example, the response time of the filter normally need not be taken into account and we can choose freely between constant bandwidth and constant percentage bandwidth. We must ensure, however, that the bandwidth B is always larger than the inverse of the repetition time:

$$B > \frac{1}{T_{rep}} \qquad (16.1)$$

(c) If we ensure that the averaging time is long enough to reduce the beat, than the result is not affected by any further increase in the averaging time.

(d) The scaling of the result is relatively simple and practically independent of the analyser used.

(e) The spectrum obtained is continuous rather than a series of spikes or lines.

On the other hand, if the duration of the transient phenomenon is much shorter than the repetition time, say, only 10 percent of T_{rep}, than the procedure may not be applicable for any of the following reasons:

(a) The dynamic range of the result decreases directly with the ratio of the transient signal length to the repetition time.

(b) If the detector is sensitive to the crest factor, then the repeated play-back may yield false results. Of course, the crest factor of the signal passing through the filter is much more important in this respect than that of the original signal. If we have an instrument that can measure the effective and peak values, than we can easily determine the crest factor of the filtered signal as the ratio of the two values.

If our instrument is capable of measuring only the r.m.s. value, then the peak value must be determined by means of an oscilloscope. When the crest factor of the signal is higher than permissible, then the displayed value is smaller than the true value.

To satisfy the requirements for the dynamic range and the crest factor, the following factors should be taken into consideration:

I. The bandwidth of the analyser

The first restriction on the bandwidth of the analyser is that it must be larger than the inverse of the repetition time [see eqn. (16.1.)]. If a bandwidth smaller than $1/T_{rep}$ is used in the analysis, than the resultant spectrum will be made up from a series of discrete peaks, and it is very hard to identify the true peaks of the spectrum among them (Fig. 16.1).
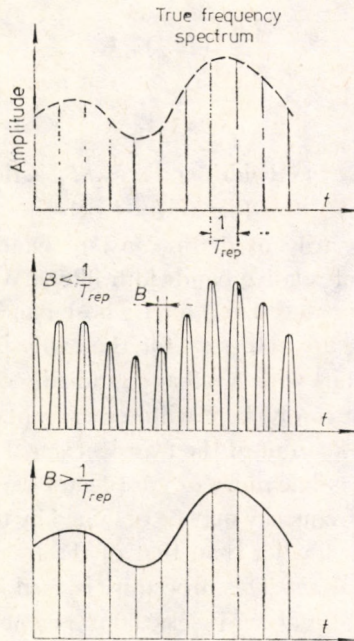
Fig. 16.1. The effect of filter bandwidth in discrete-frequency analysis

If $B \gtrsim 1/T_{rep}$, then the resultant spectrum is a continuous line, so the true maximum points can easily be seen.

The upper limit of the bandwidth of the result is given by the fact that it cannot exceed the inverse of the length T_E of the played-back signal packet, that is, $B_{max} \lesssim 1/T_E$. The narrow-band analysis, in turn, takes longer without any additional information.

We should note, however, that while the repetition time may be increased freely in order to obtain a narrower bandwidth, an increased T_{rep} will increase the chance that problems arise because of the narrowing of the dynamic range of the procedure or overstepping the tolerance of the crest factor of the indicator.

II. Averaging time

The averaging time T_A should be set at several times the repetition time T_{rep} in order to avoid fluctuation (beat), so:

$$T_A \gtrsim KT_{rep},$$

where the usual way to determine K is as follows:

$$BT_R \approx 1, \tag{16.2}$$

where T_R is the response time of the filter. Rewriting the expression:

$$\left(\frac{B}{f}\right)(fT_R) \approx 1,$$

that is:

$$bn_R \approx 1, \tag{16.3}$$

where $b = B/f$ is the relative bandwidth and $n_R = fT_R$ is the number of cycles of the signal with frequency f in T_R time (e.g., if $b = 1$ percent, then $n_R = 100$ cycles). Equation (16.2) is primarily used for constant bandwidth filters, while eqn. (16.3) is taken for constant relative bandwidth filters. When a sinusoidal signal is analysed with a one-third-octave-band filter whose bandwidth is 23.1 percent, we find that at least 4.3 cycles are necessary for the analysis. In general, the recommended procedure is to start with $K > 3$ and gradually decrease the value of this factor as long as the error can be kept within an acceptable tolerance range.

If the repetition time taken out of the transient signal is not chosen to be short enough because of the dynamic range or crest factor dependence, the components of the transient signal by frequency may be obtained by tuning the filter. When the bandwidth of the filter is smaller than that of the transient, the procedure is a constant narrow-band analysis. This procedure is used for example in such cases when the bandwidth of the analyser is selected to be one fifth of the bandwidth of the signal to be analysed, in other words, when the response time of the filter is about five times the length of the transient. In this case, the output signal of the filter is identical with the value determined by the pulse transfer characteristic of the filter, i.e. it is independent of the shape of the transient signal and depends only on the energy content in the neighbourhood of the frequency tested.

Referring to the work of Broch and Olesen [11], we know that a simple relationship exists between the spectral components and the peak value of the filter output which can be measured easily by means of a peak value detector. If the analyser is

connected to an r.m.s. measuring instrument, it is possible to use it as a sensor with appropriately short averaging time and, therefore, its output will follow the envelope curve of the filter output and, applying proper scaling, gives the actual peak values (Fig. 16.2). The parameters to be taken into account in the analysis are selected as follows:
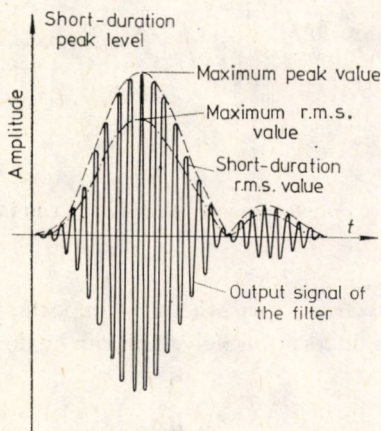
Fig. 16.2. Short-duration mean value and peak level at the output of the filter

I. The bandwidth of the analysis

It is a basic requirement that the response time of the filter must be longer than the effective length of the transient signal, so that:

$$B < \frac{1}{5T_E}, \tag{16.4}$$

where T_E is the effective length of the transient signal.

In the standard procedure, T_E is normally equal to the total length of the transient signal.

II. The response of the instrument that measures the output signal of the filter

According to the article referred to, the pulse response of the filter looks like that shown in Fig. 16.3. The envelope curve of the signal, which determines the peak values, shows the shape of the function $(\sin x)/x$ with an alternation determined by the bandwidth of the filter, while the sinusoidal fluctuation is identical with the tuned frequency f_0 of the filter. The delay time of the filter, t_L, depends on the selected phase characteristic and in practice is of the order of $1/B$ (so it is shorter than shown in the figure). According to [11], the peak value of the filter output, V_{peak}, is equal to $2B|G(f_0)|$, where $|G(f_0)|$ is the modulus of the Fourier series at frequency f_0, that is, $|G(f_0)| = \frac{V_{peak}}{2B}$. If a peak value detector is not available, an r.m.s. detector may be used under certain conditions (e.g., $f_0 \gtreqless 9\ B$).
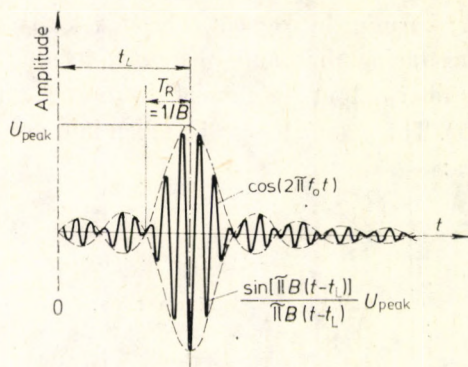
Fig. 16.3. The output response of the filter to an input pulse

III. Repetition time (T_{rep})

When a peak value detector is used, the most important task is to separate the response of the individual filters accurately. This can be done if:

$$T_{rep} \geq \frac{2}{B}.$$

In the case of very short repetition time, we see that the recorder pen cannot trace the spectrum. The pen can trace jumps of at least 20 dB magnitude, if:

$$T_{rep} \geq \frac{100}{W},$$

where W is the writing speed (for 100 mm wide chart paper). For example, for $W = 1000$ mm s^{-1}, T_{rep} should be minimum 0.1 s.

Owing to the properties of r.m.s. detectors, the following restriction must also be taken into account:

$$T_{rep} \geq 3T_A.$$

IV. Dwell time (T_D)

T_D is the time the analyser must spend on a given filter, and:

$$T_D \geq T_{rep}.$$

When $T_{rep} \geq 2/B$, the shifting of the result can be as high as half the bandwidth of the filter, which is normally acceptable.

The $B < \dfrac{1}{5T_E}$ condition is the limitation of the procedure set out in Section 16.2.2 which is practically the limitation of the constant narrow-band analysis as well. Independently of the bandwidth of the filter, the output impulse of the filter is always proportional to that part of the energy of the original transient signal which falls within the pass-band of the filter. This way it is possible to determine this

energy by means of an r.m.s. detector, provided that certain conditions are satisfied. First of all, the averaging time must be longer than the impulse—in the case of linear data averaging—only a little longer, while in the case of exponential averaging, several times longer in order that the energy be properly integrated. On the other hand, we must not overstep the peak factor and dynamic range of the sensor.

In the usual analogue analysis of transients, exponential averaging is applied. In this case it is very important to take the special features of exponential acquisition into account, especially for impulse-like input signals. According to Wahrman and Broch [139], the effective acquisition time constant for impulse signals is RC, and for steady-state signals, 2RC.

Figure 16.4 shows the output signals of acquisitions with different time constants for an oscillating transient. It can be seen that the output signal of $T_{A1} = RC$ traces
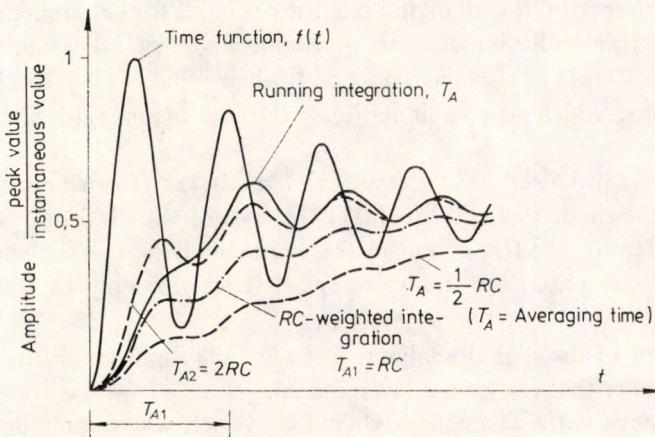
Fig. 16.4. Integration of a transient signal with RC weighting and tracing integration

the signal of linear acquisition quite well up to T_A, then the acquisition with time constant $T_{A2} = 2RC$ gives better result for the steadier section of the signal. Analogue analysers normally use $T_A = 2RC$, because they have been designed for steady-state signals. When they are applied with impulse-like signals, the result will be higher by 3 dB for the same nominal averaging time. The maximum responses of the linear and RC-type averaging are shown in Fig. 16.5 in terms of the ratio of the impulse length to the averaging time constant, T_E/T_A.
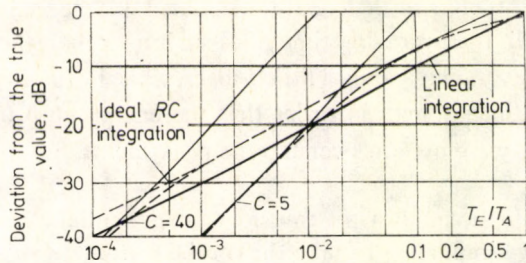
Fig. 16.5. The true r.m.s. generator plotted against T_E/T_A for different crest factors (C)

16.2.2 Constant relative bandwidth analysis

Spectrum analysers built with digital filters are suitable for determining the power spectrum of transient vibroacoustic phenomena. They allow quick analysis (several times 10 ms) of the signal applied to their input, owing to the fact that the settling time, which posed a limitation in the case of analogue filters, is practically zero.

Certain mass-produced third-octave-band analysers (for vibration analysis, 14 bands in the range of 1.6 Hz to 1.25 kHz, for noise analysis, 42 bands in the range of 25 Hz to 20 kHz) complete the whole analysis in less than 50 ms by averaging ten samples. Such analysing speed is feasible only by fully digitized systems.

At the input of the digital analyser, just after the input amplifier, we find an A-weighting filter that can be used as required.

The next stage is the analogue-to-digital converter, where sampling frequency is higher than twice the upper limit of the frequency range to be analysed in order to observe the law of sampling. If the upper band is at 20 kHz, $f_s = 66.67$ kHz may be used safely.

The signals of the analogue-to-digital converter are led to a digital filter network. To speed up operation, the digital filtering is accomplished through two parallel channels and the centre-band frequencies are switched by changing the electrical parameters by octaves. One of the channels always filters the upper band of the octave being modelled.

The next stage of the unit generates the effective value and accomplishes the averaging. At the input of this stage, there is a digital series-to-parallel signal converter. The "paralleled" signals pass through a squaring network and then go to the averaging stage capable of linear or exponential averaging. The linear average is calculated as:

$$A_r = A_{r-1} + \frac{S_r}{K},$$

where K — the number of samples to be taken into account in the averaging process,

r — the serial number of the sample,

S_r — the value of the rth sample,

A_{r-1} — the sum of the previous $r-1$ samples,

A_r — the average value of rth samples.

The exponential average is computed as:

$$A_r' = A_{r-1}' + \frac{S_r - A_{r-1}'}{K}.$$

Both types of averaging are done for a predetermined time which can be selected in steps of the power of two from 1/32 s to 128 s.

The linear averaging process finishes at the end of the preset time and the value of the average is stored until the clearing instruction is given. One advantage of this procedure is that following termination for whatever reason, the averaging process can be resumed by using the final result of the previous averaging process as the initial value of the new process, provided that the same sampling time is used again. The exponential averaging process is continuous and may be stopped only by external instruction.

Both types of averaging are accomplished through two parallel channels, one of which sums up the samples within the highest centre frequency band, and the other, all the remaining samples. The two averaging processes are compared in Fig. 16.6. At the end of the averaging stage are the square root extracting network and the linear-to-logarithmic converter.
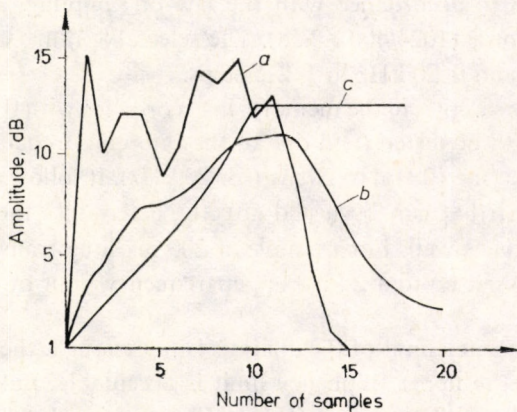
Fig. 16.6. The process of exponential and linear averaging (digital filter analysis): a — values to be averaged, b — exponential average, c — linear average

The next stage of the instrument is the display and data output unit which, on the one hand, displays the spectra on the graticuled screen and, on the other hand, outputs the data in digital or analogue form for further processing or, after digital-to-analogue conversion, for recording by means of a chart recorder.

As mentioned before, the shortest averaging time of the instrument is $1/32$ s= $= 31.25$ ms. In general, transient vibroacoustic signals of electrical machines are longer than that, so their one-third-octave-band spectra may be determined by such an instrument. If the length of the phenomenon has been determined by preliminary tests, then the averaging time can be set to match the whole signal. If the length of the phenomenon is shorter than the minimum averaging time of the instru= ment, then the play-back from memory is slowed down and the analysis may be carried out in the range 1.6 Hz to 1.25 kHz. Using the instrument, it is also possible that the signal is played back in sections and the average spectra of the individual time segments are determined separately, when the length of the phenomenon is several times longer than 31.25 ms. Furthermore, by using the A-weighting filter at the input of the instrument but "skipping" the band-pass filters, it is possible to present the A-weighted level for the total time of the transient signal packet.

16.2.3 Narrow-band analysis

Analysers whose operation is based on the principle of the Fast Fourier Transform are capable of determining 400 spectral components of transient vibroacoustic signals. As mentioned in Section 15.3.2, these instruments take samples from the input signal and these samples are saved in memory after digitization. The sampling frequency is set to 2.56 times the highest frequency component of the frequency range to be tested in accordance with the law of sampling, since the memory capacity is 1024 words ($1024/400 = 2.56$). The selectable range of the analysis can be set to 0–10 Hz and 0–20 kHz in 1–2–5 steps.

The length of the samples in the memory, in accordance with the upper frequency limit of the range to be tested (and due to the sampling frequency matched with it), varies from 40 s (for 10 Hz) to 20 ms (for 20 kHz). It follows that the length of the transient signal that can be tested directly, determines the upper frequency limit of the analysis as well. For example, a 200 ms long transient vibroacoustic signal can be analysed up to a 2 kHz upper frequency limit by means of an FFT analyser.

If the upper frequency limit of the analysis is not enough, then we can test only shorter signals. If the upper frequency limit is acceptable, but the length of the transient phenomenon is longer than it should be, the signal stored in an analogue, or preferably digital, memory must be analysed in parts.

The instruments have two built-in weighting functions, one is the constant time window and the other, the Hanning time window. The former stores and analyses the signal as it is, while the latter looks at the amplitude of the signal through the Hanning time window in their time sequence, computing the convolution of the signal and the window function.

The shape of the Hanning window function is identical with the shape of the function $2 \cos^2 \alpha$. If the shape of the stored signal is such that its amplitude is close to zero at the start and at the end of the signal, then the constant time window must be used, while in all other cases it is the Hanning window function.

When the length of the transient signal is shorter than the length of the signal packet that can be recorded for the selected frequency, the constant time window is applicable. If the transient signal can be analysed only in part because of the above reasons, then the Hanning time window must be used. In this case, the signal segments should overlap over half their length, since the Hanning window makes the start and end of the signal segment recorded for analysis zero, and weights the values away from the ends by a factor that corresponds to the value of the Hanning function at that point. If the width of the individual bands, which is the upper frequency limit divided by 400, is denoted b, then the 3 dB width of the constant time window equals $0.88b$, but for the Hanning time window it is $1.44b$.

The shape of the two weighting functions and their effect on bandwidth is illustrated in Fig. 16.7.
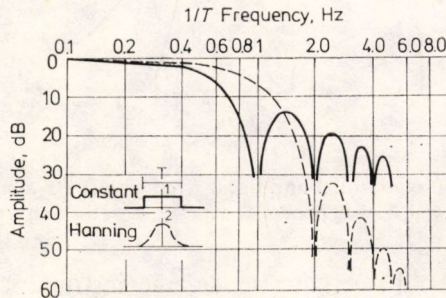
Fig. 16.7. The effect of the constant time window and of the Hanning time window on the response of the filter

Most of the instruments are suitable for the selection of three averaging modes namely the linear, exponential and maximum hold modes. The linear averaging procedure uses the following formula:

$$Y_n = \frac{(n-1)Y_{n-1} + X_n}{n}, \quad [1 \leqslant n \leqslant N],$$

where Y_n — the nth average,
        Y_{n-1} — the $(n-1)$th average,
            X_n — the nth value to be considered in the average,
            n — the serial number of the sample to be averaged,
            N — the predetermined number of averaging steps.

When $n=N$, the linear averaging process ends and holds the average value until the clearing instruction is given by the operator. The exponential averaging method is based on the following formula:

$$Y'_n = \frac{(N/2-1)Y'_{n-1}+X_n}{N/2}.$$

When $n=N/2$, the averaging process ends, but the resultant average value decreases with time.

   The two above averaging procedures are illustrated in Fig. 16.8.
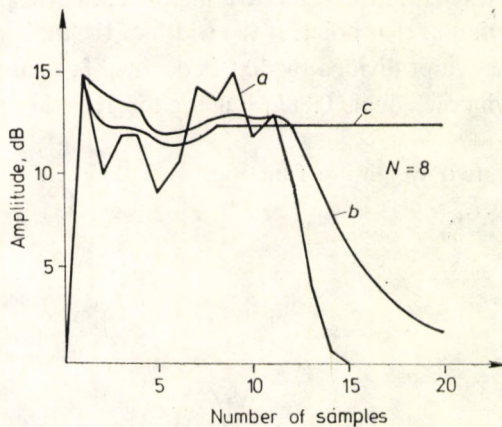
Fig. 16. 8. The process of exponential and linear averaging (FFT analysis): a — values to be averaged, b — exponential average, c — linear average

   In the maximum hold operating mode, the instrument records the largest amplitude value found in each frequency range during analysis.

   When the transient signal is analysed in sections, then linear averaging must be used, because this way the averaging process resumes for each new time segment and we finally obtain the averaged spectrum of the whole signal as a result. Moreover, the FFT analysers can display the content of their memory on the screen, so we may readily determine the necessary information from the shape of the recorded signal prior to the analysis. When the signal is displayed, only every third of the 1024 samples is used.

16.2.4 Determination of the more accurate values of the spectral components and their variation with time

The appearance of high-resolution digital FFT analysers provided new possibilities for the evaluation of transient vibroacoustic signals as well. From these possibilities, we discuss here the exact determination of the frequency by means of the band-expanding ZOOM technique and the analysis of a selected spectral component in time. The input stage of high-resolution FFT analysers is identical with that of the FFT analysers discussed in the previous section. The important difference between the two instrument types is that the former ones store 10.240 (10 K) samples in their memory instead of the 1024 (1 K) samples characteristic of FFT analysers. The first consequence is that the signal can be ten times longer for a given upper frequency limit selected for the analysis or, in turn, the upper frequency limit is increased by a factor of 10 for the same signal length. If we carry out a 400 component analysis in the normal FFT mode and find that the frequencies should be determined more accurately in the neighbourhood of a component, then by switching to the band-expanding mode of the high-resolution analyser, the range so far covering 40 components is displayed on the screen broken down into 400 components, so that we can determine the required frequency with ten times better accuracy. The 40 band range can be selected anywhere over the 400 basic components. The time analysis of any of the 400 components is feasible through the application of scanning analysis.

The content of the 10 K capacity memory may be displayed on the screen in the form of a time function. We can select a 1 K part of the 10 K sample optionally and obtain its frequency spectrum with a resolution of 400 components. This selection may be done continuously from the very beginning of the recorded signal until the end in predetermined steps. This procedure is called scanning analysis. The scanning mode may be used manually as well. During the scanning process, we can continuously observe the changes in the spectrum of the subsequent 1 K samples as they appear on the screen in sequence. In automatic mode, the length of the steps may be set in the range 8 to 1024 in binary steps and, depending on this length, the number of steps varies between 1153 and 10. Since the time required to draw up the spectrum of one sample is 110 ms, the analysis time is anywhere between 2 minutes and 1 s, depending on the number and length of the selected steps. The spectra produced during the scanning process may be summed linearly and the average spectrum comprising 400 components is at our disposal at the end of the analysis (provided that at least 37 steps have been accomplished). Unless there is a special reason to do otherwise, the Hanning time window should be used in all cases, although the constant time window could be used, too, in order to avoid unwanted distortions.

We may optionally select any component of the 400 basic spectra and draw its values recorded in the course of the scanning analysis by means of an X–Y recorder connected to the instrument and synchronized in the x direction. This facility is of particular importance when we want to carry out the identification of one significant component in time or to associate its changes with the corresponding section of the original signal. Using a high-resolution digital analyser, it is possible to record the transient vibroacoustic signal not as a function of time but of an external physical parameter that varies monotonically. In this mode, we can record and analyse the vibroacoustic signals of the transient operation of an electrical machine as a function of the r.p.m. during acceleration, braking or sudden torque changes. Now if we apply the component drawing mode of the scanning analysis, the significant values of the component can be obtained directly associated with the concrete r.p.m. value that corresponds to the phenomenon in question.

16.3 Determining the energy of the sound phenomenon

The energy of the previously recorded transient signals can be determined in various ways. If the envelope curve of the time function of the phenomenon is recorded by a level recorder as in the standard procedure, the energy may be computed. The task can be reduced to graphic integration after the time function of the squared amplitude has been drawn up. This method, however, is very time-consuming and is no longer considered up-to-date. The energy of transients recorded by tape recorders can be determined with the same analogue procedure as discussed in Section 15.3.

Finally, when the time function of the transient signal is stored digitally, the energy can be computed with high accuracy by squaring and then integrating the samples for the duration of the signal. Of course, we must ensure that the integration time is identical with the length of the impulse. When the transient signal rises above the background noise considerably, the accuracy of the measurement is not strongly affected if the integration time is longer than the length of the transient. The transient recorders normally feature a so-called pretrigger mode, which means that they can also store that part of the signal which is received before the triggering signal. If we know the mean duration of the transients to be measured, by means of the pretrigger mode we can arrange the transient signal to fall completely within the recorded and stored time segment. With a transient recorder thus set, we can reliably record subsequent transients and determine the energy of the transients continuously by means of the computer built in the measuring system, if it is set up in the required configuration.

The computerized signal processing also allows the determination of the energy of the positive and negative halves of the transient signal separately. Since the transient signals are generally not completely symmetrical, the analysis of the two halves of the signal may yield further information on the noise phenomenon.
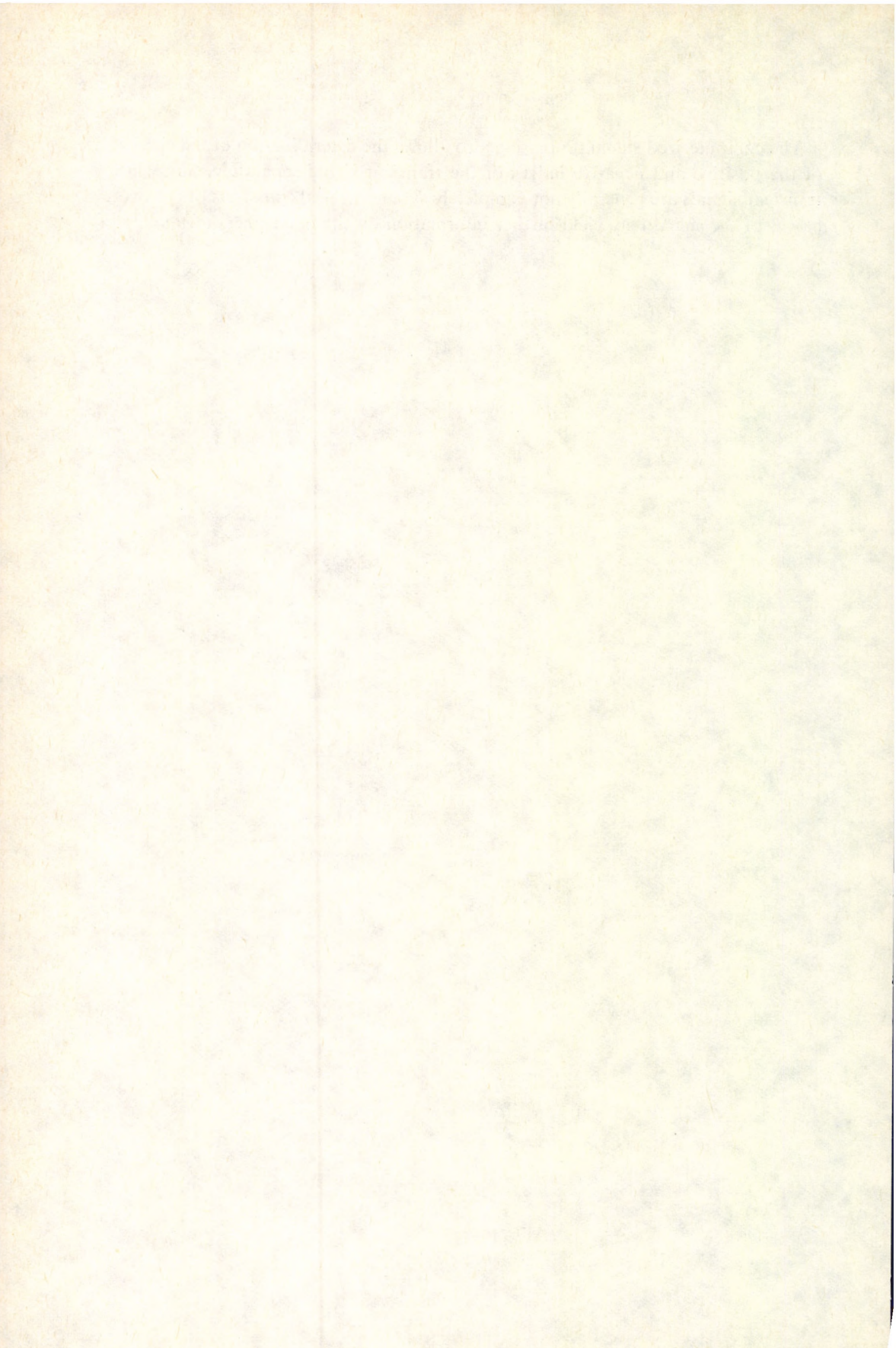
C. SOME PRACTICAL APPLICATIONS OF VIBROACOUSTIC METHODS IN THE TESTING OF ROTATING ELECTRICAL MACHINES

17. NOISE AND VIBRATION TESTING IN PRACTICE

17.1 Noise and vibration generating causes

17.1.1 Detached electric motor

First the electric motor must be subjected to a standard noise measurement to determine the noise quality grade of the motor. The sound pressure level, obtained is $\bar{L}$.

In order to separate causes of noise by their character, the ventilation noise must first be separated. When the complete standard noise measurement is repeated after the fan wheel and the enclosure have been removed, the average sound pressure level is $\bar{L}'$. The mean sound pressure level $\bar{L}_{vent}$ of ventilation origin is obtained from the following formula:

$$\bar{L}_{vent} = 10 \log (10^{0.1\bar{L}} - 10^{0.1\bar{L}'}). \tag{17.1}$$

To separate the mechanical and electromagnetic noises, the following procedure may be used. The supply voltage should be decreased from the rated value to one quarter the value. The changing voltage (flux density) does not affect noises of mechanical and aerodynamic origin, provided that the r.p.m. of the motor does not change. Noises of electromagnetic origin may change through supply variation, but whether or not it appears in the resultant noise level depends on the level of predominance of the electromagnetic component concerned. The sound pressure level versus voltage curve is continuous, since the frequency of exciting forces and the passive system characteristics remain the same and the amplitudes of exciting forces change continuously. Extrapolating the zero voltage value of the curve, we obtain the sound pressure level of mechanical origin, $\bar{L}_{mech}$. The sound pressure level of electromagnetic origin is given by the difference between the sound pressure level without the fan and the sound pressure level of mechanical origin:

$$\bar{L}_{em} = 10 \log (10^{0.1\bar{L}'} - 10^{0.1\bar{L}_{mech}}). \tag{17.2}$$

Operating the electrical motor detached and under no-load conditions without attachments (e.g., with the fan wheel removed) may yield useful information on

the origin of the cause of the noise, if our personal noise experience is completed by the instrumental frequency analysis of the noise. The use of this expression is justified, since the human ear combined with the human brain and properly trained is a noise analyser of unsurpassable dynamic characteristics even if the dynamic range, in a broader sense, is meant to cover the spanned frequency range and the modulation of noise in time in addition to the noise intensity.

The vibration tests should start with a standard vibration measurement as well. The qualification is based on standard vibration velocity values. It is worth-while investigating the voltage dependency of the vibration of the electric motor, that is, how the decreasing amplitude of the supply voltage affects the vibration of the machine. It is well known that vibration of electrical motors is made up from vibrations of electromagnetic and mechanical origin. Extrapolating the zero voltage value of the vibration velocity versus voltage curve, we obtain the value of the vibration velocity of mechanical origin, v_{mech}. The value of the vibration velocity of electromagnetic origin may be computed from the following formula:

$$v_{cm} = \sqrt{v^2 - v^2_{mech}}. \tag{17.3}$$

In order to identify the causes of vibration, it is worthwhile carrying out the frequency analysis of vibration velocity. The extremely high axial vibration velocity is generally caused by bearing defects. Particular attention must be paid to the testing of vibration directly caused by eccentricity. From the measurable variation of the vibration velocity along the stator generatrix, we can determine unambiguously the degree of dynamic eccentricity. If a purely dynamic but considerable eccentricity characterizes the rotor, then the distribution of vibration along the generatrix is symmetrical parabolic. If dynamic eccentricity is combined with static eccentricity, this parabola becomes asymmetrical. When only static eccentricity is present, the distribution along the generatrix is uniform. The vibration distribution is nearly uniform also when vibrations of electromagnetic origin dominate. For the separation of these two latter cases, the above-mentioned procedure, i.e., the investigation of the voltage-dependency of the vibration velocity, may be used. When the distribution is independent of voltage, we can be sure of the mechanical origin. Whether it is static eccentricity or a bearing defect, it can be determined by frequency analysis. The rotational frequency, which is the number of revolutions per second, is a characteristic of the balance fault. A significant part of the electromagnetic force waves can originate from eccentricity. The static eccentricity may be measured by precision instruments after the motor has been dismantled. For the direct measurement of dynamic eccentricity on assembled, operational, fully enclosed machines, no procedure has yet been worked out.

Table 17.1. Some typical noise and vibration causes

Characteristic	Cause	Result
The frequency of the vibration equals the number of revolutions per second	Eccentric rotor or the bearing ring is oval	Vibration
Randomly varying frequency and amplitude	Tight or deflected assembly	Airborne noise Structure-borne noise Vibration
The frequency of the vibration is equal to, or a multiple of, the number of revolutions per second	Rubbing parts	Airborne noise Structure-borne noise Vibration
Strong change in amplitude on slight speed variation	Resonance	Airborne noise Structure-borne noise Vibration
Tonal components in the 200 to 500 Hz range	The rolling bearing is defective	Airborne noise Structure-borne noise Vibration
The vibration amplitude is slowly changing as the motor heats up	Thermal imbalance	Airborne noise Structure-borne noise Vibration
Wide-band frequency distribution, hissing noise	Ventilation noise	Airborne noise
The frequency of the noise is an integer multiple of the number of revolutions per minute	Siren effect	Airborne noise
The frequency of the noise is an integer multiple of the rotor slot number	Siren effect of the internal ventilation	Airborne noise

Table 17.1 serves as a quick reference for the engineer who works in the industry, listing several typical phenomena and the causes that generate them.

17.1.2 Testing the noise of a group of attached machines that incorporate an electrical machine

In practice, we frequently encounter a noise complaint but have no idea at first which element of the drive that incorporates the electrical machine is the direct cause. The required action, however, is always clear: we must reduce the noise. The first step is a general survey of the possible causes of noise. Figure 17.1 helps in this respect, illustrating the logical steps of noise analysis. The two main categories shown in the figure are statements and decisions. Each statement is

```
                          ┌─────────────┐
                          │   Noise     │
                          │  complain   │
                          └──────┬──────┘
                                 │
                      ┌──────────▼──────────┐
                      │ Noise measurement   │
                      │ on the complete unit│
                      │ frequency analysis  │
                      └──────────┬──────────┘
```

Noise complain

Noise measurement on the complete unit frequency analysis

Detached electrical machine operation. Does the noise persist?
yes — no

Detached electrical machine operation in lifted position. Does the noise persist?
yes — no

Detached operation of the loading machine. Does the noise persist?
yes — no

The airborne noise of the electrical machine dominates.

The structure-borne noise of the electrical machine dominates.

The load is the main noise source.

Operating the machine with the fan detached. Does the noise persist?
no — yes

Operating the machine group with unexcited electrical machine. Does the noise persist?
no — yes

Freewheeling the machine by turning off the supply. Does the noise persist?
yes — no

Noise of aerodynamic origin dominates.

Noise of mechanical origin dominates.

Noise of electromagnetic origin dominates.

The common noise of the machine group dominates.

White noise	Interaction noise		Cause	Capability	
- (two-side ventilation) - (separate ventilating motor) - changing blade shape - changing blade material - silencer over inflow and outflow ports - sound radiating enclosure	- (removing elements close to the blade) - unevenly spaced fan blades - sound absorbing enclosure	- (installing sliding bearing) - bearing lubrication - bearing replacement - precise bearing assembly - installing plastic-cage bearing - installing closed or double-closed bearing - axial pretensioning spring in the bearing - rotor balancing - vibration insulation - new foundation	- (slot number change) - (slot shape change) - (slot skew change) - (change of winding pitch shortening) - rotor balancing, (dynamically) - magnetic key bar - precise machining of interfacing surface	- mismatching the resonant frequency of the laminated core - plastic fan housing - vibration insulation - sound absorbing material - sound absorbing enclosure	- eliminating rigid coupling (e.g. installing induction clutch) - (aligning driving and loading machines) - clutch balancing - retrimming journal - vibration insulation - new foundation - sound absorbing enclosure

preceded by a measurement. The measurement, as the indispensable tool of probing reality, raising and solving problems, is inseparable from engineering work.

The flowchart shown in the figure clearly reveals three fundamental cases. The noise source can be the electrical machine itself or another machine coupled to it, but it can also happen that each component is quiet and exhibits low vibration levels in itself, so the noise is introduced by improper coupling. Through relatively simple experiments we can quickly identify the causes of noise, where the possible methods of noise reduction are listed briefly.

17.2 Selections from test reports on noise measurements of electric motors

The subject of the noise test is a multiple-speed three-phase squirrel-cage asynchronous motor. It is capable of continuous operation both in 6-pole and 24-pole mode. The rated supply is 3×380 V, the frequency is 50 Hz, the rated output is 5.5 kW at a speed of 900 min^{-1} in the 6-pole mode and 1.37 kW at 220 min^{-1} in the 24-pole mode. The motor is placed steadily on 4 mm thick vibration absorbers (to eliminate structure-borne sound transmitting bridges) directly on the sound reflecting concrete floor of the measuring room.

The noise measurement is carried out in a workshop with a volume of about 3000 m^3. Although the walls of the workshop are not covered with sound-absorbent material, the reverberation sound field correction turns out to be less than 0.2 dB owing to the huge space dimensions, so it is negligible. According to the results of the measurement, the basic noise level is at least 10 dB lower than the noise level produced by the motor, both for the A-weighted levels and for the one-third-octave-band levels, so correction according to the basic noise is not necessary.

The noise measuring system comprises laboratory instruments, calibrated before and after the measurements. The ambient temperature during the measurement is constant within ±6 K, the relative humidity of the air is constant within ±10 percent.

The noise measurement is carried out in accordance with ISO 3744. Owing to the fact that the largest dimension of the rectangular prism that encloses the motor is 0.48 m, the condition of $d>1.5l_{max}$ is satisfied by taking a sphere radius of $R=1$ m, and the use of a hemispherical measuring surface placed on the reflecting base is justified. The surface area of the hemisphere is 2π m^2. Eight measuring points are selected over the measuring surface.

Fig. 17.1. Schematic diagram of the practical noise reducing activity (see p. 270)

17.2.1 Determining the sound power level during steady-state operation.
Noise qualification

The A-weighted sound pressure level of the motor is determined at each measur-
ing point at both r.p.m. (pole numbers) under no-load conditions with slow
time constant. The one-third-octave-band sound pressure levels are also measured
in the frequency range 100 to 10 000 Hz.

Table 17.2. The measured A-weighted sound pressure levels, in dB

Pole number	Serial number of the measuring point							
	1	2	3	4	5	6	7	8
6-pole operation	66.0	65.7	63.0	61.5	62.5	62.4	64.8	61.2
24-pole operation	52.8	53.1	55.0	55.7	49.2	50.0	51.6	51.3

Table 17.2 lists the A-weighted sound pressure levels measured at the individual
measuring points. The average A-weighted sound pressure levels at the measuring
surface, calculated by logarithmic averaging, are the following:

$L_{A,6}=63.75$ dB   in 6-pole mode,
$L_{A,24}=52.85$ dB   in 24-pole mode.

It is worth noting that logarithmic averaging always yields a more accurate mean
value than arithmetic averaging, although the latter is accepted as the standard
when the spread of the sound pressure levels is less than 5 dB. In the 6-pole mode,
the spread of the sound pressure levels is less than 5 dB. If arithmetic averaging
were used, we would obtain 63.4 dB, which is 0.35 dB less than the logarithmic
figure. In the 24-pole mode, the spread is more than 5 dB, and arithmetic aver-
aging would result in an error of 0.52 dB.

The A-weighted sound power levels:

$L_{WA,6}=71.75$ dB   in 6-pole mode,
$L_{WA,24}=60.85$ dB   in 24-pole mode.

The tested motor is fully enclosed and equipped with external ventilation. The
basis for noise qualification, according to the relevant standard, is that for the
normal noise grade; the permissible A-weighted power level is 82 dB in the 6-pole
mode at a rated output of 5.50 kW, and 74 dB in the 24-pole mode at a rated
output of 1.37 kW. Since 5 dB is allotted to each noise quality grade under the
permissible limit, the tested motor is classified as Class 3 in both the 6-pole and
24-pole modes. For machines having various speeds, noise level has to be measured

at each speed grade and the machine has to be qualified speedwise for noise according to these results. For the machine, the worst noise qualification is characteristic.

The one-third-octave-band analysis of the sound power level is carried out at each measuring point, from which the one-third-octave-band power levels listed in Table 17.3 are obtained after averaging and applying the surface correction. As an

Table 17.3. The one-third-octave-band sound power levels in dB, computed from the measured values of the one-third-octave-band sound pressure levels

f_e, The centre frequencies of the one-third-octave-band filters, Hz	6-pole operation	24-pole operation
100	57.8	53.3
125	56.9	44.2
160	60.7	42.2
200	65.1	41.2
250	68.8	52.6
315	64.5	62.8
400	63.1	48.3
500	60.0	56.0
630	62.6	55.0
800	58.1	50.0
1 000	60.7	50.2
1 250	67.0	49.7
1 600	58.3	39.5
2 000	56.9	37.3
2 500	55.4	35.9
3 150	55.6	34.8
4 000	52.6	32.4
5 000	49.8	30.3
6 300	46.8	–
8 000	45.3	–
10 000	42.8	–

example, Fig. 17.2 shows the result of the analysis carried out by an analogue measuring system. The curve has been plotted by a level recorder. (The signal measured at measuring point 6 has been analysed.)

The asynchronous motor operating at constant voltage and frequency and under constant load can be considered as a constant noise source, but this does not preclude the possibility of a slight fluctuation of certain noise components or even the A-weighted sound pressure level. The amount and frequency of fluctuations in the various frequency bands are indicated quite clearly by the properly

Potentiometer range: __50__ dB Rectifier: __r.m.s.__ Lower lim. freg: __20__ Hz Writing speed:__200__ mm s⁻¹ Paper speed:____ mm s⁻¹

Multiply frequency scale by: ____1____   Zero level: ____30 dB____   A B C Linear
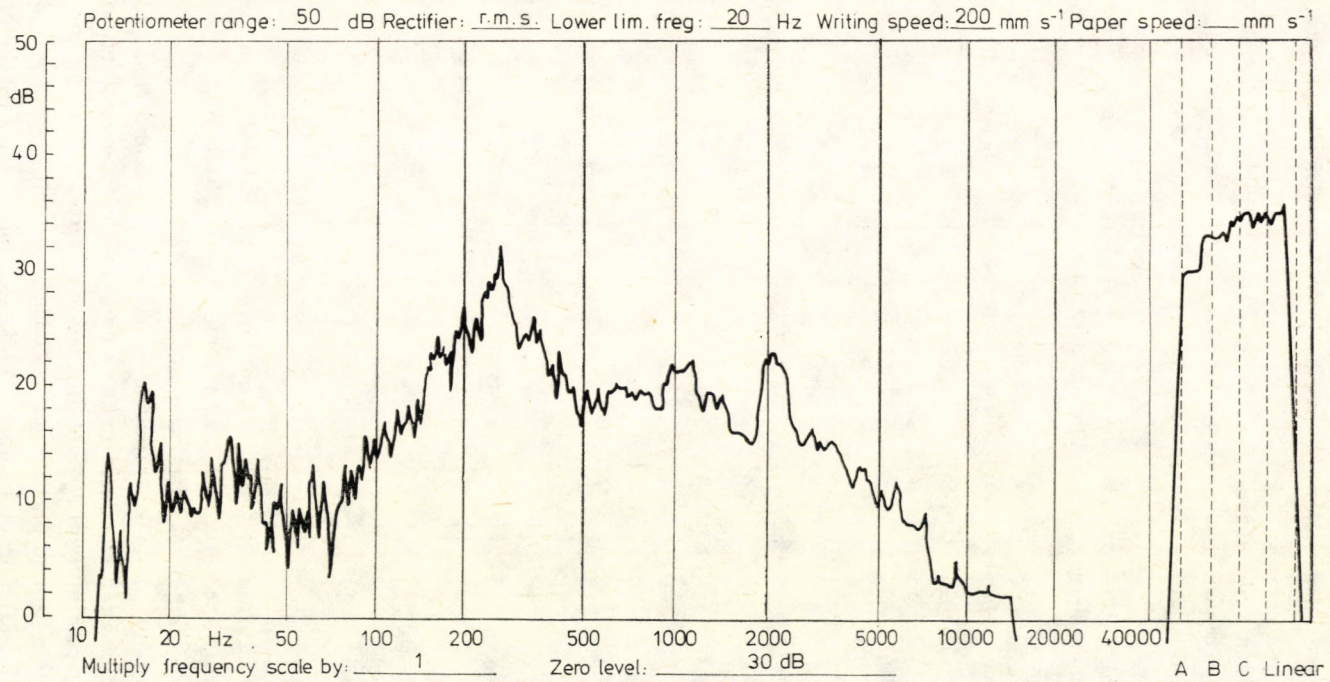
Fig. 17.2. The steady-state noise spectrum of an electrical machine running under no-load condition (in 6-pole mode)

Potentiometer range: __50__ db Rectifier: __r.m.s.__ Lower lim. freq.: __20__ Hz Writing speed: __200__ mm s⁻¹ Paper speed: ____ mm s⁻¹

Multiply frequency scale by: _____1_____   Zero level: _____30 dB_____
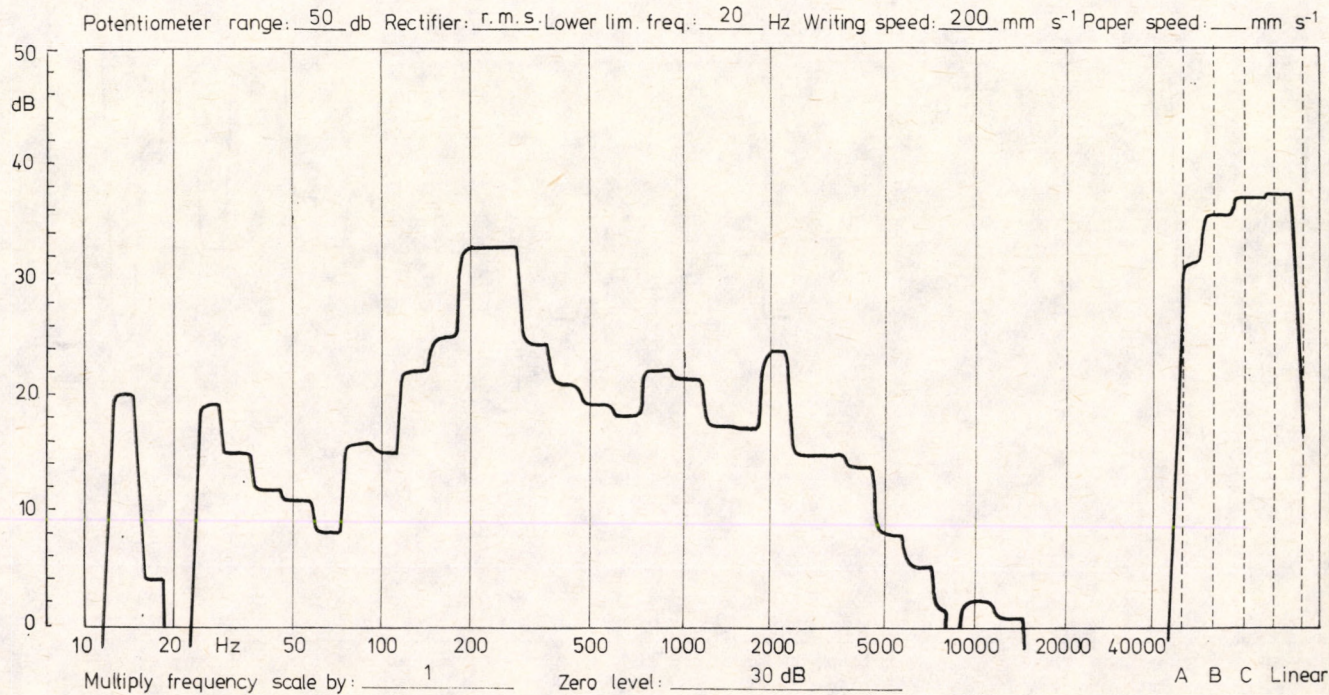
Fig. 17.3. The spectrum of a sample taken during recording the spectrum shown in Fig. 17.2
(6-pole mode)

Potentiometer range: __50__ dB Rectifier: __r.m.s.__ Lower lim. freq: __20__ Hz Writing speed: __200__ mm s⁻¹ Paper speed: ____ mm s⁻¹

Multiply frequency scale by: ____1____   Zero level: ____30 dB____   A B C Linear
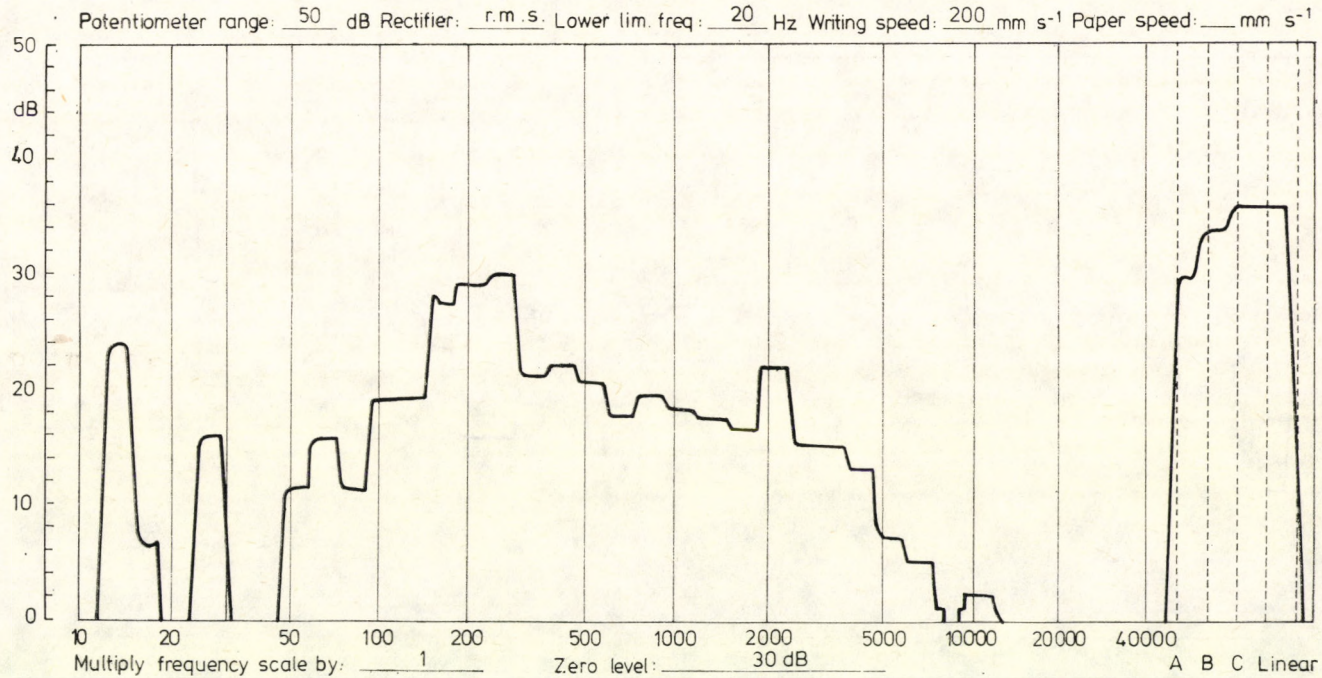
Fig. 17.4. The spectrum of another sample taken during recording the spectrum shown in Fig. 17.2. (6-pole mode)

set measuring system and the level recorder (see for example the one-third-octave-band at 250 Hz in Fig. 17.2), and therefore it may be misleading if the indirect digital measuring technique is used incorrectly. Even in the case of asynchronous motors considered as constant noise sources, we should not form an opinion on the basis of a short sample like a snapshot. Figures 17.3 and 17.4 show two spectra which were recorded indirectly, by digital sampling. The duration of each recording was 80 ms during the same time that the analogue frequency analysis was made (Fig. 17.2). The digitally recorded signal was analysed following repeated playback. As we see, the spectrum obtained this way characterizes only one instant of the motor operation and does not reflect reality.

17.2.2 Experimental testing of the starting transient noise
of a 6-pole asynchronous motor

The transient measurements are carried out at a selected measuring point. The microphone is directed to the motor at a distance of 1 m from the motor at a height of 0.4 m above the axis of the motor in a perpendicular direction. The asynchronous motor is completely detached for the test, with an inertial mass ($GD^2 = 23$ Nm^2) fixed rigidly to its drive side shaft. The motor is connected to the mains supply by means of a thyristor switch in a bounce-free fashion. This is a repeatable symmetric switching process.

The transient sound pressure signal that appears on starting is digitally recorded. The memory capacity of the instrument is 8 K, the sampling frequency is 20 kHz, the resolution is 14 bit, and so the sample length is 409.6 ms. The cut-off frequency of the low-pass filter is 5 kHz.
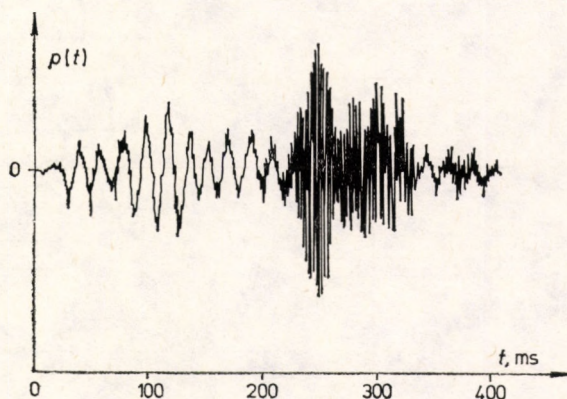
Fig. 17.5. The time function of the starting transient noise of the asynchronous machine

Potentiometer range: __50__ dB Rectifier: r.m.s. Lower lim. freq: __20__ Hz Writing speed: __200__ mm s⁻¹ Paper speed: ____ mm s⁻¹

Multiply frequency scale by: __10__   Zero level: __30 dB__   A B C Linear
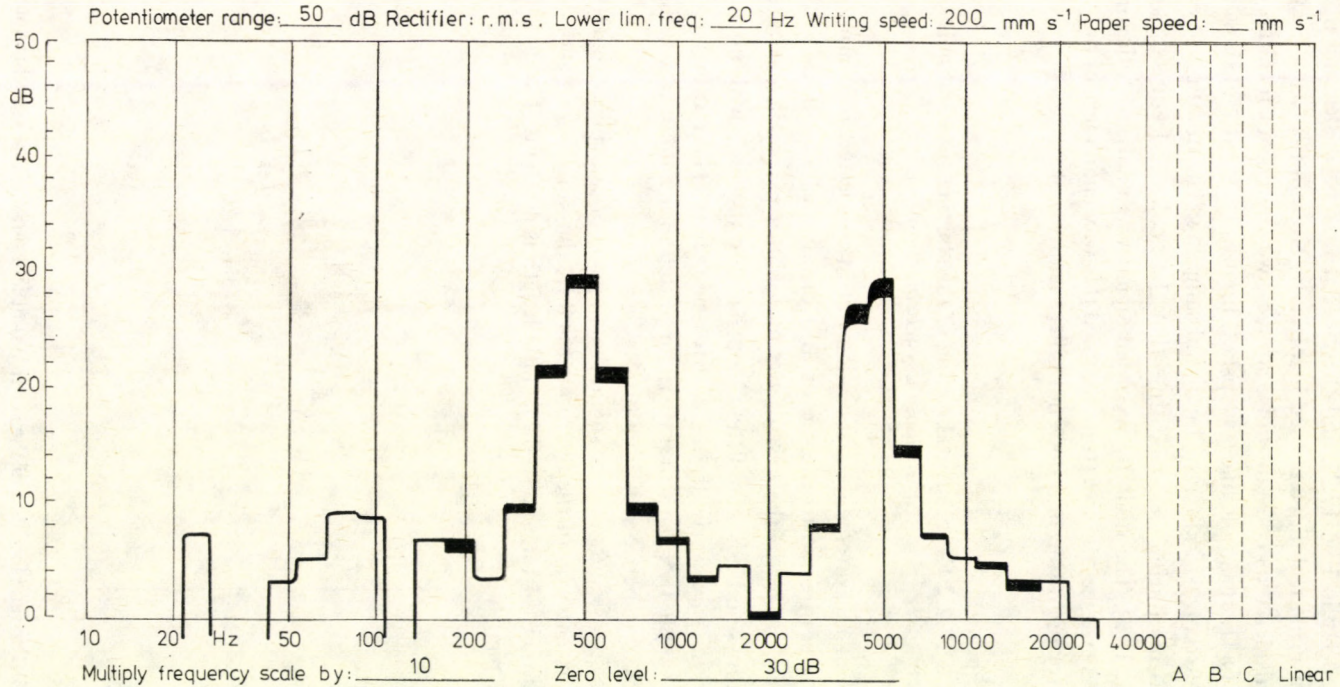
Fig. 17.6. The one-third-octave-band analysis of the transient noise signal shown in Fig. 17.5

Figure 17.5 shows the time function of the transient sound pressure signal. The signal $p(t)$, which includes the atmospheric sound pressure and the pressure variations produced by the motor, is slowed down when played back from the digital memory and recorded by an X–Y recorder. The time function clearly shows that at the instant of starting, the low-frequency signal is predominant, and strongly decreases as time goes by, while at about 250 ms the resonance at higher frequency is evident.

Now the signal packet stored digitally in the memory is made periodic and speeded up ten times to be analysed as a steady state signal by analogue instruments. Figure 17.6 shows the spectrum obtained this way. Because of the tenfold speeding (time transformation), the frequency values indicated along the x axis are obviously tenfold as well. When the spectrum is evaluated, we should bear in mind that the one-third-octave-band spectrum obtained is in effect an energetically averaged so-called equivalent spectrum, since by repeating the 409.6 ms signal packet of the recording and analysing it as a steady state signal we obtain the equivalent value relating to the time of the recording. We have to be careful, though, to ensure that the periodic signal packet includes only the transient signal and no steady state levels, not even zero levels exist, either at the leading or its trailing end. The weighted levels (e.g., the A-weighted sound pressure level) obtained from the analysis of the speeded-up signal are, of course, false, since the signals pass through the A-weighting filter of the analyser at tenfold frequencies. As we can see from the spectrum of the machine starting noise, the low-frequency component at the beginning of the transient is 50 Hz, while the high-frequency component appears near the lower frequency limit of the 500 Hz one-third-octave band. The spectra obtained by such periodization provide correct information about the frequency relations of the transient noise phenomenon, but the components appearing at different times during the transient are shown in the same spectrum and their magnitudes reflect a mean value energetically averaged over the recording time. The frequency of the higher-frequency component is determined by the narrow-band analysis of the periodic signal packet. The value obtained in our case is 452 Hz.

In the investigation of transient noise phenomena, the intensive study of the resonance phenomenon is always of utmost importance. Figure 17.7 shows the transient noise signal packet continuously passing through a constant percentage filter with fixed centre frequency of 452 Hz and with a bandwidth of 23 percent. The filter is followed by an r.m.s. network. The figure clearly shows the variation of the important resonant-frequency component with time. Owing to the settling time of the filter, the time function shown is behind the real process by several milliseconds. The signal is slowed down by a factor of 40 prior to being fed to the 452/40 Hz filter.
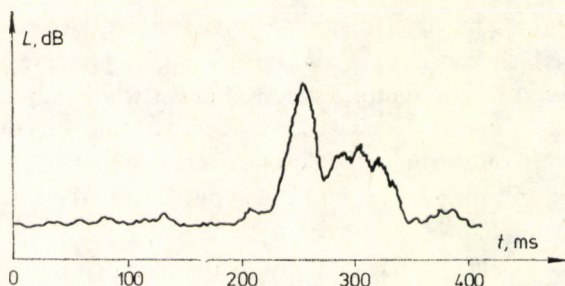
Fig. 17.7. The time function of the 452 Hz component of the transient noise signal shown in Fig. 17.5 measured with one-third-octave-band filter (r.m.s. value)

Figure 17.8 shows the variation of the r.m.s. value of the 452 Hz component obtained by scanning analysis applying the Hanning time window, one-third-octave-band filter and logarithmic amplitude scale. Scanning analysis applying the Hanning time window has developed in parallel with partial signal analysis, since if a constant time window is used for analysing a time segment, the results obtained turn out to be invalid owing to the different amplitudes at the start and end of
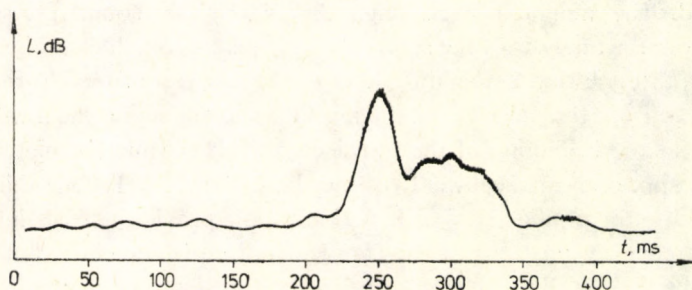
Fig. 17.8. The time function of the 452 Hz component determined by a one-third-octave band-pass filter and Hanning time window scanning (r.m.s. value)

the signal. The disturbing effect of signal segment ends can be eliminated by the Hanning time windows, although the perfect solution would be the Gaussian time window, but its realization is rather difficult.

Two practical tests are carried out applying the Hanning time window. One of them yields the result shown in Fig. 17.8. Here the time function of one component is determined by taking a 512-word sample from the signal, playing it back at the same speed it has been recorded and applying it to the selected filter, then proceeding to the next sample repeating the whole procedure in 512 cycles. This way a continuous curve is obtained from the average spectra of the 512 samples, where the settling time of the filter does not cause problems.
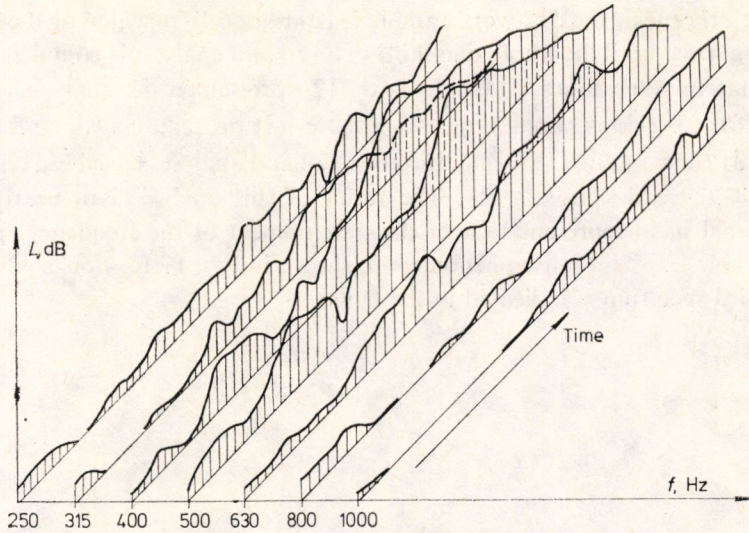
Fig. 17.9. Breaking down the transient signal by fixed frequencies

Comparing Figs 17.7 and 17.8, we see that the two time functions obtained by completely different methods exhibit close similarity, implying that the scope of analogue measuring system applications can be significantly expanded by the addition of a simple digital storage unit.

Figure 17.9 shows a three-dimensional set of curves, showing the r.m.s. value of the time functions produced by Hanning scanning in the range 250 Hz to 1000 Hz for the fixed-centre-frequency one-third-octave-bands.
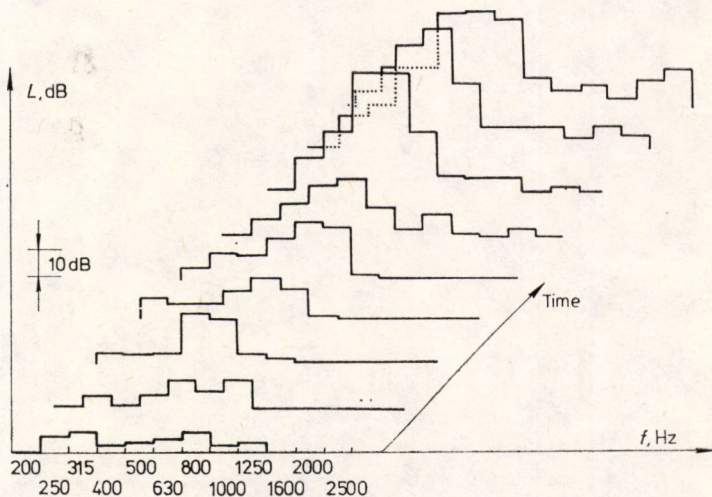
Fig. 17.10. Breaking down the transient signal by time segments

In the other test, the 512-word sample is continuously repeated at the original recording speed until the whole one-third-octave-band analysis is completed. Then we advance by 256 words and take the next 512-word sample for analysis (overlapping half the previous sample), repeating the whole procedure again and again (a total of 31 times) until all the one-third-octave-band analyses have been completed on the 8192-word sample stock. The result of this analysis is a nearly three-dimensional lucid representation of the development of the frequency spectrum of the whole transient noise phenomenon, shown in Fig. 17.10. For lucidity, only every third spectrum is indicated in the figure.

18. APPLYING VIBRATION MEASUREMENT TO ASSESSING THE TECHNICAL CONDITION OF ROTATING MACHINES AND TO SCHEDULING THEIR MAINTENANCE

18.1 The development of maintenance systems

From the moment they are put into use, the tools and machines are subject to wear and tear, they deteriorate or break down, and so sooner or later we have to provide for their replacement. Until the machine is simple, cheap and its operation can be easily detached from the other machines, the most straightforward way of catering for its replacement is to purchase and store a reserve machine and keep it ready for putting into operation at any time.

In the old days, machines were used until they became useless, then the operators took the time and replaced them. During technical development, however, processes and technologies have become more and more complex. The inter-depency of the machines and their sophisticated construction and cost prevent simple overhauling in a straightforward way. This demands today a special activity called planned preventative maintenance. Owing to the high purchase costs and the interests on the locked-up capital, we cannot afford to keep spare machines in stock, nor risk a breakdown, since the unexpected shutdown of one phase would result in the shutdown of all the other connected processes causing considerable production losses.

Different forms of maintenance planning are in general use. Simplest of all is maintenance at specified intervals. Based on statistical observation of failure frequency and on technical considerations, all the machines and equipment belonging to a given technological unit are shut down at regular intervals, the worn parts are replaced or renewed, lubricated and set, etc. This method is better than waiting for actual failure, and reduces the frequency of unexpected break-downs that cause considerable damage, but it has numerous disadvantages as well. It is based on statistical observations and consequently does not take into account the inherent difference between machines. Even among the same models, it may happen that the maintenance period is too short for one particular machine, which would not require replacement or renewal, while another may break down between two scheduled shutdowns.

In recent decades, efforts have been made to refine the fixed period maintenance method. Realizing the relationship, also statistical, that machine wear depends

on effective operating hours and, moreover, on the load, the operation of the machine was monitored by various recording instruments, and shutdown and maintenance were scheduled on the basis of this observation. This method is better than the previous one, although it is still built on indirect statistical observations and not on the actual physical-technical condition of the machine.

Fixed period maintenance, of course, may play an important role in the future as well. In applications where small and cheap machines run in high numbers, the use of failure statistics proves to be a good tool to depend on and the continuous operation can be ensured by a relatively small stock of spare parts and machines with high reliability.

In the case of expensive single-purchase units of key importance within an essential technological process (e.g., safety equipment, the basic unit of a continuous process, a machine of strategic importance, a machine in an overloaded mine, rolling mill or chemical plant, etc.), the situation is quite different. We cannot keep a spare machine in stock all the time, their repair is too costly, but, on the other hand, an unexpected breakdown is inadmissible.

Machines never break down by chance. Their operating condition gradually deteriorates, and this gradual quantitative deterioration of the parameters which characterize their technical condition transforms into a failure manifesting a
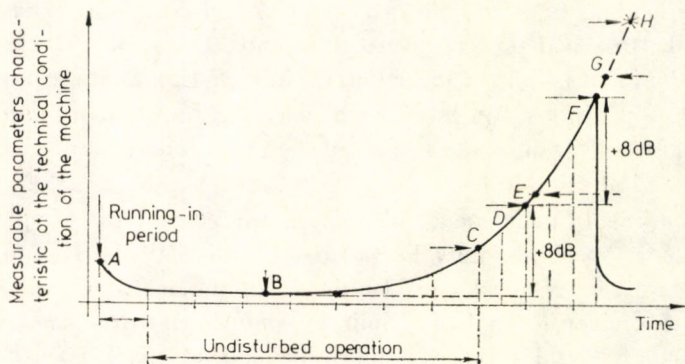
Fig. 18.1. Typical behaviour of change in the technical conditions of machines: A — new or renewed machine, B — reference value, C — the starting defect is noticed; detailed diagnosis, D — the maintenance engineer identifies the defect and makes arrangements for the necessary repair, E — first alarm level in the automatic monitoring system, F — the planned maintenance work is completed, G — second alarm level in the automatic monitoring system, H — failure of operation

qualitative change. This process is illustrated in Fig. 18.1. The character of the curve is similar for any machine. The most individual, specific parts of it are the length of the stable, undisturbed running time and the level of the parameter

measured during normal operation. First we should point out that the absolute value of any single parameter is not enough for the determination of the technical condition of the machine, but we must determine the sense and magnitude of the change of the parameter.

The technical condition of electrical rotating machines and, in particular, the commonest a.c. machines is characterized by electrical and mechanical parameters together. The most important electrical parameter is the condition of insulating materials, since their insulating capability deteriorates with time. The dielectric strength and the tendency for different types of leakage can be checked quickly by electric instruments without dismantling the machine. A discussion of these methods is outside the scope of this book.

The case of mechanical parameters, mechanical sources of defect, is completely different. The technical condition of these sources suffer the strongest deterioration during operation (e.g., bearings). The electromagnetic causes of vibration are generally rather constant. The exact determination of mechanical inaccuracies is possible only after the machine has been dismantled, so we can learn the possible fault only if we take the machine apart. To order the necessary components at this time is too late, since the machine would be out of service for a long time. On the other hand, to keep a spare for each component in stock would require considerable investment. Of course, we may find that all the components are in good operating condition. In this case, however, the cost of time and effort spent on dismantling and assembly must be recorded as loss. We have not yet mentioned that the assembly itself may serve as a source of defect, in other words, the dismantled or reassembled machine can be better or worse than before we touched it. Thus it would be good to know the real technical condition of the mechanical sources of defects during normal operation of the machine. Knowing this, we could carry out the repair, overhaul or replacement whenever it is really required, on a planned basis. We should know in advance what is needed for the repair, to stock up in time. This way we would not have unexpected trouble or shutdown, or unnecessary dismantling or maintenance.

Several decades of international professional experience and practice have dictated that the mechanical vibration of electrical machines is the right parameter to be measured, to indicate best the technical condition of the machine. Thus it is the best choice to base economic, reliable maintenance planning on.

18.2 General considerations for determining the technical condition on the basis of vibration measurements

There is a causal relationship between the mechanical vibration measurable on the surface of the electrical machine and sources of defects inside the machine.

The measuring procedures outlined in the relevant standards are generally applicable to vibration measurements of any purpose, but the use of the vibration limit values require thorough consideration beforehand. When the task is to determine the quality of a single new or reconditioned motor in terms of vibration, the motor should run detached under no-load condition for the measurement. The machine as a product can be classified on the basis of the limit values set out in standards for vibration levels. This is a relatively objective procedure, since the detached set-up of the machine is well defined from the vibrational point of view and the result of the measurement is reproducible. The standardized limit values are also acceptable for vibration qualification when we want to determine the effect of the machine on its surroundings, the building, the floor, etc., or, in general, what it is like. In this case, a general normative is required and the standards satisfy this requirement with their vibration quality grades (see, e.g., ISO 2372). This is, however, only an instant in the life of the machine, a single snapshot. In a similar way, we cannot judge the physical condition of a 40-year old man from the fact that he can lift a 20 kg weight—the only thing we know for sure is that he can do it right now. Maybe a year ago he could lift 100 kg sacks easily but because of his ulcer he can only lift 20 kg today. But maybe he has never lifted heavier weights in his life and this is the accomplishment he can do in good health for at least 50 years to come.

To be able to plan maintenance, we must know the trends of changes in the technical condition and vibrational characteristics of the machine.

The vibration of an electric motor varies during operation as shown by the curve in Fig. 18.1. The vibration curve of a motor to be tested can be determined by discrete sampling or by continuous measurement, depending on the importance, accessibility, etc. of the machine to be tested. If the machine is set up at a relatively well accessible location and several separated machines are to be measured this way, the individual points on the vibration versus time curve are determined by regular measurements. When the ascending slope of the curve is noticed, the sampling frequency must be increased. In the case of expensive, crucial or difficultly accessible machines, it is worth carrying out continuous vibration measurement and recording with a built-in automatic fault indicating facility. Devices of this kind with simple design are called vibration guards.

The question must be put again—which of the three vibratory parameters, i.e., acceleration, velocity or displacement, to measure? Based on details in Chapter

12, it is clear that when the standard qualification measurement is conducted and standard quality grade tables are to be used, the resultant r.m.s. vibration velocity must be measured in the range 10 Hz to 1000 Hz. The situation is slightly different in the case of vibration measurements to support maintenance planning. The question is the adequacy of the measurement of the resultant r.m.s. vibration velocity in however wide a frequency range, in other words, a single-value measure= ment. In our opinion, it is not adequate and what is really needed is frequency analysis, although the requirements for the measuring system and measuring time are higher. The wear or defect of a machine component will primarily alter one single component which affects only indirectly the resultant r.m.s. value through the process by which this value is derived. If the fault changes a component whose previous magnitude was negligible, then, say, a tenfold increase in this component, which can mean possible danger at the given point, is hardly noticeable in the resultant r.m.s. value. Monitoring the variation in the individual vibration com- ponents by frequency analysis of the vibration is a much more sensitive method for indicating defects. Another advantage of the spectrum analysis of the vibration signal is the general ability to identify the cause of the vibration (the source of the defect) on the basis of characteristic frequencies during normal operation, (see Chapter 17), without the need to dismantle the machine. In this way, the engineer knows before starting his maintenance work what to look for when the machine is switched off, and can make necessary preparations in time, providing for the parts and tools required. Of course, this also shortens the time required for maintenance. The autocracy of vibration velocity as the vibrational charac= teristic to be measured may be challenged by frequency analysis itself. Frequency analysis is carried out to provide information on the frequency composition of the vibration. Because of the finite dynamic range and resolution of the vibration measuring system, it is advantageous if the vibration components to be measured stay within the dynamic range of the measuring system (normally 50 dB) in the whole frequency range spanned by the system, that is, when drawing up the spec- trum by a level recorder, the level is more or less uniform. Knowing that frequency analysis breaks down the vibration into its harmonic components and that the relation $a = \omega v$ stands between the vibration velocity and vibration acceleration of the individual components, we deduce that if the energy contents of the individu= al components are nearly the same, then it is worth carrying out the analysis of vibration velocity, while if the energy content of the individual components decreases with increasing frequency, then it is better to analyse the vibration acceleration signal.

The amount of change indicating deterioration in vibration quality is another question. From experience, the literature unanimously claims that an 8 dB in-

crease in a vibrational parameter corresponds to a jump to the next lower quality grade.

The methods used so far are the following:

(1) The vibration guard. The vibration guard is simply a vibration measuring and indicating device in continuous operation. This device is used in applications where a valuable high-output machine is running at a place remote or hard to access or in explosion or radiation danger zone or otherwise hazardous area, and the unexpected breakdown of the machine would cause great losses. Also, this device is preferred in places where operating trouble may develop very quickly, such as the breaking of a turbine blade. The information-carrying signal of the vibration guard is provided by a vibration sensor placed in the machine in the factory, or mounted later. The electrical signal proportional to the vibration is led to the processing unit through a measuring cable. Here the actual vibration signal, which can be vibration acceleration or velocity, peak or r.m.s. value, in the whole frequency range or only in certain bands, is compared with the preset level(s). In multistage vibration guards, a sound of warning is triggered when the first level is reached, while the device turns on the alarm and shuts down the plant if the second, emergency level is hit. The advantages of vibration guards are their simplicity and being automatic. Their disadvantage is that this system is inherently sensitive only to serious defects and the information they pass on to the operator is too quantized, recognizing only three levels, namely, safe operation, and shutdown where the defect is expected. They do not indicate the frequency of the increasing component(s), so they cannot provide any information on the location and nature of the defect. They do not show us the trends of vibration level development, so the expected shutdown or maintenance requirement cannot be predicted in time. As they necessarily monitor a wide frequency range, their action is slow and they are sensitive only to "rough" faults. These deficiencies may be eliminated but then the vibration guard becomes too complex and transforms into a method of "continuous vibration measurement with frequency analysis and computer processing", losing its simplicity and cheapness.

(2) The SPM method. The commonest mechanical failure arises in rolling bearings, and therefore a separate method has been worked out to detect bearing defects. In the rolling bearing, a defect passing over the surface of the roller or raceway gives rise to a pulse-like excitation (shock pulse). Expanding this pulse-like excitation in a Fourier series, the high-frequency oscillations depend primarily on the running condition, the dimensions of the bearing and the rotational speed. Swedish engineers have developed an instrument for measuring the condition of bearings. This instrument has a built-in high-pass filter to suppress the usual frequencies of bearing vibrations and electromagnetic vibrations. The remaining

high-frequency (ultrasonic) components are combined to a resultant which is compared with a preset reference level. Based on the difference obtained by the comparison, the bearings are classified into three categories; good, fair, and defective. Considering the fact that in this case the high-frequency components play the dominant role, we must pay special attention to the fixation of the sensor. It must be rigid, and possibly a screwed design. The SPM method is also based on the regular measurement, since the signal obtained looks like that shown in Fig. 18.1.

To test the reliability of the SPM method, Siemens AG carried out a comprehensive series of experiments in their factory in Nürnberg and at the premises of the users of the machines manufactured in the factory [103]. Around 450 motors were involved in tests in the 200 to 2000 kW output range. The method takes into account the dimensions and the rotational speed of the bearings as modifying factors, but, according to the experiments, the high-frequency vibrations are also influenced by the location of the sensor (its distance from the bearing), the radial clearance of the bearing and even the quality of the lubricant used. These ignored factors alone can cause a change of at least one and a half in quality grade. According to the Siemens experiments, the magnitude of the high-frequency vibration values in itself, determined by the SPM method, is not decisive in judging the goodness of the bearing. Numerous bearings were found which were deemed useless on the basis of the SPM value, but in fact they ran without any problem for a considerable length of time (no other information-carrying parameter—the bearing noise, the bearing vibration measured by the standard procedure, the heat build-up in the bearing—indicated a defect). Consequently, by experience, the SPM value alone cannot serve as a basis for assessing the quality of the bearing. We may use it, among others, as an indicative factor, and especially the nature of its variation with time may provide some useful information.

(3) Cepstrum analysis. Cepstrum analysis is a tool for discovering the periodicity in the frequency spectrum, but it can identify a different kind of periodicity, namely when the spectrum includes side-bands at equal distances from one or more carrier frequencies. The existence of these side-bands is especially important in analysing the vibration signals of drives, since many defects result in the modulation of the vibration parameters of gear engagement and this modulation gives rise to side-bands in the frequency spectrum. The cepstrum can be produced in various ways—one is digitally, by an algorithm similar to the fast Fourier transformation. This is a fast and effective method requiring a digital computer. The operations are done in real-time mode. There are other techniques as well, purely analogue or hybrid analogue-digital procedures. With the spreading use of advanced measuring techniques it is anticipated that this method will be used in routine measuring practice.

18.3 The practical implementation of technical condition assessment on the basis of vibration measurement

Through the previous chapters, many methods, principles and technical considerations have been discussed and, on their basis, the technology of testing by vibration measurement can be summed up as follows.

The steps of vibration measuring:

(1) The quantity to be measured is vibration acceleration from which vibration velocity is obtained by integration, this latter being the quantity to be processed and evaluated. By means of a standard filter we must determine the resultant r.m.s. vibration velocity in the frequency range 10 Hz to 1000 Hz. Then we must determine the frequency spectrum of the vibration velocity (or the acceleration if considered better) by means of a narrow-band frequency analyser. The measuring points must be selected in accordance with the vibration measuring standards relevant to electrical machines.

(2) By vibration measurement on the new or renewed machine, we must determine the reference values for the resultant effective value and for the spectrum as well. The reference value of the resultant r.m.s. vibration velocity is obtained by adding the measuring uncertainty of the measuring system to the values measured on the new machine. The reference spectrum is obtained from the vibration velocity spectrum measured on the new machine through the following steps:

— The spectrum is shifted upwards by an amount corresponding to the measuring error of the vibration measuring system.

— The spectrum is shifted by one bandwidth to the left and to the right along the x axis. This is necessary because the supply frequency might change slightly during subsequent measurements, and the load can also change, and these result in a change of rotational speed. These changes would cause virtual changes in the vibration spectrum and turn out to be misleading.

In this way, the reference vibration values, either the resultant r.m.s. vibration velocity or any vibration component on which the time function shown in Fig. 18.1 can be built, are at our disposal.

(3) When the reference vibration values are being determined, it is worth identifying the causes of the individual vibration components. If we are uncertain about the mechanical or electromagnetic origin of a vibration component, we can carry out the experiment of switching off the supply voltage or apply the ZOOM technique that provides extremely fine frequency resolution. This may be required in the case of two-pole asynchronous motors in order to separate the $2f_1 = 100$ Hz electromagnetic and the ~ 99 Hz mechanical component, where the latter corresponds to twice the rotational frequency of the motor.

(4) The vibration measurement as in (1) must be carried out at regular intervals (one or two months for a machine in good condition) and this way we must determine the points of the curve shown in Fig. 18.1 for the resultant r.m.s. vibration velocity and for the important vibration components as well. This regular vibration measurement, of course, can also be continuous. The $+8$ dB and $+16$ dB levels with respect to the reference level must be determined as well, since these are the first and second alarm levels when the maintenance engineer or the designer must interfere and make the necessary decisions. When the first level is reached and we can see which component increases strongly, it is recommended that the possible source of the problem be identified again in order to schedule the maintenance work accordingly.

When the maintenance is completed, the whole vibration testing process recommences by determining the new reference values.

18.4 The organization levels of vibration testing

Four different organization levels can be set up for the realization of vibration testing:

(1) When only a few machines are to be tested, possibly at the same place, then manual in situ evaluation is possible in such a way that all the necessary instruments are moved to the site and the measurement, analysis and recording is carried out right on the spot. The processed results leave the site of the measurement recorded in writing. This method requires least preparation, but transport of the instruments is inconvenient and specially trained personnel is required on site.

(2) When a company intends to implement a vibration testing system on a regular basis involving more than one plant (location), it is practical to separate the measuring and evaluating function for economic use of time and skilled personnel, as well as to save the instruments. In this case, the signal measured and amplified by the sensor on the machines to be tested is stored on a mass-storage media (e.g., magnetic tape unit) and evaluated later in a central laboratory. This way the number of instruments to be moved and the time spent on the measurement decrease significantly and the actual measuring can be carried out by an intelligent skilled worker. Since numerous machines are involved in the vibration testing, each machine must have a separate file in the special central evaluating laboratory, where all the information and measurements relating to the machine concerned are stored.

(3) If many machines are to be tested, the complete evaluation process can be put on a computer. With carefully evaluated software, a digital computer, which

is capable of accomplishing technical tasks, can carry out the frequency analysis, compare the vibration values, record the results and even derive simple con-clusions.

(4) As a further step in development, the actual measurement can also be controlled by computer. In this case, the sensors must be mounted permanently and a signal cable system must be laid out between the computer centre and the machines to be tested, so the measuring period can be controlled by computer as required, or we can have continuous testing of each machine simultaneously.

On the subject of economic advantages of maintenance based on the technical condition assessed by vibration measurement, a study was written in 1978 in England, which revealed that if this method were introduced generally in industry in England, it would yield an additional 750 million pound profit annually. Since general implementation of the method is not feasible all at once, they computed that if only the highly concentrated large industrial complexes, most appropriate for this purpose, adopted the method, where the preconditions are automatically given, even then the annual profit would be 250 million pounds.

EPILOGUE WITH ECONOMIC CONSIDERATIONS

The evolution of human society indicates the ever expanding exploitation and utilization of natural resources. Our intervention in the life of nature and of the environment as a consequence of technical development is increasingly extensive. We are steadily approaching the point where modification of the living environment in one country affects the life of whole continents. It is a very regrettable fact that in too many cases decisions are made about certain elements of an extremely complicated and sophisticated system to satisfy local or peripheral interests, without following up the consequences in terms of the overall system.

Recently, we have come to realize that it is not only the mineral resources and agricultural lands—allowing various levels of cultivation—that make up our natural resources as being subject to relatively accurate quantification, but also other factors of the natural environment that can be expressed only vaguely, if at all, in numerical terms. These "secondary" elements are becoming more and more important. It cannot be sheer chance that resorts are springing up at various places of the world that have barely been touched or disturbed before, and new housing developments are gradually spreading over our hills and woods.

An environment polluted by noise and vibration is harmful to our health and simply prevents us from carrying out certain type of intellectual or physical activities. Tiredness significantly increases the number of faults made in our work, both directly and indirectly. The required protective measures are generally rather costly.

We must realize that we can sense the ramifications of the noise and vibration problem in every field from material consumption (e.g., increased dimensions due to dynamic load) through dependable operation (defects originating from vibration) to investment cost development (vibration insulating foundations). Appropriately projecting these economic effects to concrete tasks that arise, we can analyse and quantify them on a proper scale.

Among noise and vibration sources, we find electrical machines that play an important role in our technical development. Realizing their importance led to relatively early concern by the designers of electrical machines in noise and

vibration problems (e.g., various slot numbers), so the standards that specified the methods for the noise and vibration measurements of these machines had been worked out and issued before all other mechanical specifications.

Of course, the electrical machine operates in a certain environment and forms part of a certain acoustic system. To achieve a correct or acceptable noise level and to find the right strategy leading to this achievement is possible only through the cooperation of the operator, the user and the manufacturer of the electrical machine. The noise and vibration quality specifications relevant to electrical machines can be assessed only on the basis of their being in accordance with the requirements of the technical process and of the environment. It is useless to work on reducing the noise of the electric motor, if the noise level of the process it is involved in is much higher, since it would not result in any technical or economic advantage.

If, however, the electrical machine turns out to be the dominant noise source of a complex equipment, then the purchaser and manufacturer of the machine should jointly select the optimal method of noise reduction on the basis of a technical analysis. The user of electrical machines is primarily interested in the harmful noise level at the place of installation in the surroundings of the electrical machine. This is the very parameter on which the limitations of the relevant emission standards, laws and regulations are imposed, in other words, the restrictions refer to the terminal point of the acoustic system comprising the three elements, namely, the source, the path and the sensor. The task is to find the right arrangement of the noise source and noise path. Different levels of noise reduction can be achieved at any element of the acoustic system, but the optimum solution must be selected in view of the technical difficulties of the implementation, the restrictions imposed by the given environment and certain economic considerations.

Even if the electrical machine is considered to be the source of the noise, this fact must not be handled as a rigid category if we want to bring a sound technical decision. Nevertheless, it is worth breaking down this component of the complex acoustic system a little further into the real active noise source (i.e., winding, iron core, bearing, slip rings and ventilation system elements which take part directly in the electromagnetic energy conversion of the electrical machine) and the other structural components of the machine (i.e., housing, brushes, brush holder, etc.). The housing seems to be the noise source because it hardly damps (through transmission loss) the airborne sound produced inside the machine or because it transmits and emits a part of the vibrational energy produced by the active energy transforming parts in the form of structure-borne sound (e.g., the housing of large machines, the casing of a refrigerator, etc.).

The second element of the complex acoustic system, the noise path, can also

be broken down into two parts. The first is the normally gaseous medium between the noise source and the sensor, while the second is a solid body connected in series or in parallel with the first (e.g., wall, floor, etc.) that can either absorb the noise or act like a secondary sound source by radiating the structure-borne sound. Finally, the third element, the sensing human being, can be considered as a complex system comprising a receiver (including the ear, external ear, cranial bones) and a processor proper (human brain).

To observe the emission specification that relates to the very end of the acoustic system, we may interfere at any point of the system, as we have shown before, so we can hit the target in many different ways. The optimal solution can be selected only by taking all aspects (certainly including the aspects of economy) into account. As we have discussed, for example, in Chapter 7, some of the constructional methods of noise and vibration reduction, like the correct selection of slot number, correct determination and realization of rotor slot skewing, offer noise reducing methods that cost almost nothing, but cannot be realized as an after-measure. Of course, there are really expensive constructional noise reducing measures, such as increasing the thickness of the stator yoke or decreasing the flux density in the machine, etc. One certainty though is that secondary added noise reduction is almost always more costly.

APPENDIX

A.1 Vibroacoustic standards

A.1.1 The system of standards

Standards belong to the category of special legal provisions. Vibroacoustic phenomena may be approached from two aspects. One is the investigation from the direction of the source. The standards that specify the measuring procedures and limit values for the physical parameters of sources are called emission standards. When the problem is approached from the sensing element, namely, the human being, and we investigate the amount of noise or vibration that acts on the sensing human, we refer to imission standards. The emission standards and, in particular, the included standards that specify the limit values, are relevant to a given type of sources, and so they appear in the form of product standards reflecting and recording the relationship of the purchaser and the manufacturer of the product. The imission standard, in turn, is independent of the type of the source, but is a general health regulation. The operator of the machine is responsible for the observation of imission limits.

When the standards are studied, the whole system of standards must be reviewed. The investigation can lead in various directions. On the one hand, we can study the thematic hierarchy, and on the other, the hierarchy in terms of the scope of validity. By deductive classification, the levels in terms of thematic hierarchy for emission standards are as follows:

— the measuring of the parameters of vibroacoustic phenomena, in general,
— the determination of the vibroacoustic parameters of machinery noise and vibration sources,
— noise and vibration measurements on rotating electrical machines.

The hierarchy in terms of the scope of validity, progressing from the individual towards the general, is:

— national standards,
— the ST CEV (international) standards developed on the basis of an agreement on standards signed by the COMECON countries,
— general international standards, ISO, IEC.

Because of the dynamism of the process of standard framing, it is not guaranteed that every standard of this dual hierarchy is effective and functional simultaneously. It follows from the essence and final objective of the matter that the review, maintenance and updating of standards is a continuous process and in order to be able to find the way in this ever-changing mass of standards, the person who performs and evaluates the measurement must be aware of the complete system, the relationships between the individual components of the system, and their similarities and deviations.

A.1.2 Vibration measuring standards

Almost all the standards relevant to vibration testing of machines are based on the r.m.s. value of the vibration velocity. Exceptions are those which control vibration measurements on machines that act directly on the human body (e.g., hand tools). According to doctors, in these cases the important parameter is vibration acceleration.

The emission standards can be classified further. Some of them, the more elaborate, are the product standards that qualify the vibrating machine. These standards render the machine independent of its surroundings as regards vibration theory and investigate under reproducible conditions the amount of vibration produced by the detached machine. Comparing the measured value with the standardized permissible vibration values, we can determine the vibration quality grade of the machine.

The situation is not so simple if the vibration of the machine is tested at the installation site in the normal operating environment. As we have seen before, the vibration of the machine can be strongly influenced even by the rigidity of its fixation on the foundation. In addition, the vibration of the machine may be influenced by the load condition and by any other machine mechanically coupled to it, not mentioning the "background" vibrations that arrive from the surroundings through vibration transfer. It is easy to see that the evaluating and conclusion-drawing phase of vibration measurements carried out under normal operating conditions is much more complicated than a simple product qualifying vibration test. It is therefore not by mere chance that we find much fewer standards for in situ vibration measurements, and the limit values specified by them are recommendations rather than strictly observable rigid limit values.

As we see, there are quite enough standards to deal with. Fortunately, there are definite similarities between standards relevant to the same subject and certain basic principles are even identical. Most referred standards are common in that they take the largest value of vibration velocity, called as vibration severity, as

characteristic of the vibration, and the performance of the machine is judged by the vibration severity measured, and this parameter is limited by the values set out in the standards. According to the standards, the vibration testing must be carried out in the steady-state operating condition of the machine.

Standards for vibration imission, that is, measuring and classifying procedures of vibrations to which human beings are directly exposed, are just being drawn up at national and international levels. The reason why the regulation of emission measurements lags behind the emission standards is that the framing of imission regulations is not purely a technical or legal question. The objective of such measurements is the direct protection of human beings, so the targets must be set by medical science. Considering the fact that the human organism is much more complicated and diversified in its reactions than any technical invention, the determination of the parameters to be measured, the measuring procedures to be used, the measuring points and the permissible values demands prolonged scientific preparations and extended experimental investigation.

A.1.3 Noise measuring standards

Emission standards aim at the determination of the sound power level of machines. They clearly state that the airborne sound of the machine is of interest, that is, the sound power emitted directly by the machine to its surroundings. It is very hard to distinguish this, especially for large machines, from structure-borne sound of the machine at the point of sensing, because the machine transmits part of its vibrational energy to its surroundings, which, excited, becomes a secondary sound radiator. The sound energy passed on to the sound field of the measurement this way increases the sound pressure level measured at the measuring point. The amount of this increase, however, is really uncertain, and depends on the foundation, the energy converting efficiency of the secondary sound radiator, etc. In most cases, it is assumed that the structure-borne sound can be neglected. This means rounding off for safety, since the actually emitted airborne sound power is certainly not larger than the measured value.

The structure of the standard worked out recently by the International Organization for Standardization (ISO) for noise measurements is as follows. ISO 3740 provides general directives for the sound power level determination of machines as noise sources. It lists the possible standardized measuring procedures from which one should be selected to match the acoustic conditions prevailing at the place of measurement and in accordance with the objective of the work. There are seven different measuring procedures permitted by the standard, detailed in the series ISO 3741 to 3748. Table A.1 summarizes these standards.

Table A.1. Comparison of noise measuring standards

Aspects		Symbol and number of standard						
		ISO CT CEV	3741 3080	3742 3080	3743 1414	3744 1412	3745 3076	3746 1413	3747
Type of noise source	Large noise source immovable,					X		X	X
	Small noise source movable	X	X	X	X	X	X	X
Nature of noise	Steady-state broad-band	X		X	X	X	X	X
	Steady-state narrow-band pure tone		X	X	X	X	X	X
	Varying in time			0	X	X		
Accuracy class of the method	Precision	X	X			X		
	Engineering			X	X			
	Survey						X	X
Utilization of the result	Noise testing	X	X	X	X	X		
	Type testing	X	X	X	X	X		
	Comparison — different types	X	X	X	X	X		
	— same type	X	X	X	X	X	X	X
Obtainable information	Octave-band values	X	X	X	X	X		
	One-third-octave-band values	X	X		X	X		
	A-weighted levels	0	0	X	X	X	X	X
	Other weighted levels			0	0	0	0	0
	Directional characteristics				0	0		
	Other characteristics				0	0	0	0
Testing conditions	Acoustic laboratory with diffuse field	X	X					
	Diffuse field			X				
	Open space, large hall				X			
	Acoustic laboratory with anechoic chamber					X		
	In situ measurement, open space				X		X	X

× — Quantities specified by the standards as mandatory.
0 — Additional information.

The Standing Committee for Standardization of the COMECON countries has found the above structure of ISO noise standards acceptable, and evaluated COMEA standards resembling ISO standards, with minor deviations. The general noise measuring directives have been set out in the first three chapters of ST CEV 541, approved in the summer of 1977. The measuring procedures are covered in separate standards just as in the above case.

The standards mentioned above generally refer to the noise measuring of machines. There are other standards, however, which regulate the noise measurements of rotating electrical machines in particular on the basis of the general standards. This is covered by currently revised ISO 1680 that comprises two independent parts. The first is the ISO 1680/1 that describes the measuring procedure of engineering accuracy over a sound reflecting plane in the free sound field on the basis of ISO 3744. The second part, ISO 1680/2, is based on ISO 3746 and provides an approximative method. These are the two most frequently used procedures for measuring the noise of medium-sized and large electrical machines. For the rotating electrical machine as a product, noise limit values are specified by the IEC in the IEC Publication 34–9. This standard is currently being revised. The most important change in the recommendation, compared with earlier versions, is that it specifies the permissible sound power level of normal noise grade machines up to 16 MW output. We can find the counterparts of these two standards among the COMEA standards. The measuring procedure is set out in ST CEV 828, while the noise limit values are specified by ST CEV 1348.

The imission standards are not discussed here in detail, because knowledge and direct observation of these standards are health and environmental protectional tasks.

A.2 Fourier analysis

One of the commonest methods of transient signal analysis is frequency analysis, which is based on Fourier analysis.

The mathematical background of frequency analysis is the Fourier transform, which is based on the fact that any periodic function that satisfies certain mathematical conditions can be expanded in a Fourier series, that is, expressed in the form of a sum of sinusoidal and cosinusoidal signals with well defined frequency. Owing to the fact that the transient signals are not periodic, their Fourier transform exists only if the proper form of transformation is applied.

If the period of any periodic function is continuously increased, eventually we obtain a non-periodic function. It can be proved mathematically that while an optional periodic function is the sum of harmonic oscillations of discrete frequencies and different amplitudes, the non-periodic function can be expressed as

the integral of harmonic oscillations of continuously changing frequency and different amplitude density. In other words, the frequency distribution (spectrum) of periodic functions comprises discrete values, while that of non-periodic functions is continuous, that is, it can range from zero to infinity.

The Fourier series of an optional function with period T is given by:

$$f(t) = A_0 + \sum_{n=0}^{\infty} (A_n \cos n\omega_1 t + B_n \sin n\omega_1 t), \qquad (A.1)$$

where the valves of A_n and B_n are:

$$A_n = \frac{2}{T} \int_{-T/2}^{T/2} f(t) \cos n\omega_1 t \, dt,$$

$$B_n = \frac{2}{T} \int_{-T/2}^{T/2} f(t) \sin n\omega_1 t \, dt,$$

and

$$A_0 = \frac{1}{T} \int_{-T/2}^{T/2} f(t) \, dt.$$

Similarly, for non-periodic functions, the following expression may be used:

$$f(t) = \int_{0}^{\infty} [a(\omega) \cos \omega t - b(\omega) \sin \omega t] \, d\omega. \qquad (A.2)$$

The amplitude densities $a(\omega)$ and $b(\omega)$ are given by the following formulae:

$$a(\omega) = \frac{1}{\pi} \int_{-\infty}^{\infty} f(u) \cos \omega u \, du,$$

$$b(\omega) = \frac{1}{\pi} \int_{-\infty}^{\infty} f(u) \sin \omega u \, du.$$

The coefficients A_n and B_n give the amplitude of the nth harmonic of the Fourier series, while $a(\omega)$ and $b(\omega)$ of the Fourier integral mean amplitude density, and not the amplitude that corresponds to the angular frequency ω but rather the amplitude per unit angular frequency interval. If the spectrum is continuous, a given frequency cannot have a finite amplitude, since in any infinitesimal neighbourhood of this frequency there is an infinite number of other frequencies with

amplitudes in the same order of magnitude, thus adding up to an infinitely large resultant value.

We might say that a non-periodic function is the sum of sinusoidal and co-sinusoidal oscillations [$b(\omega)d\omega \sin \omega t$ and $a(\omega)d\omega \cos \omega t$, respectively] with increasing accuracy as the value of $d\omega$ is chosen smaller and smaller.

The Fourier series and Fourier integral can be written in complex form by expressing the sine and cosine functions in eqn. (A.1) by exponential functions using the well known Euler's formula:

$$f(t)= \sum_{n=0}^{\infty} \left(A_n \frac{e^{jn\omega_1 t}+e^{-jn\omega_1 t}}{2}+B_n \frac{e^{jn\omega_1 t}-e^{-jn\omega_1 t}}{2} \right),$$

after rearranging:

$$f(t)= \sum_{n=0}^{\infty} \left[\frac{A_n+jB_n}{2} e^{-jn\omega_1 t}+\frac{A_n-jB_n}{2} e^{jn\omega_1 t} \right],$$

and introducing

$$\frac{A_n+jB_n}{2}=\bar{C}_{-n} \quad \text{and} \quad \frac{A_n-jB_n}{2}=\bar{C}_n,$$

the expression may be rewritten in the following form:

$$f(t)= \sum_{n=-\infty}^{\infty} \bar{C}_n e^{jn\omega_1 t}. \tag{A.3}$$

If the function $f(u)$ is known, then the coefficients $\bar{C}_n$ can readily be determined from:

$$C_n=\frac{1}{T} \int_{-T/2}^{T/2} f(u)e^{jn\omega_1} \, du.$$

To obtain the complex form of the Fourier integral, substitute the value of $\bar{C}_n$ into the formula of $f(t)$ in eqn. (A.3):

$$f(t)= \sum_{n=-\infty}^{\infty} \frac{\omega_1}{2\pi} \int_{-T/2}^{T/2} f(u)e^{jn\omega_1(t-u)} \, du.$$

If T is increased to infinity, ω_1 becomes infinitesimally small. Denoting this by $d\omega$, the expression can be rewritten as:

$$f(t)= \sum_{n=-\infty}^{\infty} \frac{d\omega}{2\pi} \int_{-T/2}^{T/2} f(u)e^{jn \, d\omega(t-u)} \, du.$$

This expression can be interpreted in the following way. Let us consider a fixed

point in time, t, then the value of the integral will only depend on $n\,d\omega$. If we determine the value of the function:

$$\int_{-T/2}^{T/2} f(u)e^{j\omega(t-u)}\,du = \varphi(\omega, t),$$

at the points of $d\omega, 2d\omega, \ldots, nd\omega = \omega$ (now t is only a parameter) and produce the sum $\sum_{n=-\infty}^{\infty} d\omega\varphi(\omega, t)$ for $T \to \infty$, then we get:

$$f(t) = \frac{1}{2\pi} \int_{-\infty}^{\infty} \left[\int_{-\infty}^{\infty} f(u)e^{j\omega(t-u)}\,du \right] d\omega.$$

Rearranging the formula we obtain:

$$f(t) = \frac{1}{2\pi} \int_{-\infty}^{\infty} \left[\int_{-\infty}^{\infty} f(u)e^{-j\omega u}\,du \right] e^{j\omega t}\,d\omega. \tag{A.4}$$

Finally, the complex amplitude density or complex spectrum is found as:

$$f(t) = \int_{-\infty}^{\infty} \bar{S}(\omega)e^{j\omega t}\,d\omega,$$

where

$$\bar{S}(\omega) = \frac{1}{2\pi} \int_{-\infty}^{\infty} f(u)e^{-j\omega u}\,du.$$

From this, the original function can be determined, therefore this is called the inverse transform (or inversion integral) of the Fourier transform. Using the usual denotation:

$$F\{f(t)\} = \bar{S}(\omega) \quad \text{and} \quad F^{-1}\{\bar{S}(\omega)\} = f(t).$$

To obtain the amplitude density coefficients $a(\omega)$ and $b(\omega)$ of eqn. (A.2), we must develop and reduce the integral (A.4). Then we arrive at the following formula:

$$f(t) = \frac{1}{\pi} \int_{0}^{\infty} \int_{-\infty}^{\infty} f(u) \cos \omega(t-\omega)\,du\,d\omega.$$

Substituting the expression of $\cos (t-u)$:

$$f(t) = \frac{1}{\pi} \int_{0}^{\infty} \int_{-\infty}^{\infty} [f(u) \cos \omega u \cos \omega t + f(u) \sin \omega u \sin \omega t]\,du\,d\omega,$$

from which we obtain the value of the amplitude densities $a(\omega)$ and $b(\omega)$ and the real and imaginary parts of the complex spectrum:

$$\text{Re } \{\bar{S}(\omega)\}=\frac{1}{2}a(\omega) \quad \text{and} \quad \text{Im } \{\bar{S}(\omega)\}=-\frac{1}{2}b(\omega),$$

that gives:

$$\bar{S}(\omega)=\frac{a(\omega)}{2}-j\frac{b(\omega)}{2}.$$

In practice, the Fourier spectrum is mostly determined from its absolute value and phase angle, where

$$S(\omega)=\sqrt{(\text{Re } \{\bar{S}(\omega)\})^2+(\text{Im } \{\bar{S}(\omega)\})^2}$$

is the amplitude spectrum and

$$\Theta(\omega)=\tan^{-1}\frac{\text{Im } \{\bar{S}(\omega)\}}{\text{Re } \{\bar{S}(\omega)\}}$$

is the phase spectrum, that is,

$$\bar{S}(\omega)=S(\omega)e^{j\Theta(\omega)}.$$
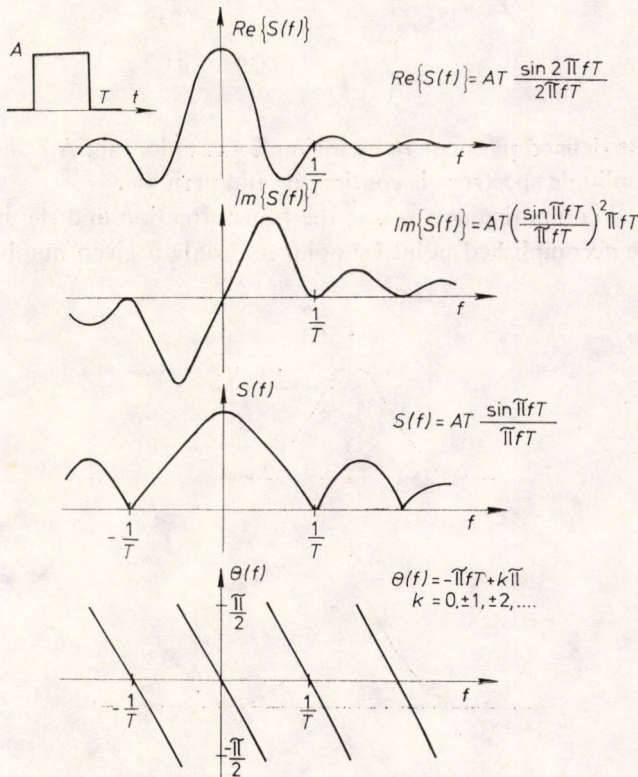
Fig. A.1. The components of the Fourier transform of a square pulse in various forms

As an example, Fig. A.1 shows the components of the complex spectrum of a square pulse of amplitude A and length T, as well as its amplitude and phase spectrum.

A.3 The Fourier transform

Now let us consider signals that are not continuous in time but are characterized by a series of points taken at equal time intervals. Such a case is most frequently encountered right after digitization or, in other words, sampling that directly precedes the digital processing of the signals concerned. The discrete Fourier transform is suitable for the analysis of such signals.

Let Δt denote the time intervals, f_s the frequency of sampling and t_n the time coordinate of the nth point $(t_n = n\Delta t)$. If the points belong to the function $g(t)$, then:

$$\bar{S}(f) = \sum_{n=-\infty}^{\infty} g(t_n)e^{j2\pi ft..}, \qquad (A.5)$$

$$g(t_n) = \frac{1}{f_s} \int_{-f_s/2}^{f_s/2} \bar{S}(f)e^{j2\pi ft..} \, df.$$

Illustrating the defined parameters by a simple example, Fig. A.2 shows that the frequency–amplitude spectrum is continuous and periodic.

In the digital computing procedure, the transformation and the inverse transformation are accomplished point by point and only a given number of points,
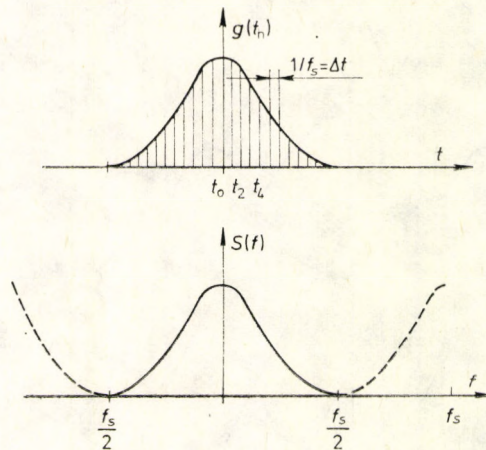
Fig. A.2. The periodic frequency spectrum of a discrete time function

N, are taken into consideration. This limitation is frequently imposed by the limited capacity of the digital memory or stems from the requirement of reducing calculation time.

The expression of the transformation is:

$$\bar{S}(k)=\frac{1}{N}\sum_{n=0}^{N-1}g(n)e^{-j\frac{2\pi kn}{N}}, \tag{A.6}$$

while the expression of the inverse transformation is:

$$g(n)=\sum_{k=0}^{N-1}\bar{S}(k)e^{j\frac{2\pi kn}{N}},$$

where k selects the frequency f_k and n identifies the point of time t_n. This procedure is called the discrete Fourier transform (DFT).

It is easy to see that while N frequency spectrum samples are produced from the N time samples or vice versa, N^2 complex multiplications must be accomplished. The time required to complete these operations is rather long even for the most up-to-date units.

A.4 The Fast Fourier Transform

In order to speed up the discrete Fourier transformation, Cooley and Tukey worked out a procedure in 1965, called the Fast Fourier Transform (abbreviated FFT). The algorithm involves $N\log_2 N$ multiplications, so the number of operations (and therefore the time required) decreases in a ratio of $N/\log_2 N$. If $N=1024\simeq 2^{10}$, this ratio is larger than 100.

Equation (A.6) can be written in the form of a matrix equation as

$$\bar{S}_k=\frac{1}{n}\bar{A}_{kn}\bar{g}_n,$$

where $\bar{S}_k$ and $\bar{g}_n$ are column vectors consisting of the N frequency spectrum samples and the N time samples, respectively, $\bar{A}_{kn}$ is a square matrix of degree N comprising the unit vectors of $e^{-j2\pi kn/N}$. For $N=8$, the matrix equation is quite simple (Fig. A.3). The FFT algorithm is produced by factorizing the matrix $\bar{A}$

Fig. A.3. The matrix form of the equation $\bar{S}_k=\frac{1}{n}\bar{A}_{kn}\bar{g}_n$.

Serial number in $\bar{B}$ $\bar{B}$ Serial number in $\bar{A}$

0 0 0 (0)   0 0 0 (0)

0 0 1 (1)   1 0 0 (4)

0 1 0 (2)   0 1 0 (2)

0 1 1 (3)   1 1 0 (6)

1 0 0 (4)   0 0 1 (1)

1 0 1 (5)   1 0 1 (5)

1 1 0 (6)   0 1 1 (3)

1 1 1 (7)   1 1 1 (7)

$\bar{X}$ $\bar{Y}$ $\bar{Z}$
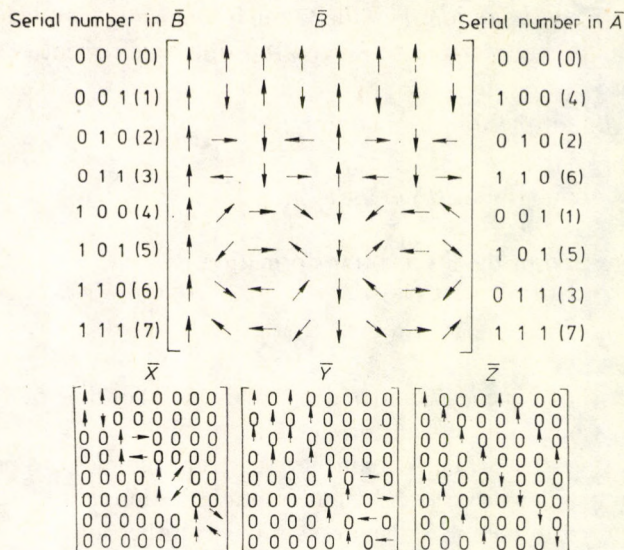
Fig. A.4. The matrix $\bar{B}$ and its components, $\bar{X}$, $\bar{Y}$, $\bar{Z}$.

into $\log_2 N$ matrices, or rather not the matrix $\bar{A}$ itself but one of its variants produced by interchanging certain rows. This variant, $\bar{B}$, is expressed as a product of three ($\log_2 8 = 3$) matrices, $\bar{X}$, $\bar{Y}$ and $\bar{Z}$, shown in Fig. A.4. These matrices are common in that only two elements are non-zero in each row and one is always a unit. Multiplying by these matrices means only N operations (one for each row), so making the product of all these matrices means $N \log_2 N$ operations. The result, of course, yields the interchanged rows of the matrix $\bar{B}$ but to restore the right sequence of rows is a much faster operation than the multiplication of matrices. Taking advantage of other matrix properties, the operations can be further simplified.

So far we have not differentiated between the values of $\bar{S}_k$, $\bar{g}_n$ and the samples in time, although in practice the samples in time are real and only the values of $\bar{S}_k$ and $\bar{g}_n$ are complex. If this fact is ignored, it leads to redundancy for two reasons:

— The memory area allocated to the imaginary part of all the input data will store zeros.

— One half of the resultant spectrum (from $-f_N$ to f_N) will contain negative frequencies (from $-f_N$ to zero). As these are the complex conjugates of the positive frequencies, their storage is also redundant.

This redundancy may be eliminated by filling the N real input data by means

of an algorithm in $N/2$ complex memory and determining only one half of the resultant spectrum. Considering the time taken by the operations necessary to interpret the results, the time saving is about half of that originally required. This reduction of the calculation time allowed the introduction of real-time analysis. By applying two digital memories, the signal being tested can be processed continuously without any part being lost (Fig. A.5). An analysis can be considered real-time when $T_r > T_c$ is guaranteed. The upper limit of T_r is set by the capacity of digital memories, but is also related to the sampling frequency f_s.
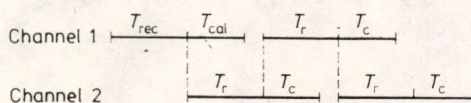
Fig. A.5. Dual channel continuous sampling

A.5 Digital filters

A digital filter is an operational unit that operates on the signal given by the digital data applied to its input, with output signal data that follow the time flow of the input signal but also reflect the impact of the required filter. The main feature of the so-called recursive digital filtering technique is the continuous nature of the procedure in which all output data are derived from the input data, that is, its characteristics are similar to those of analogue filters. Theoretically, we can design such digital "filters" that are not feasible physically in the form of analogue filters.

As an introduction to the discussion of digital filters, let us acquaint ourselves with a low-pass RC filter, the kind also used for the "exponential acquisition" of the components of the frequency spectrum in the analysis of random signals (i.e., the corresponding components of subsequent samples are summed in terms of an exponential function and not linearly). Following each sampling period, the sample is multiplied by A and then added to the sum of the previous samples produced in the same way times B. For the digital filter presented as an example, $A = 0.1$, $B = 0.9$ and the sum of the previous samples is stored in the delay element (Fig. A.6). A and B are independent parameters. By changing the value of these parameters, the characteristics of the filter can be varied over a wide range. In our case their sum is unity in order to get unit resultant amplification for the filter. The minimum number of samples that yields an average value of the tested samples at the output of the filter depends on the values of A and B, while the averaging time, measured from the start of sampling, depends on the length of the sampling cycle. In other words, the cut-off frequency of the low-pass filter is
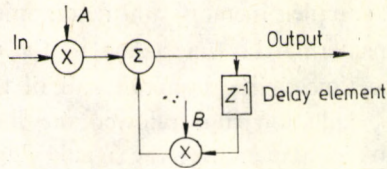
Fig. A.6. Schematic diagram of a one-pole digital filter

determined by the frequency of sampling. In the present case, the time constant RC is about 10 sampling periods, while the averaging time is equal to the time of about 20 sampling periods.

A.5.1 The Z transform

By definition:

$$G(z) = \sum_{n=-\infty}^{\infty} g(n\Delta t)z^{-n}, \tag{A.7}$$

where $z = e^{j2\pi f \Delta t}$ (circle with unit radius). Substituting the expression for z we see that the formula obtained is identical with eqn. (A.5) of the discrete Fourier transform;

$$\bar{S}(f) = \sum_{n=-\infty}^{\infty} g(t_n)e^{-j2\pi f t_n}.$$

The sampling frequency f_s is found on the unit circle at the point $z = e^{j2\pi} = 1$ applying the relation $f_s(=1/\Delta t)$, while the Nyquist frequency, f_n, which, according to Shannon's sampling rule, is equal to $f_s/2$, is found at the point $z = -1$.

Figure A.7 illustrates the Z plane. It can be shown that the Z transform relates to the discrete Fourier transform just as the Laplace transform relates to the Fourier integral, but the former is applied to discrete time samples. This relationship with the Laplace transform is reminiscent of the fact that a filter which is described by a differential equation of the Nth order has N poles in the Laplace plane.
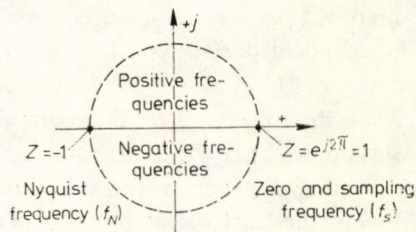
Fig. A.7. Frequencies in the Z domain

The same applies to the Z transform in the case of differential equations of
Nth order (which can even be the characteristic equation that describes the system).
In our present discussion, we want to know how the delay corresponds to the
integration and how it relates to the commonest, simple low-pass RC filters that
are described by the following differential equation:

$$\frac{di(t)}{dt} = -\frac{i(t)}{RC}.$$ (A.8)

The solution of this equation for unit step function is:

$$i(t) = e^{-t/RC}.$$

For infinitesimal changes:

$$\frac{\Delta i}{\Delta t} = -\frac{i}{RC},$$

or

$$\frac{i(n) - i(n-1)}{\Delta t} = \frac{-i(n-1)}{RC},$$

from which it follows that:

$$i(n) = i(n-1)\left(1 - \frac{\Delta t}{RC}\right).$$ (A.9)

This expression shows how the value of $i(n)$, which is the integral of di/dt, can
be derived from $i(n-1)$ by using the constant $\Delta t/RC$. According to the above
equation, the simple integration is identical with a delay. Cyclically applying the
recursive formula (A.9), we obtain:

$$i(n) = i(0)\left(1 - \frac{\Delta t}{RC}\right)^{n}.$$ (A.10)

Figure A.8 illustrates the weighting factors of the exponential summing of the
samples in the case when $i(0)$ and $\Delta t/RC$ are both equal to 0.1.
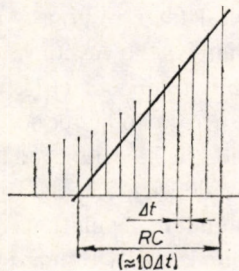
Fig. A.8. The weighting of the various samples in digital exponential averaging

A.5.2 The general multipole filter

A differential equation with two time constants describes a two-pole (second-order) filter. A general two-pole filter is illustrated in Fig. A.9.

All known filters (Butterworth, Tchebyscheff, etc.) can be realized in digital form or approximated to a degree where the error can be considered negligibly
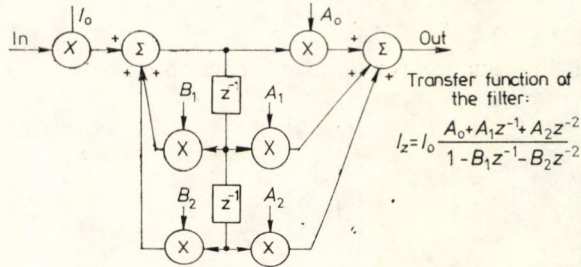
Fig. A.9. Generalized diagram of a two-pole recursive filter

small. Multipole filters can be constructed from two-pole filters by carefully selecting the parameters.

One advantage of digital filters is that a filter with arbitrary characteristic can be produced by the same procedure, only the constants must be adjusted accordingly. For example, the same calculation can be used for the design of low-pass and high-pass filters, and the cut-off frequencies can easily be shifted, etc. Once the filter is calculated, it will never change its parameters so it need not be retuned. For the realization of logarithmic frequency scale and constant relative bandwidth filters, the application of digital filters is much easier than that of FFT, which is characterized by linear frequency scale and constant bandwidth.

A.5.3 Digital filter responses

Analogue filters may be copied by digital filters, but there is always a deviation between the analogue and digital filter responses mainly because the frequency of digital filters is periodic, that is, the response curve continues even for frequencies higher than the Nyquist frequency (Fig. A.10). This could give rise to considerable distortion, but the error can be reduced to negligible levels by proper dimensioning. On the other hand, the incorporated low-pass filter affects the whole filter response. In spite of these deficiencies, the digital filters in their final form satisfy the requirements of all standard regulations and, for example, a bandwidth variation of 1 : 10 is feasible quite easily within a decade at any frequency. Therefore their application is frequently justified and their spreading rate is striking.
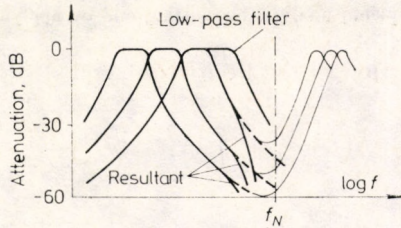
Fig. A.10. Digital filter response with low-pass filter

A.6 Applied digital analysis

In the following pages we review the practical applications of FFT analysis for single-channel and dual-channel signal processing.

A.6.1 FFT with spectrum refining (ZOOM-FFT)

As we have seen, FFT analysis ranges from zero to the Nyquist frequency, and its resolution depends on f_N and N. It is frequently required to know the spectrum in a small fraction of the frequency range, but with much more refined resolution. The so-called spectrum refining FFT or ZOOM-FFT procedure makes this possible (Fig. A.11).
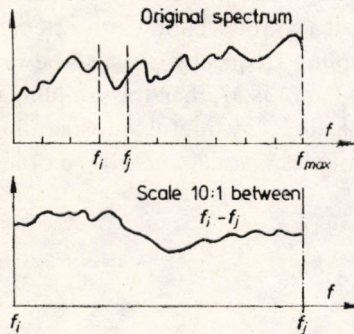
Fig. A.11. The original spectrum after tenfold refining

A.6.1.1 Digital frequency analysis by shifting and by applying a low-pass filter

If we look at the expression of the Fourier integral

$$\bar{S}(f_k) = \frac{1}{T} \int_{-T/2}^{T/2} g(t)e^{-j2\pi f_k t}\, dt$$

where $f_k = kf_1$, $f_1 = 1/T$ and $k = 0, \pm 1, \pm 2, \ldots \pm n$, we see that the unit vector $e^{-j2\pi f_k t}$ actually shifts the point $f = 0$ to the point $f = f_k$, as shown in Fig. A.12.
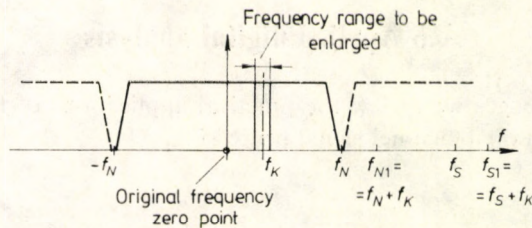
Fig. A.12. The frequency-shifting effect of multiplying by a rotating unit vector

In other words, if a signal is multiplied by a unit vector that rotates at a frequency of f_k, then the value that corresponds to the zero frequency is shifted to the frequency f_k and, in general, all the other values (i.e., the spectrum) are shifted by f_k. The resultant complex signal must be filtered so that outside the tested neighbourhood of the frequency f_k no other components are being tested in order to avoid distortions. In this way, it is possible to reduce the sampling frequency f_s (Fig. A.13). For example, if the total bandwidth after "filtering" is one tenth of the original, then the sampling frequency can also be reduced to one tenth of it.

In general, if the refining factor is M, then the sampling frequency can be reduced to an Mth part without losing any useful information. When the sampling is repeated only one of M samples is used, and all the others are filtered out.
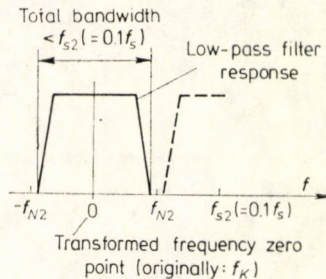
Fig. A.13. The compressed frequency range and the reduced $f_{s2} = 0.1 f_s$ after repeated sampling

When a time function is analysed by the FFT procedure, the resultant spectrum will range from 0 to a well defined maximum frequency, f_{max}. The resolution will be determined by the number of digital samples tested (e.g., 1024=1 K) and by the number of components in the resultant spectrum (e.g., 400), that is, $\Delta f=$ $=f_{max}/400$ or, in terms of sampling frequency, $\Delta f=f_s/400$. In other words, for a given f_{max}, the resolution of the FFT analysis can be increased (Δf decreased) only if the number of samples used for the transformation is increased. In this procedure, when the usual 1 K samples are analysed, the frequency f_{max} is decreased by a factor of M, but only in the neighbourhood of frequency f_k. (In the case of normal FFT analysis, this could only be possible by increasing the number of samples by a factor of M.)

Since the operation of the low-pass filter is always associated with the sampling frequency, repeated refining is possible by data feedback (see dashed line in Fig. A.14), that is, raising M to powers (for $M=2$, the powers 4, 8, 16, 32, ... will
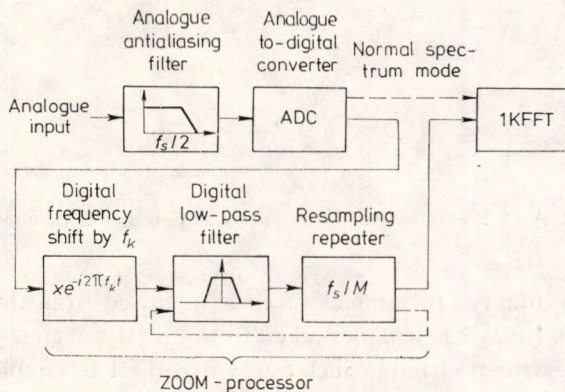
Fig. A.14. Digital spectrum refining (ZOOM-FFT) with frequency shift and low-pass filter

appear). This spectrum refining procedure works in the real-time mode, since it directly processes the signals coming from the analogue-to-digital converter. Summing up the features of the spectrum refining procedure that applies a low-pass filter and frequency shifting, we have:

— arbitrarily large refining factor,
— real-time procedure,
— the original time function is lost.

A.6.1.2 High-resolution digital recording of the time function

This procedure is used for 1 : 10 spectrum refining e.g. in the Brüel and Kjaer 2033 high-resolution digital signal analyser. The operation of the instrument is illustrated by the block diagram in Fig. A.15. To increase frequency resolution (to
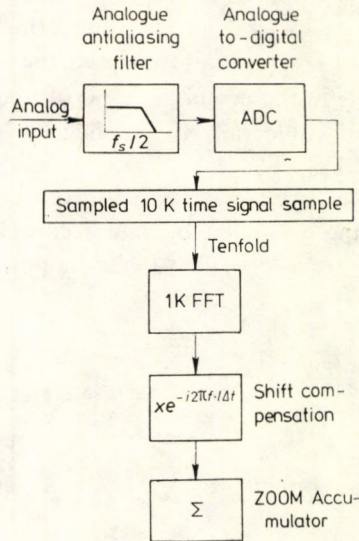
Fig. A.15. Block diagram of a high-resolution digital analyser

decrease Δf), the number of samples taken is increased from the usual 1 K to 10 K, and the ten times 1 K samples taken from the data memory are processed into a 400-component spectrum in such a way that the 1 K samples are collected by repeated sampling of the 10 K sample according to the procedure shown in Fig. A.16. In other words, each 1 K sample represents the whole recorded time function and the sum of the ten 1 K samples is equal the 10 K sample. Since the Fourier transform is linear, the result is that the sum of the spectra produced by the processing of the 1 K samples yields the spectrum of the original signal. As the 1 K samples are taken with a certain shift, this shift must be compensated for prior to summing. The calculating procedure is illustrated in Fig. A.17. The ten 1 K FFT analysers, the shift compensating unit (with coefficient $W_{10,240}^{l\,k}$) and the summation can be seen clearly.

The frequency spectrum produced from the 10 K sample gives 5120 independent components, but only those from 0 to 4000 are taken into account in order to achieve the required accuracy, that is, in the spectrum refining procedure only 400 components are produced. (In eqn. (1) in the figure, K takes 512 subsequent
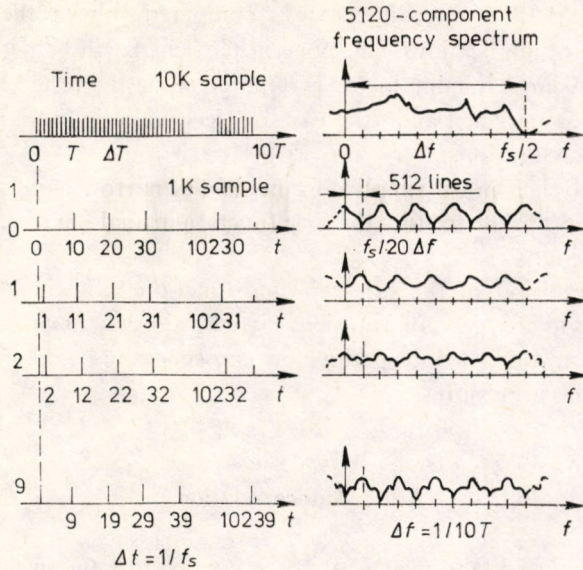
In the lth sub-analysis the shift compensation
of the kth component is $\Delta\phi_{lk} = -2\pi l k / 10240$

Fig. A.16. The principle of 10 K FFT process with tenfold 1K transformation

values.) The original time function remains intact during the analysis and can be used again.

Summarizing the main features of the procedure is based on high resolution digital signal recording:

— the refining factor is 10,
— the analysis is not real-time,
— the original time function remains intact.

$$(1)\ X(k) = \sum_{l=0}^{9} W_{10240}^{lk}\, G_l(k)$$

$$0 \leqslant k \leqslant 4000$$

$$(2)\ W_{10240}^{lk} = \exp\left(-j\,\frac{2\pi l k}{10240}\right)$$
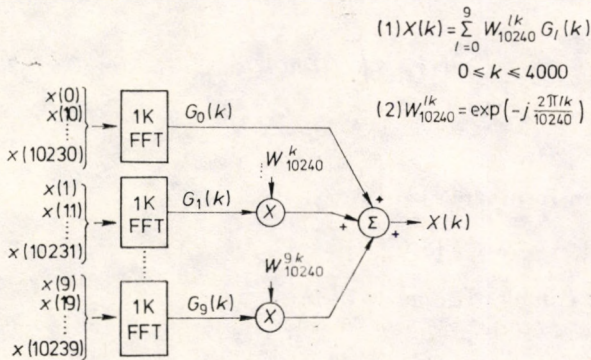
Fig. A.17. The computing process of the refined spectrum

The two ZOOM-FFT procedures can be compared only on the basis of their respective scope of applications, since one in particular will be better for solving different tasks. A large refining factor is required when the tested signal contains many "sharp" components, as in the case of electrically induced phenomena or rotating machine vibrations.

Real-time analysis is mostly applied in the field of narrow-band signal analysis, otherwise it is appropriate to store the time function in analogue or digital memory for later processing.

The intact condition of the original time function following the analysis is required mostly in the case of transient signals, since it may be very hard to reproduce them and the various parameters can generally be determined only by different analysing procedures.

A.6.2 Autocorrelation

Autocorrelation reveals the degree of correspondence between a signal and its variant shifted in time, as a function of the extent of shifting.

The autocorrelation function $R_{xx}(\tau)$ is defined from the original time function $f_x(t)$ as:

$$R_{xx} = \lim_{T \to \infty} \frac{1}{T} \int_{-T/2}^{T/2} f_x(t) f_x(t+\tau) \, dt. \tag{A.11}$$

As we see, for $\tau = 0$ the mean square of $f_x(t)$ is obtained for one period. In many cases, the autocorrelation is expressed in a normalized form produced by dividing it by the mean square value (thus its maximum value cannot exceed 1). Let us compare the expression of autocorrelation with the convolution integral, which is:

$$g(\tau) = \int_{-\infty}^{\infty} f(t) h(-t+\tau) \, dt. \tag{A.12}$$

Let

$$F\{f_x(t)\} = F_x(f) \tag{A.13}$$

(the Fourier transform) and

$$F\{f_x(-t)\} = F_x(-f) = F_x^*(f), \tag{A.14}$$

where F^* is the complex conjugate of F.
From these

$$F\{R_{xx}(\tau)\} = F\{f_x(t)\} F\{f_x(-t)\} = F_x(f) F_x^*(f) = |F_x(f)|^2 \tag{A.15}$$

which is precisely the power spectrum of $f_x(t)$. The FFT technique allows quick determination of the value of R_{xx} by the inverse transformation of the power spectrum, since applying the discrete Fourier transform:

$$S_{xi} = \frac{\Delta t}{n} |X_i|^2, \qquad (A.16)$$

where S_{xi} — the spectral component obtained from the ith sample of the tested signal.

Applications of autocorrelation:

(a) Determination and shape analysis of reflected signals.

(b) Selection of a periodic signal from a very noisy background. After prolonged summing of the power spectrum components, the interfering signals will soon fall out.

A.6.3 The power cepstrum

According to the original definition, the power cepstrum is the logarithm of the power spectrum. It is easily derived mathematically as:

$$F_x(f) = F\{f_x(t)\}, \qquad (A.17)$$

$$F_{xx}(f) = |F_x(f)|^2, \qquad (A.18)$$

$$C_x(\tau) = |F\{\log [F_{xx}(f)]\}|^2. \qquad (A.19)$$

As opposed to this, the autocorrelation $R_{xx}(\tau)$ is:

$$R_{xx}(\tau) = F^{-1}\{F_{xx}(f)\}. \qquad (A.20)$$

The independent variable of the power cepstrum, τ, was given the artificial name "quefrency", although its dimension is time and it means just the same as in the case of autocorrelation.

Bogert, who introduced the notion of cepstrum, first used cepstra for the evaluation of seismic signals, because this method is more sensitive to reflected signals. The power cepstrum is applied when mixed signals of two phenomena are detected. Let us consider the case when the resultant may be written as the product of the two component phenomena:

$$U(f) = V(f)Y(f). \qquad (A.21)$$

Taking the logarithm of the equation:

$$\log [U(f)] = \log [V(f)] + \log [Y(f)].$$

Because of the linearity of the Fourier transform, it can be applied to functions expressed in the form of a sum:

$$F\{\log[U(f)]\}=F\{\log[V(f)]\}+F\{\log[Y(f)]\}. \tag{A.22}$$

The two functions become easily recognisable by separating their parameters. It should be borne in mind that the unit of power cepstrum is dB^2, but there are users who generate amplitude cepstrum by a further transformation, and the unit of amplitude cepstrum is dB.

Several practical applications:

(a) determination of reflected signals, measurement of their delay time,
(b) identification of resonant machine parts during machine vibration analysis,
(c) additional noise detection.

A.6.4 The complex cepstrum

Despite its name, the complex cepstrum is a real function, but as opposed to the power cepstrum it is derived from the complex spectrum in order to save phase information. Because of this, the procedure is reversible. By definition, the complex cepstrum is the inverse Fourier transform of the complex logarithm of the complex spectrum. The complex spectrum, of course, is obtained by Fourier transformation of the signal to be tested.

Expressing eqn. (A.13) in exponential form:

$$F_x(f)=A(f)e^{j\Phi(f)}.$$

Taking the logarithm:

$$L(f)=\ln A(f)+j\Phi(f),$$

from which the complex cepstrum $K(\tau)$ may be defined as;

$$K(\tau)=F^{-1}\{L(f)\}. \tag{A.23}$$

Complex cepstrum applications:

(a) correction of acoustic recordings, e.g., the elimination of the effects of the transmission system,
(b) separation of the original signal from its echo.

A.6.5 Cross correlation and spectrum

The cross correlation function describes the correlation between two functions in terms of the time shifting between them.

(a) The cross correlation of $f_x(t)$ and $f_y(t)$ is:

$$R_{xy}(\tau) = \lim_{T \to \infty} \frac{1}{T} \int_{-T/2}^{T/2} f_x(t) f_y(t + \tau)\, \mathrm{d}t. \tag{A.24}$$

If the value of R_{xy} is divided by $\sqrt{R_{xx}(0)R_{yy}(0)}$, the normalized cross correlation is obtained. When $f_x(t) = f_y(t)$, $R_{xy}(\tau)$ gives the autocorrelation function.

(b) The cross spectrum of $f_x(t)$ and $f_y(t)$ can be obtained as the Fourier transform of the cross correlation R_{xy}. It is denoted $F_{xy}(f)$. The cross spectrum is normally a complex function whose real part is called cospectrum, and imaginary part, quadspectrum.

The cross spectrum can be produced from the Fourier transforms of $f_x(t)$ and $f_y(t)$ as well:

$$F_{xy}(f) = F_x^*(f) F_y(f), \tag{A.25}$$

where $F_x^*(f)$ is the complex conjugate of $F_x(f)$.

It can be seen that $F_{xy}(f)$ is identical with the power spectrum when $F_y(f) = F_x(f)$

Of course, the cross correlation can be obtained by the inverse Fourier transformation of the cross spectrum. Note that these procedures are applicable to transient signals, in which case the dimension of the cross spectrum is power rather than energy and the factor $1/T$ is also redundant.

Applications:

(a) cross correlation
— to determine the degree to which the measured signal originates from the suspected source and how long its delay is in time,
— to detect the presence of a signal (not only periodic) against a very strong background noise,
(b) cross spectrum
— to determine the transfer function,
— to determine the frequency-dependent time delay (phase shift).

A.6.6 The transfer function

The transfer function of a tested system is the ratio of the Fourier transforms of the input and output signals as a function of time:

$$H_{xy}(f)=\frac{F_y(f)}{F_x(f)}, \tag{A.26}$$

where $F_y(f)$ — the Fourier transform of the output signal,
   $F_x(f)$ — the Fourier transform of the input signal.

Multiplying the denominator and the numerator by $F_x^*(f)$:

$$H_{xy}(f)=\frac{F_y(f)F_x^*(f)}{F_x(f)F_x^*(f)}=\frac{F_{xy}(f)}{F_{xx}(f)}. \tag{A.27}$$

We have found here that the transfer function is equal to the cross spectrum of the input and output signals divided by the power spectrum of the input signal.

Applications:

   (a) Determination of the mechanical impedance of a mechanical system. If $f_x(t)$ is the acting force and $f_y(t)$ is the velocity due to the force, then $H_{xy}(f)$ is the inverse of the mechanical impedance of the system.
   (b) Analysis of systems by modelling.
   (c) Elimination of the effect of the transmission system from the output signal.
   (d) Determination of the output signal of a system with the knowledge of the input signal and the transfer function by the inverse Fourier transformation of $F_y(f)$.

A.6.7 Coherence

If we cannot be sure that the output signal $f_y(t)$ of a system is produced by the suspected input signal $f_x(t)$, then it is practical to calculate the coherence of the signals which, by definition, is found as:

$$\gamma_{xy}^2(f)=\frac{|F_{xy}(f)|^2}{F_{xx}(f)F_{yy}(f)}, \tag{A.28}$$

where $F_{xy}(f)$ is the cross spectrum determined as the average of several measure= ments, as for the power spectra $F_{xx}(f)$ and $F_{yy}(f)$. As a first approximation, the coherence is always unity if $f_x(t)$ and $f_y(t)$ really correspond to each other, since:

$$F_{xy}(f)=F_x^*(f)F_y(f)=|F_x(f)||F_y(f)|_{\varphi_y-\varphi_x} \tag{A.29}$$

$$|F_{xy}(f)|^2 = |F_x(f)|^2 |F_y(f)|^2, \tag{A.30}$$

and moreover:

$$F_{xx}(f) = |F_x(f)|^2 \quad \text{and} \quad F_{yy}(f) = |F_y(f)|^2,$$

from which:

$$|F_{xy}(f)|^2 = F_{xx}(f) F_{yy}(f). \tag{A.31}$$

Under the influence of strong noise or foreign signal, the coherence is always smaller than 1.

Applications:

(a) Checking the correctness of the cross spectrum and the transfer function. If they are correct, the coherence is 1.

(b) Approximative identification of noise sources by total output noise analysis of the system.

A.7 Several applied concepts of mathematical statistics

In the field of vibroacoustic signal measurement, methods of mathematical statistics can be very useful. One of the physical parameters of the continuously varying noise, e.g., the sound pressure level, is considered as a one-dimensional random variable characterized by a density function $f(x)$ or a distribution function $F(x)$. Since the density function and the distribution function are normally not known, they must be determined by measurement.

It is assumed that any sample of the elements $L_1, L_2, \ldots, L_n$, obtained by sound pressure level measurements is a result of n independent measurements. In this case, the independent quantities, $L_1, L_2, \ldots, L_n$ can be considered as random variables with the same density function. The empirical distribution function of this sample, $F(L)$, is a non-decreasing step function for which $F(-\infty) = 0$ and $F(+\infty) = 1$.

The empirical distribution function roughly gives the probability that a given element of the sample is smaller than, or equal to, the argument of the function. If the number of elements in the sample is increased, the empirical distribution function approximates the theoretical distribution function better and better.

In acoustic measurements, instead of the mathematical distribution function, the function $1 - F(L)$ is in general use. The value of this function means the probability that the measured sound pressure level is higher than L. From the measured data, this so-called integral distribution function can easily be determined. If the number of measurements is known in advance, we can calculate the points of the integral distribution function by checking for each value of L the

percentage of the results higher than L. The curve obtained is similar to that shown in Fig. A.18a.

The amplitude distribution of the noise can be characterized quite well by means of the integral distribution function. If we find the sound pressure level L_N that corresponds to N percent on the curve, various statistical parameters of
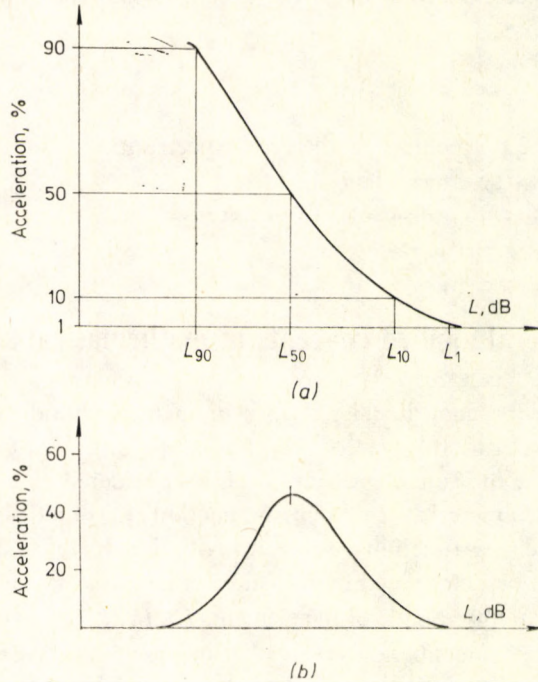
Fig. A.18. (a) Distribution function, (b) density function

the sample are obtained depending on the value of N. For example, L_{50}, called the sample mean or median, gives the average sound pressure level (from experience, the symmetry of the density function about the median can be assumed in most cases). L_{99}, compared with which 99 percent of the elements are higher, can be considered as background noise, while L_1, by a statistical interpretation, is the maximum level of the signal segment tested. The variation of the signal, that is, the fluctuation of its amplitude, in usually characterized by the difference $L_{10} - L_{90}$. These quantities are especially important in the calculation of the so-called perceived noise level.

The derivative of the distribution function is the density function or the differential distribution function. The value of $f(L)\, dL$ is the probability that the result

of the sound pressure level measurement will fall in the dL interval about L. The shape of the density function is similar to the curve shown in Fig. A.18b, but the density function is very seldom used directly as a characteristic feature in acoustic measurement. The instruments which carry out the statistical analysis, however, measure the density function and derive the distribution function from it.

REFERENCES

1 Amey, W. and Pohl, H.: Massnahmen zur Geräuschminderung bei Hochspannungsmotoren mittlerer Leistung *Siemens–Zeitschrift*, Vol. 47, No. 6, 1973, 466–469.

2 Amey, W. and Tikvicki, M.: Modulares System zur Geräuschminderung bei röhrengekühlten Hochspannungsmotoren. *Siemens–Energietechnik*, Vol. 5, No. 1, 1983, 33–37.

3 Augusztinovicz, F.: Determining the sound power of machines (in Hungarian). Thesis, Technical University of Budapest, 1982.

4 Baberad, L.: Asynchronous motors with reduced vibration and noise level (in Czech). *Elektrotechnik*, Praha, Vol. 26, No. 1, 1971, 6–13.

5 Belmans, R., Geysen, W., Jordan, H. and Vandenput, A.: Unbalanced magnetic pull and homopolar flux in three phase induction motors with eccentric rotors. *Proc. ICEM'82*, Budapest 1982, 916–921.

6 Benaragama, B. S., Ward, D. M. and Tavner, P. J.: Unbalanced magnetic pull on the eccentric rotor of a turbo-alternator. *Proc. ICEM'82*, Budapest 1982, 922–925.

7 Bendat, J. S. and Piersol, A. G.: *Analysis and Measurement Procedures*. Wiley, New York 1971.

8 Beranek, L. L.: *Noise reduction* (in Hungarian). Műszaki Könyvkiadó, Budapest 1967.

9 Beranek, L. L.: *Noise and Vibration Control*. McGraw–Hill Book Company, New York 1971.

10 Bradford, M.: Unbalanced magnetic pull in a 6-pole induction motor. *Proc. IEE*, 115, 1968, 1619–1627.

11 Broch, J. T.: Mechanical Vibration and Chock Measurements. Brüel and Kjaer handbook, Copenhagen 1984.

12 Brozek, R.: No-load to full-load airborne noise level change on high-speed polyphase induction motors. *IEEE Trans. Ind. Appl.* IA-9, 2, 1973, 180–184.

13 *Brüel and Kjaer Technical Review*, Statistical distribution analysis, 1, 1984.

14 Burmeister, J.: Probleme bei der geräuscharmen Belüftung von kleinen, oberflächenge-kühlten elektrischen Maschinen. *Siemens–Zeitschrift*, Vol. 49, No. 2, 1975, 103–108.

15 Carter, F. W.: Magnetic noise in dynamo-electric machines. *Engineering*, 134, 1932, 548–579.

16 Chapman, F. T.: The production of noise and vibrations by certain squirrel-cage induction motors. *J. A. IEE*, Vol. 61, No. 1, 1922, 39.

17 Coers: Magnetische Schallerzeugung bei Drehstromasynchronmotoren mit Schleifringläufer. Dissertation. T. H. Hannover 1961.

18 Crawford, W. G.: Unbalanced magnetic pull as a cause of vibration in two-pole induction motors. *Proceedings of Electrical Machines in the Seventies, Dundee, 1970*, 48–1, 48–4.

19 Cremer, L. and Heckl, M.: *Körperschall*. Springer Verlag, Berlin 1967.

20 Ellison, A. J. and Moore, C. J.: Acoustic noise and vibration of rotating electric machines. *Proc. IEE,* Vol. 115, No. 11, 1968, 1633–1640.

21 Ellison, A. J. and Moore, C. J.: Calculation of acoustic power radiated by short electric machines. *Acustica,* 21, 1969, 10–15.

22 Ellison, A. J. and Yang, S. J.: Acoustic noise measurements on nominally identical small electrical machines. *Proc. IEE,* Vol. 117, No. 3, 1970, 555–560.

23 Ellison, A. J. and Yang, S. J.: Calculation of acoustic power radiated by an electric machine. *Acustica,* 25, 1978, 28–34.

24 Ellison, A. J., Moore, C. J. and Yang, S. J.: Methods of measurements of acoustic noise radiated by an electric machine. *Proc. IEE,* 1969, 1419–1431.

25 Erdélyi, E.: Predetermination of sound pressure levels of magnetic noise of polyphase induction motors. *J. A. IEE,* Part III, Vol. 94, No. 12, 1955, 1269–1280.

26 Fahy, F.: *Sound and Structural Vibration.* Academic Press, London 1985.

27 Foster, S. L. and Reiplinger, E.: Characteristics and control of transformer sound. *IEEE Trans. PAS,* Vol. 100, No. 3, 1981, 1072–1077.

28 Freise, W. and Jordan, H.: Einseitige magnetische Zugkräfte in Drehstrommaschinen. *ETZ-Arch.,* Vol. 83, No. 9, 1962, 299–303.

29 Frohne, H.: Über die primären Bestimmungsgrössen der Lautstärke bei Asynchronmotoren. Dissertation, T. H. Hannover 1959.

30 Fudeh, H. R. and Ong, C. M.: Modelling and analysis of induction machines containing space harmonics. *IEEE Trans. PAS,* Vol. 102, No. 8, 1983, 2608–2628.

31 Fuge, R.: Schwingunsmessung zur Schadenfrüherkennung in energietechnischen Anlagen. *VDI-Berichte,* 454, 1982, 65–70.

32 Galincev, J. V.: The effect of rotor and stator slot numbers on asynchronous motor characteristics (in Russian). *Elektrotekhnika,* Moscow, Vol. 43, No. 8, 1972, 44–48.

33 Géher, K. *Linear Networks* (in Hungarian). Műszaki Könyvkiadó, Budapest 1972.

34 Haase, H., Jordan, J. and Kovács, K. P.: Störung der Laufruhe von Drehstrom-Asynchronmotoren infolge elektromagnetischer Anfachungen. *ETZ-Arch.,* Vol. 94, No. 2, 1973, 73–76.

35 Halt, H. G.: Lärmarme Elektromotoren. *VDI-Berichte,* 239, 1975, 117–122.

36 Hardeous, H. and Weidermann, B.: Pendelmomententwicklung bei der stromrichtergespeisten Asynchronmaschine mit Berücksichtigung des welligen Zwischenkreisstroms. *Arch. Elektrotech.,* 64, 1982, 297–305.

37 Harris, C. M.: *Handbook of Noise Control.* McGraw-Hill Book Company, New York 1957.

38 Hassall, J. R. and Zaveri, K.: Acoustic noise measurements. Brüel and Kjaer handbook, Copenhagen, 1979.

39 Hasse, H., Jordan, H. and Kovács, K. P.: Rüttelkräfte infolge von Wellenflussen bei zweipoligen Induktionmaschinen. *ETZ-Arch.* Vol. 93, No. 9, 1972, 485–486.

40 Heller, B. and Hamata, V.: *Harmonic Field Effects in Induction Machines.* Elsevier Scientific Publishing Company, Amsterdam, Oxford, New York 1977.

41 Hoffmann, R., Jordan, H. and Weis, M.: Ersatzstrahler zur Ermittlung der Schalleistung von rotierenden elektrischen Maschinen. *Lärmbekämpfung,* 1, 1966, 7–11.

42 Hribar, A. E., White, D. and Teplitzky, A. M.: Development of a low noise FOA transformer cooler. *IEEE Trans. PAS,* Vol. 100, No. 5, 1981, 2424–2432.

43 Hübner, G.: Geräuschbildung von Radiallüftern. *Siemens-Zeitschrift,* Vol. 33, No. 8, 1959, 499–505.

44 Hübner, G.: Enstehung und Bekämpfung der Geräusche elektrischer Maschinen. *ETZ-Arch.* Vol. 82, No. 24, 1961, 771–781.

45 Hübner, G.: Geräuschproblemen bei elektrischen Maschinen. *Bull. SEV Rev.* Vol. 54, No. 21, 1963, 878–891.

46 Hübner, G.: Qualification procedures for free field conditions for sound power determination of sound sources. *INTER-NOISE'73,* conference paper, Copenhagen 1973.

47 Hübner, G.: Analysis of errors in measuring machine noise under free field conditions. *The Journal of the Acoustical Society of America,* Vol. 54, No. 4, 1973, 967–977.

48 Hübner, G.: Minderung von Maschinengeräuschen. *ETZ-B.,* Vol. 29, No. 8, 1977, 245–248.

49 Hübner, G.: Investigation of the establishment of International Standards for the measurement of noise emitted by machines – newer aspects of uncertainties in the determination of the sound power. *Proc. INTER-NOISE'79,* 1979, 405–410.

50 Hübner, G. and Meurers, H.: Investigation of sound propagation over non-ideal reflecting planes and the influence of the measurement distance on the accuracy of sound power determination of sound sources operating outdoors. *A.A.S.E.,* Le bruit des machines et l'environnement. Paris 1975, 559–567.

51 Ito, M., Fujimoto, N., Okuda, H. and Takahashi, H. Miyata, T.: Analytical model for magnetic field analysis of induction motor performance. *IEEE Trans. PAS,* 100, 1981, 4582–4590.

52 Jaenicke, P. and Jordan, H.: Berechnung der elektromagnetischen Radialkraft von Drehstromasynchronmaschinen mit excentrischer Verlagerung des Läufers. *Siemens Forsch. & Entwicklungsber.,* Vol. 5, No. 5, 1976, 249–255.

53 Jordan, H.: *Der Geräuscharme Elektromotor.* W. Girardet, Essen 1957.

54 Jordan, H.: Newest results in vibration testing of electrical machines (in Hungarian). *Elektrotechnika,* Budapest, Vol. 57, No. 6, 1964, 202–212.

55 Jordan, H. and Röder, G.: Über den Einfluss des Gehäuses auf die Resonanzfrequenzen des Ständers elektrischen Maschinen. *Acta Techn. CSAV,* 5, 1969, 536–561.

56 Jordan, H. and Uner.: Berechnung der Eigenfrequenzen in den Statorblechpaketen von Drehstrommotoren. *Konstruktion,* Berlin, 3, 1964, 57–60.

57 Jordan, H. and Weis, M.: Die Nutenschrägung und ihre Wirkungen. *ETZ-Arch.,* Vol. 88, No. 10, 1967, 528–533.

58 Jordan, H., Klima, V. and Kovács, K. P.: *Asynchronmaschinen.* Akadémia Kiadó, Budapest 1975.

59 Jordan, H., Röder, G. and Weis, M.: Das Schwingungsverhalten der Ständer elektrischer Maschinen. *Tech Rundsch,,* Vol. 47, No. 10, 1967, 33—37.

60 Kabrhel, I.: Problems of measurement and propagation of transformer noise (in Czech). *Transformatory,* Vol. 18, No. 3, 1982, 17–19.

61 Kako, F., Tsuruta, T., Nagaishi, K. and Kohmo, H.: Experimental study on magnetic noise of large induction motors. *IEEE Trans. PAS,* Vol. 102, No. 8, 1983, 2805–2810.

62 Ketteler, K. H.: Über den Einfluss der Wicklungsschaltung in Induktionmaschinen auf die Zusatzverluste und den einseitigen magnetischen Zug. *ETZ-Arch.* Vol. 6, No. 3, 1984. 99–106.

63 Kirkham, H. and Gajda, W. J.: A mathematical model of transmission line audible noise. *IEEE Trans. PAS* Vol. 102, No. 3, 1983, 710–728.

64 Kleinrath, H.: *Stromrichtergespeiste Drehfeldmaschinen.* Springer, Vienna 1980.

65 Kovács, E.: *Noise and vibration problems of shorted three-phase motors* (in Hungarian). *Elektrotechnika,* Budapest, Vol. 57, No. 6, 1964, 213–225.

66 Kovács, K. P.: *Transient Phenomena in Electrical Machines* Elsevier, Amsterdam and Akadémiai Kiadó, Budapest 1984.

67 Kovács, K. P.: Two-pole induction motor vibrations caused by homopolar alternating fluxes. *IEEE Trans. PAS,* Vol. 96, No. 4, 1977, 1105–1108.

68 Kováts, A.: *Noise Protection Theory and Practice* (in Hungarian). Tankönyvkiadó, Budapest 1984.

69 Kranen, H. H.: Möglichkeiten der Geräuschminderung bei grösseren elektrischen Maschinen. *VDI Berichte,* 239, 1975, 99–107.

70 Krondl, M.: Self-excited radial vibrations of the rotor of induction machines with parallel paths in the winding. *Bull. Assoc. Suisse Electr.,* 47, 1956, 581–588. Research reports (70 through 73).

71 Lachonius, L.: The water-cooled electrical motor solves noise problems (in German). *Antriebstechnik,* 9, 1974, 533–535.

72 Lahti, T. and Starck, J.: Industrial impulse noise measurements. *International Symposium on effects of impulse noise on hearing.* Malmö, 25–27, August 1980.

73 Lazaroiu, D. F. and Bichir, H.: Noise of electrical machines and transformers (in Russian). *Energiya,* Moscow 1973.

74 Lehmann, S.: Kraftswellen-Ordnungszahlen und Frequenzen magnetischer Geräusche bei elektrischen Maschinen. *ETZ-Arch.* Vol. 82, No. 24, 1961, 782–788.

75 Lipcsey, L.: The effect of ferromagnetic slots and special pole shoes on the magnetic noise of salient-pole synchronous machines (in Hungarian) *GVM News,* 11, 1972, 40–43.

76 Liska, J.: Zur Nutschrägung der Asynchronmotoren. Separatum. *Period. Polytech. Electr. Eng.* Vol. 3, No. 2, 1959.

77 Martin, G.: Geräuschminderung bei elektrischen Maschinen mittlerer Leistung. *VDI-Berichte,* 239, 1975, 127–129.

78 Maruvada, P. S., Dallaire, R. D., Norris-Elye, O. C. Thio, C. V. and Goodman, J. S.: Environmental effects of the Nelson River HVDC transmission lines. *IEEE Trans. PAS,* Vol. 101, No. 4, 1982, 951–959.

79 Medvegjev, V. T.: The effect of non-sinusoidal and asymmetrical supply voltage on the vibroacoustic properties of three-phase squirrel-cage asynchronous machines (in Russian). Thesis, MEI, Moscow 1976.

80 Molnár, L. L. and Timár, P. L.: The role of the electrical motor in the development of noise in compression-type refrigerating machines (in Hungarian). *Elektrotechnika,* Vol. 67, Nos 1–2, 1974, 68–73.

81 Moore, C. J.: A solution to the problem of measuring the sound field of a source in the presence of a ground surface. *J. Sound & Vib.,* 16, 1971, 269–282.

82 Narolski, B.: Beiträge zur Berechnung des magnetischen Geräusches von Asynchronmotoren. *Acta Tech. CSAV,* 2, 1965, 156–171.

83 Novacek, M.: Lärmbekämpfung an niederpoligen Käfigläufermotoren mittlerer Leistung. *Brown Boveri Rev.,* 12, 1972, 582–584.

84 Oberretl, K.: Über die Sättigungsoberfelder in Induktionsmaschinen. *Elektrotechnik und Maschinenbau,* Vol. 78, No. 8, 1961, 285–294.

85 Ploner, B.: Aerodynamische Geräusche bei mittleren Asynchronmotoren. *Brown-Boveri Rev.,* 8, 1976, 493–499.

86 Ponomarjov, Sz. D.: *Strength Calculations in Mechanical Engineering,* Vol. 7 (in Hungarian). Műszaki Könyvkiadó, Budapest 1966.

87 Prediger, A.: Extrem geräuscharmer 31,5 MVA Transformator. *BBC Nachr.,* 3/4, 1982, 71–73.

88 Rácz, I.: *Electrical Drives* (in Hungarian). Tankönyvkiadó, Budapest 1971.

89 Reiplinger, E.: Dämmung von Transformatorgeräuschen um mehr als 10 dB(A). Sonderdruck. *Trafo-Union*, 1971.

90 Reiplinger, E.: Massnahmen zur Geräuschminderung in Umspannanlagen. *Tech. Mitt. AEG-Telefunken*, Vol. 62, No. 2, 1972, 66–70.

91 Reiplinger, E. and Stelter, H.: Geräuschprobleme. *ETZ-Arch.*, Vol. 98, No. 3, 1977, 224–228.

92 Rentsch, H.: Luftströmungsgeräusche in elektrischen Maschinen. *ETZ-Arch.*, Vol. 82, No. 24, 1961, 792–797.

93 Report on the research (project aiming) at the noise reduction of asynchronous motors (in Hungarian). (sponsored by: Ganz Electric) Technical University of Budapest, Department of Electrical Machines, 1980.

94 Research of noise reduction possibilities for squirrel-cage asynchronous machines (in Hungarian). (sponsored by: EVIG—United Electric Machine Works) Technical University of Budapest, Department of Electrical Machines, 1977.

95 Retter, Gy.: The Unified Theory of Electrical Machines (in Hungarian). Műszaki Könyvkiadó, Budapest 1976.

96 Révész, J. and Timár, P. L.: Vibration and rotor unbalance in asynchronous motors (in Hungarian). *Elektrotechnika*, Budapest, Vol. 68, Nos 4–5, 1975, 179–188.

97 Sattler, Ph. K. and Strötgen, E.: Auswirkung der Versorgung einer stromrichtergespeister Asynchronmaschine aus dem 16 2/3 Hz-Netz auf die Pendelmomententwicklung. *ETZ Arch.*, Vol. 6, No. 1, 1984, 25–32.

98 Schuisky: Magnetischer Zug bei elektrischen Maschinen infolge der Exzentrizität des Läufers. *Elektrotechnik und Maschinenbau*, Vol. 88, No. 9, 1971, 391–399.

99 Sebestyén, B.: *Computer-controlled Measuring Systems* (in Hungarian). Műszaki Könyvkiadó, Budapest 1976.

100 Sequenz, H.: Die Wahl der Nutenzahlen bei Käfigankermotoren. *Elektrotechnik und Maschinenbau*, Vol. 50, No. 8, 1932, 428–434.

101 Shenoy, P. K.: Polyphase induction motors and noise. *Westinghouse Engineer*, 3, 1971, 46–50.

102 Smetana, C.: *Noise and Vibration Measurement* (in Hungarian). Műszaki Könyvkiadó, Budapest 1975.

103 Sperling, P. G.: Elektromagnetisch erzeugte mechanische Schwingungen und Geräusche in elektrischen Maschinen. *Siemens-Zeitschrift*, Vol. 48, No. 2, 1974, 106–113.

104 Starck, J. and Lahti, T.: Impulse noise measurements in a hearing damage study. *NAS-80 Proceedings*, 1980, 10–12.

105 Stephen, D. D. and Davies, R. J.: Discussion on acoustic noise and vibration of rotating electrical machines. *Proc IEE*, Vol. 117, No. 1, 1970, 127–129.

106 Stepina, J.: Theorie des Asynchronmotors mit elliptischer Bohrung. *ETZ-Arch.*, H. 4, 1972, 187–189.

107 Stiel, W.: Experimentelle Untersuchung der Drehmomentverhältnisse mit Kurzschlussmotoren verschiedener Stabzahl. *Forschungsarbeiten auf dem Gebiete des Ingenieurwesens*, 212, 1919.

108 Stork, P.: Beitrag zur Theorie der elektromagnetischen Körperschallerzeugung bei Drehstrom-Käfig-Läufermotoren mittlerer Leistung. Thesis, TH Hannover 1960.

109 Subcommittee Report: A comparison of methods for calculating audible noise of high voltage transmission lines. *IEEE Trans. PAS*, Vol. 101, No. 10, 1982, 4090–4099.

110 Subov, I. G.: Noise and vibration of electrical machine (in Russian). *Energiya*, Leningrad 1974.

111 Swann, S. A.: Effect of rotor eccentricity on the magnetic field in the air gap of a non-salient-pole machine. *Proc. IEE,* Vol. 110, No. 5, 1963, 903–915.

112 Szentmártony, T.: *Noise Elimination* (in Hungarian). Műszaki Könyvkiadó, Budapest 1963.

113 Szentmártony, T. and Kurutz, J.: *The Fundamentals of technical acoustics* (in Hungarian). Tankönyvkiadó, Budapest, 1981.

114 Taegen, F.: Die Bedeutung der Läufernutschlitze für die Theorie der Asynchronmaschine mit Käfigläufer. *Arch. Elektrotech.,* Vol. 48, No. 5, 1964, 373–386.

115 Theoretical analysis of asynchronous machines with solid-state supply system (in Hungarian). (sponsored by: EVIG – United Electric Machine Works) Technical University of Budapest, Department of Electrical Machines, 1975.

116 Theoretical and experimental analysis of transient noise and vibration phenomena (in Hungarian). (sponsored by: KVI) Technical University of Budapest, Department of Electrical Machines, 1983.

117 Thrane, N.: The discrete Fourier transform and FFT analysers. *Brüel and Kjaer Technical Review,* 1, 1979.

118 Tikvicki, M.: Sekundäre Massnahmen zur Geräuschminderung an elektrischen Maschinen im mittleren Leistungsbereich. *Siemens-Energietechnik,* Vol. 2, No. 1, 1980, 23–26.

119 Timár, P. L.: Measuring the vibration of electrical motors (in Hungarian). *Villamosság,* Vol. 20, No. 8, 1972, 233–240.

120 Timár, P. L.: Technical-economical analysis of the possibilities of vibration and noise reduction in three-phase asynchronous motors with 0.75 to 30 kW output (in Hungarian). Thesis, Technical University of Budapest, 1974.

121 Timár, P. L.: Die Auswirkung der Stromrichterspeisung auf das Geräuschverhalten des Asynchronmotors mit Schleifringläufer. *I. Symposium régional contre le bruit,* Varna 1975. Conference paper.

122 Timár, P. L.: System theory in the teaching of the noise of electromagnetic origin in asynchronous machines (in Hungarian). *Elektrotechnika,* Vol. 69, Nos 8–9, 318–325.

123 Timár, P. L.: Noise problems of the asynchronous machine fed by an inverter. *ICEM'76,* Vienna 1976. Conference paper.

124 Timár, P. L.: The effect of controllable solid-state device applications on the noise and vibration of slip-ring asynchronous machines (in Hungarian) *Elektrotechnika,* Budapest, Vol. 70, No. 3, 1977 100–104.

125 Timár, P. L.: Calculating the noise and vibration of electromagnetic origin in asynchronous machines (in Hungarian). Thesis for Ph.D., Budapest 1978.

126 Timár, P. L.: Vibroacoustic considerations related to asynchronous motors (in Hungarian). *MTI Textbook,* Budapest 1981.

127 Timár, P. L. and Bagi, I.: Vibrations of electromagnetic origin in rotating electrical machines (in Hungarian). *Elektrotechnika,* Budapest, Vol. 72, No. 7, 1979, 184–188.

128 Timár, P. L. and Bagi, I.: The mechanical natural frequency of rotating electrical machines equipped with mounting legs (in Hungarian). *Elektrotechnika,* Budapest, Vol. 72, No. 8, 1979, 222–225.

129 Timár, P. L. and Csiszár, Gy.: The ventilation noise of aerodynamic origin in rotating electrical machines (in Hungarian). *Elektrotechnika,* Budapest, Vol. 68, No. 9, 1975, 350–353.

130 Timár, P. L. and Ellison, A.: The effect of loading on asynchronous motor noise (in Hungarian). *Elektrotechnika,* Budapest, Vol. 76, Nos 10–11, 1983, 352–355.

131 Timár, P. L. and Palatinszky, J.: Modelling the sound radiating electrical machine (in Hungarian). *Elektrotechnika,* Budapest, Vol. 66, Nos 7–8, 1973, 313–319.

132 Timár, P. L. and Poloujadoff, M.: Method of comparative measurement as a survey process to determine the A-weighted sound power level of rotating electrical machines. *IEEE Trans. PAS,* Vol. 103, No. 7, 1984, 1816–1821.

133 Timár, P. L. and Takács, S.: Low noise level motors of the Ganz Electric Works. *Transelektro News,* 25, 1980, 70–77.

134 Timár, P. L. and Yang, S. J.: Measurement and evaluation errors in the determination of the sound power of electrical machines and equipment (in Hungarian). *Elektrotechnika,* Budapest, Vol. 72, No. 12, 1979, 338–344.

135 Timár, P. L.: Theory of the vibration and noise of asynchronous machines and the experimental investigation (in Hungarian). Thesis for D.Sc., Budapest, 1985.

136 Tsivitse, P. J. and Weihsmann, P. R.: Polyphase induction motor noise. *IEEE Trans. IGA,* Vol. 7, No. 3, 1971, 339–358.

137 Valkó, I. P.: *The Fundamentals of Electroacoustics* (in Hungarian). Akadémia Kiadó, Budapest 1973.

138 Vincze, I.: *Mathematical Statistics* (in Hungarian). Műszaki Könyvkiadó, Budapest, 1975.

139 Wahrman, C. G. and Broch, J. T.: On the averaging time of RMS. *Measurements, Brüel and Kjaer Technical Review,* Nos 2–3, 1975.

140 Weh, H.: Zur elektromagnetischen Schwingungsanregung bei Asynchronmaschinen. *ETZ-Arch.,* Vol. 85, No. 7, 1964, 193–197.

141 Wright, M. T., Gould, D. S. M. and Middlemiss, J. J.: The influence of unbalanced magnetic pull on the critical speed of flexible shaft induction machines. *Proc. Int. Conf. Electr. Mach.—Design and Application,* London 1982.

142 Yang, S. J.: Pulsating noise from small electrical machines. *Proc. ICEM'74,* London 1974, B7.1–B7.8.

143 Yang, S. J.: Effect of length-diameter ratio on noise radiation from electrical machines. *Acustica,* Vol. 32, No. 4, 1975, 255–261.

144 Yang, S. J.: Acoustic noise from small 2-pole single-phase induction machines *Proc. IEE,* Vol. 122, No. 12, 1975, 1391–1396.

145 Yang, S. J.: Noise and vibration of inverter-fed induction motors. *Proc. ICEM'76,* Vienna, 1976, I.9.1–I.9.10.

146 Yang, S. J.: *Low-noise Electrical Motors.* Clarendon Press, Oxford 1981.

147 Yang, S. J. and Akindele, K.: Unipolar flux waves in a single-phase machine. *Proc. ICEM'82,* Budapest 1982, 318–321.

148 Yang, S. J. and Elison, A. J.: *Machinery Noise Measurement.* Clarendon Press, Oxford 1985.

149 Yang, S. J. and Timár, P. L.: The effect of harmonic currents on the noise of a three-phase induction motor. *IEEE Trans. PAS,* Vol. 99, No. 1, 1980, 307–310.

150 Zavadil, I. and Ondruska, E.: The influence of the ventilation system on the operating noise of electrical machines (in Czech). *Elektrotechnický Obzor,* Prague, Vol. 57, No. 10, 1968, 583–588.

Standards

151 ISO 1680/1.2 Test code for the measurement of airborne noise emitted by rotating electrical machinery—Engineering method, survey method.

152 ISO 3740, Acoustics—Determination of sound power levels of noise sources—Guidelines for the use of basic standards and for the preparation of noise test codes.

153 ISO 3741, Acoustics—Determination of sound power levels of noise sources—Precision methods for broad-band sources in reverberation rooms.

154 ISO 3742, Acoustics—Determination of sound power levels of noise sources—Precision methods for discrete-frequency and narrow-band sources in reverberation rooms.

155 ISO 3743, Acoustics—Determination of sound power levels of noise sources—Engineering methods for special reverberation test rooms.

156 ISO 3744, Acoustics—Determination of sound power levels of noise sources—Engineering methods for free-field conditions over a reflecting plane.

157 ISO 3745, Acoustics—Determination of sound power levels of noise sources—Precision methods for anechoic and semi-anechoic rooms.

158 ISO 3746, Acoustics—Determination of sound power levels of noise sources—Survey method.

159 ISO 3747 DP Determination of sound power levels of noise sources—Survey method using a reference sound source.

160 ISO 3748 DP Determination of sound power levels of noise sources. Simplified engineering method for portable sources and essentially free field conditions over a reflecting plane.

161 ISO 6920, Acoustics—Determination of sound power levels of noise sources—Characterization and calibration of reference sound sources.

162 ISO/TR 7849 Estimation of airborne noise emitted by machinery from vibration measurement.

163 IEC Publications 34–9 Rotating electrical machines. Noise limits.

164 ISO 2372 Mechanical vibration of machines with operating speed from 10 to 200 rev/s. Basic for specifying evaluation standards.

165 ISO 2373 Mechanical vibration of certain rotating electrical machinery with shaft heights between 80 and 400 mm—Measurement and evaluation of vibration severity.

166 ISO 3945 Mechanical vibration of large rotating machines with speed range from 10 to 200 rev/s—Measurement and evaluation of vibration severity in situ.

167 ISO 2954 Mechanical vibration of rotating and reciprocating machinery—Requirements for instruments for measuring vibration severity.

168 ISO/DIS 7919/1 Mechanical vibration of non-reciprocating machines. Measurements on rotating shafts and evaluation.

SUBJECT INDEX

The authors have written a systematic study summarizing all the knowledge so far available about the vibroacoustic effects accompanying the fundamental energy conversion of electrical machines.

Beginning with a discussion of the noise generation in the machines and a detailed field analysis used in the computation of the noise of electromagnetic origin in rotating electrical machines, the authors then expand the investigation to the noise of inverter-fed asynchronous motors and to the influence of the loading. In addition the book deals with the noise of transformers and high voltage power lines, and demonstrates the theory and different practical methods of the noise and vibration reduction as well.

The second part of the book is devoted to the vibroacoustical measurements. Beside the classical noise measurements carried out in steady-state condition of the investigated machine, the authors present practical analogue and digital methods for measuring the noise characteristics of the machines in transient mode of operation and at impulsive-like noise phenomena.

With international trade in mind the authors also provide the critical review of international standards on noise and vibration measurements and evaluation, together with the newly developed methods being in status of draft proposal.

The book is intended to assist designers, engineers, scientific workers, students and technicians by extending their knowledge of the vibration and noise of electrical machines, and of problems related to the experimental investigation of vibroacoustic character of machines generally.